2022-11-01

An Improved Bio-based Activated Carbon for the Water Treatment of a Lagoon in Northern Mexico Based on Life Cycle Assessment Methodology

Leticia Elizabeth Rodriguez
University of Texas at El Paso

AN IMPROVED BIO-BASED ACTIVATED CARBON FOR THE WATER TREATMENT OF A LAGOON IN NORTHERN MEXICO BASED ON THE LIFE CYCLE ASSESSMENT METHODOLOGY

LETICIA E. RODRIGUEZ

Doctoral Program in Environmental Science and Engineering

APPROVED:

Peter Golding, Ph.D., Chair

Luis Rene Contreras, Ph.D.

Diane Elisa Golding, Ph.D.

Luis G. Perez, Ph.D.

Stephen L. Crites, Jr. Ph.D.
Dean of the Graduate School

Dedication

I dedicate this work to my mother, who, although she is no longer with us, continues and will continue to inspire me to be a better professional and person. Mother, wherever you are, with all my love and admiration, I dedicate this work to you.

AN IMPROVED BIO-BASED ACTIVATED CARBON FOR THE WATER TREATMENT OF A LAGOON IN NORTHERN MEXICO BASED ON THE LIFE CYCLE ASSESSMENT METHODOLOGY

by

LETICIA E. RODRIGUEZ, M.S.

DISSERTATION

Presented to the Faculty of the Graduate School of

The University of Texas at El Paso

in Partial Fulfillment

of the Requirements

for the Degree of

DOCTOR OF PHILOSOPHY

Environmental Science and Engineering Program

THE UNIVERSITY OF TEXAS AT EL PASO

December 2022

Acknowledgments

I would like to thank Shahrouz Jafarzade Ghadimi, Li Chen, and Dr. Shane Walker for their help, advice, and assistance with the ICP analysis. I also want to thank Truman Word and Diego Hernandez for their assistance with the SEM/EDS analysis. My sincere thanks to Dr. Peter Golding, Annalisa Perez, and Ana Cram for their time, support, help, work and for sharing their knowledge and experience with me. Thank you so much to all my professors, advisors, committee members, and the University of Texas at El Paso for educating me and helping me achieve this goal and be a better professional. A special thanks to my husband, Rene Medina, for his constant support and to God for always being present in my life and projects.

Table of Contents

List of Tables

List of Figures

List of Illustrations

Chapter 1: Introduction

The Bustillos lagoon (Laguna de Bustillos) is in the central part of the state of Chihuahua, México, near the municipality of Cuauhtémoc (Illustrations 1.1 and 1.2). The National Commission for the Knowledge and Use of Biodiversity (CONABIO, for its Spanish acronym) considers this lagoon an essential ecosystem for migratory and native aquatic birds in México. Furthermore, the International Program of Important Areas for Bird Preservation (AICA) recognizes the lagoon as an important area for the conservation of birds (Ochoa et al., 2017; Quintana et al., 2015).

Illustration 1.1: lagoon Cuauhtémoc, Chihuahua, Mexico (Source: Google Earth 2020).

Illustration 1.2: Bustillos' lagoon aquatic birds (Source: El Heraldo de Chihuahua, 2020).

The primary discharges into Bustillos' lagoon are runoffs from an intensive agricultural area and wastewater from the industrial and domestic sectors. These mainly originate from the three ethnic groups inhabiting the area around the lagoon: (1) The Mennonite villages located on the west side; (2) The Mexican rural communities located on the east and south sides; and (3) The Tarahumara communities, located at the northwest, and in colonies within the Mexican communities. Illustration 1.3 shows the diverse ethnicity around the lagoon. Some authors attribute these runoffs and wastewater discharges as the primary causes of pollution in the lagoon, affecting the surrounding communities (INEGI, 2003; INEGI, 2010; Amado, 2012; Ochoa et al., 2017; Quintana et al., 2017).

Illustration 1.3: Various ethnic groups that inhabit the communities around the Bustillos lagoon (Source: Ah Chihuahua journal, 2015).

Additional factors, such as low wages, negatively impact these communities. In December 2016, 27.3% of the economically active population received an income lower than the value of the basic food basket. Illustration 1.4 shows two regional agricultural economic activities, apple, and dairy production. Furthermore, the mortality rate in children under five years of age is high due to the lack of access to health services. In addition, the deficiency in parents' education and the inadequate maternal and child nutrition position the community at a social disadvantage (Vittrup et al., 2016).

Illustration 1.4: Depiction of economic activities around the Bustillos lagoon area (Source: El Heraldo de Chihuahua, 2018 and Geo-mexico.com, 2020).

The United Nations (UN-Habitat) measured the communities' progress using the Cities Prosperity Index (CPI) to promote collective welfare. Illustration 1.5 shows the results for the six different categories measured: (1) Productivity (55.66); (2) Infrastructure (62.00); (3) Life quality (57.37); (4) Equity and social inclusion (73.39); (5) Environmental sustainability (37.92); and (6) Urban governance and legislation (27.49). Table 1.1 shows the breakdown for each category with their corresponding indicators. Reviewing the Cities Prosperity Index, any category, sub-category, or indicator below 49.9 indicates a weak rating. The economic growth sub-category ranked at 35 receives a weak rating. In addition, the Gini coefficient, which measures the equitability of income distribution among individuals, marked a great disparity of income. Furthermore, the UN study, which used the salary-food basket ratio, identified that the poverty rate indicator scored a weak result of 33.96.(INEGI, 2010; Vittrup et al., 2016).

In addition to these indicators, the local environmental sustainability category also falls into the weak rating for various reasons. The state treats only 60% of the municipality's sewage water. Additionally, as no entity monitors local air and water quality, this estimate comes from the total wastewater state-level data. (SEMARNAT-CONAGUA, 2015). The absence of these observations are additional indicators of poor environmental security. Moreover, the nonexistence of clean, renewable energy sources significantly reduced the CPI score, placing this municipality at an environmental disadvantage.

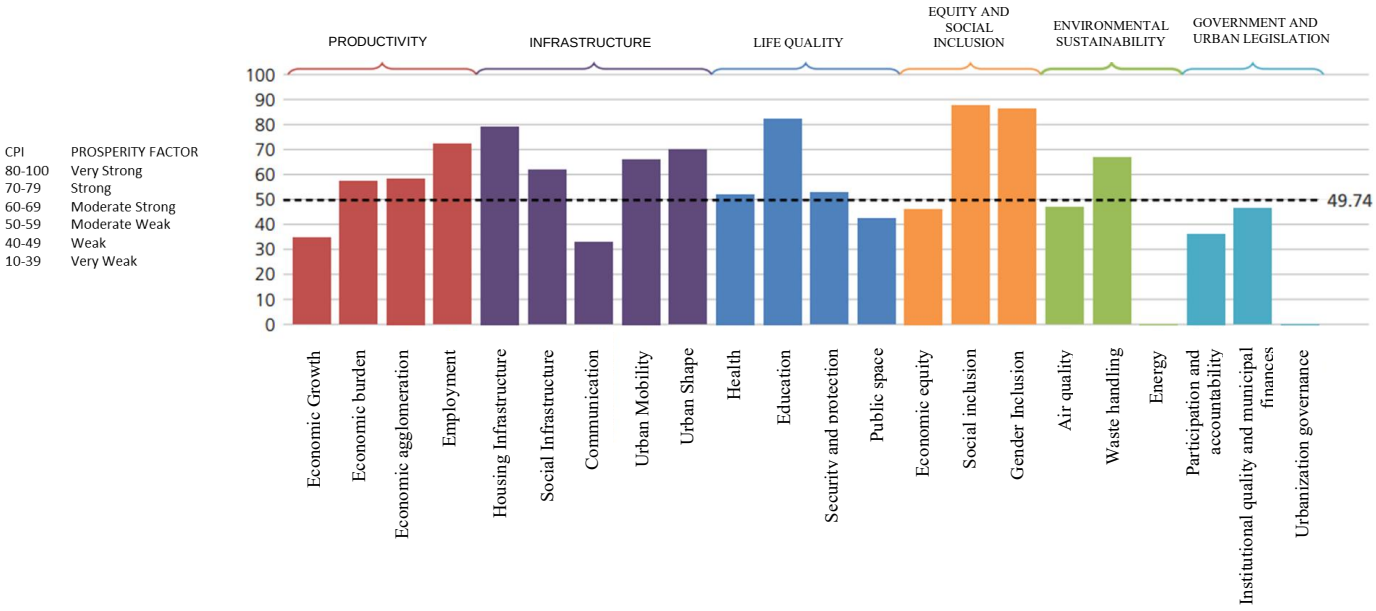

Illustration 1.5: Cities Prosperity Index (CPI) (Source: UN-Habitat, 2015).

Table 1.1: Cities Prosperity Index (CPI) structure.

Categories	Sub-categories	Indicators	Score
1. Productivity	1.1 Economic growth	1.1.1 Urban product per capita	34.67
	1.2 Economic burden	1.2.1 Elderly dependency ratio	57.31
	1.3 Economic agglomeration	1.3.1 Economic density	58.43
	1.4 Employment	1.4.1 Unemployment rate	86.93
		1.4.2 Employment-population relationship	57.53
2. Infrastructure	2.1 Housing Infrastructure	2.1.1 Durable housing	97.60
		2.1.2 Access to improved water	99.03
		2.1.3 Enough living space	100.00
		2.1.4 Population density	20.11
	2.2 Social Infrastructure	2.2.1 Physicians density	61.96
	2.3 Communication	2.3.1 Internet access	22.54
		2.3.2 Bandwidth speed	43.44
	2.4 Urban Mobility	2.4.1 Mass transport length	-
		2.4.2 Traffic fatalities	66.10
	2.5 Urban Shape	2.5.1 Road interconnection density	85.06
		2.5.2 Road density	45.69
		2.5.3 Surface for roads	78.57
3. Life Quality	3.1 Health	3.1.1 Life expectancy at birth	59.45
		3.1.2 Under-5 mortality rate	44.67
	3.2 Education	3.2.1 Alphabetization rate	96.57
		3.2.2 Schooling average years	68.07
	3.3 Security and Protection	3.3.1 Homicide rate	52.59
	3.4 Public space	3.4.1 Accessibility to public spaces	73.29
		3.4.2 Green areas per capita	11.53
4. Equity and social inclusion	4.1 Economic Equity	4.1.1 Gini coefficient	58.44
		4.1.2 Poverty rate	33.96
	4.2 Social Inclusion	4.2.1 Slum housing	93.73
		4.2.2 Youth unemployment	81.48
	4.3 Gender Inclusion	4.3.1 Educational Equity	86.35
5. Environmental sustainability	5.1 Air Quality	5.1.1 Monitoring stations number	0.00
		5.1.2 Particulate matter levels	95.00
		5.1.3 CO_2 concentration	46.08
	5.2 Waste Handling	5.2.1Solid waste collection	73.42
		5.2.2 Sewage treatment	60.05
	5.3 Energy	5.3.1 Renewable energy usage	0.00
6. Government and Legislation	6.1 Participation	6.1.1 Electoral participation	36.25
	6.2 Institutional finances	6.2.1 Spending efficiency	100.00
		6.2.2 Tax collection	24.74
		6.2.3 Debt	13.97
	6.3 Urbanization	6.3.1 Urban planning	0.00

Reports of high pollutant levels in the Bustillos Lagoon confirm the CPI assessment performed by the UN-Habitat (Quintana et al., 2015; Amado et al., 2016; Ochoa et al., 2017). Quintana et al. (2015) found aluminum and iron levels exceeding Mexican irrigation standards (NOM-001/002-SEMARNAT-1996), and the levels of nickel and chromium were at the threshold limit. Similarly, Amado et al. (2016) reported high nitrates, coliform bacteria levels, and low levels of dissolved oxygen in the lagoon. In addition, Ochoa et al. (2017) documented high concentrations of Dichlorodiphenyltrichloroethane (DDT), including metabolites, nitrates, magnesium, and Sodium Adsorption Ratio (SAR).

More recently, Rodriguez et al., states in pending publication of a heavy metal study conducted in the Bustillos lagoon. Their results show the presence of mercury (Hg), arsenic (As), and uranium (U) in levels above drinking water and irrigation standards (US EPA, NOM-001/002-SEMARNAT-1996, NOM-003-SEMARNAT-1997). According to this study, the highest concentrations occurred during the fall, right after harvest. However, the levels of arsenic and uranium were concentrated in the lacustrine zone, whereas the levels of mercury were more constant throughout the lagoon.

Heavy metals exceeding water standards, like those found by Rodriguez et al., increase the potential negative impacts of water used for agricultural irrigation or livestock consumption since these metals resist degradation. Another concern is that plants and animals bio-accumulate these elements and thus enter the human food chain. Several studies have found that mercury, arsenic, and uranium show adverse acute and chronic health effects in humans, birds, and aquatic life (US EPA, 2009; US EPA Health Effects Notebook, 2016; CDC-ATSDR, the Agency for Toxic Substances and Disease Registry).

Addressing the heavy metal pollution in the Bustillos lagoon, this study proposes the development of a Bio-based Activated Carbon (BBAC) to remove arsenic, with higher or comparable adsorption properties, lower production cost, and better environmental performance than conventional activated carbon. Furthermore, the proposed BBAC will treat the polluted water lagoon to achieve irrigation standards for agricultural purposes. In turn, using the proposed BBAC can potentially improve the life quality of the surrounding communities.

Chapter 2: Relevance and Research Goal

Many adsorbent methods for water treatment have been developed and are commercially available (zeolites, synthetic polymeric adsorbents, activated alumina, activated carbon). However, AC is the most commonly used adsorbent since it performs exceedingly well in several process applications. Specifically, ACs appear to have the most favorable characteristics for adsorption in water treatment processes, mainly due to their wide range of pore size that provides a large organic molecules storage capacity. Examples of the organic molecules that ACs can store include (1) Natural Organic Matter (NOM); (2) Synthetic Organic Compounds (SOC) (pesticides/herbicides); (3) Solvents; and (4) fuels.

ACs remove disinfection by-products (DBP), colors, tastes, and odors. In addition, ACs are usually less expensive than zeolites, synthetic polymeric adsorbents, and activated alumina. Recently, treating ACs with different chemical species (e.g., ammonia, ferric hydroxide, and iron) allows for an increase in their adsorption capacity. Examples of materials that treated AC can adsorb include: (1) Bromated; (2) Perchlorate; (3) Some anionic species; (4); Heavy metals, and (4) Arsenic (Crittenden et al., 2012; Hongmei et al.,2018; Arena et al., 2016; Jeswani et al., 2015; Hadi et al., 2015; Zhang et al., 2005; Xu et al., 2016). Traditionally, ACs come from hard coals (fossil-based materials). However, environmental awareness has provided a market opportunity for alternative, renewable, and low-impact bio-based products, including ACs (Hongmei et al., 2018; Arena et al., 2016; Crittenden et al., 2012).

The high volumes of agricultural residue serve as feedstock to create ACs. However, further assessments of these bio-products will help to determine their environmental effectiveness compared to fossil fuel-based ACs. For instance, the Life Cycle Assessment (LCA) methodology is a comprehensive, input-output material and energy-based analysis used to quantify the potential

environmental impacts associated with all the life cycle stages of a product, process, or service. This study will evaluate the manufacturing process for ACs following the LCA methodology to compare different scenarios that can provide a starting point for the environmental improvement of the proposed BBAC. Implementing an LCA at the design stage helps prevent potential adverse environmental impacts in mass production. (Corsi et al., 2018). Therefore, some authors consider LCA a powerful tool for supporting eco-design and decision-making (Corsi et al., 2018; Hongmei et al., 2018; Arena et al., 2016).

This research aims to develop an innovative Bio-based Activated Carbon using locally available agricultural residues with better or equal arsenic adsorption capacity, lower cost, and better potential environmental impacts than the commercial coal-based AC.

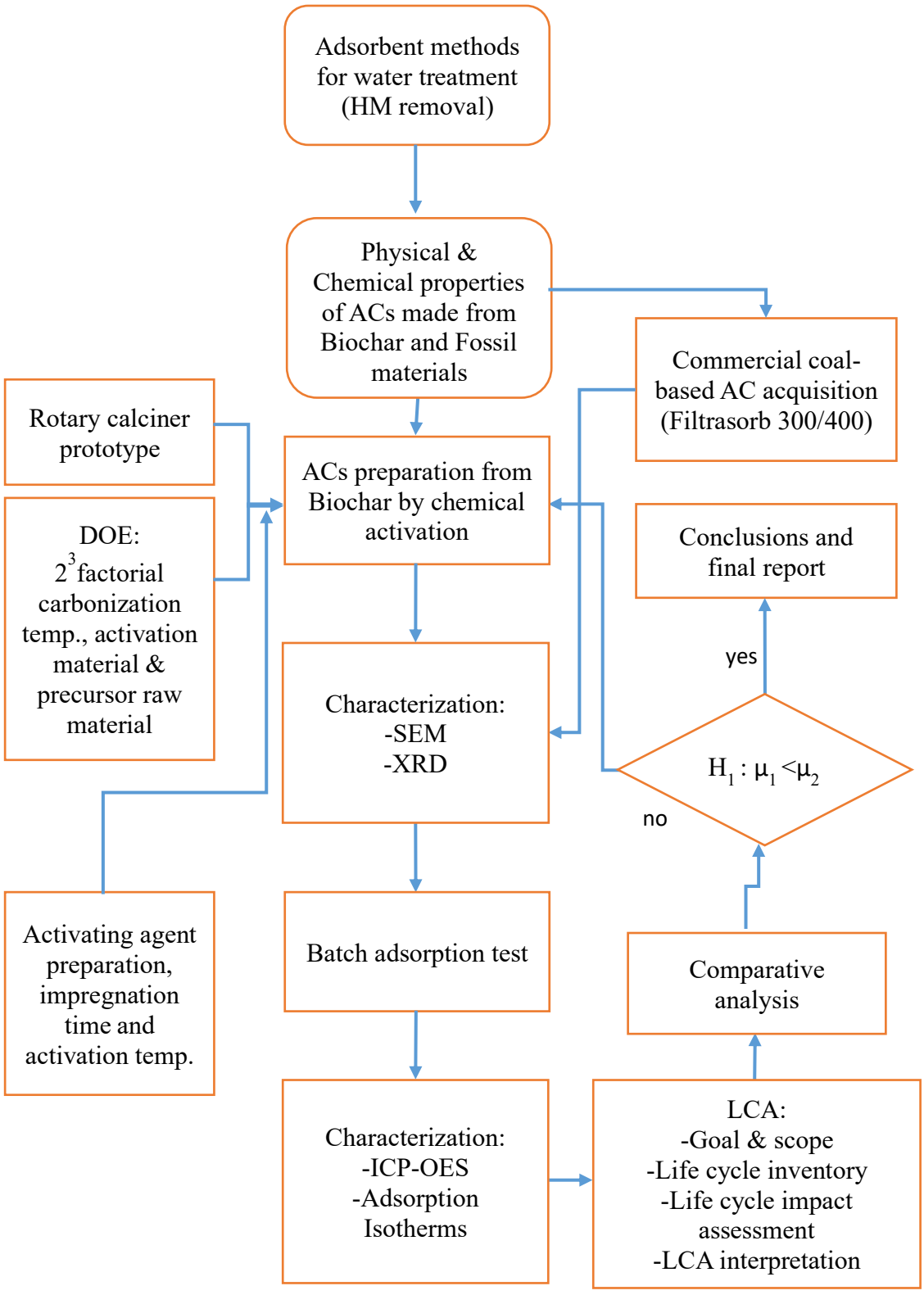

Figure 2.1: Flow Chart Diagram of the Project.

Chapter 3: Goal and Objectives

This study aims to create a new Bio-based Activated Carbon (BBAC) to remove arsenic from water in the Bustillos lagoon. Regional biomass, including rice husk and peanut shells, will create the essential biochar needed for the BBAC. Additionally, the goal is to produce a BBAC with better or equal physical adsorption properties, better environmental performance, and lower cost than the commercially Coal-based Activated Carbon (CCAC) (Filtrasorb 300 or 400).

3.1 OBJECTIVES

To reach the main goal, during the preparation stage, three specific objectives must be achieved. A DOE matrix is used to identify and evaluate the most important factors and their interactions for the adsorption capacity and carbon content in these materials. The BBACs and CCAC environmental performance and cost are also evaluated for comparative purposes

3.1.1 Objectives for physical properties

The adsorption capacity of the proposed BBACs should be equal to or higher than the adsorption capacity of CCAC. The BBAC preparation stage entails improving the porosity and surface area physical characteristics to reach this objective. The adsorption capacity of the CCAC and the proposed BBACs will be measured using ICP-OES equipment, adsorption isotherms, elemental analysis (EDS), and a scanning electron microscope (SEM). These evaluations aim to find arsenic concentration, porous size, porous distribution, and particle size. An Analysis of Variance (ANOVA) will take place, using the previous evaluation results to determine if the new BBAC has comparable or better adsorption properties to the CCAC.

The physical properties optimized by manipulating the controllable input factors while preparing the BBAC include 1) Pyrolysis temperature, 2) Pyrolysis time, and 3) activation

material. The optimal parameters are determined with a 2^3 full factorial Design of Experiments (DOE with three factors at two levels).

3.1.2 Objectives for environmental performance

A comprehensive Life Cycle Assessment (LCA) of the proposed BBAC and the CCAC will show environmental comparisons. This comparison uses the scores obtained from the mid-point impact categories according to the LCIA-TRACI "Tool for Reduction and Assessment of Chemicals and other Impacts," developed according to Environmental Protection Agency (EPA) standards. The categories that LCIA-TRACI considers are: (1) Global warming potential, (2) Eutrophication potential, (3) Ozone depletion potential, (4) Ecotoxicity Air, (5) Acidification potential, (6) Human Health Particulate Air, (7) Human toxicity, cancer, (8) Human toxicity, non-cancer, (9) Resources, Fossil fuels, and (10) Smog Air (GaBi Software, 2020). The system boundary considered is from "cradle-to-grave" that aligns with the ISO14040 series on LCA (ISO-14040, 2006; ISO-14044, 2006).

3.1.3 Objectives for cost

The total production BBACs cost should be equal to or lower than the sale price of CCAC in retail stores. The BBACs improvement is based on biomass, energy (electricity and natural gas), water, and all other required inputs. The raw material acquisition, energy consumption, and other production costs will be optimized using agricultural wastes available in the region and improving the production conditions at the preparation stage.

Chapter 4: Background and Literature Review

Many researchers have studied the Activated Carbon (AC) composition, properties, uses, advantages, and disadvantages. Crittenden et al. (2012) observed that several processes manufacture AC from natural, carbonaceous materials. It is a very effective adsorbent due to its highly developed porosity, large surface area, variable surface chemistry characteristics, and high degree of surface reactivity, making AC a very versatile material. ACs have several useful purposes, such as removing pollutants from gaseous or liquid phases and purifying or recovering chemicals. (Dias et al., 2007; Derbyshire et al., 2001).

According to Crittenden et al. (2012), AC is available in two particle size ranges: powdered activated carbon (PAC), which means that the particle size is from 20 to 50 μm, and granular activated carbon (GAC) with a 0.5 to 3 mm particle size. Currently, the most common GACs applications in water treatment are for toxic organic compounds control, barriers to occasional odor and taste in surface waters, disinfection by-products, and dissolved organic carbon control. Worldwide water treatments mainly use powdered activated carbon for seasonal taste and odor compound control. Synthetic organic compounds (SOC) such as pesticides, herbicides, tetrachloroethene, and benzene are removed with GAC because less of this adsorbent is required compared to PAC. (Crittenden et al., 2012; Ioannidou & Zabaniotou, 2007).

Currently, there are many studies regarding AC development from agricultural residues. The results are encouraging as they contribute to decreasing the costs of production and waste disposal. Therefore, they help to protect the environment and present similar or even better characteristics than conventional ACs (Dias et al., 2007). Ioannidou and Zabaniotou (2007) mentioned that the main processes in AC production consist of first, pyrolysis applied to biomass and secondly, activation applied to the resulting char. Pyrolysis is a thermal treatment that has the

potential to generate char. The thermal treatment removes the biomass moisture and the volatile matter contents. The remaining solid or char shows different characteristics than the original raw materials. These changes in the properties usually lead to high reactivity; hence, an alternative usage of char as an adsorbent material becomes possible. The char becomes an attractive by-product, which includes AC. Any material with high carbon content and low inorganics are suitable raw material for AC production. Agricultural by-products have proven to be a promising source of raw materials for AC production because they are available at cost-effective prices (Ioannidou & Zabaniotou, 2007; Dias et al., 2007). They can be used to produce AC with a high adsorption capacity, considerable mechanical strength, and low ash content (Savova et al., 2001; Ioannidou & Zabaniotou, 2007; Dias et al., 2007) (See Table 4.1).

Table 4.1: Agricultural residues proximate and ultimate analysis.

Agricultural Wastes	**Fixed Carbon %ww**	**Moisture %ww**	**Ash %ww**	**Volatiles %ww**	**C %ww**	**H %ww**	**O %ww**	**N %ww**	**S %ww**
Rice Husk	15.36	10.427	12.223	61.982	39.84	5.03	28.4	0.56	0.11
Peanut Shell	26.53	5.79-8	2.86	62.73	45.44	6.69	36.06	1.07	0.02

Literature comprised of multiple research studies indicates that there have been many experiments to obtain low-cost and more eco-friendly AC from agricultural wastes. Examples of agricultural waste in these experiments include wheat straw, corn straw, olive stones, bagasse, birch wood, miscanthus, sunflower shell, pinecone, rapeseed, cotton residues, pine raye, and sugar cane bagasse. Also used are almond shells, peach stones, grape seeds, straw, oat hulls, corn stover, apricot stones, cotton stalks, cherry stones, peanut hulls, nut shells, rice hulks, rice straw, coconut shells, walnut shells, coffee bean husk, coffee residues, and woody biomass (Ioannidou &

Zabaniotou, 2007; Dias et al., 2007). Research shows that both physical and chemical activation contributes to the AC preparation from agricultural residues. The raw material's structure dramatically influences the best parameters needed to obtain specific AC. It is possible to obtain AC with different pore textures by varying the activation conditions, thus optimizing their production for a specific purpose (Ioannidou & Zabaniotou, 2007; Dias et al., 2007).

Several treatment purposes have benefitted from AC prepared from various agricultural wastes. Kadirvelu et al.'s (2003) research showed that AC prepared from agricultural wastes removed significant amounts of different types of dyes, Hg (II) and Ni (II). According to Kadirvelu et al. (2001), AC made from coir pith can potentially remove toxic heavy metals from industrial wastewater. Chemical activation processes seem more frequent than physical activation in preparing AC from agricultural wastes. The agents more frequently used are H_3PO_4, KOH, and $ZnCl_2$ (Dias et al., 2017).

Dias et al. (2007) mentioned that AC prepared from woody materials appears to be very effective in adsorbing heavy metals such as chromium and copper. It can also remove dyes, and organic compounds (phenol), from an aqueous phase. However, preparing AC with high surface areas and good porous texture using woody materials should be carefully optimized to obtain the adsorption behavior required by manipulating preparation parameters. Studies using both physical and chemical activation have prepared AC from woody materials. (Gu et al., 2018; Lo et al., 2012, Danish & Ahmad, 2018, Hadi et al., 2015).

Ioannidou and Zabaniotou (2007) reviewed several AC manufacturing processes from agricultural residues. They observed different effects when a change occurs in the process parameters in the pyrolysis and the activation stage. The resulting pyrolytic char gained suitable conditions for removing heavy metals, dyes, and organic compounds. Zhang et al. (2005), studied

oak, wood wastes, corn hulls, and corn stover carbonization and chemical activation to remove Hg II. In the studies of Yakout et al. (2016), Stavropoulos et al. (2005), and Demiral et al. (2011), researchers heated chars obtained from olive residues to gasify under steam and nitrogen atmosphere as well as chemical activation using potassium hydroxide (KOH) and phosphoric acid (H_3PO_4). AC obtained in these studies showed effective adsorbing capacities for dye removal. Sugarcane bagasse, rice hulls, rice straw, and pecan shells are other examples of raw materials studied by Bansode et al. (2003), Zhang et al. (2015), Wu et al. (2013), and Taha et al. (2011). The biochar was created in an atmosphere of nitrogen gas at 750 °C and physically and chemically activated in a high-temperature fluidized bed reactor. According to Ioannidou and Zabaniotou (2007), pyrolysis temperature has the most significant effect, followed by pyrolysis heating rate and the pyrolysis residence time.

There are two main steps for the preparation of AC: (1) the carbonization of the carbonaceous raw materials below 800 °C in the absence of oxygen, and (2) the activation of the carbonized product (char), which is either physical or chemical (Ioannidou & Zabaniotou, 2007; Dias et al., 2007; Crittenden et al., 2012).

Chemical activation is a two-step process carried out simultaneously, with the precursor mixed with chemical activating agents as dehydrating agents and oxidants (Crittenden et al., 2012). According to Dias et al. (2007), and Ioannidou and Zabaniotou (2007), the most common chemical agents are $ZnCl_2$, KOH, and H_3PO_4, less common chemical is K_2CO_3. They mentioned that chemical activation offers several advantages since, in a single step, it combines pyrolysis and activation performed at lower temperatures and develops a better porous structure. Although, environmental concerns of using chemical agents for activation could arise (Ioannidou & Zabaniotou, 2007; Dias et al., 2017; Crittenden et al., 2012). Besides, it is possible to recover part

of the added chemicals.(Tsai et al., 1998 & 2001; Zhang et al., 2004). Chemical activation was used in the preparation of AC using corn cob and corn straw as precursors to remove Hg II, Ni II, Congo red, methylene blue, and rhodamine 3 (Tsai et al., 1998 & 2001; Zhang et al., 2005; Kadirvelu et al., 2003, Dias et al. 2007). Many different agricultural residues appeared in the articles of Ioannidou and Zabaniotou (2007), Sung and Webley (2010); Ketcha et al. (2012), and Dias et al. (2007) discussing AC preparation by chemical activation. Studies included the use of olive stones used as precursors for AC by Stavropoulos and Zabaniotou (2005), Dias et al. (2007), Yakout and Sharaf (2016). As was rice husks used as precursors by Van and Luong (2014), Hieu et al. (2015), Ioannidou and Zabaniotou (2007), Dias et al. (2007), Daifullah et al. (2002), Pode R. (2016), and Hegazi H.A. (2013). Other studies used rice straw as precursors Park (2002), and Fierro et al. (2010). Another study used fruit peels as precursors (cassava, pomelo) Sun et al. (2016) and Sudaryanto et al. (2006). Nutshells, in particular, macadamia, hazelnut, almond, walnut, and pistachio, were used as precursors for AC which as developed by Ahmadroup and Do (1997), Aygun et al. (2003), Yang and Lua (2003), Ahmedna et al. (2004), Ioannidou and Zabaniotou (2007), and Dias et al. (2007). Peanut shells were used as a precursor for AC to remove heavy metals, dyes, and organic compounds by Zhang et al. (2015), Wu et al. (2013), Georgin et al. (2016), Girgis et al. (2003), and Ricordel et al. (2001). Apricot stones were used in the studies of Ioannidou and Zabaniotou (2007), Dias et al. (2007), and Aygun et al. (2003). Cherry stones were used as precursors by Angin D. (2014), Ioannidou and Zabaniotou (2007), Dias et al. (2007), and Aygun et al. (2003). Wheat straw served as a precursor by Biswas et al. (2017), Yang et al. (2010), Ioannidou and Zabaniotou (2007), and Dias et al. (2007). Coconut shells were analyzed as precursors in the AC development by Arena et al. (2016) and Anirudhan and Sreekunan (2011). Studies of biomass occurred regarding cocoa shells by Rivas et al. (2015), coffee residues by

Lamine et al. (2014), and woody biomass as precursors for AC preparation by chemical activation by Gu et al. (2018), Danish and Ahmad (2018), and Zhang et al. (2004) (see Table 4.2).

According to Ioannidou and Zabaniotou (2007), physical activation involves the carbonization of a carbonaceous material followed by the activation of the resulting char at elevated temperature in the presence of suitable oxidizing gases such as carbon dioxide, steam, or their mixture. The activation gas is usually CO_2 since it is clean, easy to handle, and facilitates control of the activation process due to the slow reaction rate at temperatures around 800 °C. Carbonization temperature ranges between 400 and 850 °C, and activation temperature ranges between 600 and 900 °C. (Ioannidou and Zabaniotou, 2007). Research literature indicates the use of physical activation in the subsequent studies where AC is developed from different raw materials: corn on the cob and corn straw (Tsai et al., 2001; Yang et al., 2017; Lanzetta & Di Blasi, 1998), olive bagasse *(*Demiral et al., 2011), peanut shells (Wu et al., 2013; Georgin et al., 2016), rice husk and rice straw (Pode R, 2016; Hegazi H.A., 2013), barley straw (Pallares et al., 2018), oak, moso, and bamboo wood *(*Jung & Kim, 2014). However, according to Ioannidou and Zabaniotou (2007), AC produced by physical activation does not achieve desirable characteristics to be used as adsorbents or as filters compared with AC produced by chemical activation (Ioannidou & Zabaniotou, 2007). Crittenden et al. (2012) considered that carbons produced by chemical activation have a low-density structure and, without special treatment, have a low micropores proportion, making them less suitable for use in the removal of micropollutants and odor-causing substances. They also considered carbons produced for water treatment must utilize an endothermic thermal activation process (Crittenden et al., 2012). This activation involves contacting a gaseous activating agent, typically steam, with the char at elevated temperatures, typically 850 to 1000 °C. It causes a slight reduction in the size of the adsorbent grain caused by

external oxidation as the oxidizing gas diffuses into the internal carbon domain. The raw material or occasionally pretreatment determines the pore structure. The type of activating agent, activation length, and temperature can significantly influence the adsorbent properties (Crittenden et al., 2012).

According to Crittenden et al. (2012) and Ioannidou and Zabaniotou (2007), the most critical factors and properties of carbonaceous materials used for AC preparation are the surface area and pore size. These properties determine the number of adsorption sites and the accessibility of the sites for adsorbates. Generally, there is an inverse relationship between the pore size and surface area: the smaller the pores for a given pore volume, the greater the surface area available for adsorption. During the carbonization step, volatile components are released, forming graphite. Furthermore, the carbon realigns to form a pore structure that develops during the activation process. In the activation step, carbon is removed selectively from an opening of closed porosity, increasing the micropore's average size. For most thermally activated carbons, a maximum surface area per weight of original char is about 40 to 50 % mass burn-off. Activation up to this point opens closed pores and enlarges existing pores, resulting in a net increase in surface area. The types of base materials can influence the distribution of the pores.

The International Union of Pure and Applied Chemistry (IUPAC) classifies the pore sizes as (i) micropores with a diameter less than 2 nm., (ii) mesopores with a diameter between 2 nm and 50 nm., and (iii) macropores with a diameter greater than 50 nm. (Crittenden et al., 2012). Coconut shell carbons are considered a microporous carbon because most of their total void volume is micropores. (Crittenden et al., 2012). Wood-based carbons have a more even distribution of micro, meso, and macropores. Biomass is a renewable organic material comprised of cellulose, hemicellulose, and lignin (Crittenden et al., 2012).

Materials with a greater content of lignin (grape seeds, cherry stones) develop ACs with macro-porous structures. Raw materials with higher content of cellulose (coconut shells, apricot stones, almond shells) yield ACs with a predominantly microporous structure. The surface area of char is essential because it may strongly influence the reactivity and combustion behavior. In the Tsai et al. (1997 & 1998) studies, surface areas decreased at higher pyrolysis temperatures and soaking time but increased at higher activation temperatures.

Ioannidou & Zabaniotou (2007) research shows that ACs from corn stover and oat hulls yield a larger pore volume. In contrast, olive stone carbons, when being activated, have a high percentage of char yield (76%). The higher surface area (S_{BET}) is achieved by pyrolyzing rice straws and activating the carbons with KOH. However, remarkable surface areas can be taken from corn cob, olive stones, and cassava peel. The chemical nature of ACs influences its adsorptive, electrochemical, catalytic, and other properties. Generally, ACs with acidic surface chemical properties are favorable for basic gas adsorption, such as ammonia, while ACs with basic surface chemical properties are suitable for acidic gas adsorption, such as sulfur dioxide. The AC produced from peanut hulls, and rice straws serves as the adsorption of methylene blue and trace metals. The AC made from rice husk, and orange peel can remove acid dyes. The AC produced from palm kernel fiber can remove ions and arsenic. Pitch-based carbons serve as adsorption of atrazine, wheat straw carbon removes nitrate and pesticides, and wastewater treatment uses rice husk carbon. Olive stones carbons have several uses: groundwater treatment, drinking water purification, heavy metals removal, effluent gas streams purification, mercury vapors removal, volatile organic compounds (VOCs) removal, nitrates and sulfates removal, and removal of phenolic compounds (Ioannidou & Zabaniotou, 2007).

Dias et al. (2007), describe the fundamentals of the adsorption process when using AC. The study showed that the adsorption process results from interactions between the carbon surface and the adsorbate. These interactions can be electrostatic or non-electrostatic. When the adsorbate is an electrolyte that dissociates in an aqueous solution, electrostatic interactions occur; the nature of these interactions, which can be attractive or repulsive, depend on (i) the charge density of the carbon surface, (ii) the chemical characteristics of the adsorbate, and (iii) the ionic strength of the solution. Non-electrostatic interactions are always attractive and can include: (i) van der Waals forces, (ii) hydrophobic interactions, and (iii) hydrogen bonding. An electric charge occurs when the AC is in contact with an aqueous solution. This charge results from either the carbon functional groups' dissociation or the ions' adsorption from the solution and strongly depends on the solution pH and the surface characteristics of the adsorbent *(*Li et al., 2002). There are three different mechanisms to remove ions from water. Dias et al. (2007) discuss that the first mechanism is an ion exchange process that stems from electrostatic adsorbate-adsorbent interactions dependent on carbon surface functionality. The second mechanism suggests that enhanced adsorption potentials, which occur in the narrowest micro-porosity, have enough strength to adsorb and retain ions. The third mechanism stems from the concept of acids and bases. The oxygen, hydrogen, nitrogen, and sulfur atoms, can be found in AC (Dias et al., 2007). These atoms, which may have originated in the raw material or could be introduced during preparation or further treatments (Radovic et al., 2000), influence the charge, hydrophobicity, and electronic density of the AC surface (Dias et al., 2007).

According to Crittenden et al. (2012) and Benjamin M. (2015), the adsorbate affinity for an adsorbent is quantified using adsorption isotherms. This describes the extent of adsorbate, which is adsorbed by an adsorbent at equilibrium. In most water treatment applications, the amount

of adsorbate adsorbed is usually a function of the aqueous-phase concentration, and this relationship is commonly called an isotherm. Adsorption isotherms are performed by exposing a known quantity of adsorbate in a fixed volume of liquid to various dosages of adsorbent. Equations developed by Langmuir, Freundlich, Brunauer, Emmet, and Teller (BET isotherm) describe the equilibrium capacity of adsorbents and is applied in this study (Crittenden et al., 2012., and Benjamin M., 2015).

Ioannidou and Zabaniotou (2007), mentioned that biomass pyrolysis is generally a complex process, so it is challenging to develop kinetic models that explain the mechanism of thermal decomposition. However, since agricultural residues are mixtures mainly composed of cellulose, hemicellulose, and lignin, their decomposition comprises a large number of reactions in parallel and in series. Thus, the number of reactions that occur simultaneously in the simplest pyrolysis process is so great that it is practically impossible to develop a kinetic model that considers all these reactions. Dias et al. (2007), reviewed many studies related to the adsorption of organic pollutants and heavy metals in AC prepared from agricultural solid wastes. Many of these studies report that heavy metals removal by AC is economically favorable and technically effortless. Literature regarding heavy metals removal such as cadmium, chromium, mercury, iron, and copper are in a review by Huang (1978), Zhang et al. (2005), Chen and Wu (2004), Nadeem et al. (2006), Goel et al. (2005), Liu et al. (2007), Park et al. (2006), Madhava Rao et al. (2006), Youssef et al. (2004), Erdogan et al. (2005), and Kadirvelu et al. (2001 & 2003). Most revised studies showed that these materials could compete with a commercial AC, and some have even better behavior than conventional ones.

Ioannidou & Zabaniotou (2007), mentioned in their article that peanut husks carbon is an effective adsorbent for the removal of Pb^{2+}, Cd^{2+}, Zn^{2+}, and Ni^{2+} from aqueous solutions. Peanut

husks would be helpful for the economic wastewater treatment containing these heavy metals (See Table 4.2).

Although many AC studies discuss agricultural residues, only ACs made from coconut shells have been manufactured on an industrial scale. Despite all the advantages that studies have found in AC from agricultural residues, their use remains small in water treatment processes compared to conventional AC (Ioannidou & Zabaniotou, 2007).

Table 4.2: Applications of Activated Carbon made from agricultural wastes.

RAW MATERIAL	ACTIVATION AGENT CHA	ACTIVATION AGENT PHA	CONTAMINANTS REMOVED	REFERENCE
CHERRY STONE	$ZnCl_2$		INDUSTRIAL WASTE GASES AND WASTEWATER	ANGIN. ET AL. (2014) IOANNIDOU AND ZABANIOTOU. (2007) DIAS ET AL. (2007)
COCOA SHELL	$KOH+Al(NO_3)+Na_2SO_4$		RV-5 DYE	RIBAS ET AL. (2014)
CORN COB	KOH K_2CO_3 KOH $ZnCl_2$	CO_2	HEAVY METALS AND DYES	TSAI ET AL. (2014) SUN AND WEBLEY. (2010) TSAI ET AL. (1997)
OAKWOOD WASTE, CORN HULLS/STOVER		CO_2	Hg (II)	ZHANG ET AL. (2004)
WOOD MATERIALS	H_3PO_4, KOH, and $ZnCl_2$	STEAM AND CO_2	DYES, PHENOL, ORGANICS, Cr (VI), Cu (II), Hg (II), Pb (II)	DANISH AND AHMAD. (2018), DIAS ET AL. (2007)
FOX NUTS	H_3PO_4		INDUSTRIAL WASTE GASES AND WASTEWATER	KUMAR AND MOHAN-JENA. (2016)
FRUIT STONES AND NUTSHELLS	$ZnCl_2$		PHENOL, METHYLENE BLUE	AYGUN ET AL. (2003)
OLIVE BAGASSE		STEAM	HERBICIDES	DIAS ET AL. (2007)
OLIVE SEED WASTE	KOH		METHYLENE BLUE	STRAVROPOULOS AND ZABANIOTOU. (2005)
PEANUT HUSKS	NaOH		HEAVY METALS (Pb, Hg and Cu)	TAHA ET AL. (2011) IOANNIDOU AND ZABANIOTOU (2007)
PEANUT SHELLS	K_2CO_3 AND Fe_3O_4	CO_2	HEAVY METALS, DYES, AND ORGANIC COMPOUNDS.	WU ET AL. (2013) ZHANG ET AL. (2015) GEORGIN ET AL. (2016) GIRGIS ET AL. (2003) RICORDEL ET AL. (2001)
PECAN SHELL	H_3PO_4	STEAM AND CO_2	HEAVY METALS (Cu, Pb, and Zn)	BANSODE ET AL. (2003)
RICE STRAW	KOH		METHYLENE BLUE	HWAN-OH AND ROE-PARK. (2002) FIERRO ET AL. (2010)
RICE HUSK	KOH HCl NaOH		HEAVY METALS (Fe, Mn, Zn, Cu, Cd, and Pb)	DAIFULLAH ET AL. (2003) LE VAN AND LUONG-THI. (2014) IOANNIDOU AND ZABANIOTOU. (2007) PODE. (2016)
COFFEE RESIDUES	H_3PO_4		PHENOL	MOHAMED-LAMINE ET AL. (2014)
BAGASSE PITH		STEAM	HEAVY METALS Hg	ANOOP-KRISHNAN AND ANIRUDHAN. (2002)
COCONUT BUTTONS AND SHELLS	H_2SO_4, $NaHCO_3$, NaCl, HCl, NaOH, AND H_2SO_4		HEAVY METALS (Pb, Hg, and Cu)	ANIRUDHAN AND SREEKUMARI. (2011) ARENA ET AL. (2016)
COCONUT TREE, SAWDUST, SILK COTTON HULL, AND BANANA PITH)	H_2SO_4		DYES AND METAL IONS. (RHODAMINE-B, CONGO RED, METHYLENE BLUE, METHYL VIOLET, MALACHITE GREEN, Hg (II), AND Ni (II).	KADIRVELY ET AL. (2003)
COIR PITH			HEAVY METALS	KADIRVELU ET AL. (2001)
POMELO PEEL			CIPROFLOXACIN	SUN ET AL. (2016)
APRICOT STONES	$ZnCl_2$, KOH, H_3PO_4, and K_2CO_3		HEAVY METALS (Hg (II), Ni (II)) AND DYES	IOANNIDOU AND ZABANIOTOU. (2007)

The need for a systematic evaluation of the environmental impacts of products and processes is widely recognized, and a growing body of literature is endorsing life cycle assessment (LCA) as a valid tool for this purpose (Gavankar et al., 2012). The United Nations Environment Program (UNEP) and the Society of Environmental Toxicology and Chemistry (SETAC) launched the Life Cycle Initiative (Hauschild et al., 2008). This initiative developed practical tools for evaluating the opportunities, risks, and other factors associated with products and services over their entire life cycle to achieve sustainable development (Hauschild et al., 2008). Furthermore, to identify recommended practices for conducting life cycle assessment (LCA) within the framework spelled out by the International Organization for Standardization (ISO) standards and to make the data and methodology for performing LCA available and applicable worldwide (Hauschild et al., 2008). Environmental awareness among industries, businesses, people, and governments worldwide, has started to shift their attention to pollution prevention. Many businesses and industries now offer environmentally conscious products and use environmentally conscious processes in their manufacturing plants. The environmental impact of new products and processes has become a vital issue, which is why companies are watchful to avoid or diminish adverse effects on the environment (Manjare & Khan, 2006*)*. The LCA is a tool that helps with pollution prevention. This tool systematically quantifies environmental performance and can complement conventional process analysis (Manjare & Khan, 2006). The LCA evaluates the potential environmental impacts associated with the AC production process from bio-wastes according to Bernardo et al. (2016), Gu et al. (2017), and Arena et al. (2016). Gu et al. (2017), developed an LCA of AC made from woody biomass from cradle-to-gate and compared it with commercial coal-based AC showing about 35 percent less energy demand. Consequentially, the greenhouse gas emissions were less than that of coal AC production. Biochar AC from the study above suggests a

potential high-value market for woody biomass derived from forest restoration and wildfire suppression activities. Arena et al. (2016) developed an LCA for AC made from coconut shells. This study found that the impact categories of Global Warming Potential, Human Toxicity Potential, and Acidification Potentials can improve by reducing the electrical energy consumption in the process units using biomass and electrical energy produced from renewable sources. Hjaila et al. (2013) implemented the LCA to quantify the potential environmental impacts of the AC production process from olive-waste cakes in Tunisia. The results showed that impregnation using phosphoric acid (H_3PO_4) and electricity presented the highest environmental impacts for the majority of the indicators tested: global warming potential, acidification potential, eutrophication, ozone depletion potential, human toxicity, and terrestrial eco-toxicity. Bernardo et al. (2016) developed a survey literature article looking for the environmental risk assessment and eco-toxicity of AC made from bio-wastes. That study concluded that there is a significant lack of studies dealing with the ACs production environmental risk assessment through bioassays. Furthermore, no studies discuss the LCA for the entire life of ACs. According to Bernardo et al. (2016), there is a lack of information about the environmental performance of the overall chain of bio-waste-derived AC production. Kim et al. (2019) reported the environmental impacts of AC production from wood waste, considering one tonne of wood waste as a functional unit, cradle to grave, and comparing it to the process using coals. This study utilized the boundary expansion method to analyze the wood waste recycling process for AC production. The results showed that the activated carbon system using one tonne of wood waste has an environmental benefit of 163 kg CO_2-eq. for reducing global warming potential compared with the same amount of wood waste disposal by landfilling. Noijuntira & Kittisupakorn (2010) compared AC production using coconut shells as precursor material and AC made from palm-oil shells. The study showed that the AC production

processes using coconut shells as precursor material is higher than that using palm-oil shells in most life cycle impact assessment categories. Additionally, the AC scored specifically higher in the acidification potential and eutrophication categories. (Noijuntira & Kittisupakorn, 2010).

Chapter 5: Methodology

The methodology employed in the proposed BBAC includes the following steps: (1) BBAC preparation; (2) Adsorption experiments; (3) Analysis and characterization; and (4) Life Cycle Assessment.

5.1 BBAC PREPARATION

There are two main processes for preparing AC: (1) Pyrolysis; and (2) Chemical or physical activation. Pyrolysis is a process in which the raw material is carbonized in the absence of oxygen, followed by the activation of the resulting char with a chemical dehydrating substance, such as KOH or CaCl. Chemical activation can be a one or two-step process that involves the impregnation of the biochar with the chemical agent and/or biochar heating after the impregnation process (Crittenden et al., 2012 and Benjamin M., 2015). Pyrolysis and activation processes will be statistically evaluated through a Design of Experiments (DOE) to determine the ideal conditions in the manufacture of BBAC to obtain the best physical properties for the adsorption of arsenic from water.

5.1.1 Feedstock processing

A sufficient quantity of agricultural residues (rice husk and peanut shells) will be washed with deionized water. The materials will be dried in the oven at a low temperature (105°C) or allowed to air dry. Materials will be crushed (~2.5 mm).

5.1.2 Pyrolysis

Rotary calciner prototype, design, and fabrication (pilot-scale 15:1 meters), fuel with LP gas will be used to produce char. An optional process includes using a lab-scale furnace with a retort in an inert atmosphere with nitrogen gas for AC preparation. A sufficient quantity of crushed materials is placed in the calciner under the following DOE parameters: rice husk carbonization

conditions: 600°C-800°C / 1 h and 500°C-600°C/ 3 h and peanut shell carbonization conditions: 600°C-800°C / 1 h and 500°C-600°C/ 3 h.

5.1.3 Activation

After cooling the calciner to room temperature, the carbonized materials (biochar) will be subject to a chemical activation process. Rice husk will be impregnated (ratio 1:3) with KOH and CaCl for 24 hours at room temperature and the peanut shells will be impregnated (ratio 1:3) with KOH and CaCl for 24 hours at room temperature. After that, drain as much of the remaining activating agent from the impregnation container as possible. The biochar should be wet but not saturated.

5.1.4 Heating

Heat the biochar for 2 hours to completely activate it as follow: rice husk and peanut shell at 300-500°C/ 2 h

5.1.5 Cooling and washing

After cooling the AC to room temperature, the activated material will be washed with distilled water.

5.1.6 Drying

The activated material will be oven-dried at 110°C for four hours and cooled at room temperature.

5.1.7 Crushing

The carbon will be ground and sieved to -80+230 mesh size, with an average diameter of 0.096 mm, and stored in a desiccator for further use.

5.2 ADSORPTION EXPERIMENTS

Batch adsorption test on AC: ~2.0 mg of AC will be added to 200 mL with different concentrations of arsenic standard solutions (~0.025, ~0.050, ~0.100, ~0.150, and ~0.250 mg/L). The solution will be mixed using a magnetic stirrer for at least 2 hours at 100 rpm, at room temperature (~25°C). The next step is to allow the solids to settle for 2 hours. Settled solids will be removed using a filtration procedure. A sample of water will be acidified and analyzed in the ICP-OES equipment.

5.3 ANALYSIS AND CHARACTERIZATION METHODS

After completing the preparation and adsorption experiments, the data obtained allow for the following analysis.

5.3.1 Development of Adsorption Isotherms

The amount of arsenic adsorbed onto the ACs at equilibrium will be quantified using Inductively Coupled Plasma Optical Emission Spectroscopy (ICP-OES) equipment. The adsorption isotherms will be developed to know the affinity of the adsorbate (As) for the adsorbent (ACs) at equilibrium and at a constant temperature. Adsorption isotherms will be developed by exposing a known quantity of adsorbate (As) in a fixed volume of liquid and a known dosage of adsorbent (ACs).The removal rate will be measured using the concentration of the element adsorbed and the concentration remaining in the solutions using eq. 1.1.

$$Removal\ \% = -\left(\frac{C_e}{C_i}\right) * 100 + 100 \qquad \text{Eq. 1.1}$$

Where C_i is the initial concentration (mg/L), C_e is the concentration at the final equilibrium (Karnib et al., 2014; Zabihi et al., 2009*)*. The adsorption equilibrium isotherms will be plotted in a graph.

5.3.2 Elemental analysis

An energy-dispersive X-ray spectroscopy (EDS) analysis will be developed to obtain chemical information about the adsorbents. The identification and quantitative determination of the elements present in the samples will be carried out using this characterization method.

5.3.3 Scanning Electron Microscope (SEM)

A SEM analysis of the adsorbents will obtain information about the surface morphology, porous size, and porous distribution. This SEM analysis also includes the shape and size of the particles. With all the information obtained in this stage, the statistical analysis will be completed using Minitab® 18.

5.4 LIFE CYCLE ASSESSMENT METHODOLOGY

Life Cycle Assessment (LCA) methodology is an input-output material and energy-based analysis used to quantify the potential environmental impacts associated with all the life cycle stages of a product, process, or service (Hauschild et al. 2008, and Rosenbaum et al. 2008). There are four main steps in LCA, as suggested in ISO 14040 series:

a) Goal and scope definition (ISO 14041)

b) Life cycle inventory (LCI) (ISO14042)

c) Life cycle impact assessment (LCIA) (ISO 14043)

d) Life cycle assessment interpretation (ISO 14044)

Figure 5.1 show the interaction between the LCA's components.

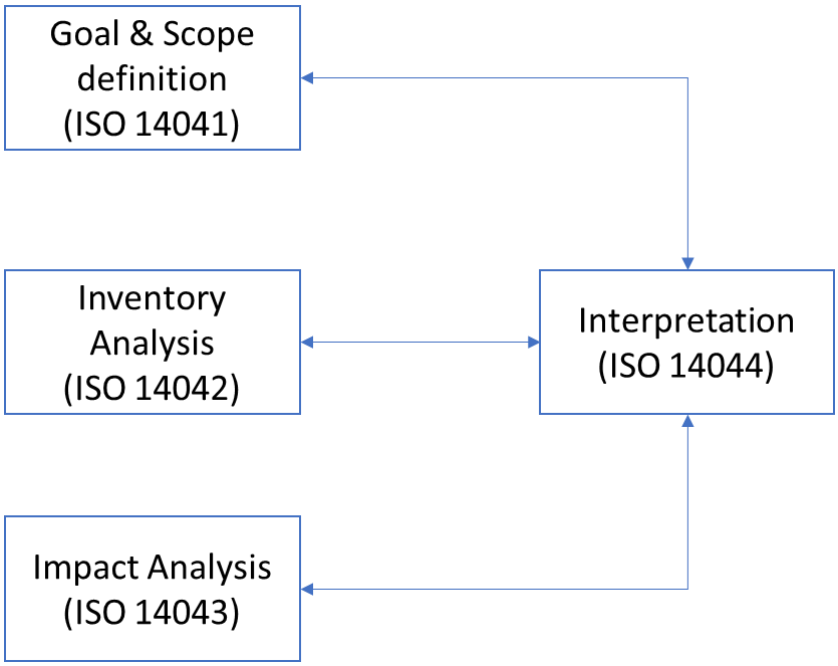

Figure 5.1: Components of LCA.

5.4.1 Goal and scope

This study will evaluate and compare the potential environmental impacts of activated carbons made from hard coal-based materials with activated carbons made from agricultural residues (peanut shell, rice husk). The functional unit is an equivalent performance of a product used as a reference unit in an LCA study. A constant functional value must be selected to make this comparison.

The functional unit used in this study is 1 kg of activated carbon used for water treatment. The LCA's studies conducted will follow ISO 14040/44 guidelines. The GaBi® software will perform the LCAs. Required data to perform these LCA's will be obtained from literature, the software database, data obtained from the experimental process, local agencies' available data, and other available databases.

The system boundaries are defined from cradle-to-grave (Figure 5.2). The stages considered in this system include raw materials acquisition and processing, production, end-of-life, and final disposal.

The BBAC production made from agricultural residues, from raw material acquisition until its disposal, includes ten main unit processes. These can also include subprocesses, depending on the output characteristics required. Figure 5.3 shows each main unit BBAC processes: (1) Raw materials acquisition and transportation; (2) Batch preparation (washing); (3) Crushing; (4) Pyrolysis; (5) Activation; (6) Washing; (7) Drying; (8) Crushing, and (9) Use and End of Life Disposal: landfill. All the inputs and outputs within the system boundaries are associated with the main unit processes.

The CCAC process includes all stages of the cradle-to-grave analysis, from raw materials acquisition to disposal. Figure 5.4 illustrates each central unit CCAC process: (1) Raw material acquisition and transportation; (2) Raw material processing; (3) Crushing; (4) Impregnation; (5) Activation; (6) Washing; (7) Drying; (8) Crushing and packaging; (9) Transportation to retailer store and customer, and (10) Use and end of life disposal: landfill.

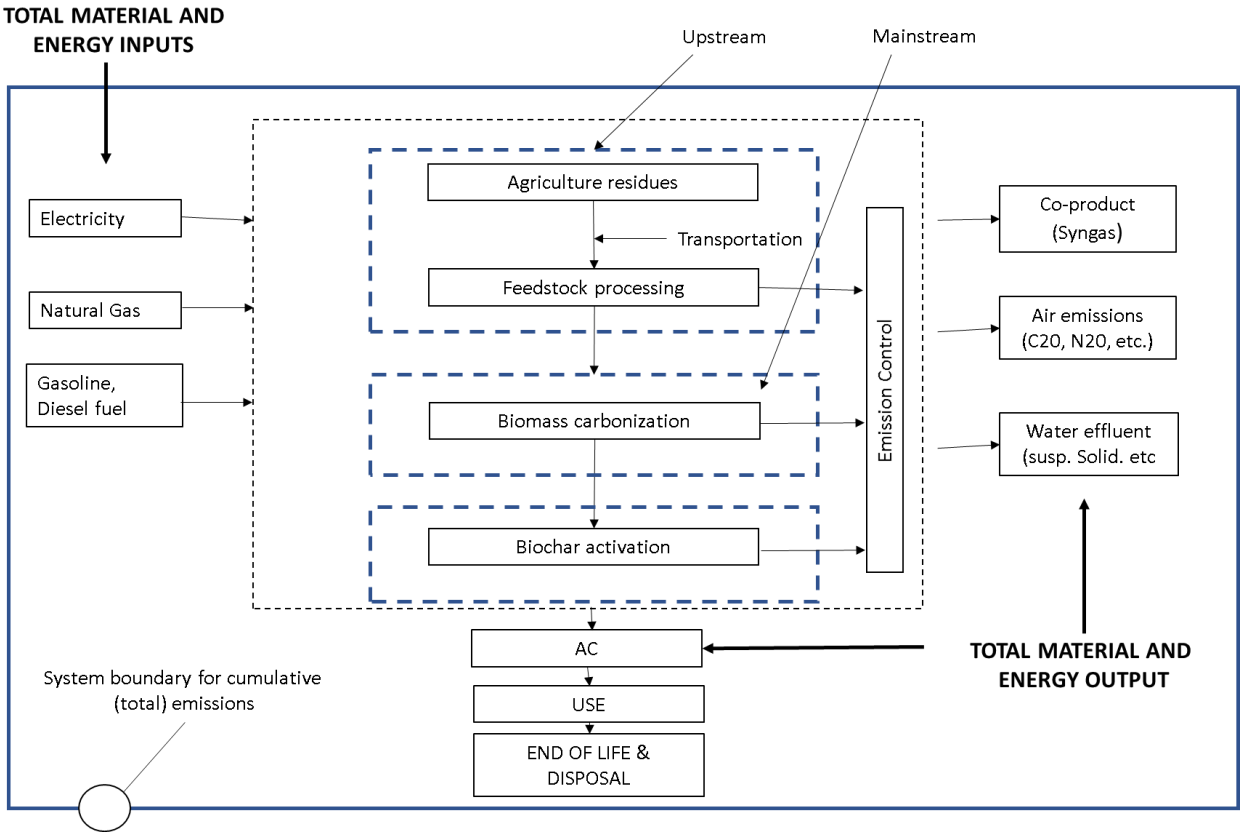

Figure 5.2: BBAC System boundaries. (Gu et al., 2018)

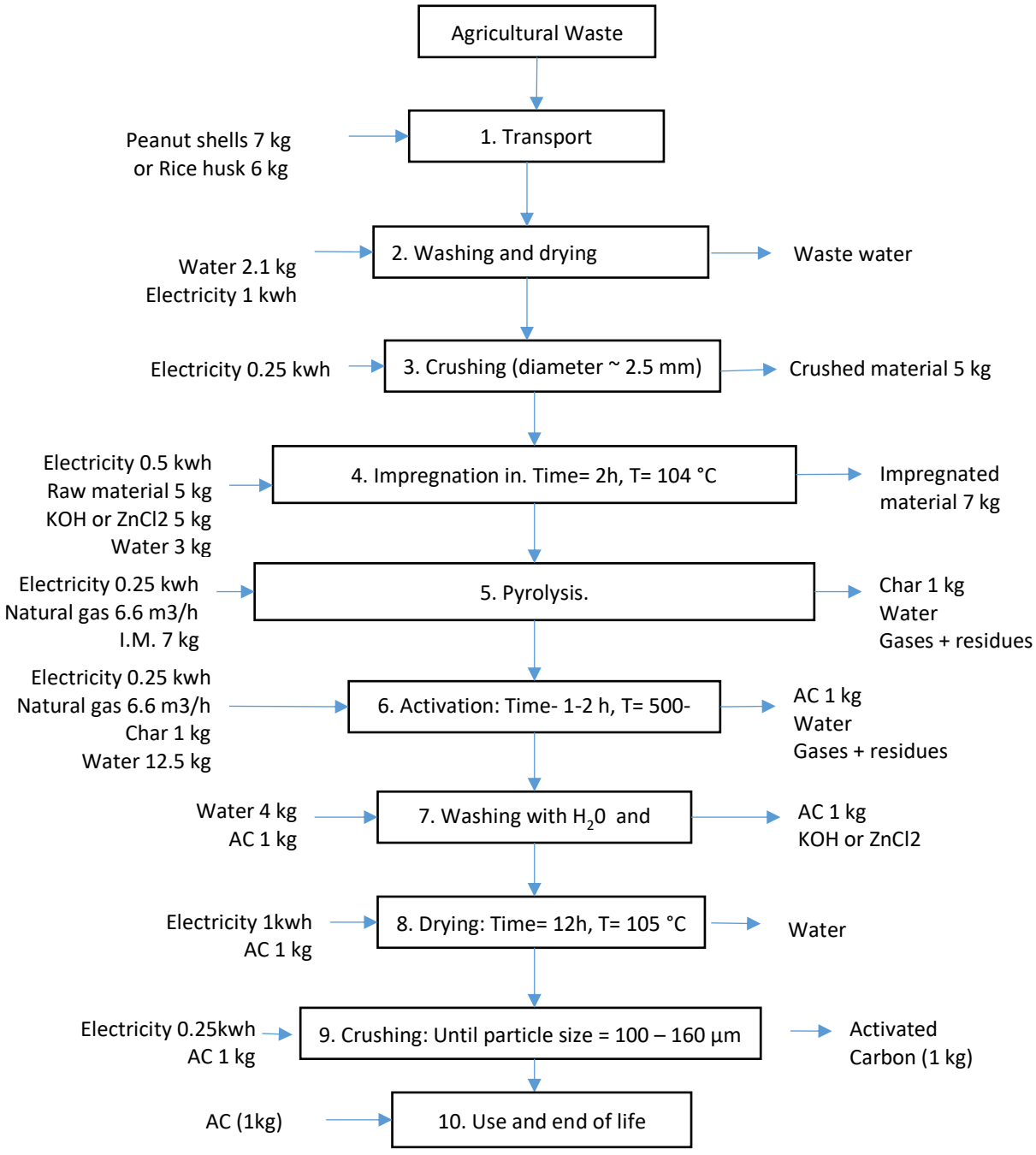

Figure 5.3: BBAC preparation process flow diagram.

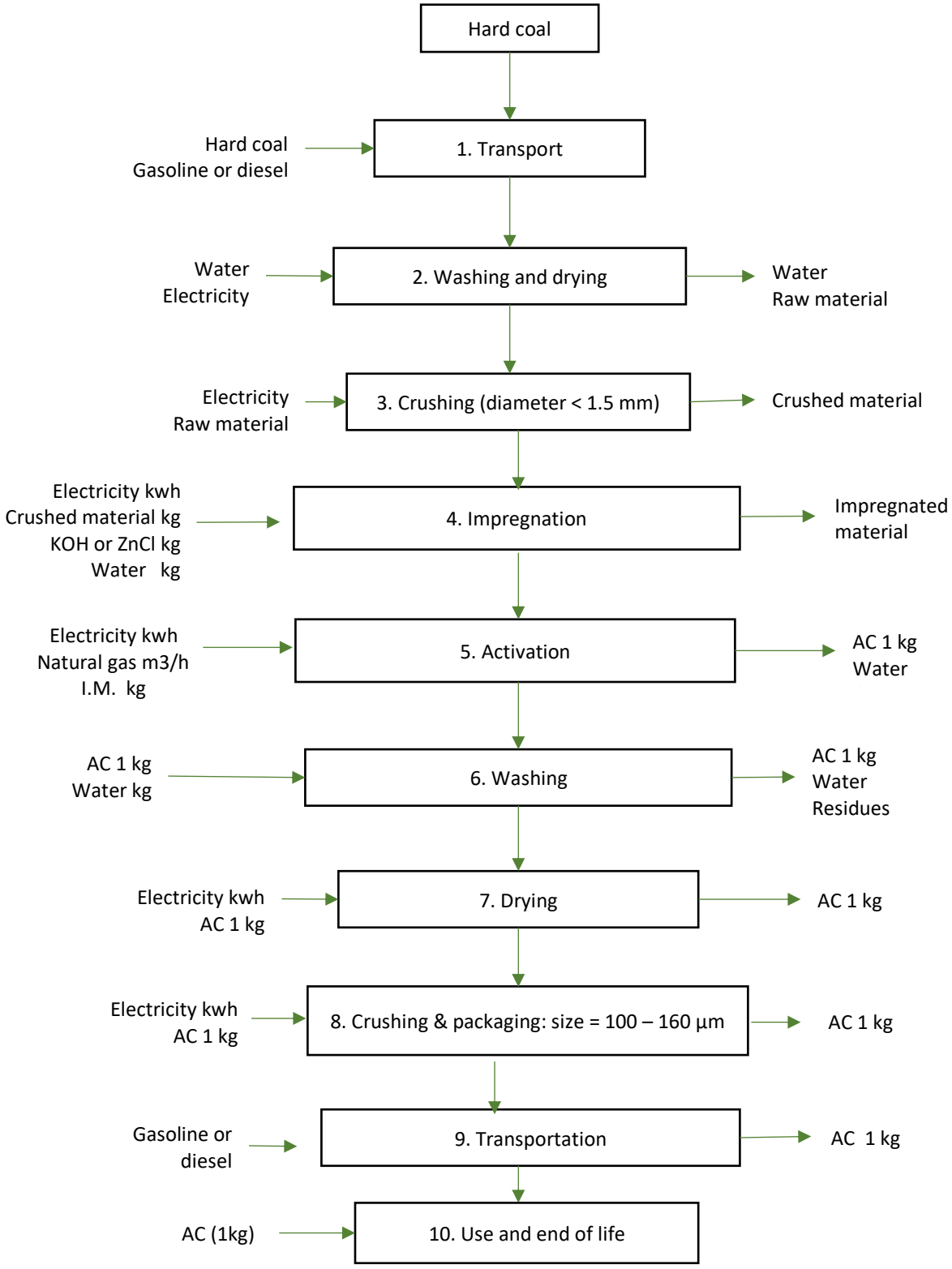

Figure 5.4: CCAC preparation process flow diagram.

5.4.2 Life Cycle Inventory (LCI)

The LCA inventory includes the inputs and outputs values for all the processes within the boundaries (Table 5.1 and 5.2). The input values include materials and energy requirements to produce 1 kg of BAC and 1 kg of CAC. The output values include the products and co-products produced and emissions and wastes. Database from GaBi 6.0, literature, and other sources, will all be employed to perform the BBACs and CCACs LCAs.

The Life Cycle Inventory in this study uses the following parameters: (1) Raw materials and raw material processing facilities are near to the ACs facilities; (2) The use of U.S Electric and natural gas data ; (3) The CCACs LCA assumes a manufacturing facility using a kiln-fired with natural gas; (4) The CCACs LCA assumes that the Best Available Technology (BAT) is used, producing significantly low levels of emissions and wastes; and, (6) Residues and other particulates leaving the system boundaries are not considered.

Table 5.1: The Life Cycle Inventory (LCI) of BBACs production, using a rotary calciner.

Inputs		Process	Outputs
Corn straw, rice husk, or peanut shells		Raw material processing	Crushed materials Batch 6 kg
Corn straw	6 kg.	Washing, Drying &	
Rice husk	6 kg.	Crushing (Batch preparation)	
Peanut shell	6 kg.		
Water	2.10 kg.		
Electricity	1.0 kWh		
Batch	5 kg.	Impregnation	Impregnated material 6 kg
Chemical substance	5 kg		
Water	3 kg		
Mix Batch	6 kg	Pyrolysis	Carbonized material 1 kg.
Natural Gas	6.6 m^3 /h		
Electricity	1.0 kWh		
Carbonized material	1 kg.	Activation	AC 1 kg.
Electricity	1.0 kWh		
Water	12.5 kg		
Natural gas	6.6 m^3 /h		
AC	1 kg.	Washing & Drying	AC 1 kg
Water	4.10 kg		
Electricity	1.0 kWh		
Electricity	0.25 kWh	Crushing & Packaging	AC 1 kg
AC 1 kg (filter)		Use & end of life	Used AC 1 kg.
Used AC	1 kg.	Transportation	Bulk of used product
Diesel (500 km travel distance)			
Used product	1 kg.	Landfill disposal	Used product 1 kg.

Table 5.2: The Life Cycle Inventory (LCI) of CCAC production.

Inputs		Process	Outputs
Coal-based matls.	1.0 kg.	Raw material acquisition, processing & and transportation.	Coal 0.9 kg.
Water Coal	4.0 kg. 0.9 kg	Batch preparation (Wash & dry)	Mix batch 1 kg.
Electricity Mix Batch	0.155 kWh 1 kg.	Crusher	Crushed material
Natural gas Electricity Crushed material	1.1 m^3 /h 1.6 kWh 1 kg.	Activation	AC 1 kg.
Electricity Water Natural gas	1.10 kWh 12.5 kg 1.1 m^3 /h.	Washing, Drying &Crushing	AC 1 kg.
Activated carbon Diesel (500 km travel distance)	1 kg.	Packaging & transportation	AC bulk/pallet.
AC final product (filter)	1 kg	Use	Used product 1 kg.
Used product	1 kg.	End-of-life & landfill disposal	Used product 1 kg

Table 5.3: The Life Cycle Inventory (LCI) and Cost analysis of AC production.

Inputs	Process	Outputs	CCAC Cost	BBAC Cost
Rice husk **Peanut shell** **Hard coal**	Raw material processing	Raw materials	 49USD/TON	28.18USD/TON 20.45USD/TON
Diesel Lt (0.85USD.) **A Rice husk 900km** **Peanut shell 150 km** **Hard coal 1500 km**	Transportation		 427.71 USD	 256.6 USD 42.77 USD
Raw material 6-7 kg. **Water 2.10 Kg.** **Electricity 1 kWh** **Electricity 25 KWh**	Washing, Drying & Crushing (Manually) Hard coal crushing	Batch 6-7 kg	 0.826 USD	9.5×10^{-5} USD 0.033 USD
Mix Batch 6-7 kg **Natural Gas 6.6 m^3 /h** **Electricity 1.0 kWh**	Pyrolysis	Carbonized material 1 kg.	N/A N/A	1.82 USD 0.033 USD
Biochar 1 kg. **Electricity 1 kWh** **Water 12.5 kg** **Natural gas 6.6 m^3 /h**	Activation (steam in CCAC)	AC 1 kg.	0.033 USD 5.4×10^{-4} USD 1.82 USD	0.033 USD 5.4×10^{-4} USD 1.82 USD
AC 1 kg. **Water 4.10 kg** **Electricity BBAC 1 kWh** **Electricity CCAC 25 KWh**	Washing & drying	AC 1 kg	1.8×10^{-4} USD 0.826 USD 0.826 USD	1.8×10^{-4} USD 0.033 USD N/A
Electricity 25 kWh	Crushing (manually in BBAC) & Packaging	AC 1 kg		
AC 1 kg **BBAC (Rice husk)** **BBAC (Peanut shell)** **Hard coal (store price)**	Use & end of life	Used AC 1 kg.	 **16.29 USD**	 **4.0976 USD** **3.8356 USD**
Used AC 1 kg.	Landfill disposal	Used product		

5.4.3 Life Cycle Impact Assessment (LCIA)

The impact assessment establishes a relationship between the product/process or service and its potential impacts on the environment. The LCI results and the potential environmental impacts are associated using the mid-point and end-point approaches (Figure 5.5). The LCIA mid-point is a problem-oriented approach in the middle pathway in each impact category, between the LCI results and the end-point (Jolliet et al., 2014 & Sharaai et al., 2010*).*

The end-point LCIA is a damage-oriented approach located at the end of the impact pathway. The end-point considers human health, natural environmental quality, and man-made environment (Sharaai et al., 2010*).* Bare et al. (2008) state that the end-point impact category is less comprehensive and implies a higher uncertainty level than the mid-point impact category.

Figure 5.5: Impact pathway connecting the emission to several categories (Sharaai et al., 2010)

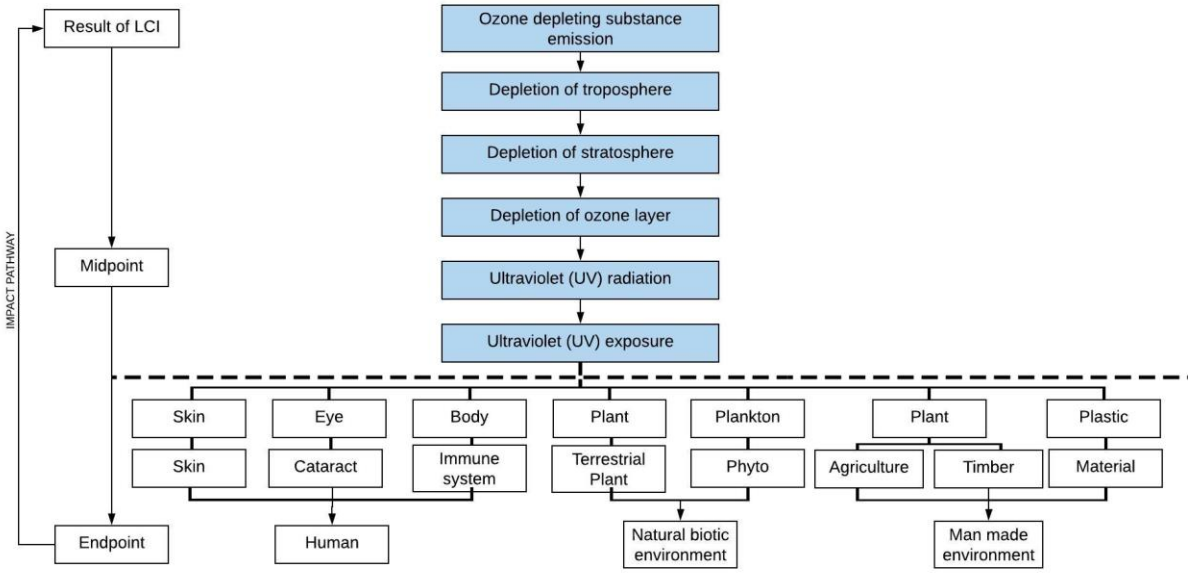

The EPA developed TRACI, which uses the mid-point approach (Jolliet et al., 2014). This tool facilitates the characterization of the environmental stressor, which can result in potential environmental impact categories, such as global warming, eutrophication, ozone depletion, eco-

toxicity, human health criteria-related effects, and fossil fuel depletion (Sharaai et al., 2010). The categories considered in this study are as follows:

5.4.3.1 Acidification potential

Acidic gases such as Sulphur dioxide (SO_2) react with water in the atmosphere to form "acid rain", also known as acid deposition. When acid rain falls, it causes ecosystem impairment on varying levels. Gases that cause acid deposition include ammonia (NH_3), nitrogen oxides (NOx), and Sulphur oxides (SOx). Acidification potential is expressed in kg SO_2 equivalent. The model does not consider regional differences regarding which areas are more or less susceptible to acidification. It accounts only for acidification caused by SO_2 and NOx. This includes acidification due to fertilizer use, according to the method developed by the Intergovernmental Panel on Climate Change (IPCC) (Acero et al., 2015).

5.4.3.2 Climate change/Global warming potential

Climate change or Global Warming Potential (GWP) is the change in global temperature caused by the greenhouse effect (Acero et al., 2015). The Greenhouse Effect involves the release of greenhouse gases (GHG) created by anthropogenic activity. In recent scientific consensus, these increases in GHG emissions are having a noticeable effect on climate. The continuously increasing average global temperature is expected to cause climatic disturbance, desertification, rising sea levels, and the spread of disease. The environmental profiles characterization model is based on factors developed by the UN's IPCC. GWP can be quantified in different time horizons; the most common is 100 years (GWP100). Its measured reference unit is in kg CO_2 equivalent (Acero et al., 2015).

5.4.3.3 Deletion of abiotic resources

Depletion of abiotic resources considers different sub-impacts categories. This impact category generally refers to the consumption of non-biological resources, such as fossil fuels, minerals, metals, and water. The value of the abiotic resource consumption of a substance (e.g., lignite or coal) is a measure of the scarcity of a substance. This measurement depends on the amount of the resources and their extraction rate. Some models measure the number of depleted resources in antimony equivalents (kg Sb equivalents), water consumption (m^3), mineral depletion (kg), and fossil fuels (MJ) (Acero et al., 2015).

5.4.3.4 Eutrophication potential

Eutrophication is the build-up of a concentration of chemical nutrients in a water ecosystem, which leads to abnormal productivity. This abnormal productivity causes excessive plant growth, like algae in rivers, leading to severe reductions in water quality and animal populations. Emissions of ammonia, nitrates, nitrogen oxides, and phosphorous all have an impact on eutrophication. This category is based on the work of Heijungs & Guinee (1993) and is expressed in kg PO_4 equivalents. Direct and indirect impacts of fertilizers are included in the method. Direct impacts come from fertilizers used, and indirect impacts are measured using the IPCC method (Acero et al., 2015).

5.4.3.5 Ozone layer depletion (Stratospheric ozone depletion)

Ozone-depleting gases cause damage to the ozone layer. There is not enough information about the combined effects of different gases in the stratosphere. All chlorinated and brominated compounds which reach the stratosphere can impact the ozone layer. Major causes of ozone depletion are attributed to Chlorofluorocarbons (CFCs), halons, and hydrochlorofluorocarbons (HCFCs) (Acero et al., 2015). Damage to the ozone layer increases the amount of carcinogenic

UVB light that reaches the earth's surface. The World Meteorological Organization (WMO) states that the reference substance is chlorofluorocarbon-11 (CFC-11), expressed in kg CFC-11 equivalent (Acero et al., 2015*).* The results of the Life Cycle Impact Assessment (LCIA) of CAC from a cradle-to-grave approach (Figure 5.6) at the midpoint impact categories (TRACI) obtained from the modeling analysis are provided in Figure 5.7 and will be used for comparative purposes.

5.4.3.6 Ecotoxicity

This category examines the potential adverse effects of chemical outputs on abiotic ecosystems or non-living organisms. Impact scores are based on the identity and amount of toxic chemicals as outputs to air. Impact characterization factors use chronic toxicity hazard values based on the same non-cancer chronic data used for human health. The USEtox model is the basis for the human health cancer, non-cancer, and eco-toxicity categories (http://nepis.epa.gov/Adobe/PDF/P100HN53.pdf).

5.4.3.7 Human health particulate

Particulate matter (PM) is a group of minuscule particles in ambient air that can potentially cause adverse human health effects, including respiratory illness and death (Humbert 2009; US Environmental Protection Agency 2008n). Common sources of particulate matter are combustion from different materials and dust particles. These sources are the most common precursors to sulfur dioxide (SO2) and nitrogen oxide (NOx) particulates (US Environmental Protection Agency 2008n). The human health impacts calculation method includes modeling fate and exposure into intake fractions. These intake fractions are a function of the amount of the emitted substance into the air and the rate at which the population is exposed. Emitted substances were measured using PM2.5 as the reference unit (Humbert 2009; US Environmental Protection Agency 2008n).

5.4.3.8 Human health cancer and non-cancer

This category examines the potential adverse effects of chemical substances on human health. Impact characterization factors are based on chronic and acute toxicity hazard values using the toxicity potentials for over 3000 substances (Hauschild et al. 2008, Rosenbaum et al. 2008). The USEtox model adopted many of the best features of several models developed previously (Hauschild et al. 2008, Rosenbaum et al. 2008). These categories and eco-toxicity are measured in characterization factors: CTUh and CTUe.

5.4.3.9 Smog formation

Smog is created when nitrogen oxides (NOx) and volatile organic compounds (VOCs) chemically react. Adverse human health effects can result in different respiratory illnesses and negative ecological impacts, including damage to various ecosystems and crop damage due to ozone. The main contributors to smog formation are exhaust from motor vehicles, electric power generating facilities, and industrial facilities (Hauschild et al. 2008, Rosenbaum et al. 2008, US Environmental Protection Agency 2008e). This category is measured in kg of ozone equivalent.

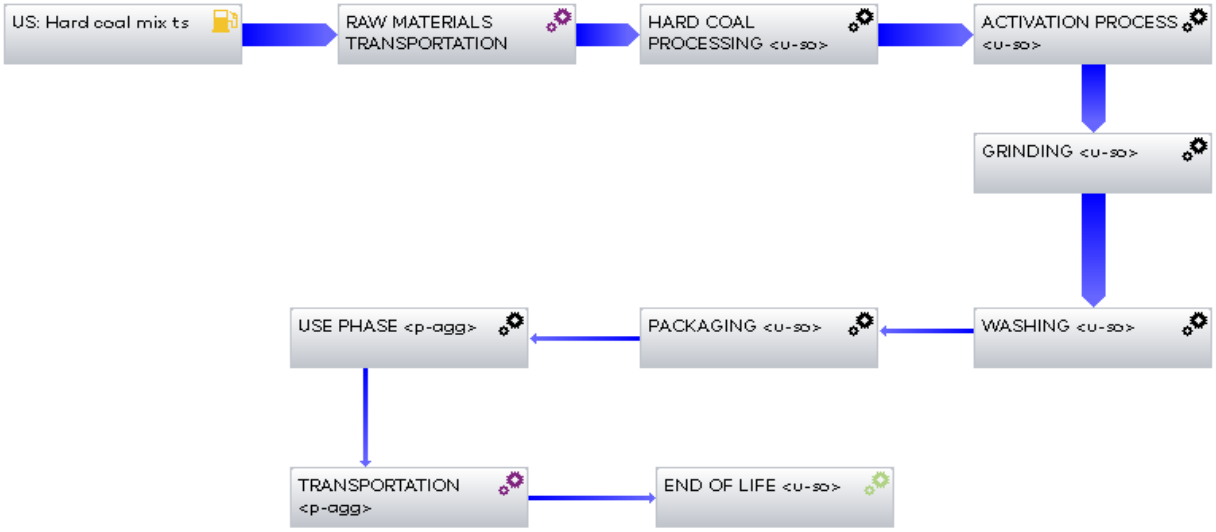

Figure 5.6: Example of process simulation using GaBi® software for commercial activated carbon life cycle from a cradle-to-grave approach.

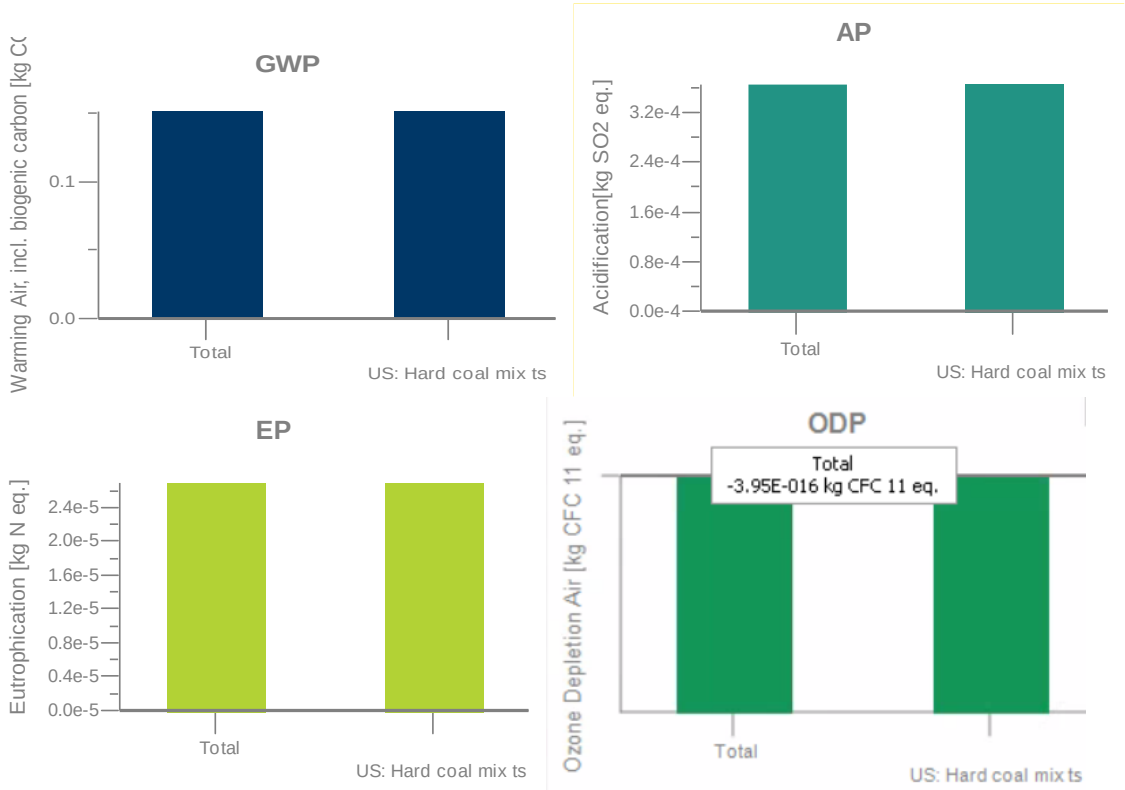

Figure 5.7: Example of Life Cycle Impact Analysis ((LCIA) of product (TRACI standard categories using GaBi® software)

Chapter 6: Results and Comparative Analysis

The results obtained from different analysis and tests are listed below. Using all the information, comparative analysis was performed and is discussed in greater detail below.

6.1 ACTIVATED CARBONS CHARACTERIZATIONS (SEM and EDS ANALYSIS)

Once the physical, chemical and structural characteristics of ACs are known through the Scanning Electron Microscope (SEM) and energy-dispersive X-ray spectroscopy analysis (EDS), their nature can be established. For the SEM/EDS analysis, a small amount of BBAC was placed on carbon tape, as shown in Illustration 6.1. The high-resolution images obtained from the surface area of the samples, the different experiments, and the respective repetitions can be compared with each other and against the CCAC. The samples are labeled and analyzed according to the arrangement of the DOE matrix.

Illustration 6.1: Images of AC and carbon tape needed to place the sample under the SEM/EDS.

Below is the DOE matrix, Table 6.1, used to prepare the samples and run the experiments. This matrix identifies the sample number and associated iterations.

Table 6.1: Design of experiments matrix

Design of experiments full factorial 2^3 (3 factors at two levels)			
	Factor 1: Precursor material	**Factor 2: CarbonizationTemp.**	**Factor 3: Activation agent**
Levels	**(A.Peanut shell/B.rice husk)**	**(A.High=600-800°C/ B.Low=500-600°C)**	**(A.KOH/B.CaCl)**
Sample #			
1	Peanut shell	High	KOH
2	Peanut shell	Low	KOH
3	Peanut shell	High	CaCl
4	Peanut shell	Low	CaCl
5	Rice husk	High	KOH
6	Rice husk	Low	KOH
7	Rice husk	High	CaCl
8	Rice husk	Low	CaCl
9	Peanut shell 2	High	KOH
10	Peanut shell 2	Low	KOH
11	Peanut shell 2	High	CaCl
12	Peanut shell 2	Low	CaCl
13	Rice husk 2	High	KOH
14	Rice husk 2	Low	KOH
15	Rice husk 2	High	CaCl
16	Rice husk 2	Low	CaCl
17	Peanut shell 3	High	KOH
18	Peanut shell 3	Low	KOH
19	Peanut shell 3	High	CaCl
20	Peanut shell 3	Low	CaCl
21	Rice husk 3	High	KOH
22	Rice husk 3	Low	KOH
23	Rice husk 3	High	CaCl
24	Rice husk 3	Low	CaCl

6.1.1 Sample 1, 9 and 17

Precursor material: peanut shell

Carbonization temperature and time: 600-800°C/ 1H

Activation method and agent, temperature, and time: chemical activation/KOH at 300-500°C/3 H

SEM Observations:

The mean particle size is in an approximate range of 3µm to 500µm; therefore, considered a granular activated carbon (GAC) (above180 µm is considered GAC) because a higher percentage of the particles in the sample are in the GAC range size. The surface area is very irregular and has a high pore volume with characteristics observed at 500, 100, 50, and 20 µm magnification.

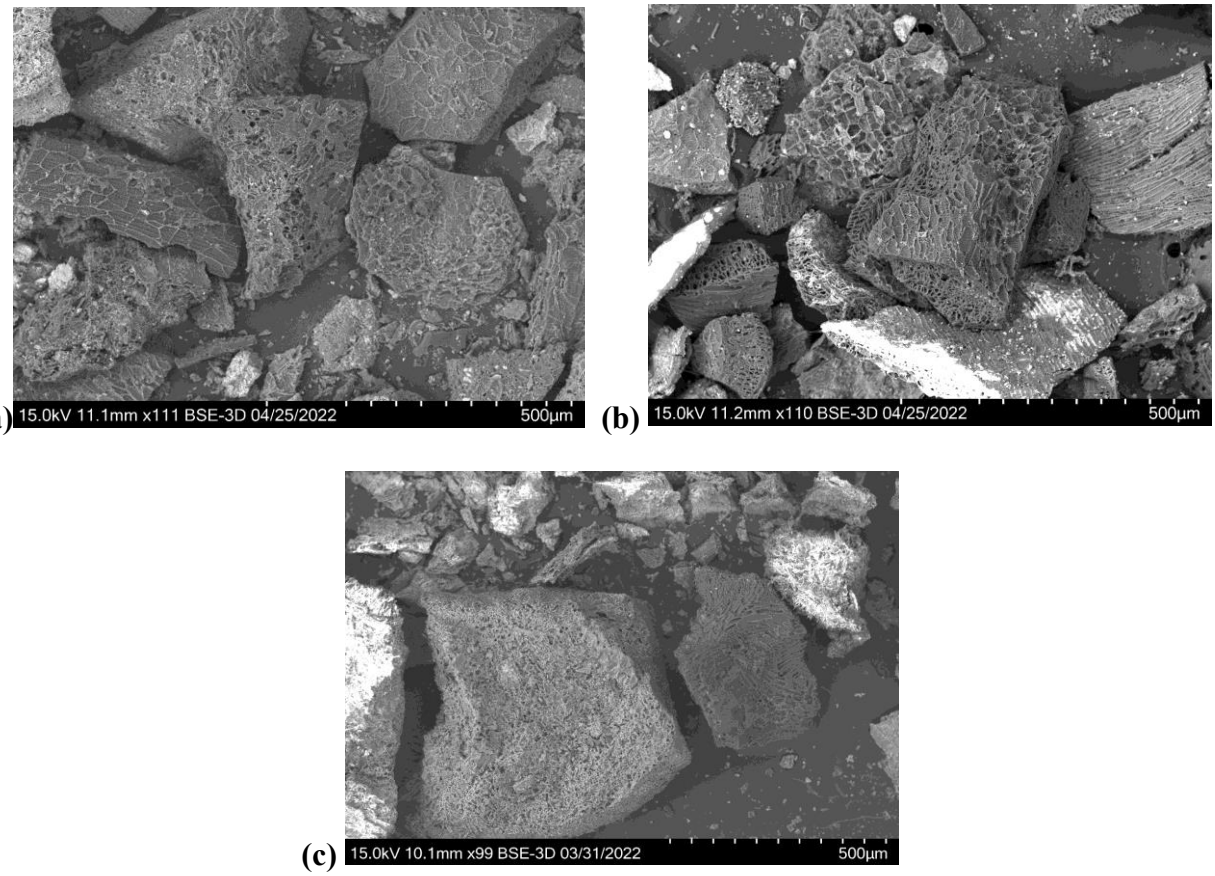

Figure 6.1.1.1 SEM images of samples 1, 9, and 17 (particle size, shape, and surface area)

(a) SEM image of sample 1. (b) SEM image of sample 9 (repetition of experiment 1. (c) SEM image of sample 17 (repetition of experiment 1). These SEM micrographs for peanut shell-based activated carbon show particle size and a high proportion of porous in the surface area. The scale lines are the interval of the white marks; this micrograph is 500µm.

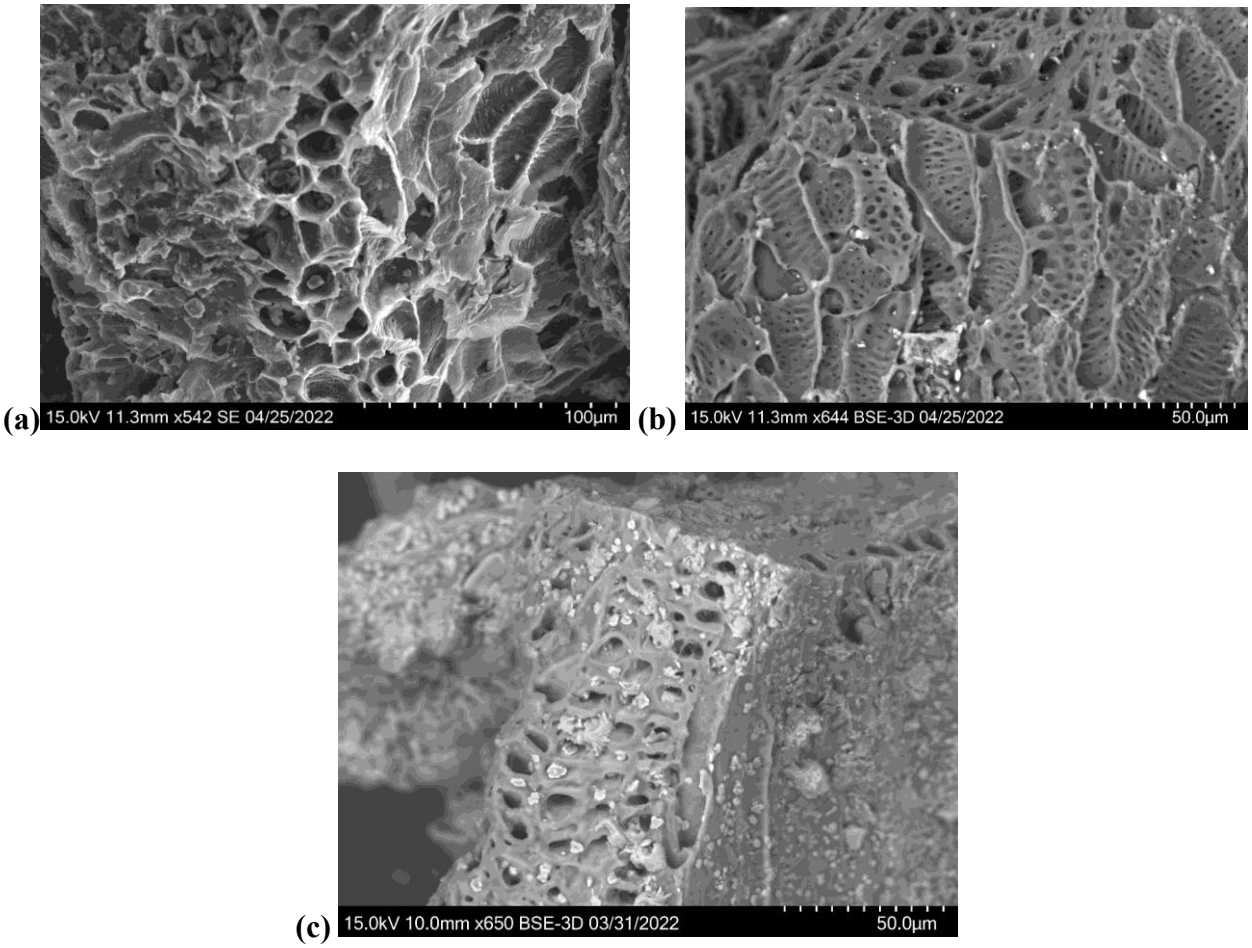

Figure 6.1.1.2: SEM images of samples 1, 9, and 17 (porosity).

(a) SEM image of sample 1 at 100µm of magnification. (b) SEM image of sample 9 (repetition of experiment 1) at 50µm of magnification. (c) SEM image of sample 17 (repetition of experiment 1) at 50µm of magnification. SEM micrographs for peanut shell-based activated carbon showing macropores and mesopores in the samples. The scale lines are the interval of the white marks.

(a) 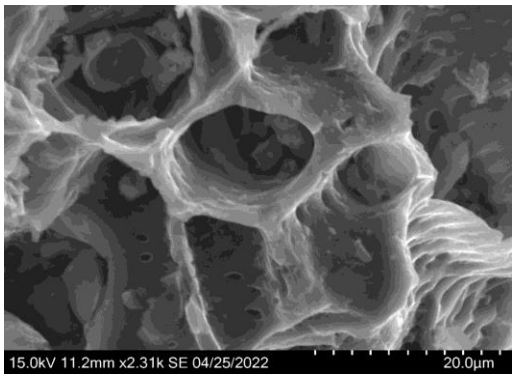

(b) 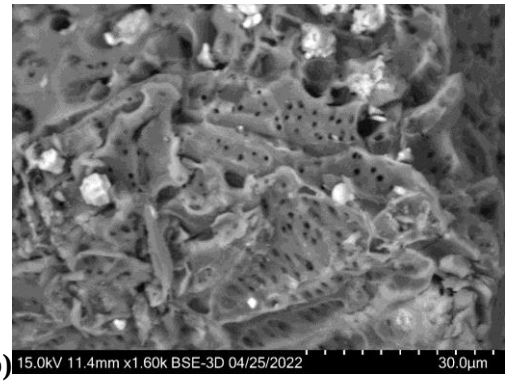

Figure 6.1.1.3: SEM images of samples 1, 9, and 17 (pores size).

(a) SEM micrograph of sample 1 at 20µm of magnification. (b) SEM micrograph of sample 9 (repetition of experiment 1) at 30µm of magnification. The mean pore size in both images is larger than 50nm; some pores are between 2 and 20µm, and some smaller pores are between 500nm and 1µm inside the larger pores. According to IUPAC standards, most of the pores are in the range size of macropores and mesopores.

Elemental analysis (EDS)

The energy-dispersive X-ray spectroscopy was used for the elemental analysis or chemical characterization of the BBACs samples. The chemical elements present in the sample and relative abundance (measured as a percentage in the sample) are as follows: (a) 48.9% carbon, 17.9% oxygen, 26.8% potassium, and 6.4% calcium. The presence of calcium is considered contamination due to the potassium hydroxide used as an activating agent.
(b) 86.2% carbon, 12.2% oxygen, and 1.5% potassium. (c) 47.7% carbon, 33.9% oxygen, 17.3% potassium, and 1.1% silicon. The 1.1% silicon is due to the raw material's small rocks and is considered a contaminant.

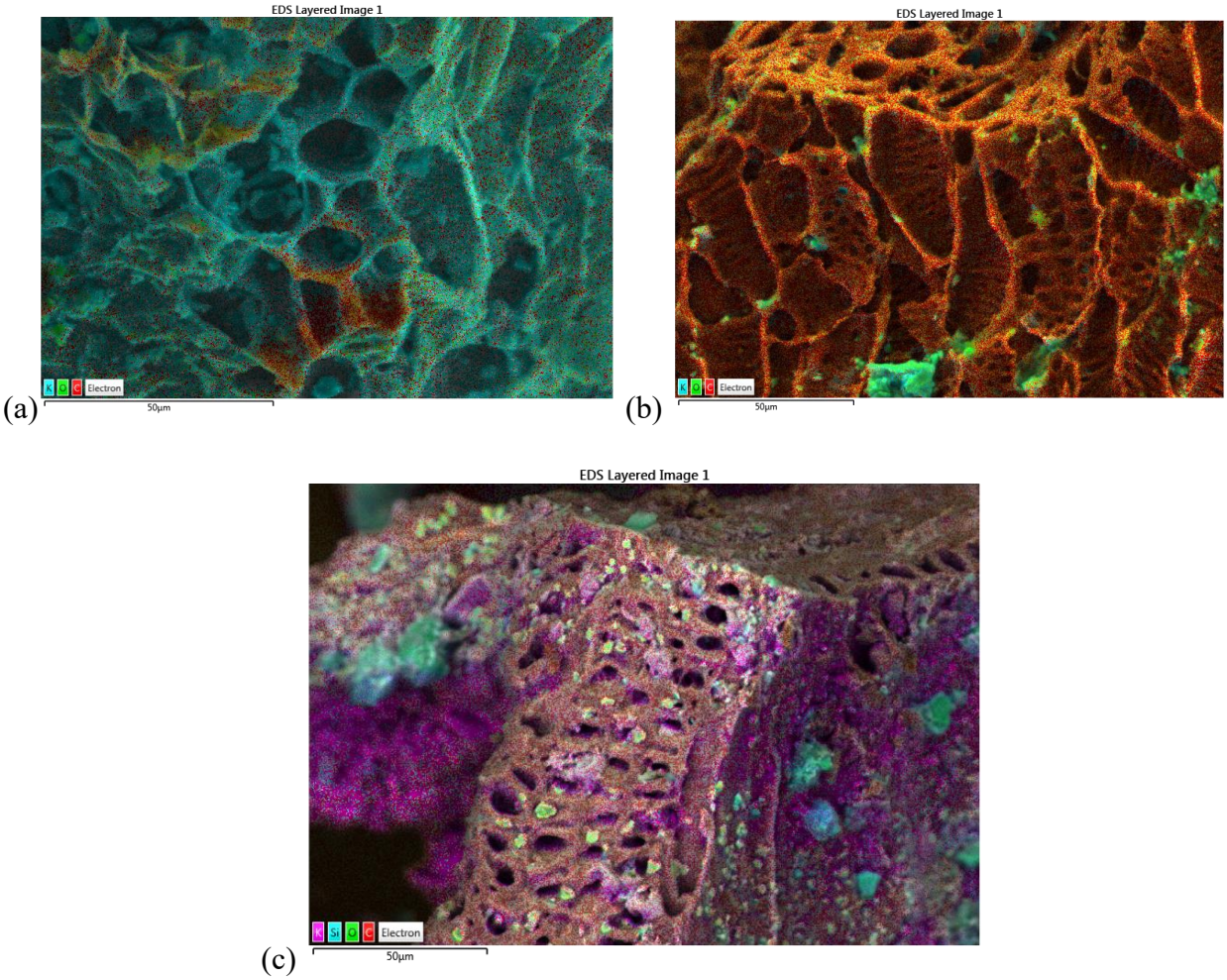

Figure 6.1.1.4: Elemental analysis (EDS) of samples 1, 9 and 17

Elemental analysis (EDS) images show chemical elements in the sample in different colors. (a) sample 1, (b) sample 9, and (c) sample 17. The images show carbon with small particles on the surface of the activating agent potassium hydroxide.

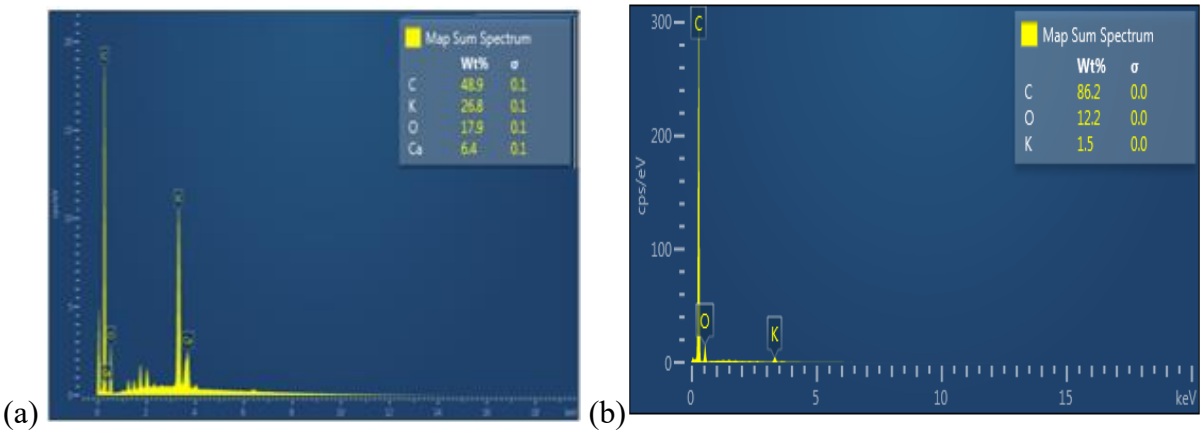

(c) 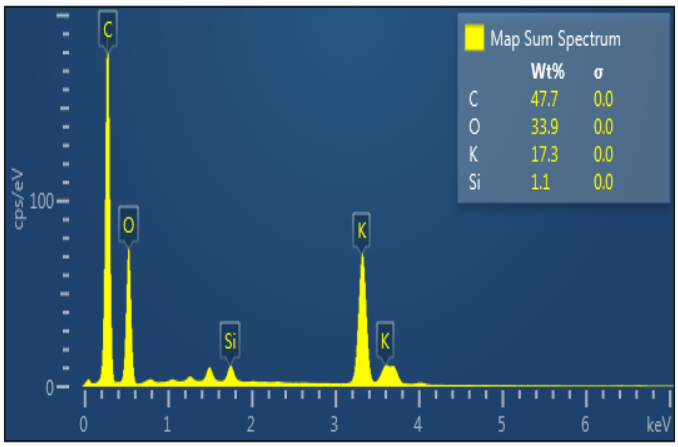

Figure 6.1.1.5: EDS graphs showing weight percentage of samples 1, 9 and 17

(a) sample 1, (b) sample 9, and (c) sample 17. EDS graphs show the weight percentage of the chemical elements found in samples 1, 9, and 17.

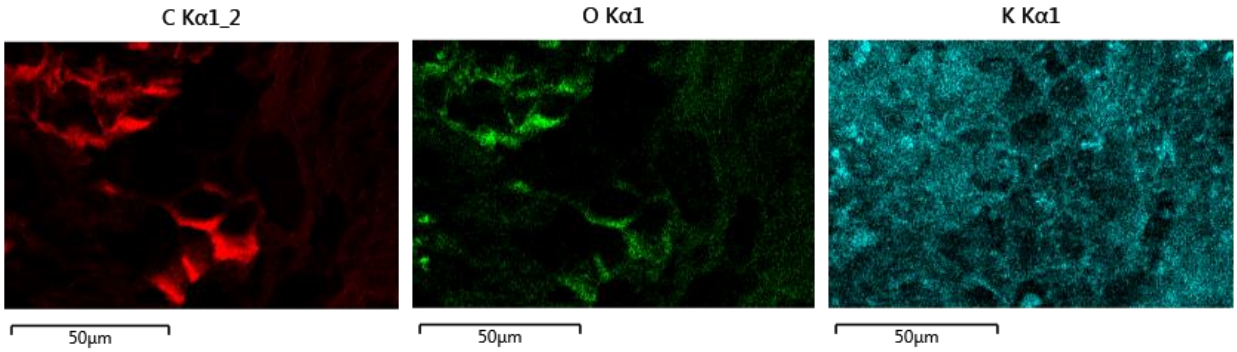

Sample 1.

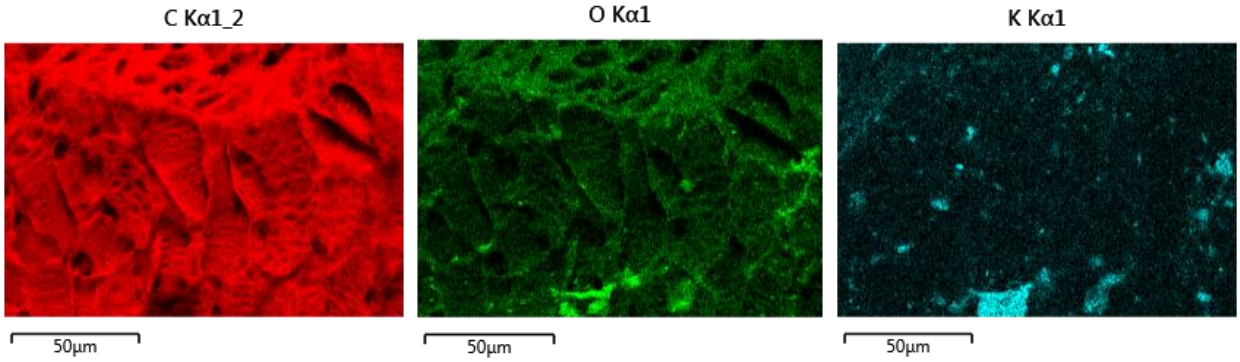

Sample 9.

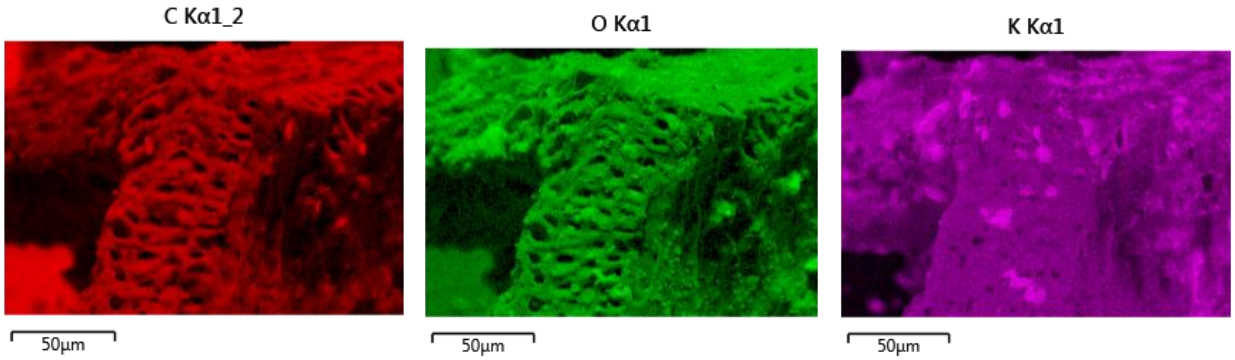

Sample 17

Figure 6.1.1.6: EDS images showing elements present in samples 1, 9 and 17

EDS images show the distribution of chemical elements in the sample. Carbon in red, oxygen in green, and potassium in blue in samples (a) and (b), and purple in sample (c).

6.1.2 Sample 2, 10, and 18

Precursor material: peanut shell

Carbonization temperature and time: 500-600°C/ 3H

Activation method and agent, temperature, and time: chemical activation/KOH, 300-500°C/2 H

SEM Observations:

The mean particle size is in an approximate range of 3µm to 500µm; therefore, considered a GAC because a higher percentage of the particles in the sample are in the GAC range size. The surface area is very irregular and has a high pore volume with characteristics observed at 500 and 200 µm magnification.

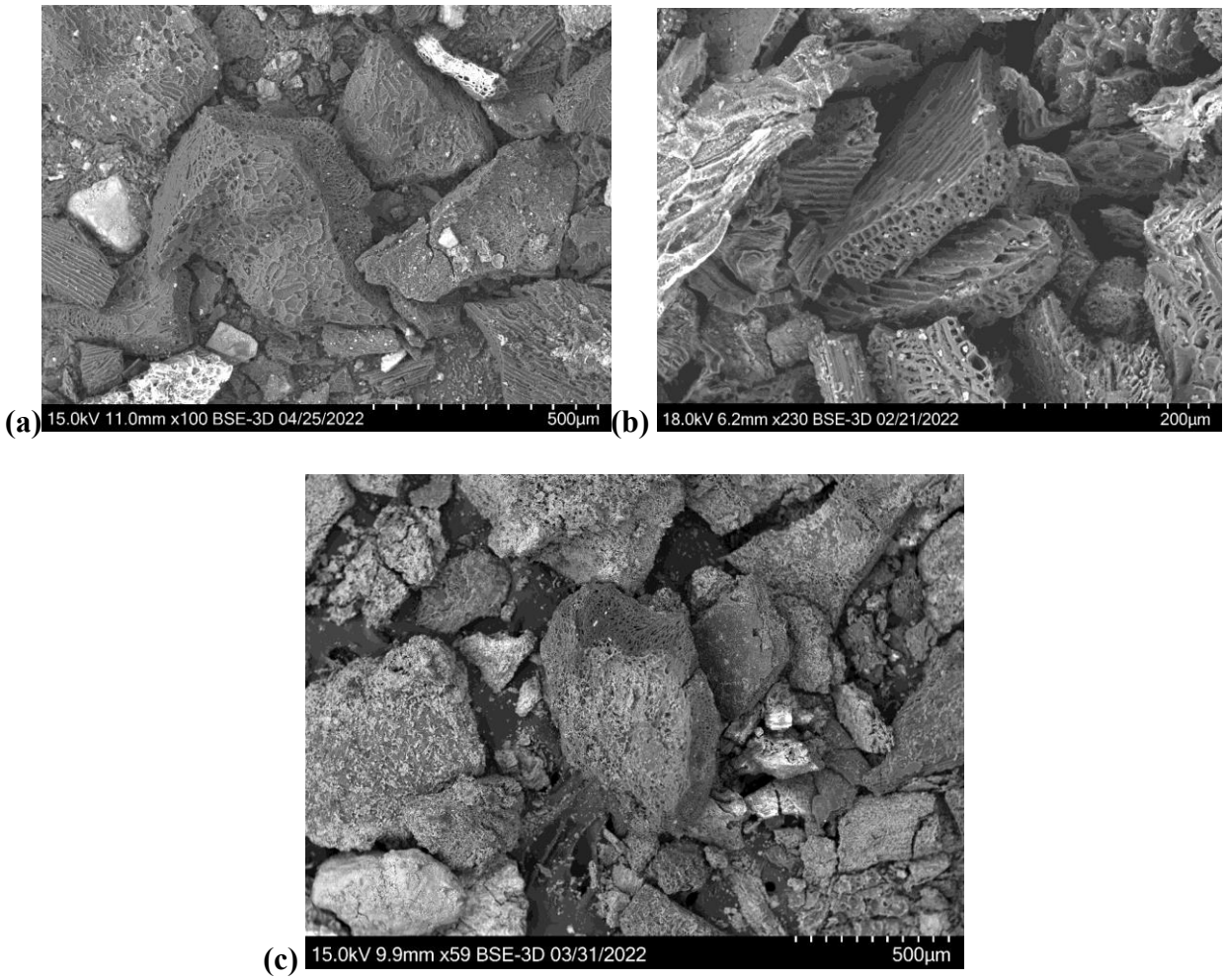

Figure 6.1.2.1: SEM images of samples 2, 10, and 18 (particle size and shape)

(a) SEM image of sample 2. (b) SEM image of sample 10 (repetition of experiment 2. (c) SEM image of sample 18 (repetition of experiment 2). These SEM micrographs for peanut shell-based activated carbon show particle size and a high proportion of porous in the surface area. The scale lines are the interval of the white marks.

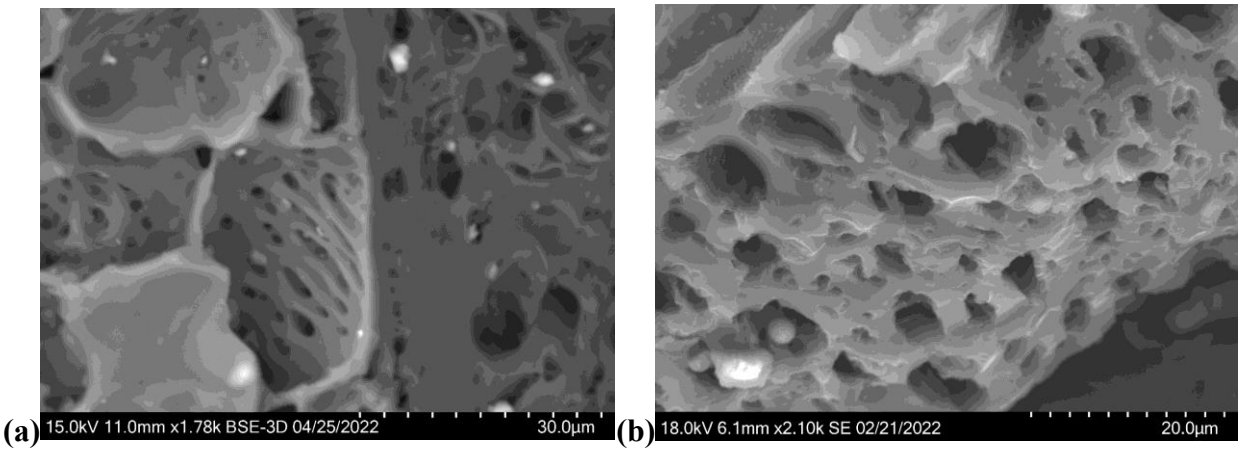

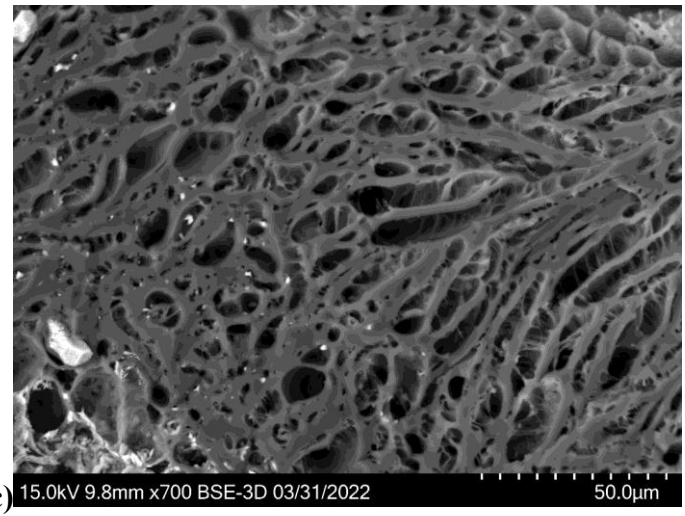

(c)

Figure 6.1.2.2: SEM images of samples 2, 10, and 18 (surface area and porosity)

SEM for peanut shell-based activated carbon samples show an area with a high amount of macropores and mesopores. (a) SEM image of sample 2. (b) SEM image of sample 10 (repetition of experiment 2. (c) SEM image of sample 18 (repetition of experiment 2). The scale lines are the interval of the white marks. According to IUPAC (International Union of Pure and Applied Chemistry), some smaller pores are visible; therefore, most are in the range size of macropores and mesopores.

Elemental analysis (EDS)

The energy-dispersive X-ray spectroscopy was used for the elemental analysis or chemical characterization of the BBAC sample. The chemical elements present in the sample and relative abundance (measured as a percentage in the sample) are as follows: (a) sample 2 with 85.0% carbon, 12.9% oxygen, and 1.2% potassium, (b) sample 10 with 70.6% carbon, 19.6% oxygen, and 9.9% potassium, and (c) sample 18 with 75.4% carbon, 20.1% oxygen, and 4.5% potassium. Other elements present are considered contamination.

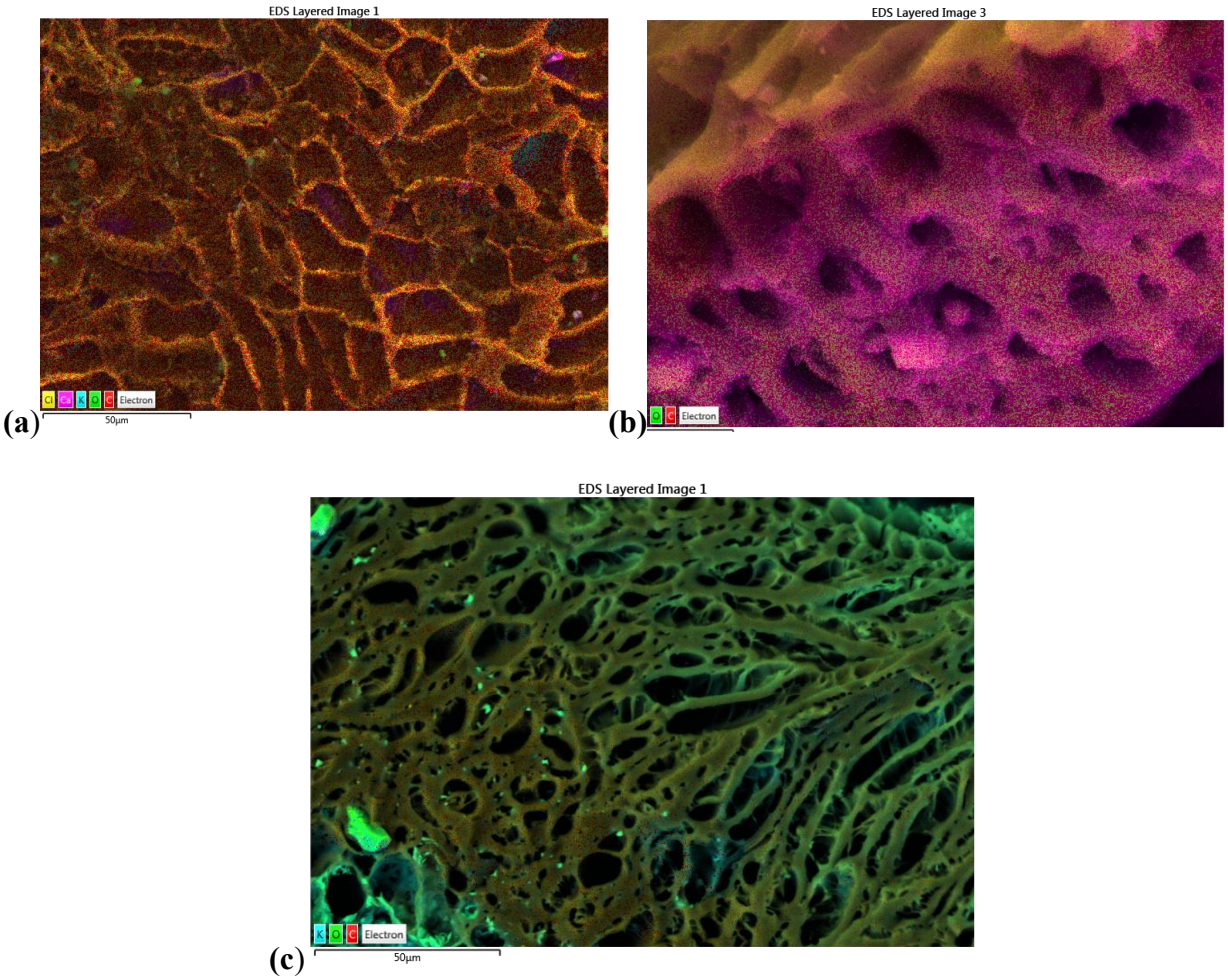

Figure 6.1.2.3: Elemental analysis (EDS) of samples 2, 10 and 18

EDS image shows chemical elements present in the sample in different colors**.** (a) EDS image of sample 2. (b) EDS image of sample 10 (repetition of experiment 2. (c) EDS image of sample 18 (repetition of experiment 2).

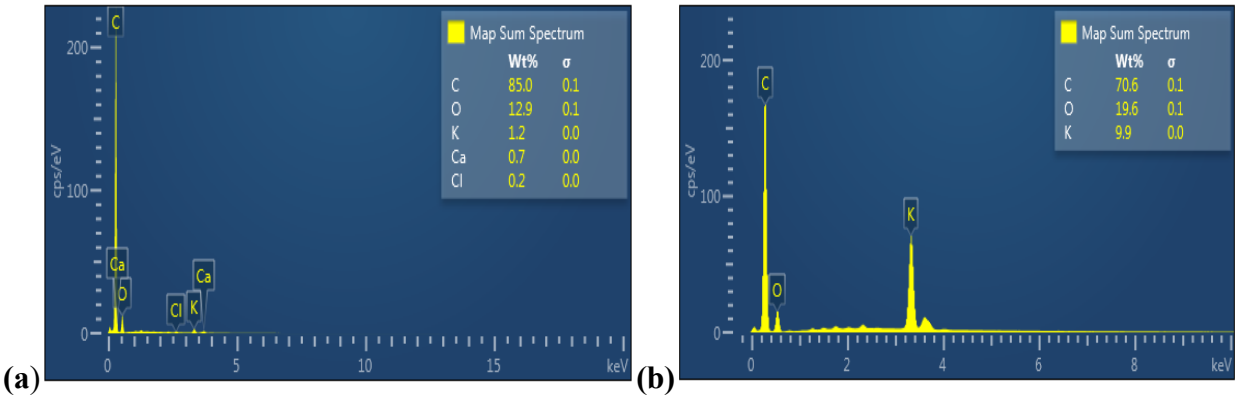

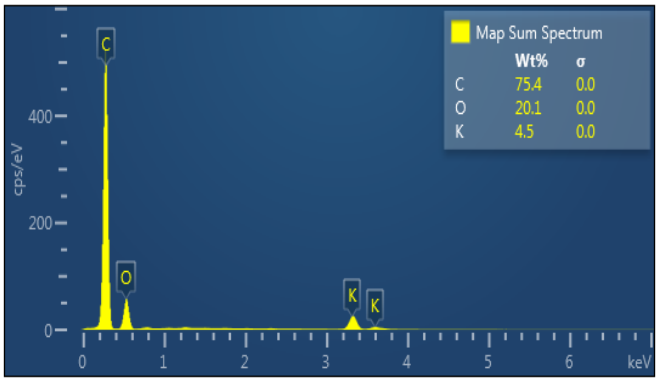

(c)

Figure 6.1.2.4: EDS graphs showing the weight percentage of samples 2, 10 and 18

EDS graphs show the weight percentage of the chemical elements found in the sample**.** (a) EDS graph of sample 2. (b) EDS graph of sample 10. (c) EDS graph of sample 18.

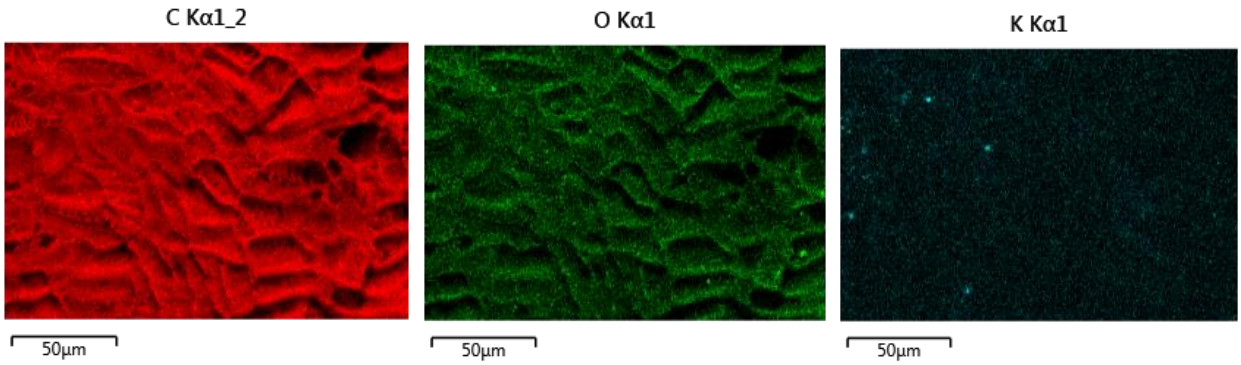

(a) sample 2

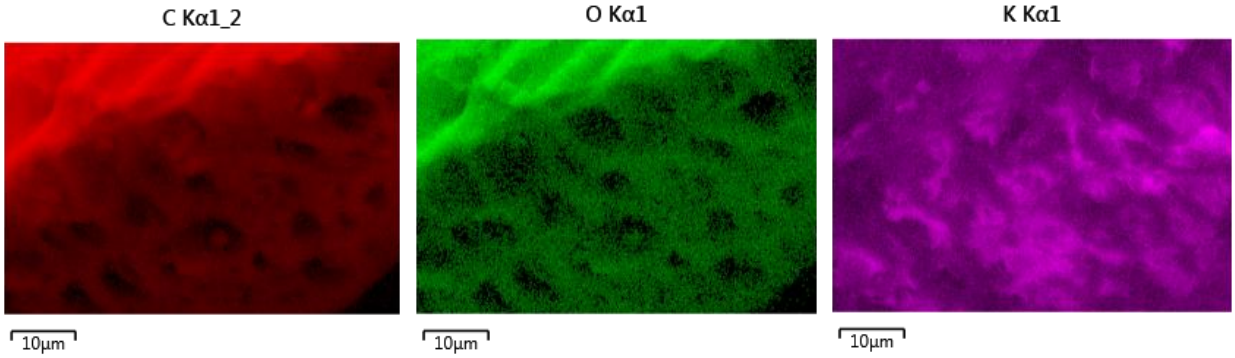

(b) sample 10

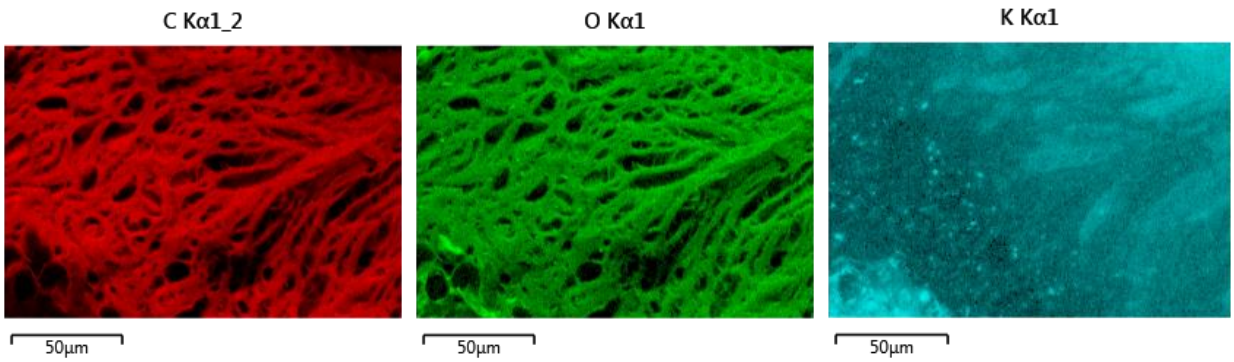

(c) sample 18

Figure 6.1.2.5: EDS images showing distribution of elements present in samples 2,10 and 18

EDS images show the distribution of chemical elements in the sample. Carbon in red, oxygen in green, and potassium in blue color in samples (a) and (c), and purple in sample (b).

6.1.3 Samples 3, 11, and 19

Precursor material: peanut shell

Carbonization temperature and time: 600-800°C/ 1H

Activation method, agent, temperature, and time: chemical activation/CaCl at 300-500°C/2 H

SEM observations:

The mean particle size is in an approximate range of 3µm to 600µm; therefore, considered a GAC because a higher percentage of the particles in the sample are in the GAC range size. The surface area is very irregular and has a high pore volume with characteristics observed at 500 and 200 µm magnification.

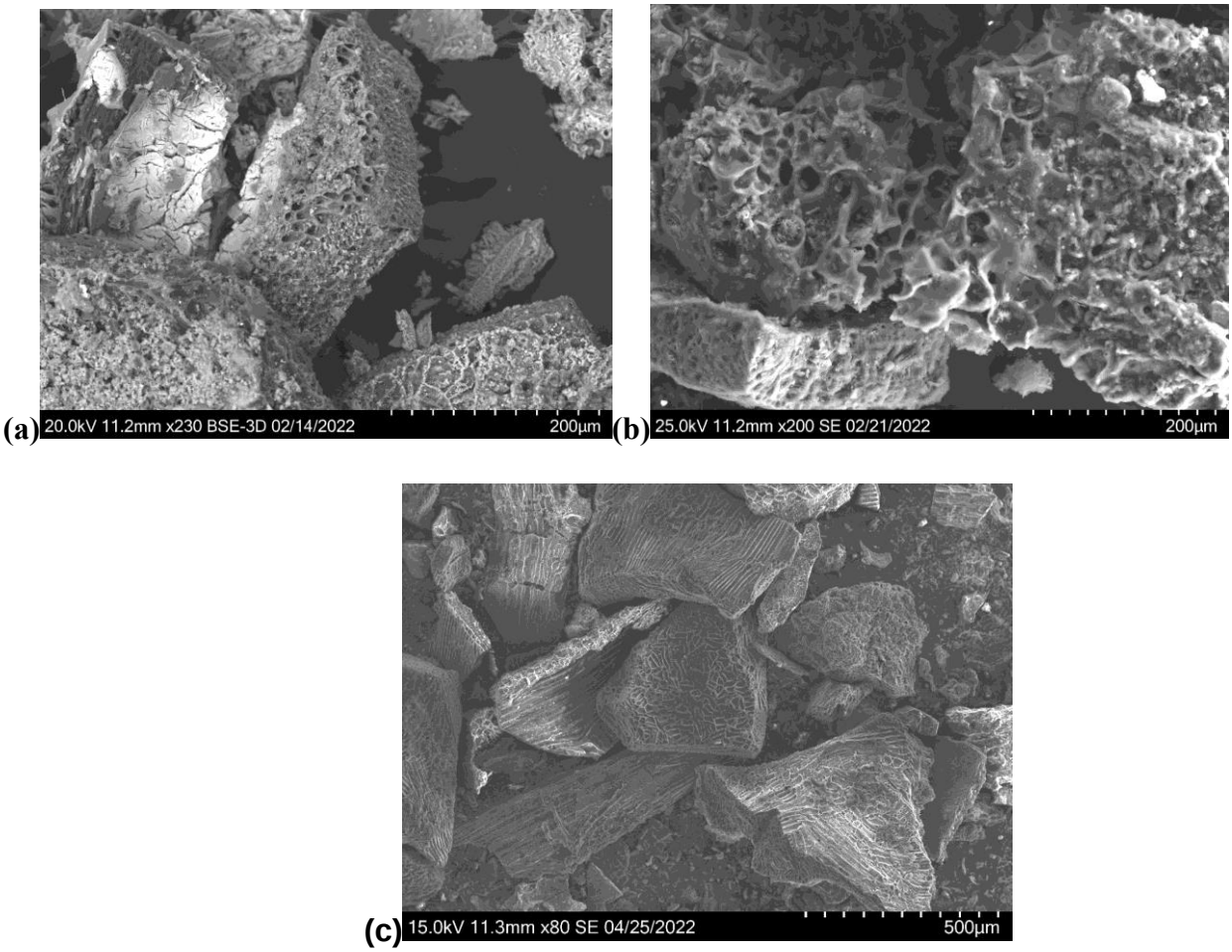

Figure 6.1.3.1: SEM images of samples 3, 11, and 19 (particle size and shape)

SEM for peanut shell-based activated carbon samples show particles and porosity in the surface area. The scale lines are the interval of the white marks**.** (a) SEM image of sample 3. (b) SEM image of sample 11 (repetition of experiment 3). (c) SEM image of sample 19 (repetition of experiment 3).

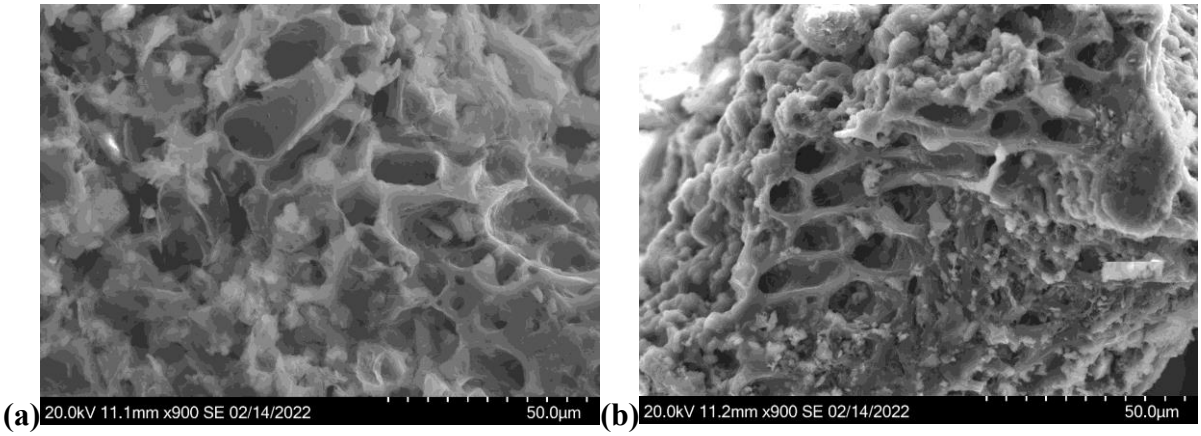

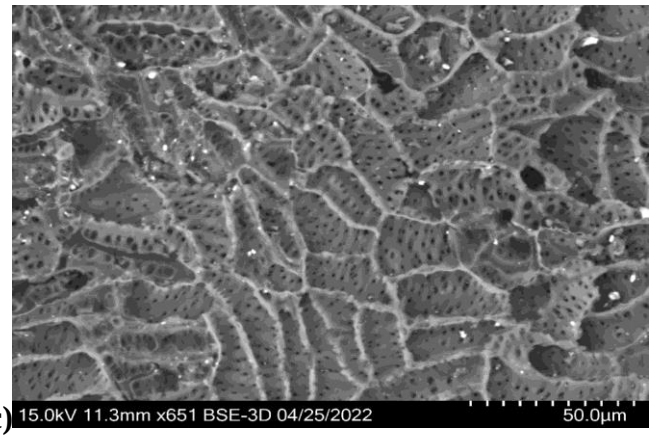

(c)

Figure 6.1.3.2: SEM images of samples 3, 11, and 19 (surface area and porosity)

(a) SEM image of sample 3. (b) SEM image of sample 11. (c) SEM image of sample 19. The mean pore size is larger than 50nm in the three samples; most pores are between 20 and 3µm, in the range size of macropores according to IUPAC standards.

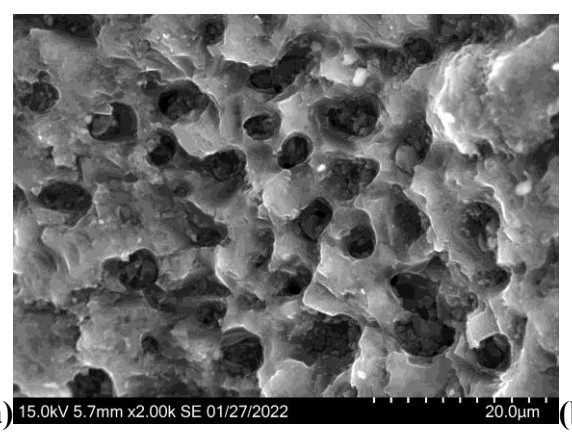

(a)

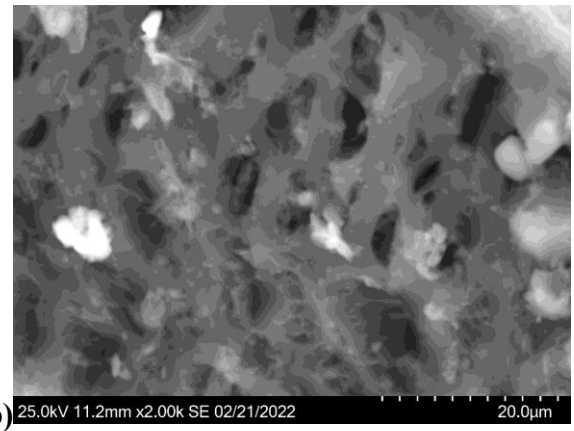

(b)

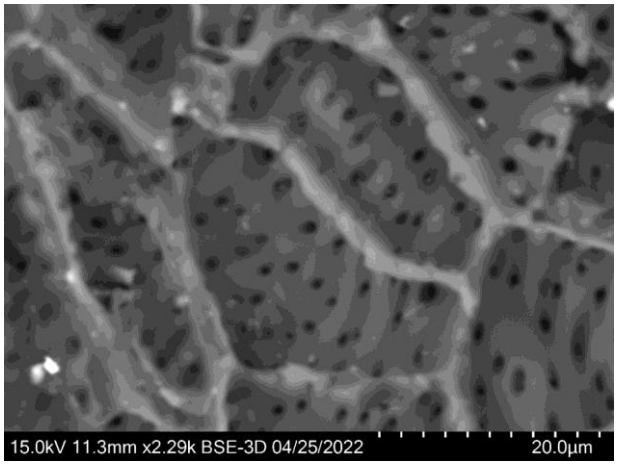

(c)

Figure 6.1.3.3: SEM images of samples 3, 11, and 19 (pore size)

(a) SEM image of sample 3. (b) SEM image of sample 11 (repetition of experiment 3). (c) SEM image of sample 19 (repetition of experiment 3). SEM micrographs show a large proportion of macropores. The scale lines are the interval of the white marks.

Elemental analysis (EDS)

The energy-dispersive X-ray spectroscopy was used for the elemental analysis or chemical characterization of the BBAC sample. The chemical elements present in the sample and relative abundance (measured as a percentage in the sample) are as follows: sample (a) 72.4% carbon, 8.1% oxygen, 12.7% chlorine, and 6.8% calcium. Sample (b) 80.3% carbon, 12.0% oxygen, 5.0% chlorine, and 2.6% calcium. Sample (c) 86.0% carbon, 12.8% oxygen, 0.4% chlorine, and 0.8% calcium.

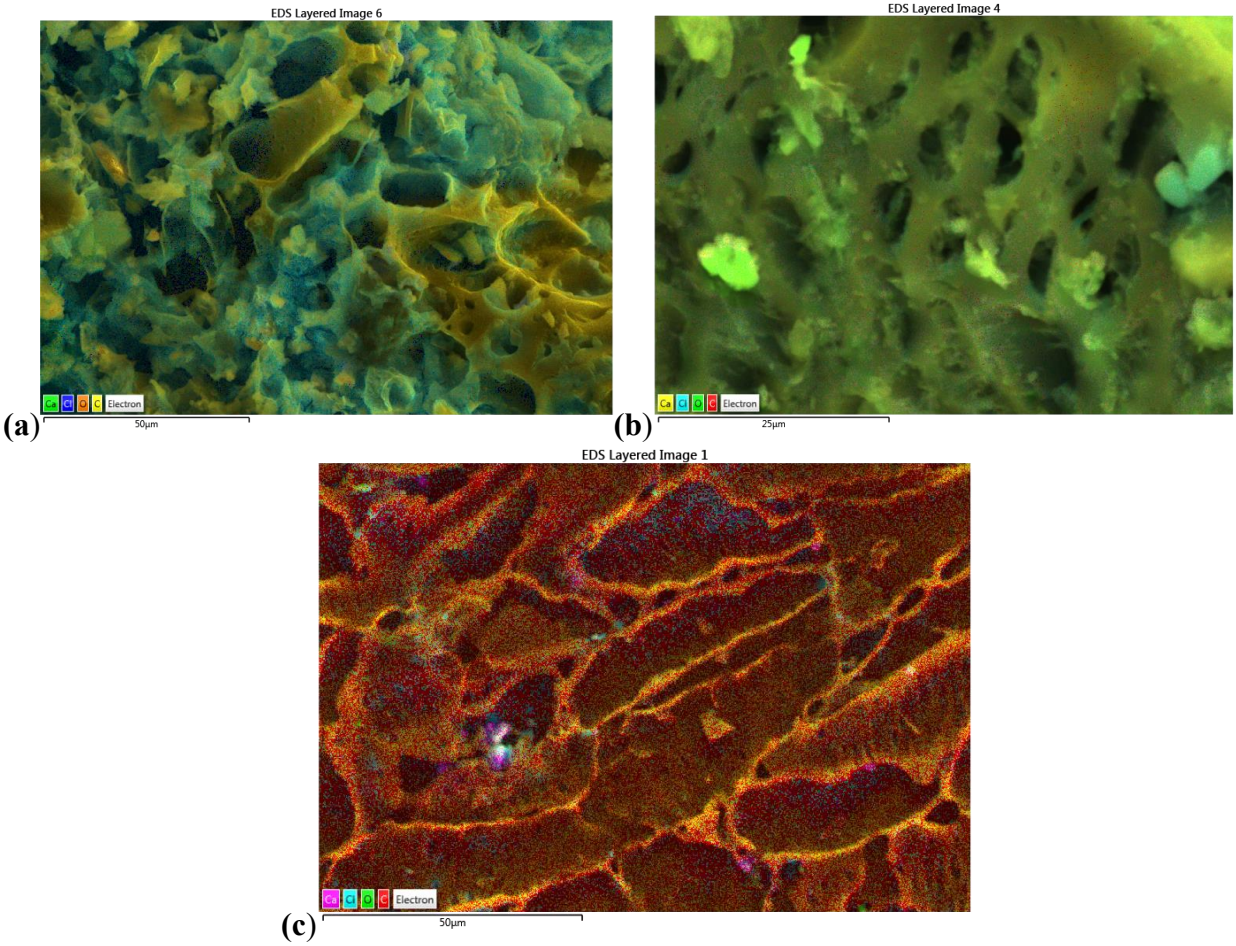

Figure 6.1.3.4: EDS elemental analysis of samples 3, 11 and 19

(a) EDS image of sample 3. (b) EDS image of sample 11 (repetition of experiment 3). (c) EDS image of sample 19 (repetition of experiment 3). EDS images show chemical elements present in the sample in different colors. The image show carbon with small particles on the surface of the activating agent, calcium chloride.

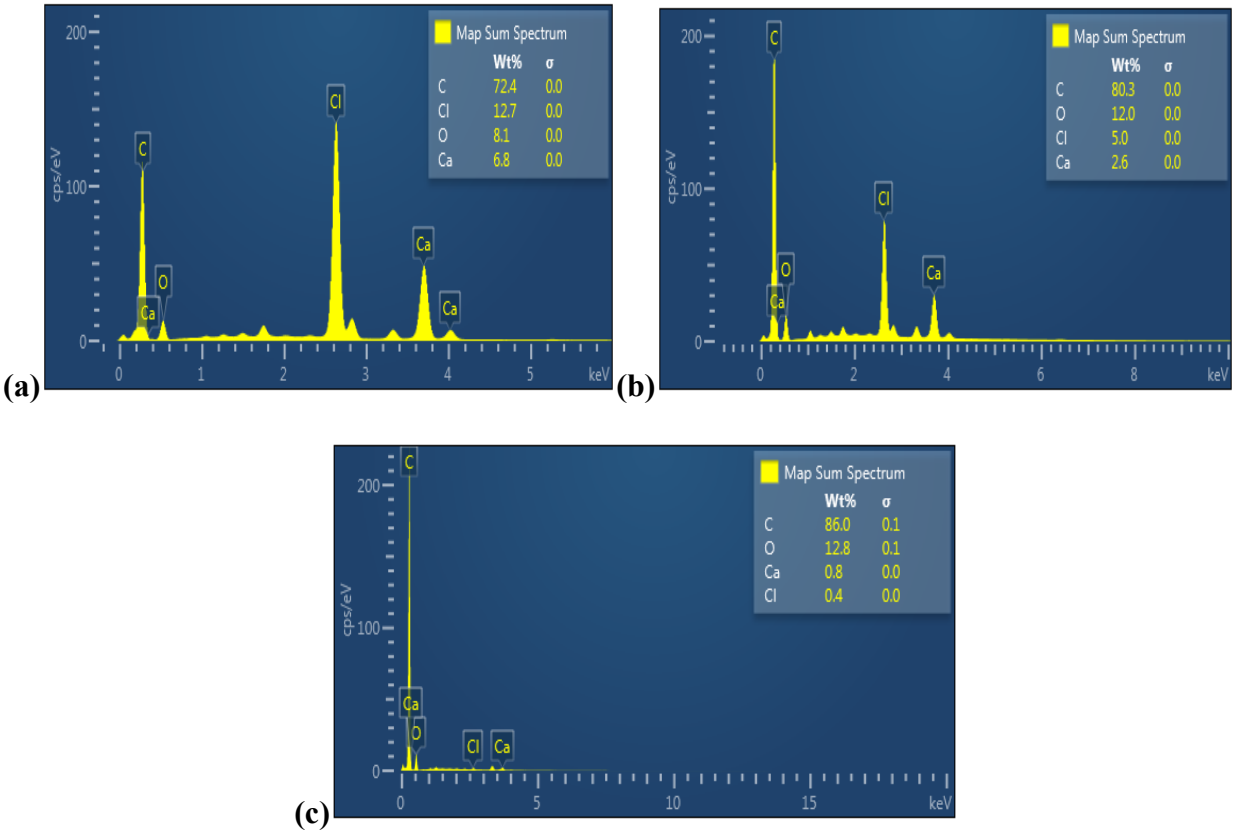

Figure 6.1.3.5: EDS graphs showing weight percentage of elements in samples 3,11 and 19

EDS graph showing the weight percentage of the chemical elements found in the sample. (a) EDS graph of sample 3. (b) EDS graph of sample 11 (repetition of experiment 3). (c) EDS of sample 19 (repetition of experiment 3).

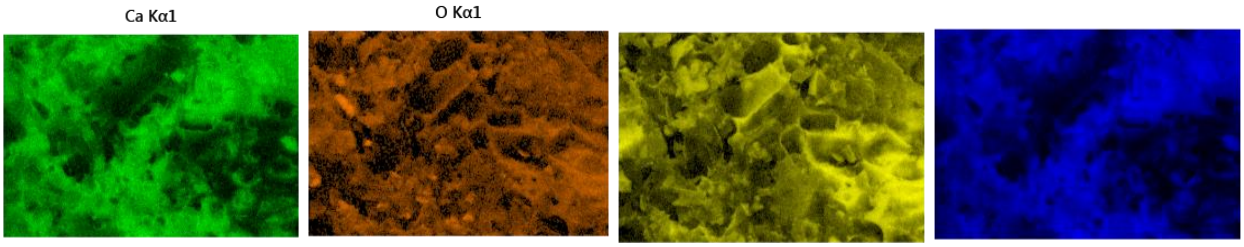

(a) Sample 3

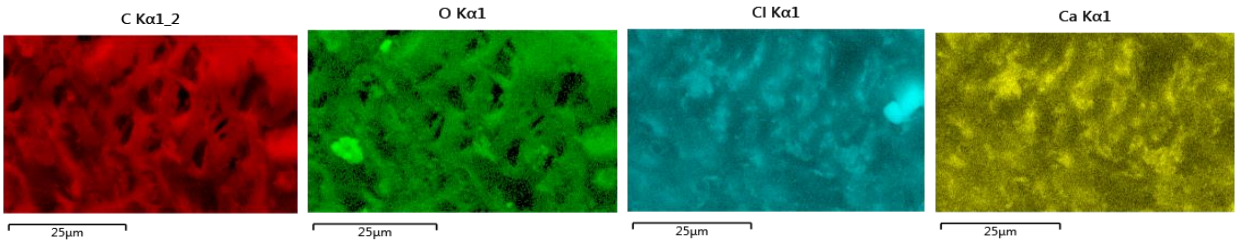

(b) Sample 11

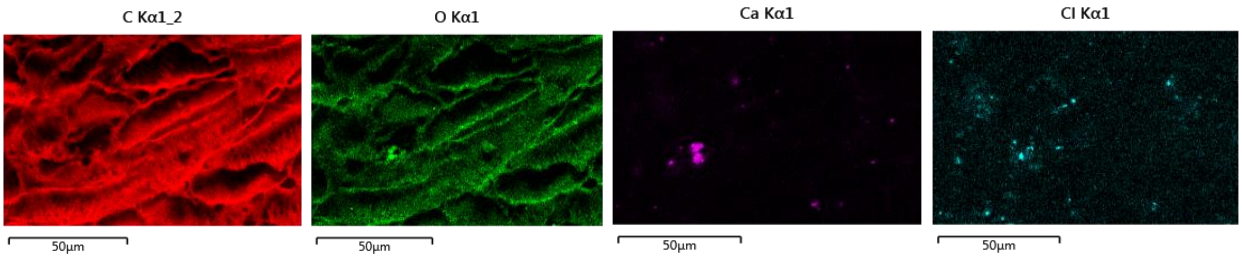

(c) Sample 19

Figure 6.1.3.6: EDS images showing distribution of elements present in samples 3,11 and 19 EDS images show the distribution of chemical elements in the sample in different colors.

6.1.4 Samples 4,12, and 20

Precursor material: peanut shell

Carbonization temperature and time: 500-600°C/ 3H

Activation method and agent, temperature, and time: chemical activation/CaCl, 300-500°C/2 H

SEM Observations:

The mean particle size is in an approximate range of 3µm to 700µm; therefore, considered a GAC because a higher percentage of the particles in the sample are in the GAC range size. The surface area is very irregular and has a high pore volume with characteristics observed at 2000, 1000, and 500 µm magnification.

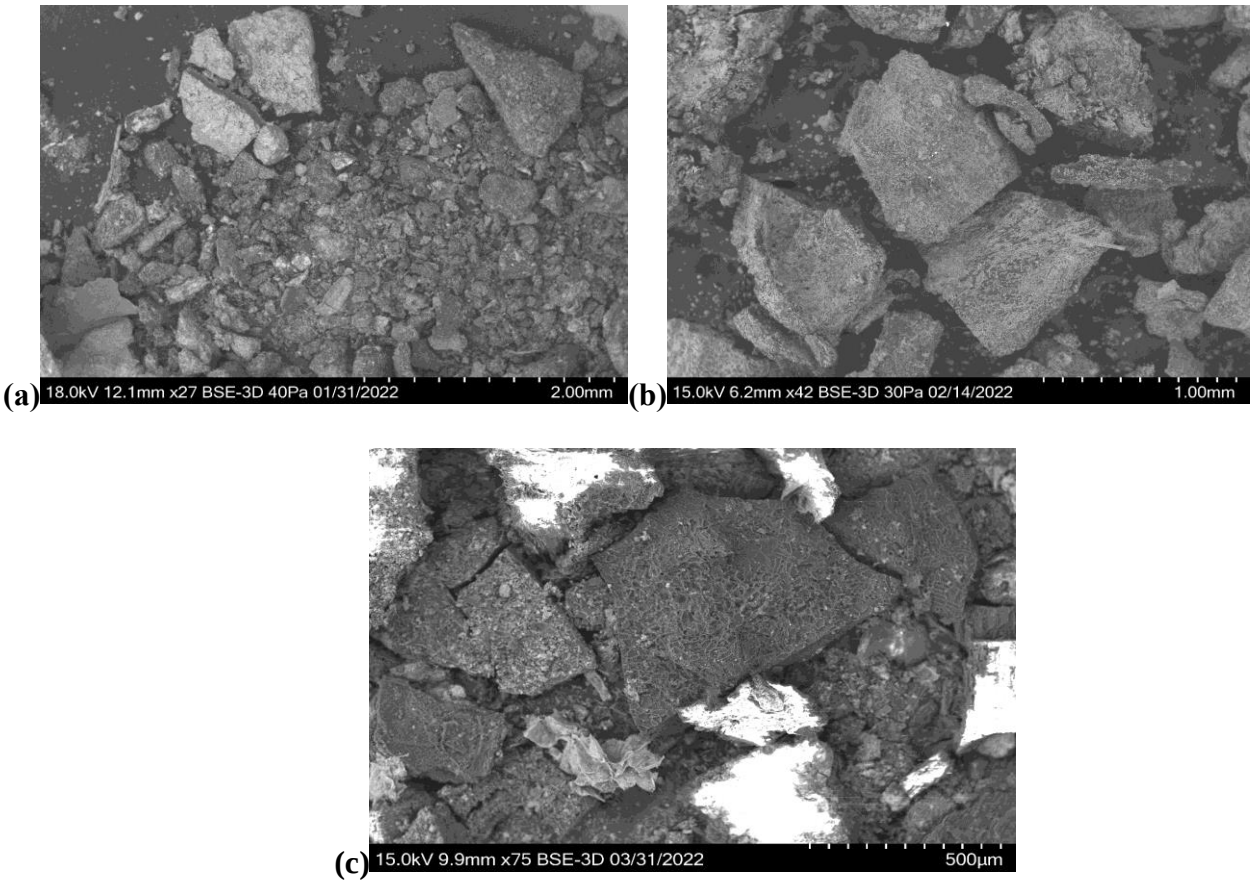

Figure 6.1.4.1: SEM images of samples 4, 12, and 20 (particle size and shape)

(a) SEM image of sample 4. (b) SEM image of sample 12 (repetition of experiment 4). (c) SEM image of sample 20 (repetition of experiment 4). SEM micrographs for peanut shell-based activated carbon showing particles and porosity in the surface area. The scale lines are the interval of the white marks.

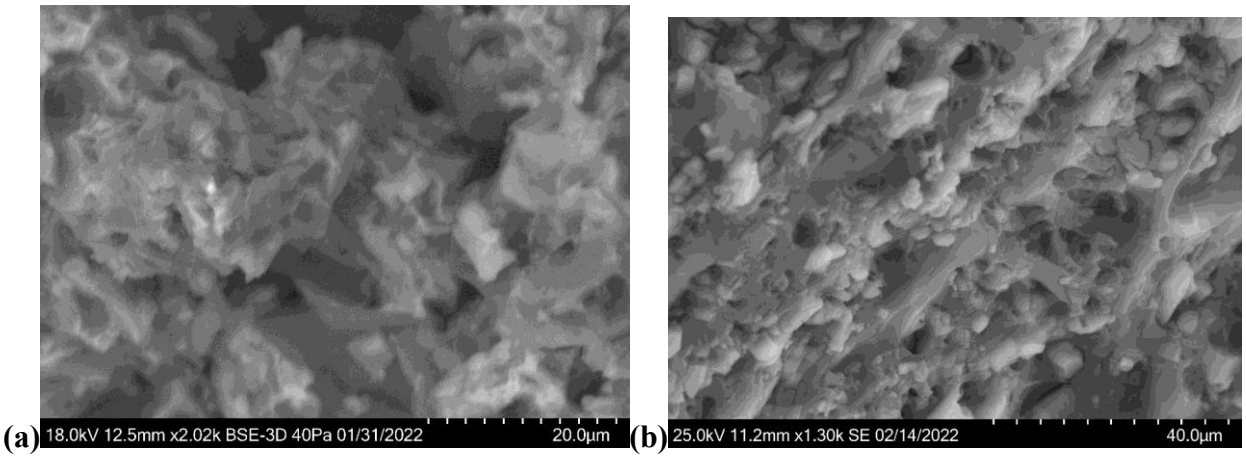

(c) 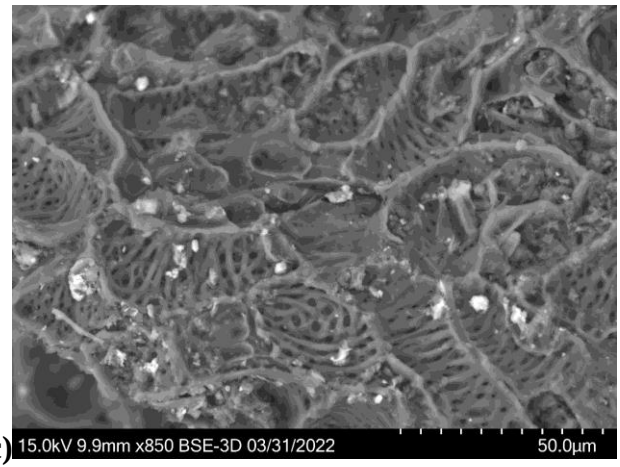

Figure 6.1.4.2: SEM images of samples 4, 12, and 20 (porosity and surface area).

(a) SEM image of sample 4. (b) SEM image of sample 12 (repetition of experiment 4). (c) SEM image of sample 20 (repetition of experiment 4). SEM images for peanut shell-based activated carbon show an area with a high percentage of macropores and mesopores. Pore size is larger than 50nm, and most of the pores are in the range size of macropores according to IUPAC standards.

Elemental analysis (EDS)

The energy-dispersive X-ray spectroscopy was used for the elemental analysis or chemical characterization of the BBAC sample. The chemical elements present in the sample and relative abundance (measured as a percentage) are distributed as follows: (a) 62.9% carbon, 17.4% oxygen, 11.5% chlorine, and 5.3% calcium. (b) 66.8% carbon, 6.2% oxygen, 17.0% chlorine, and 9.0% calcium. (c) 78.0% carbon, 20.7% oxygen, 0.6% chlorine, and 0.6% calcium. Other elements present, such as potassium and silicon, are considered contamination.

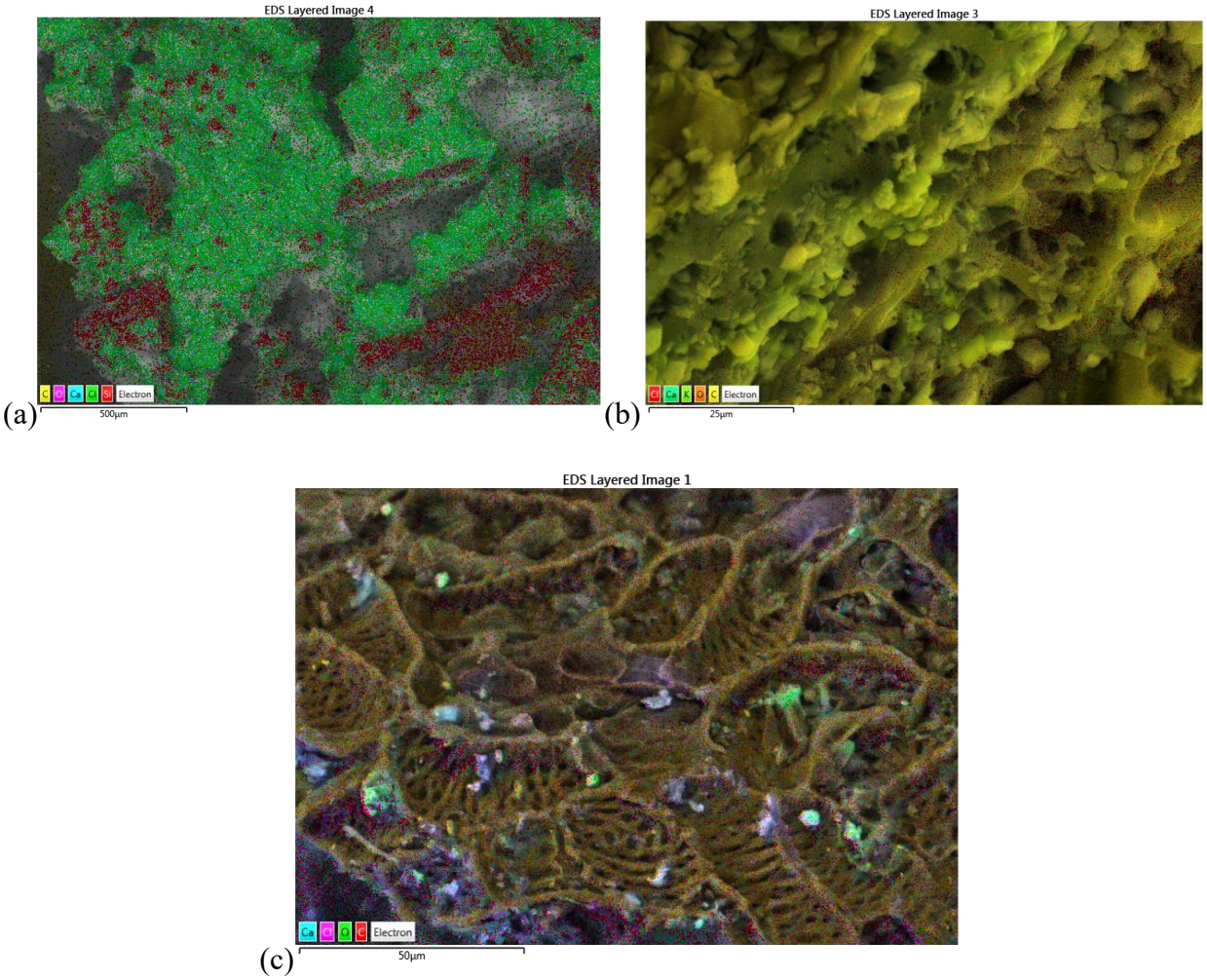

Figure 6.1.4.3: EDS elemental analysis of samples 4, 12, and 20.

(a) EDS image of sample 4. (b) EDS image of sample 12 (repetition of experiment 4). (c) EDS image of sample 20 (repetition of experiment 4). EDS images show chemical elements present in the sample in different colors. The image show carbon with small particles on the surface of the activating agent, calcium chloride.

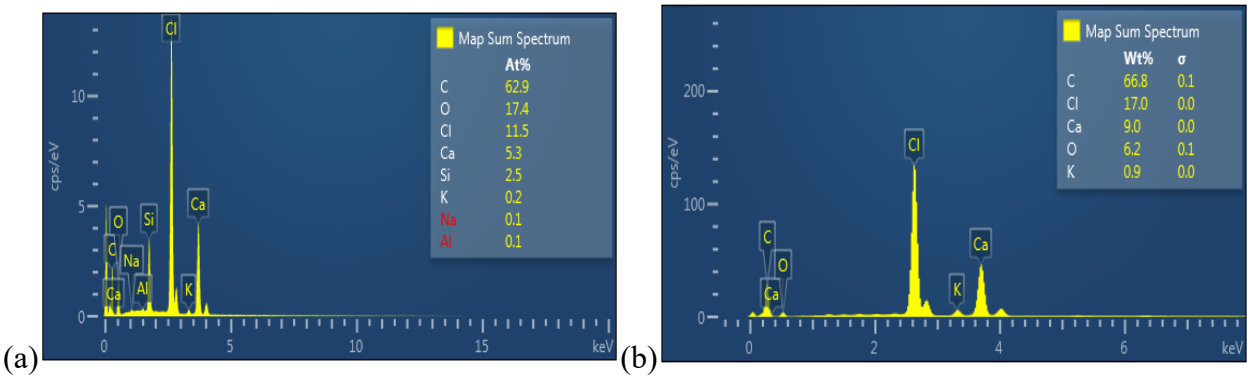

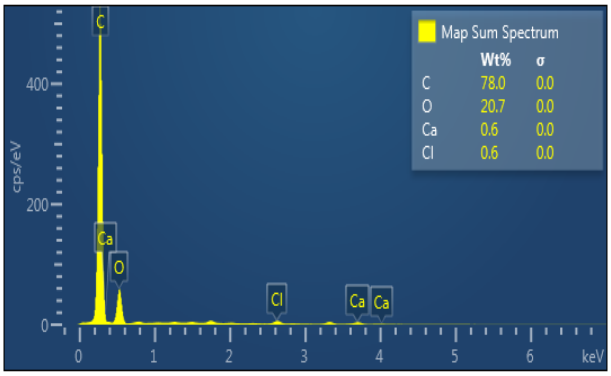

(c)

Figure 6.1.4.4: EDS graphs showing weight percentage of elements in samples 4,12, and 20.

EDS graphs show the weight percentage of the chemical elements found in the sample. (a) EDS graph of sample 4. (b) EDS graph of sample 12 (repetition of experiment 4). (c) EDS graph of sample 20 (repetition of experiment 4).

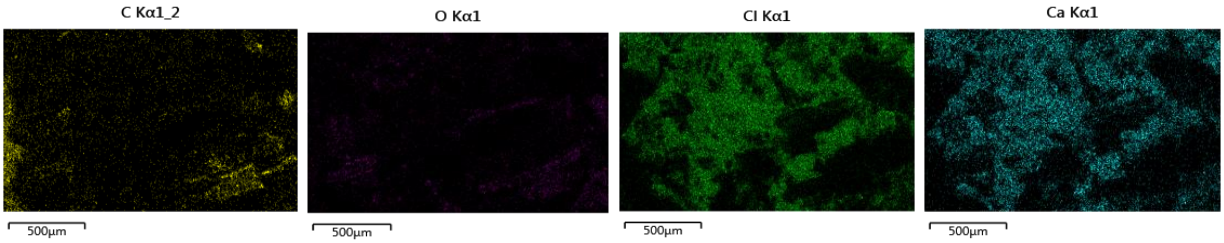

(a) sample 4

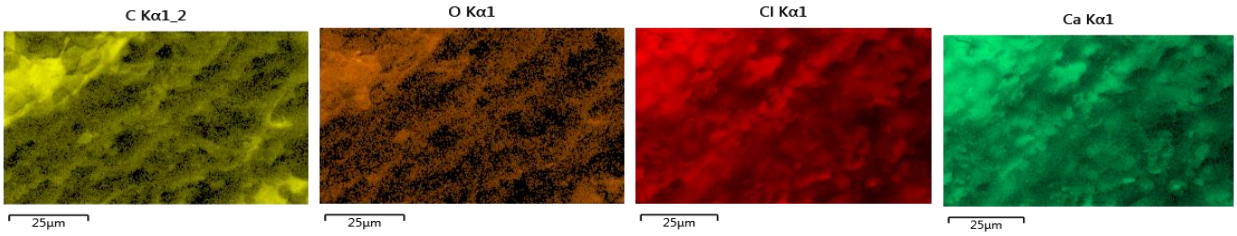

(b) sample 12

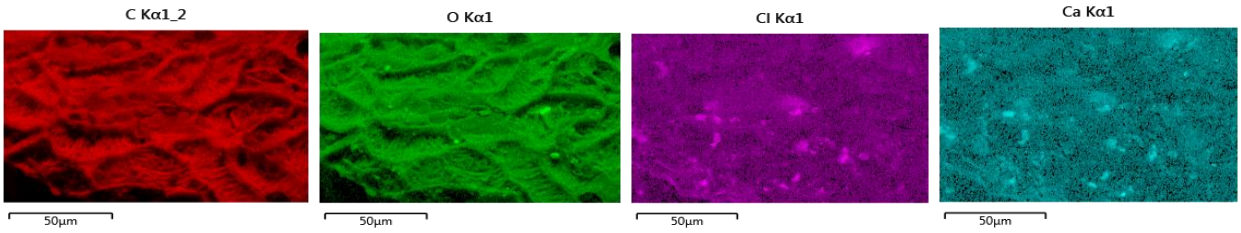

(c) sample 20

Figure 6.1.4.5: EDS images showing distribution of elements present in samples 4,12, and 20.

EDS images show the sample's distribution of chemical elements in different colors.

6.1.5 Sample 5, 13, and 21

Precursor material: rice husk

Carbonization temperature and time: 600-800°C/ 1H

Activation method and agent, temperature, and time: chemical activation/KOH, 300-500°C/3 H

SEM Observations:

The particle size is in an approximate range of 3µm to 600µm (in the largest dimension); therefore, it is considered a granular activated carbon (above180 µm is considered GAC). The surface area is very irregular and has a high pore volume with many cracks with characteristics observed at 1000, 500, 400, 50, and 30 µm magnification.

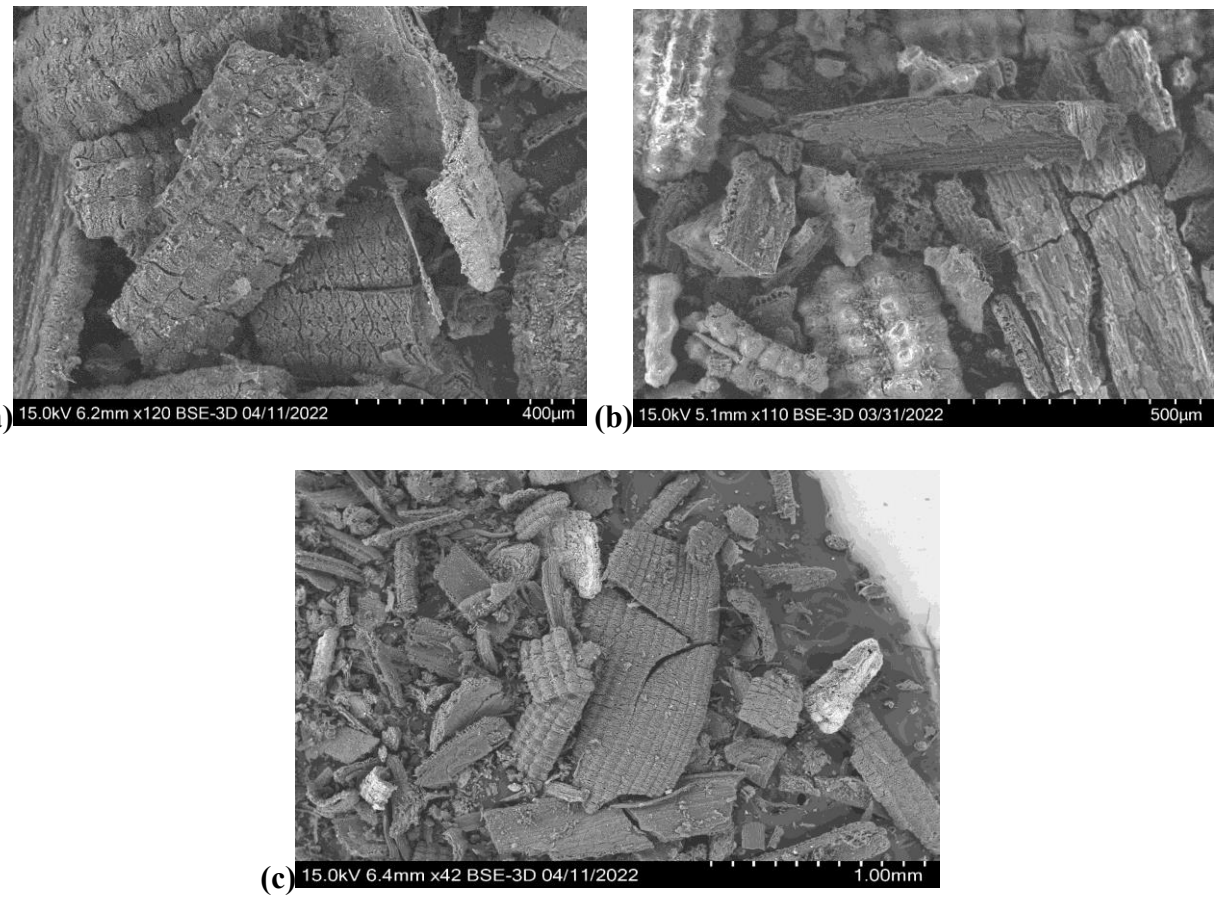

Figure 6.1.5.1: SEM images of samples 5, 13, and 21 (particle size and shape).

(a) sample 5, (b) sample 13 (repetition of experiment 5), (c) sample 21 (repetition of experiment 5). SEM micrographs for rice husk-based activated carbon showing particle's shape and size.

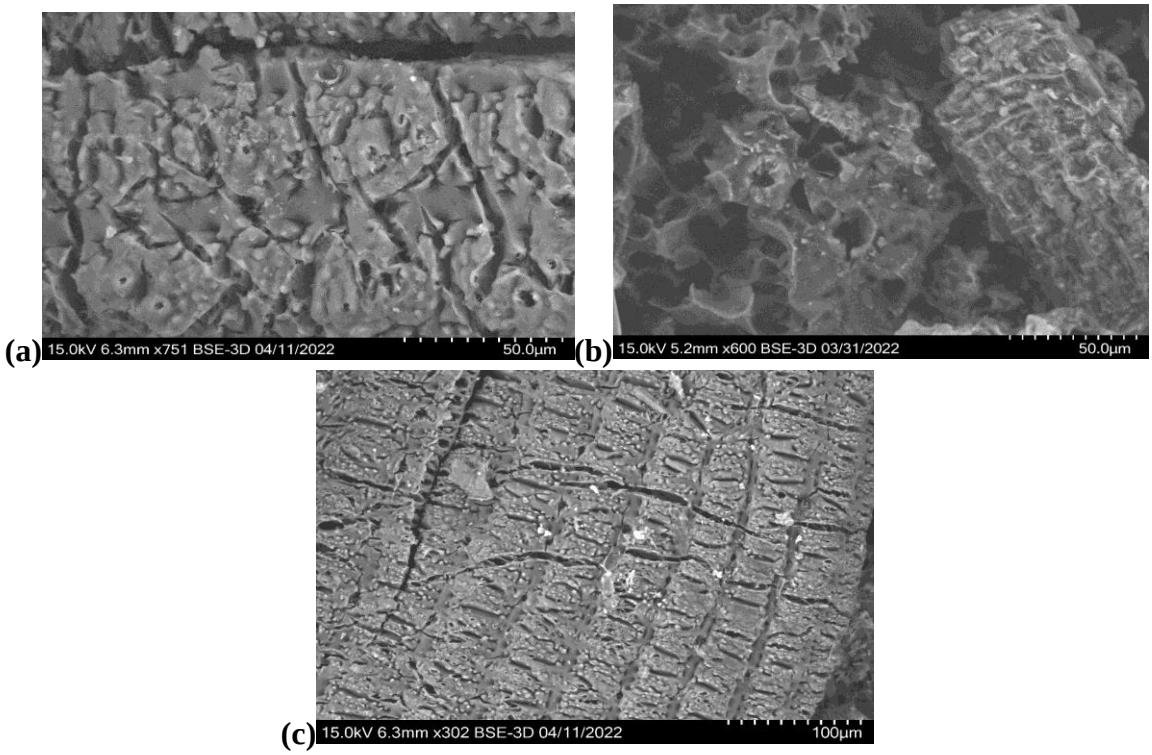

Figure 6.1.5.2: SEM images of samples 5, 13, and 21 (surface area and porosity).

(a) sample 5, (b) sample 13, (c) sample 21. SEM micrographs show the particle's surface area with a high proportion of cracks and pores.

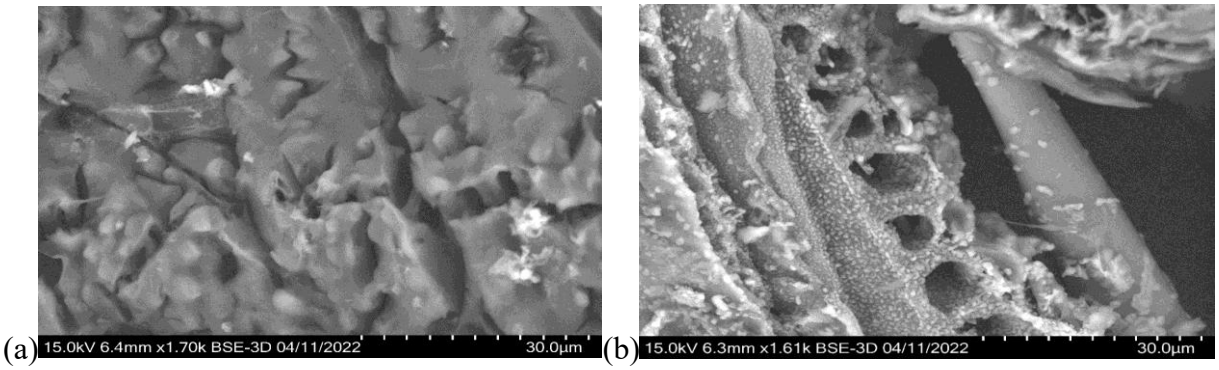

(c) 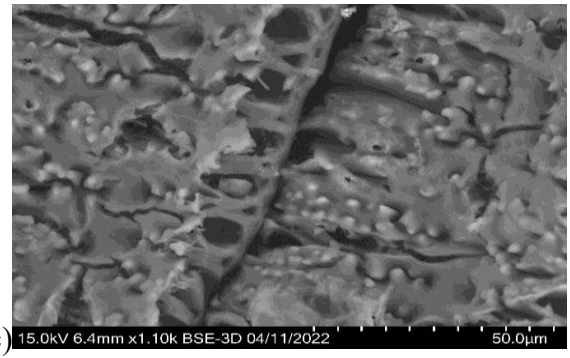

Figure 6.1.5.3: SEM images of samples 5, 13, and 21 (pore size).

SEM micrographs show the particle's surface area at 30 and 50 µm magnification. The mean pore size is larger than 50nm, and some pores are between 5 and 10µm; therefore, most are in the macropores range according to IUPAC standards.

Elemental analysis (EDS)

The energy-dispersive X-ray spectroscopy was used for the elemental analysis or chemical characterization of the BBAC sample. The chemical elements present in the sample and relative abundance (measured as a percentage in the sample) are distributed as follows: (a) 55.7% carbon, 29.1% oxygen, 9.1% potassium, and 5.9% silicon. (b) 60.0% carbon, 30.7% oxygen, 0.5% potassium, and 8.7% silicon, and (c) 67.9% carbon, 21.7% oxygen, and 6.3% potassium. The presence of other elements is considered contamination.

(a) 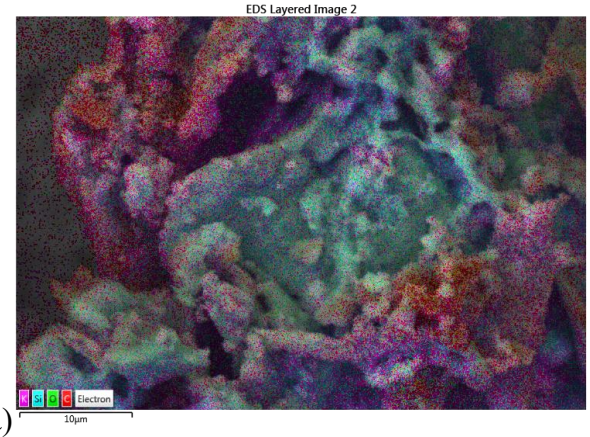

(b) 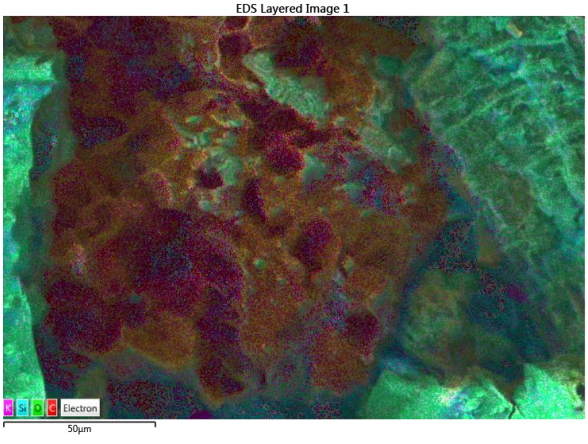

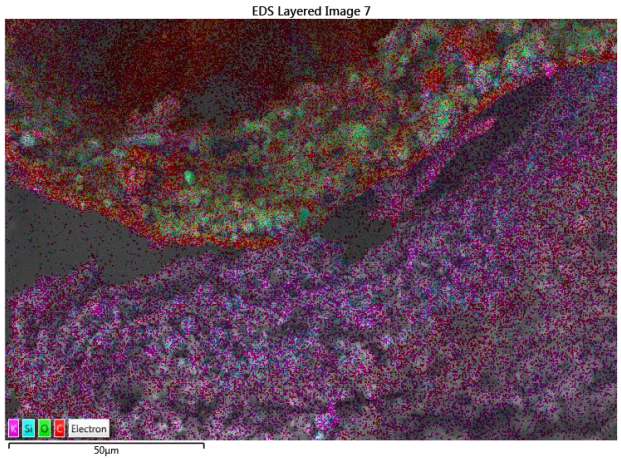

(c)

Figure 6.1.5.4: EDS elemental analysis of samples 5, 13, and 21.

(a) sample 5, (b) sample 13 (repetition of experiment 5), (c) sample 21 (repetition of experiment 5). Elemental analysis (EDS) image shows chemical elements in the sample in different colors. The image show carbon with small particles on the surface of the activating agent potassium hydroxide.

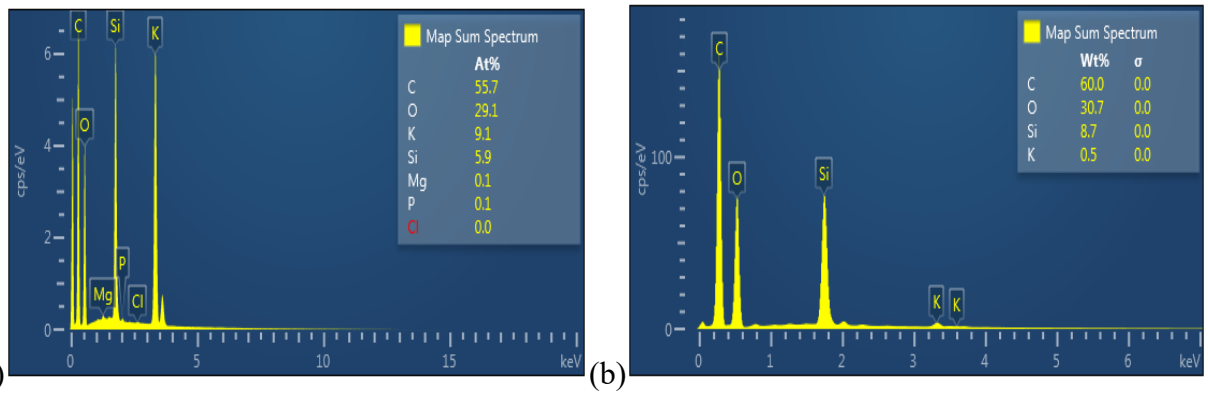

(a) (b)

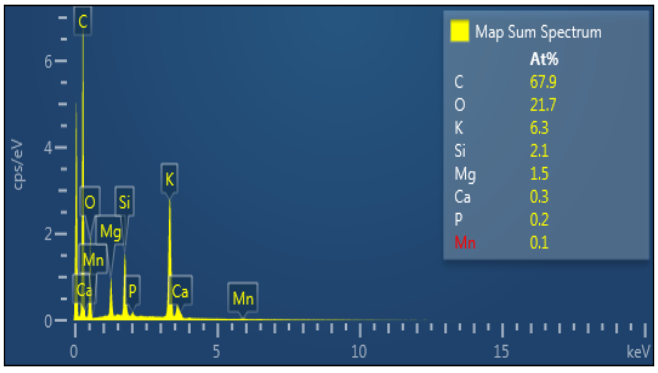

(c)

Figure 6.1.5.5: EDS graphs showing weight percentage of elements in samples 5,13, and 21.

(a) sample 5, (b) sample 13, (c) sample 21. EDS graphs show the weight percentage of the chemical elements found in the sample.

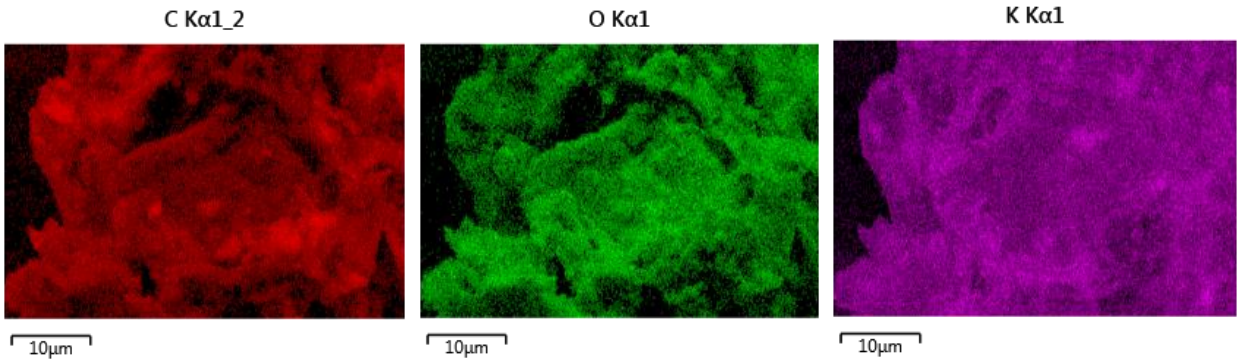

(a) sample 5

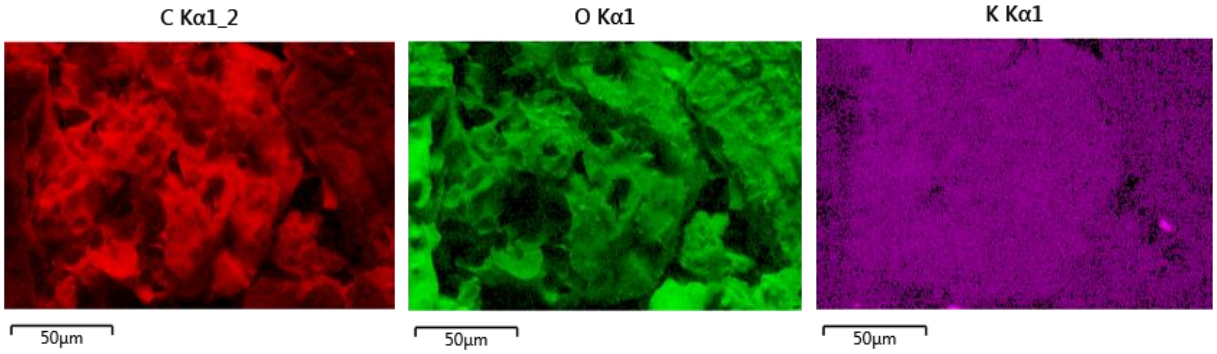

(a) sample 13

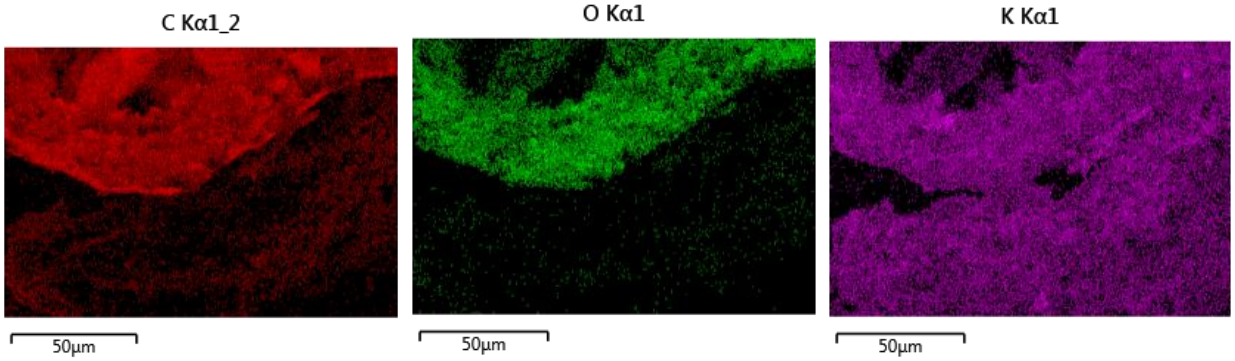

(b) sample 21

Figure 6.1.5.6: EDS images showing distribution of elements present in samples 5,13, and 21.

EDS images show the distribution of chemical elements in the sample. Carbon in red, oxygen in green, and potassium in purple.

6.1.6 Sample 6, 14, and 22

Precursor material: rice husk

Carbonization temperature and time: 400-600°C/ 3H

Activation method and agent, temperature, and time: chemical activation/KOH, 300-500°C/2 H

SEM Observations:

The particle size is in an approximate range of 3µm to 600µm (in the largest dimension); therefore, considered a GAC because a higher percentage of the particles in the sample are in the GAC range size. The surface area is very irregular and has a high pore volume with characteristics observed at 500, 50, 40, 30, and 20 µm magnification.

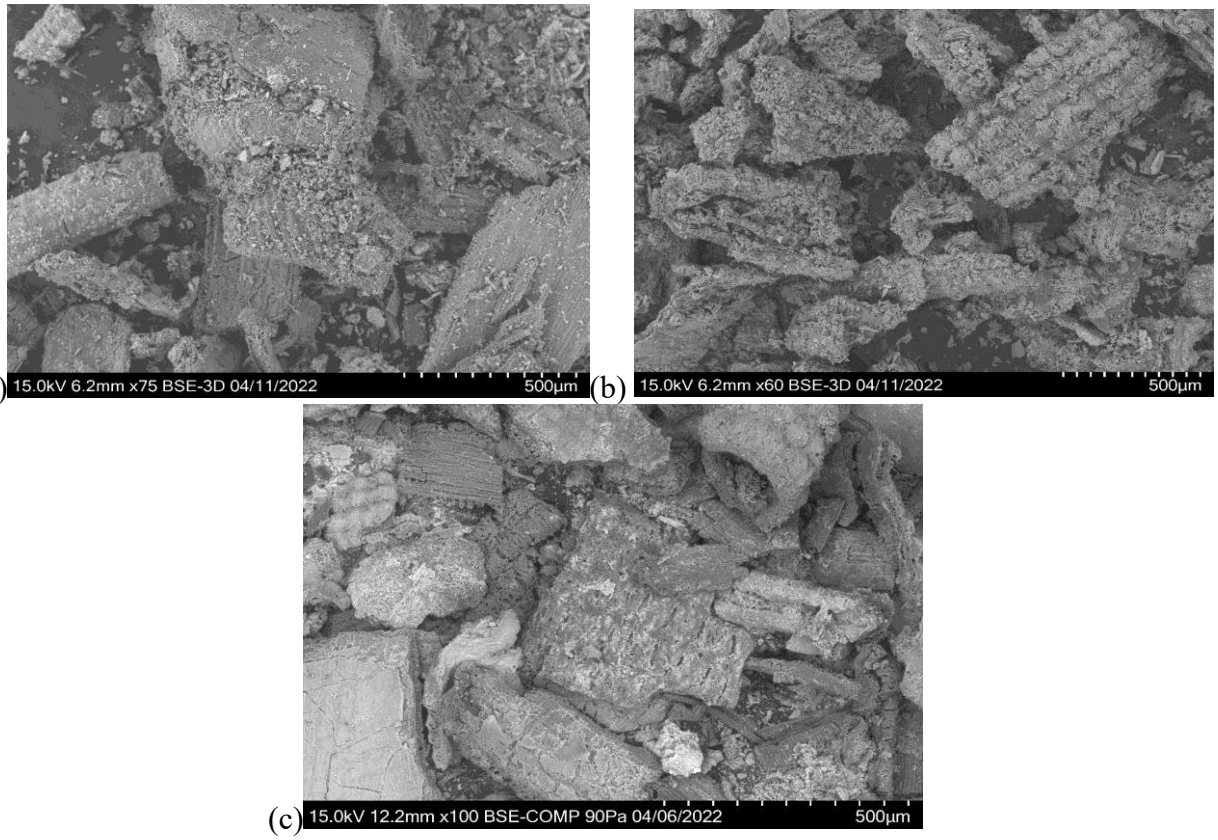

Figure 6.1.6.1: SEM images of samples 6, 14, and 22 (particle size and shape).

(a) sample 6, (b) sample 14 (repetition of experiment 6), (c) sample 22 (repetition of experiment 6). SEM micrographs for rice husk-based activated carbon showing particle's shape, size, and surface area. The scale lines are the interval of the white marks.

(a) 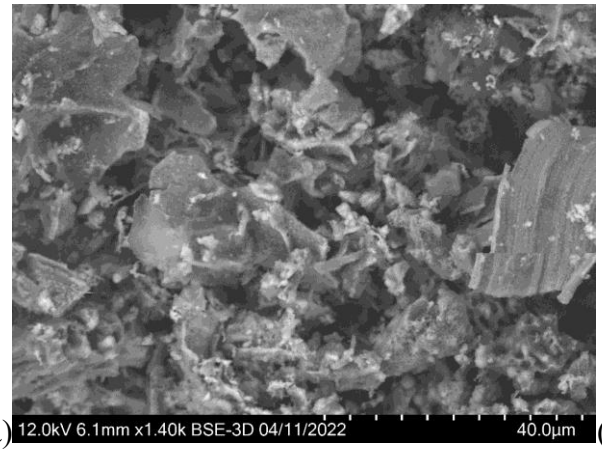

(b) 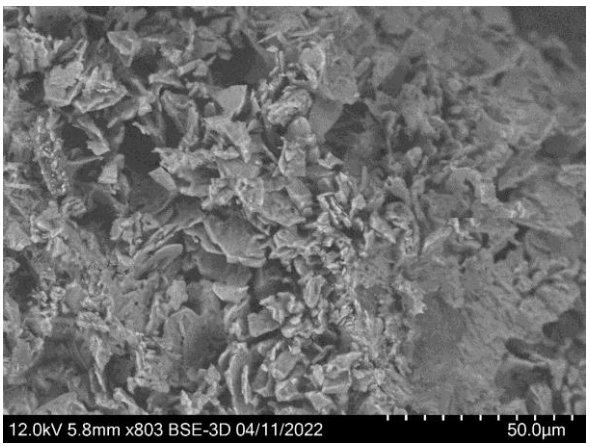

Figure 6.1.6.2: SEM images of samples 6, 14, and 22 (surface area and porosity)

(a) sample 6, (b) sample 14 (repetition of experiment 6), (c) sample 22 (repetition of experiment 6). SEM micrographs show the particle's surface area of samples (a) and (b). Micrographs showing surface area with a high proportion of lumps.

(a) 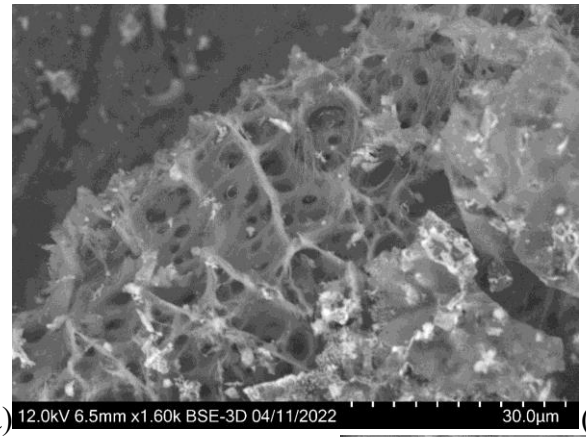

(b) 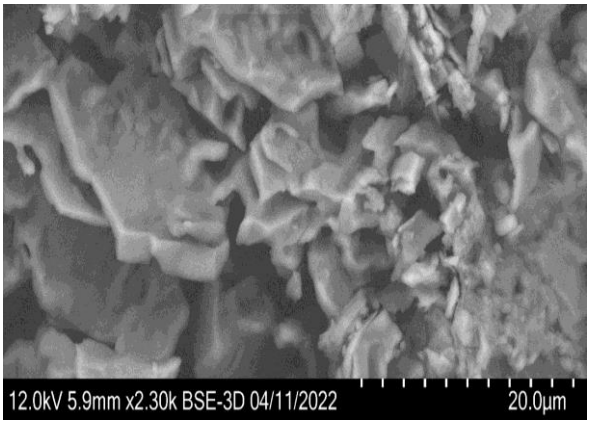

(c) 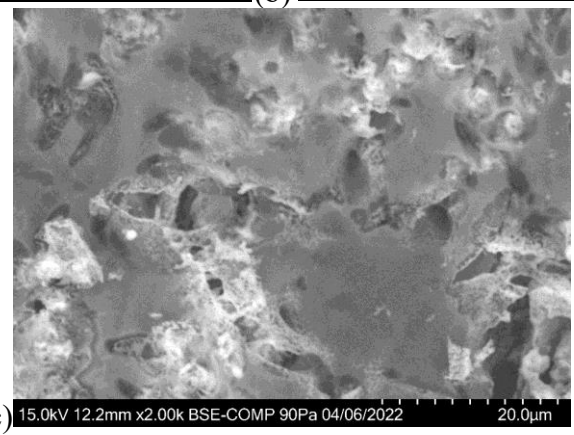

Figure 6.1.6.3: SEM images of samples 6, 14, and 22 (pore size)

SEM micrographs show the particle's surface area at 20 magnification on (b) and (c) and 30 µm on (a). In addition, micrographs show the particle's surface area and porosity. The mean pore

size is larger than 50nm, and some pores are between 2 and 10µm; therefore, most are in the macropores range according to IUPAC standards.

Elemental analysis (EDS)

The energy-dispersive X-ray spectroscopy was used for the elemental analysis or chemical characterization of the BBAC sample. The chemical elements present in the sample and relative abundance (measured as a percentage in the sample) are distributed as follows: (a) 56.1% carbon, 30.3% oxygen, and 13.6% potassium, (b) 22.3% carbon, 50.5% oxygen, and 25.6% potassium, and (c) 44.0% carbon, 24.9% oxygen, and 24.6% potassium.

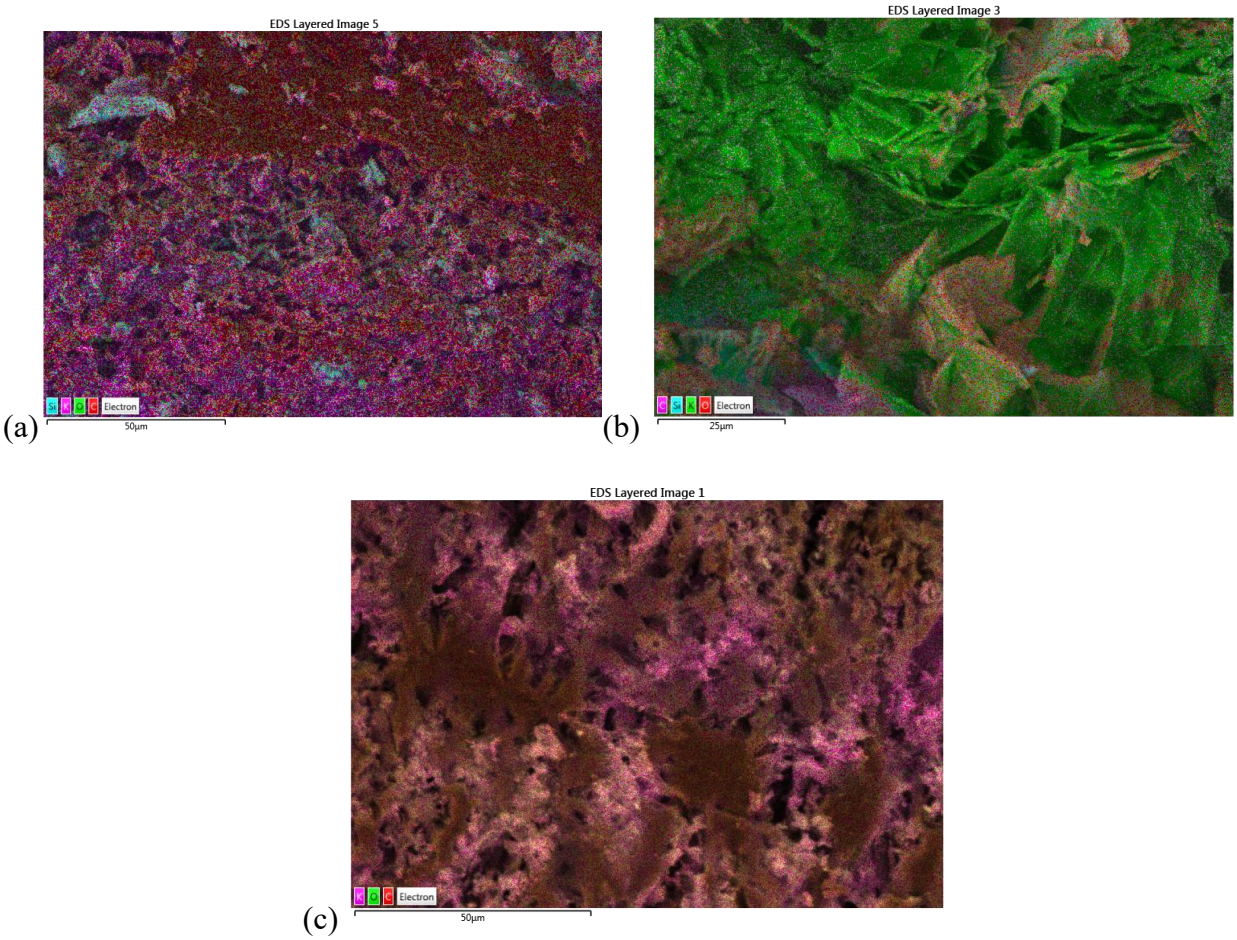

(a) (b) (c)

Figure 6.1.6.4: EDS elemental analysis of samples 6, 14 and 22

(a) sample 6, (b) sample 14 (repetition of experiment 6), (c) sample 22 (repetition of experiment 6). Elemental analysis (EDS) image shows chemical elements in the sample in different colors.

The image show carbon with a small amount on the surface of the activating agent potassium hydroxide.

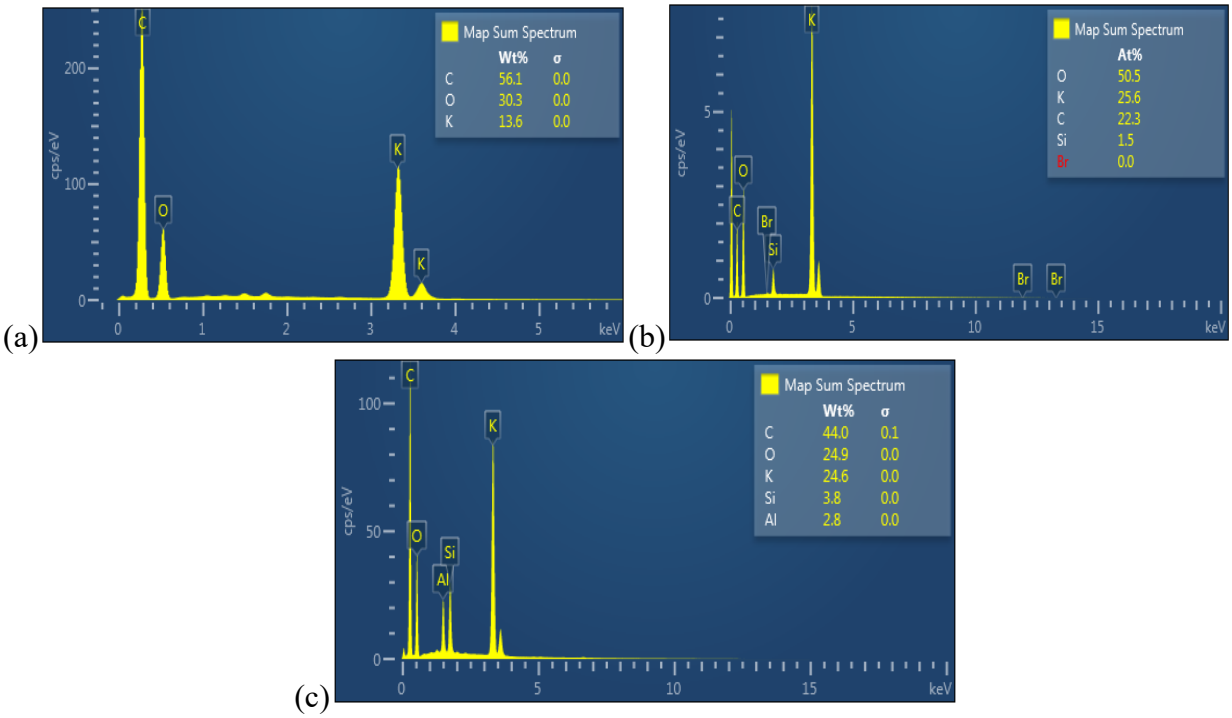

Figure 6.1.6.5: EDS graphs showing weight percentage of elements in samples 6,14 and 22

(a) sample 6, (b) sample 14, (c) sample 22.EDS graph showing the weight percentage of the chemical elements found in the sample.

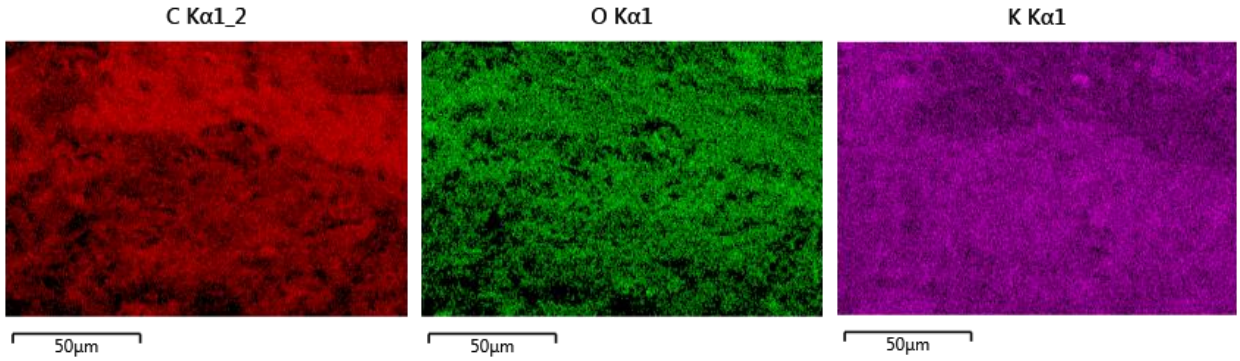

(a) sample 6

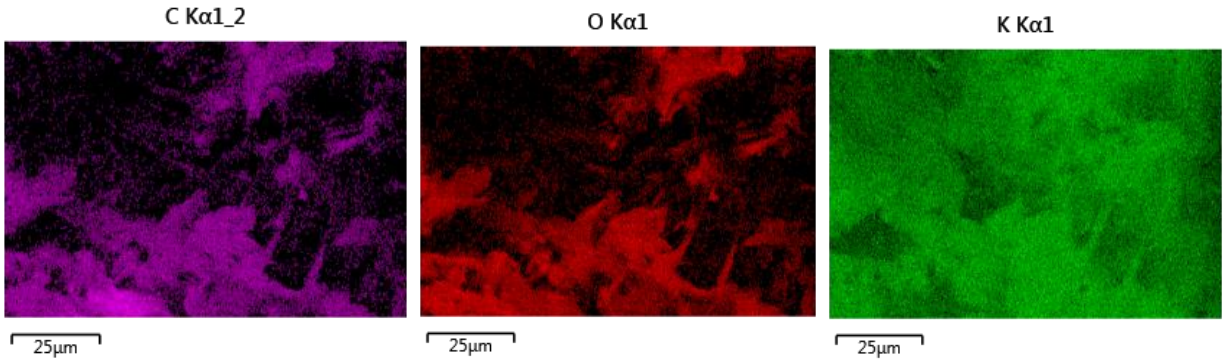

(b) sample 14

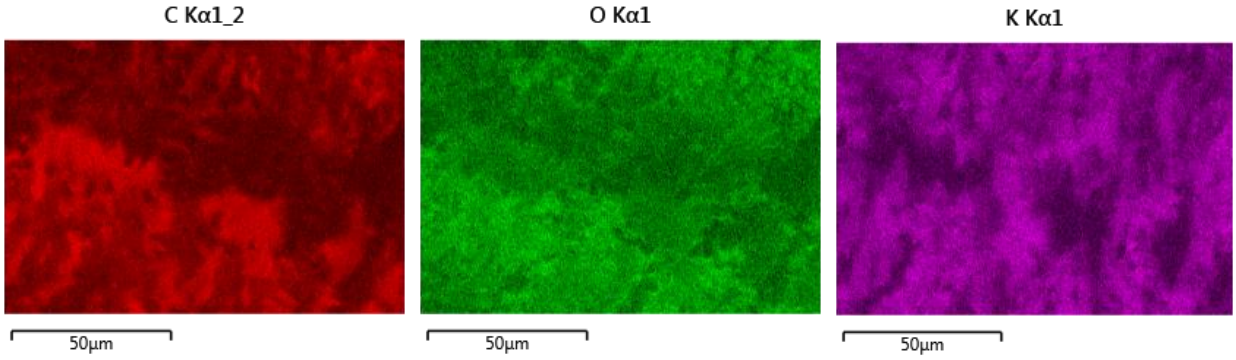

(c) sample 22

Figure 6.1.6.6: EDS images showing distribution of elements present in samples 6,14, and 22.

EDS images show the distribution of chemical elements in the sample. Carbon in red in samples (a) and (c), purple in sample (b); oxygen in green in samples (a) and (c), red in sample (b); and potassium in purple color in samples (a) and (c), and green in sample (b).

6.1.7 Sample 7, 15, and 23

Precursor material: rice husk

Carbonization temperature and time: 600-800°C/ 1H

Activation method and agent, temperature, and time: chemical activation/CaCl, 300-500°C/3 H

SEM Observations:

The particle size is in an approximate range of 3µm to 600µm (in the largest dimension); considered a GAC because a higher percentage of the particles in the sample are in the GAC

range size. The surface area is very irregular, with characteristics observed at 500, 300, 50, 40, and 20 µm magnification.

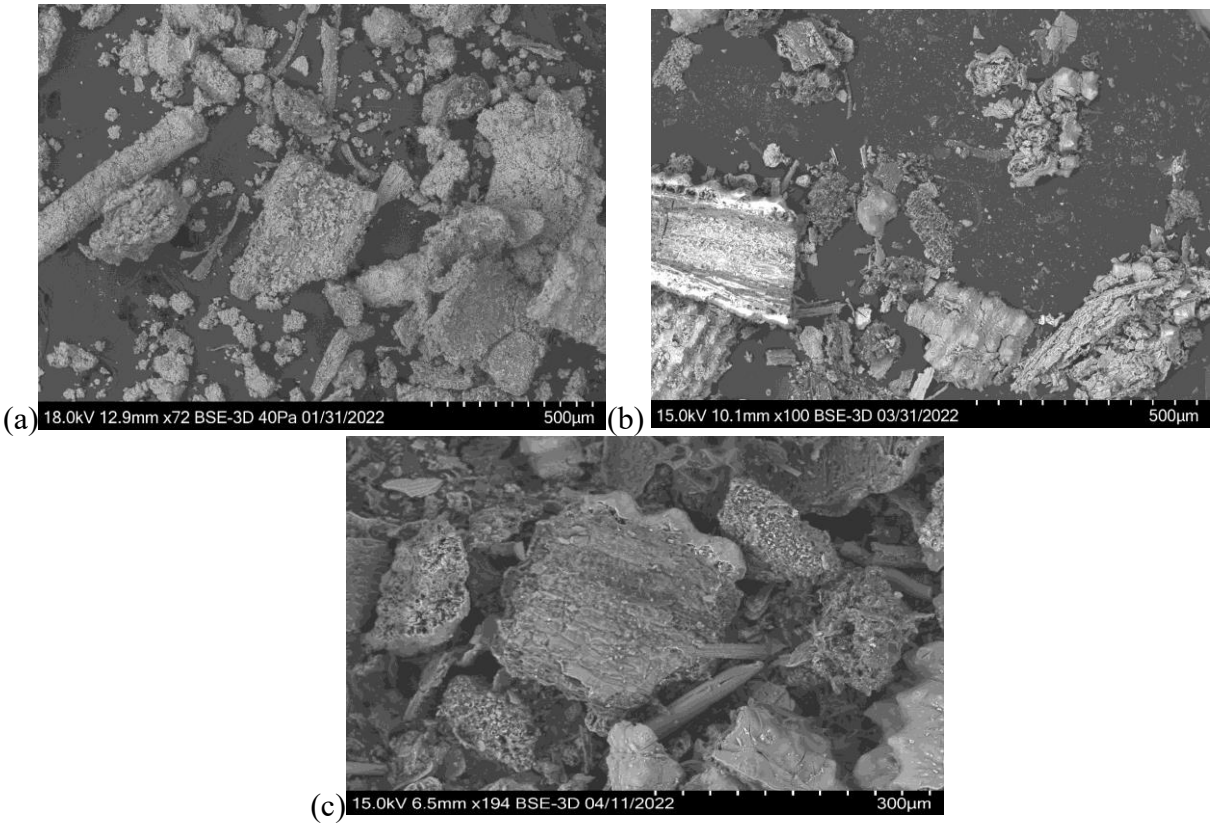

Figure 6.1.7.1: SEM images of samples 7, 15, and 23 (particle size and shape).

(a) sample 7, (b) sample 15 (repetition of experiment 7), (c) sample 23 (repetition of experiment 7). SEM images for rice husk-based activated carbon showing particle's shape and size. The scale lines are the interval of the white marks.

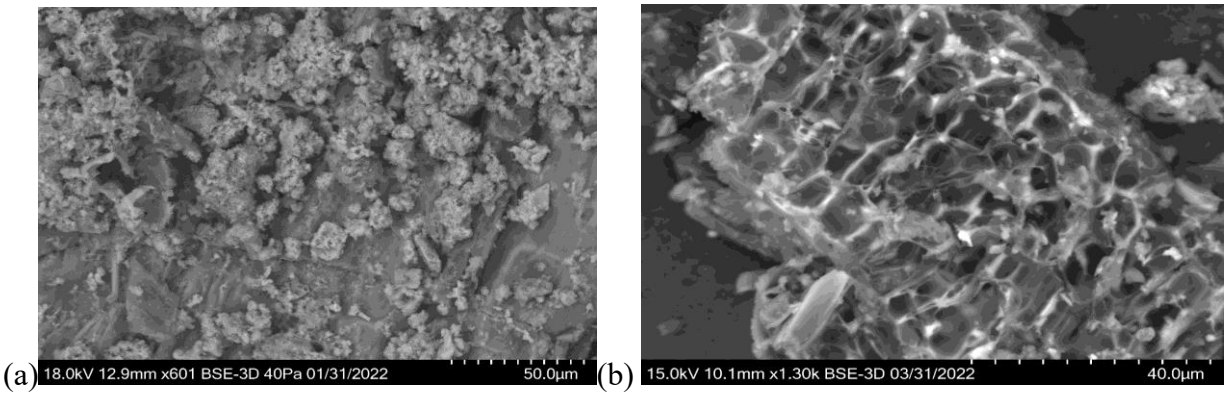

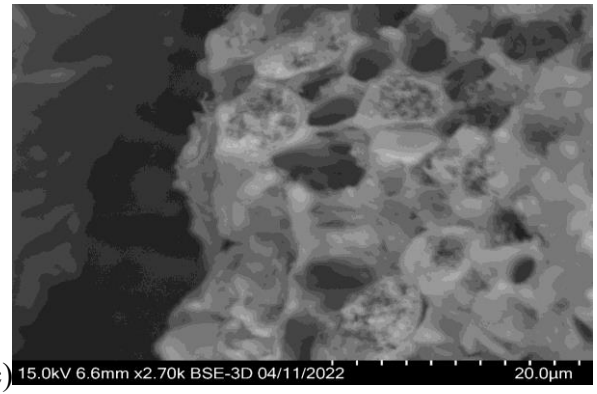

(c)

Figure 6.1.7.2: SEM images of samples 7, 15, and 23 (surface area and porosity).

(a) sample 7, (b) sample 15 (repetition of experiment 7), (c) sample 23 (repetition of experiment 7). The mean pore size is larger than 50nm, and some pores observed in this micrograph are between 1 and 2µm; therefore, most of them are in the range size of macropores according to IUPAC standards.

Elemental analysis (EDS)

The energy-dispersive X-ray spectroscopy was used for the elemental analysis or chemical characterization of the BBAC sample. The chemical elements present in the sample and relative abundance (measured as a percentage in the sample) are distributed as follows: (a) 80.0% carbon, 10.9% oxygen, 5.3% chlorine, and 2.7% calcium, (b) 71.0% carbon, 16.2% oxygen, 5.8% chlorine, and 3.3% calcium, and (c) 59.2% carbon, 30.5% oxygen, 0.3% chlorine, and 0.1% calcium. The other elements found are considered contamination in the samples.

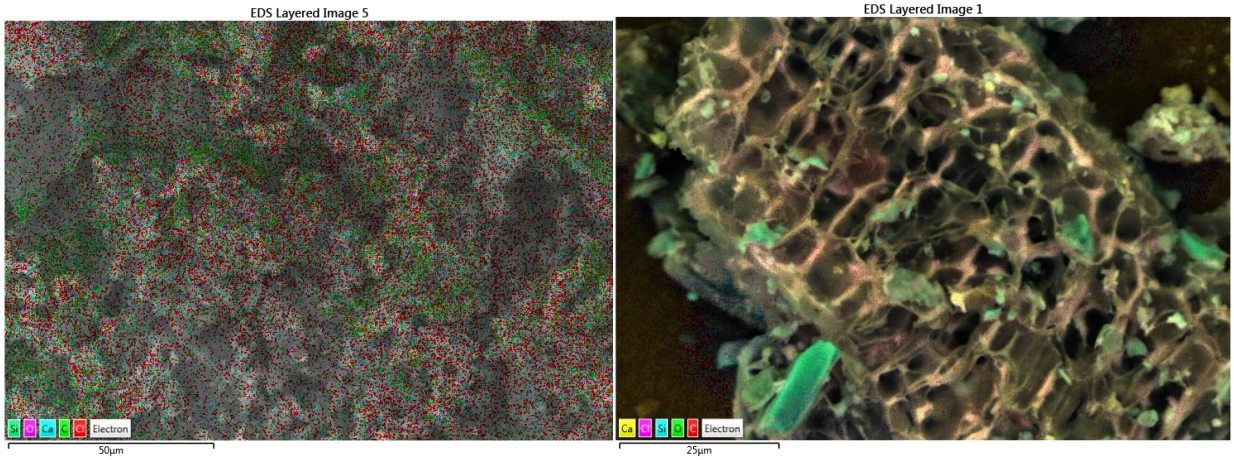

(a) (b)

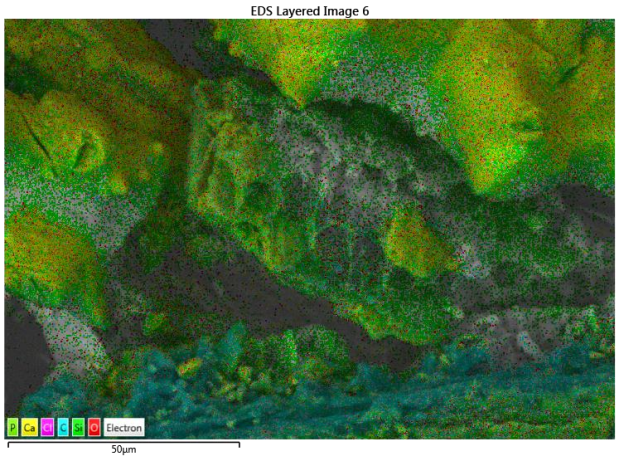

(c)

Figure 6.1.7.3: EDS elemental analysis of samples 7, 15, and 23.

(a) sample 7, (b) sample 15 (repetition of experiment 7), (c) sample 23 (repetition of experiment 7). EDS images show site and chemical elements in the sample in different colors. The image show carbon with a small amount on the surface of the activating agent, calcium chloride.

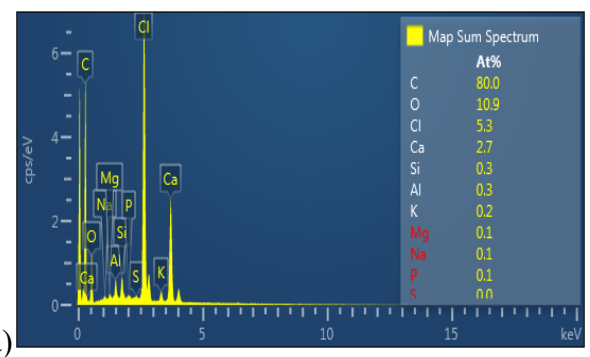

(a)

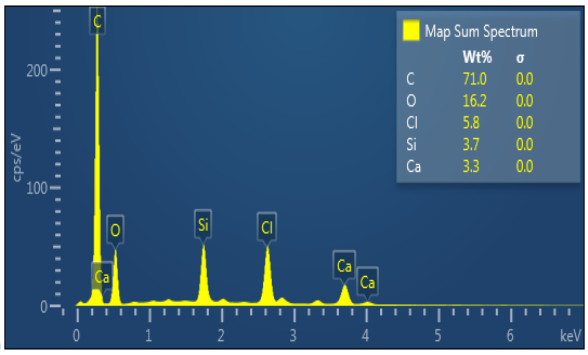

(b)

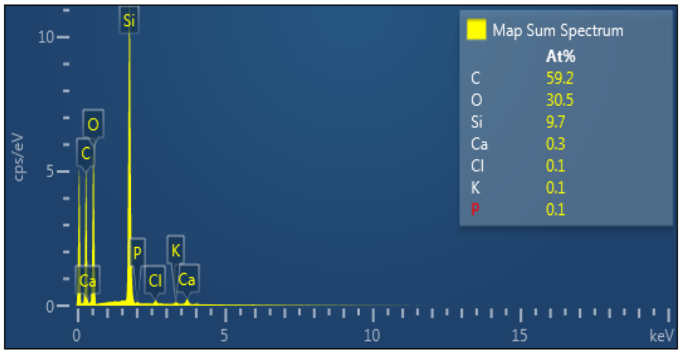

(c)

Figure 6.1.7.4: EDS graphs showing weight percentage of elements in samples 7,15 and 23

(a) sample 7, (b) sample 15, (c) sample 23.EDS graphs show the weight percentage of the chemical elements found in the sample.

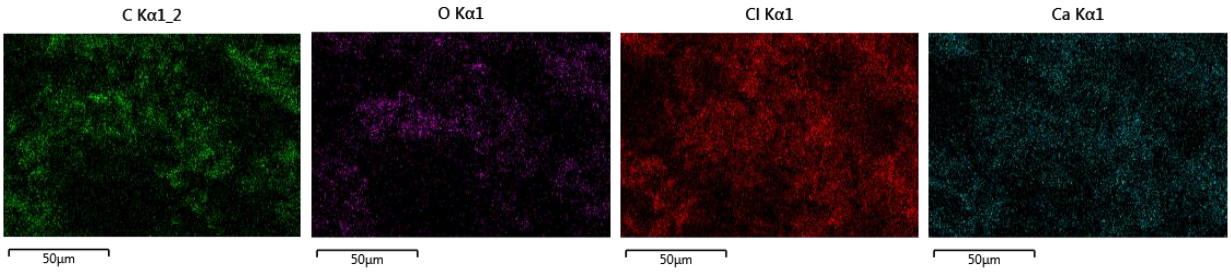

(a) sample 7

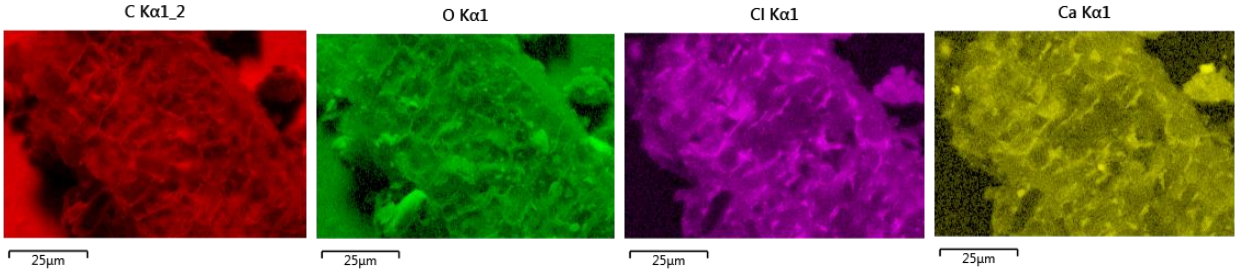

(b) sample 15

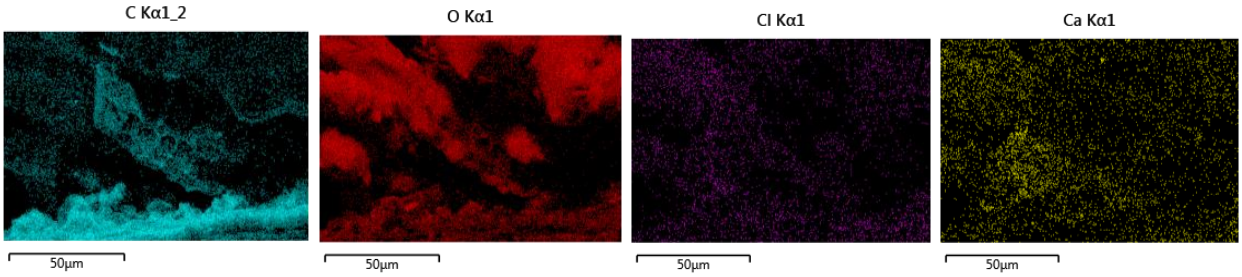

(c) sample 23

Figure 6.1.7.5: EDS images showing distribution of elements present in samples 7,15 and 23

6.1.8 Sample 8, 16, and 24

Precursor material: rice husk

Carbonization temperature and time: 500-600°C/ 3H

Activation method and agent, temperature, and time: chemical activation/CaCl, 300-500°C/3 H

SEM Observations:

The particle size is in an approximate range of 3µm to 600µm (in the largest dimension); therefore, considered a GAC because a higher percentage of the particles in the sample are in the GAC range size. The surface area is very irregular, with characteristics observed at 500, 200, and 20 µm magnification.

(a) 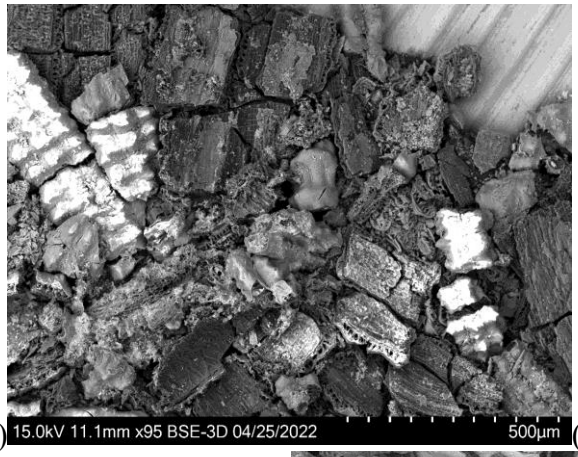

(b) 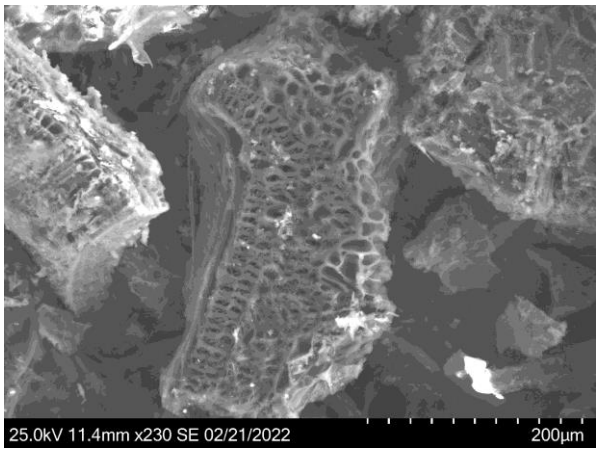

(c) 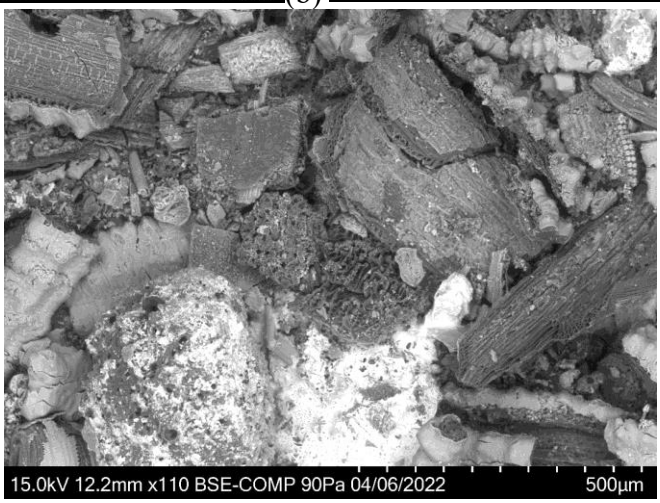

Figure 6.1.8.1: SEM images of samples 8, 16, and 24 (particle size and shape)

(a) sample 8, (b) sample 16 (repetition of experiment 8), (c) sample 24 (repetition of experiment 5). SEM micrographs for rice husk-based activated carbon showing particle's shape and size. The scale lines are the interval of the white marks.

(a) 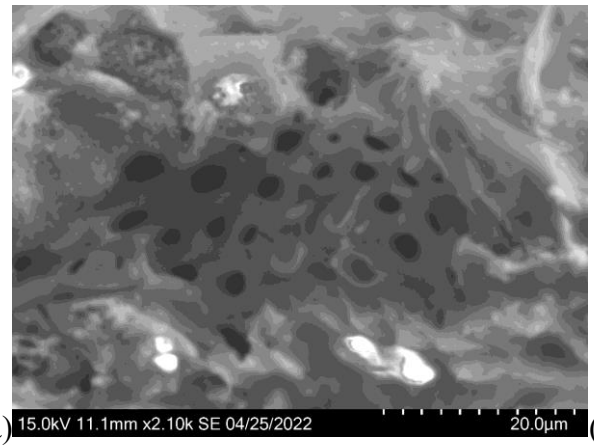

(b) 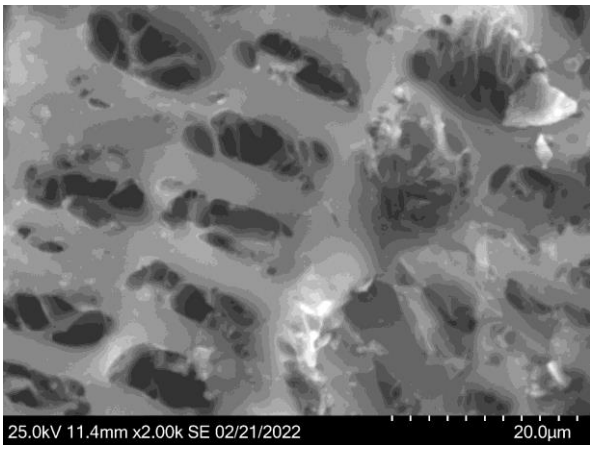

(c) 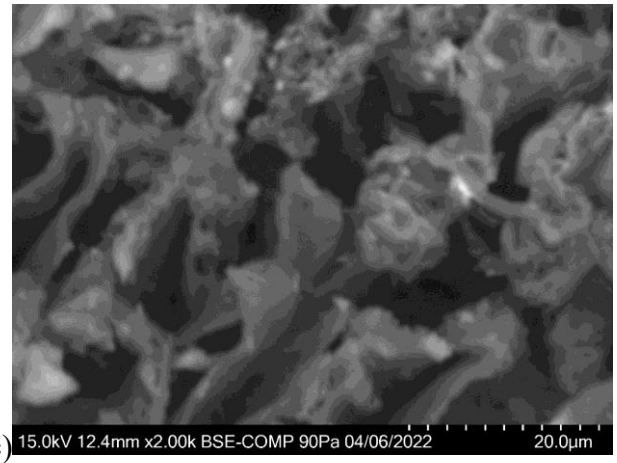

Figure 6.1.8.2: SEM images of samples 8, 16, and 24 (surface area and porosity).

(a) sample 8, (b) sample 16 (repetition of experiment 8), (c) sample 24 (repetition of experiment 8). The mean pore size is larger than 50nm, and some pores observed in this micrograph are between 1 and 2µm; therefore, most of them are in the range size of macropores and mesopores, according to IUPAC standards.

Elemental analysis (EDS)

The energy-dispersive X-ray spectroscopy was used for the elemental analysis or chemical characterization of the BBAC sample. The chemical elements present in the sample and relative abundance (measured as a percentage in the sample) are distributed as follows: (a) 38.9% carbon, 31.0% oxygen, 11.6% chlorine, and 6.3% calcium, (b) 83.0% carbon, 14.1% oxygen, 1.3% chlorine, and 0.9% calcium, and (c) 61.0% carbon, 21.4% oxygen, 5.7% chlorine, and 3.6%

calcium. The silicon and other element particles are contaminants because the small rocks were not completely removed from the samples.

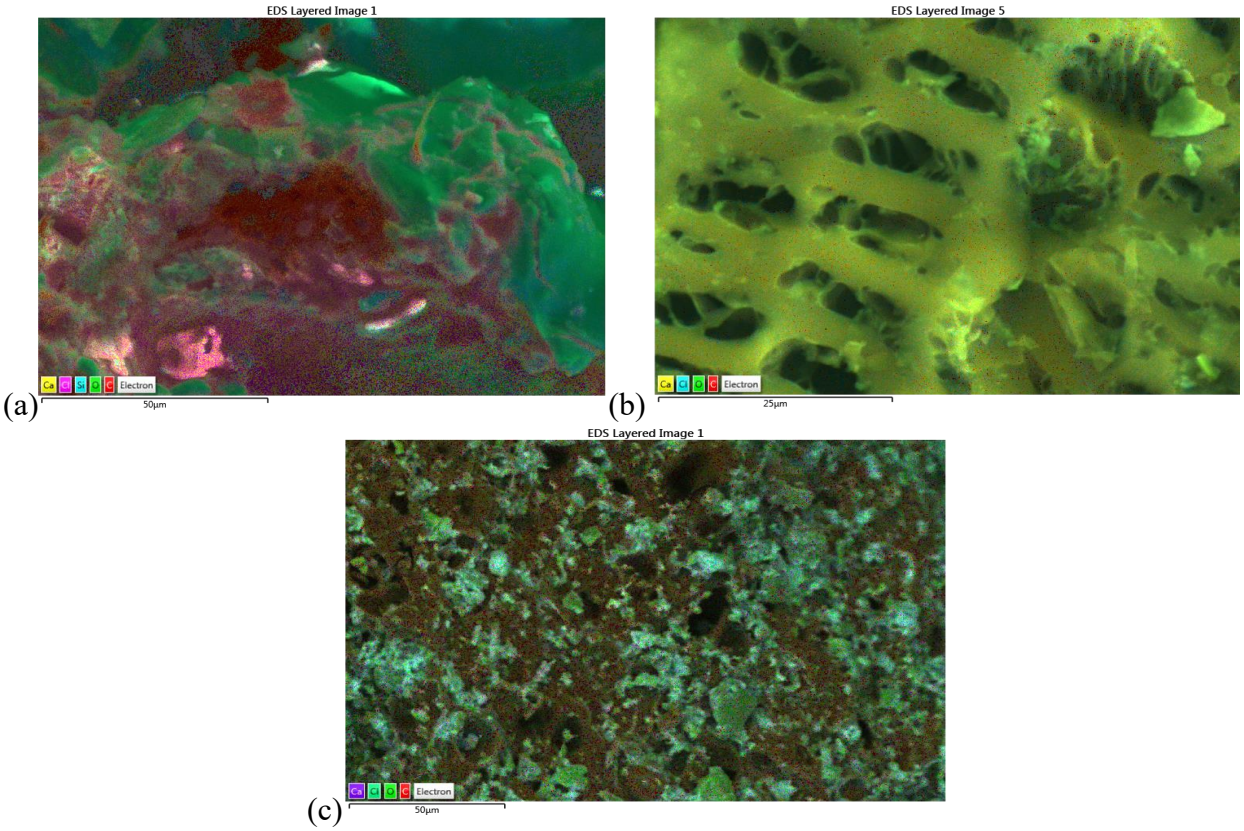

(a) (b) (c)

Figure 6.1.8.3: EDS elemental analysis of samples 8, 16, and 24.

(a) sample 8, (b) sample 16 (repetition of experiment 5), (c) sample 24 (repetition of experiment 5). Elemental analysis (EDS) images show chemical elements in the sample in different colors.

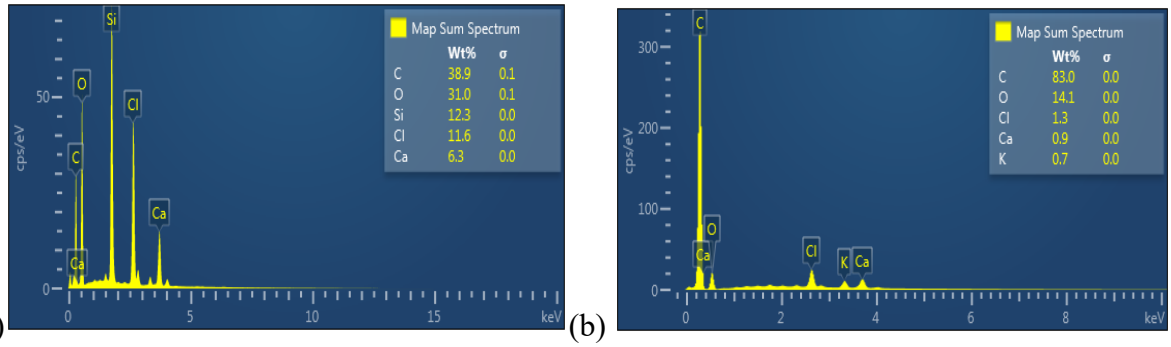

(a) (b)

(c) 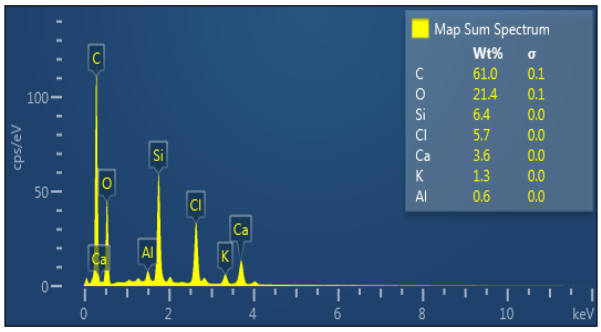

Figure 6.1.8.4: EDS graphs showing weight percentage of elements in samples 8,16, and 24.

(a) sample 8, (b) sample 16, (c) sample 24.EDS graphs show the weight percentage of the chemical elements found in the sample.

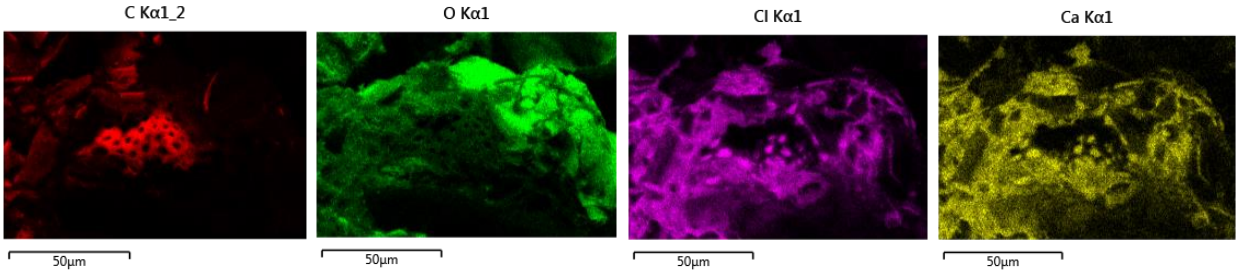

(a) Sample 8

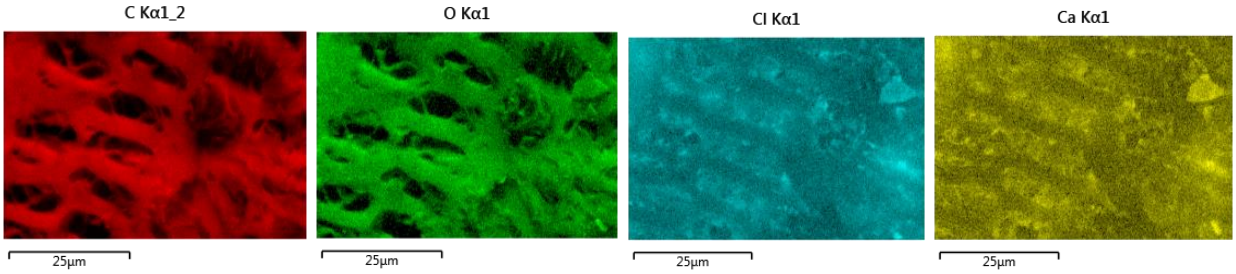

(b) Sample 16

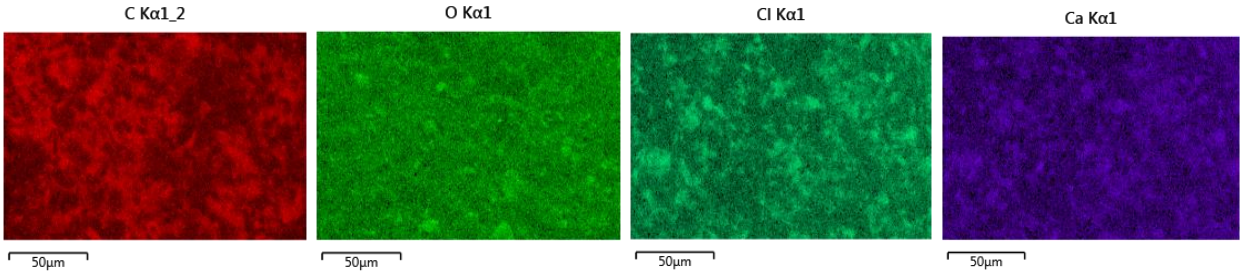

(c) Sample 24

Figure 6.1.8.5: EDS images showing distribution of elements present in samples 8,16 and 24

EDS images show the distribution of chemical elements in the sample. Carbon in red, oxygen in green, calcium in yellow in (a) and (b), and purple in (c), and chlorine in purple color in (a), blue in (b), and green in (c).

6.1.9 Commercial coal-based activated carbon sample

SEM Observations:

The particle size is in an approximate range of 300µm to 900µm (in the largest dimension); therefore, considered a GAC. The surface area is very irregular, with characteristics observed at 500, 20, and 10 µm magnification.

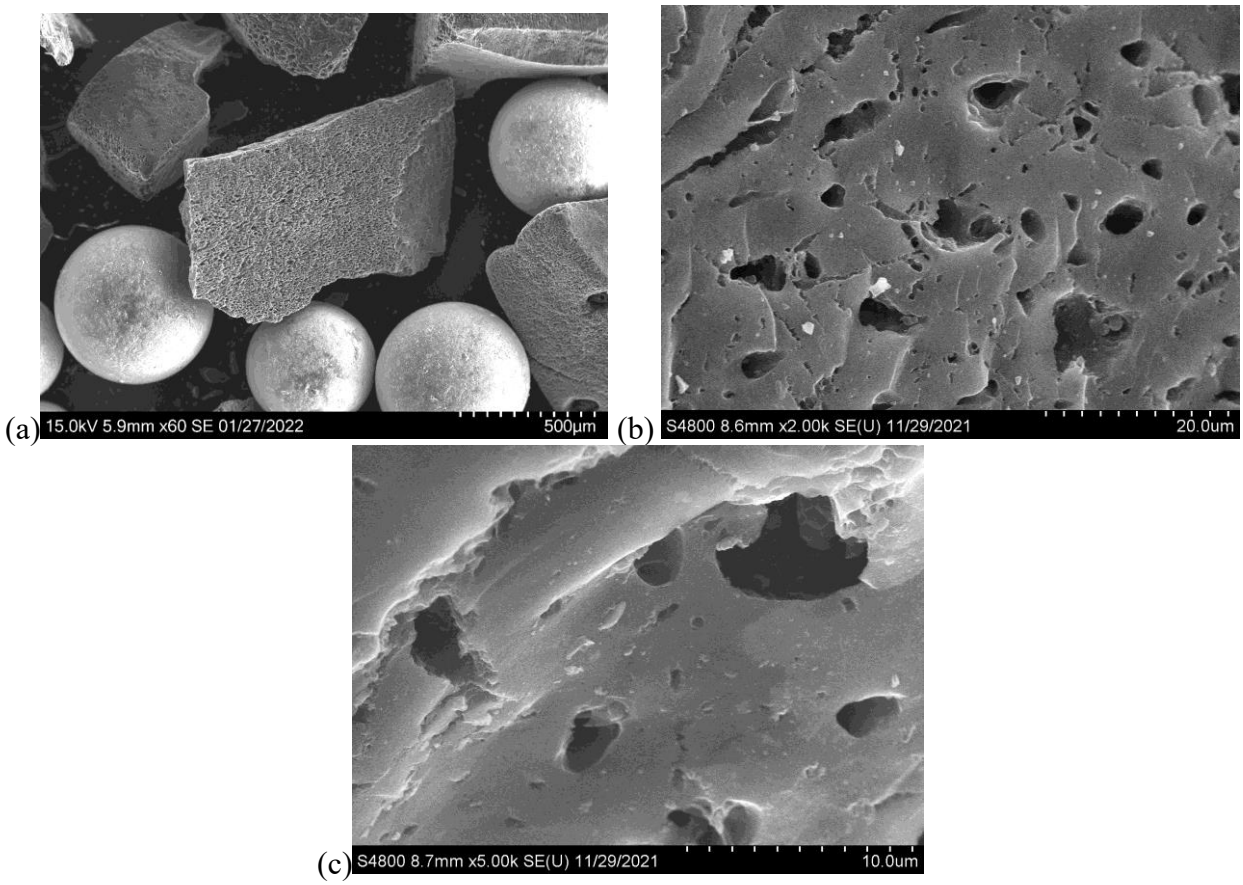

Figure 6.1.9.1: SEM images of commercial coal-based AC (particle size and shape).

(a) CCAC sample micrograph at 500 µm of magnification showing particles' shape and size, (b) CCAC sample at 20 µm of magnification showing the surface area with a high number of pores, (c) CCAC sample at 10 µm of magnification showing micropores and mesopores on the particle's surface area.

Elemental analysis (EDS)

The energy-dispersive X-ray spectroscopy was used for the elemental analysis or chemical characterization of the CCAC sample. The chemical elements present in the sample and relative abundance (measured as a percentage in the sample) are distributed as follows: (a) 80.2% carbon, 18.6% oxygen, 0.5% potassium, and 0.7% aluminum.

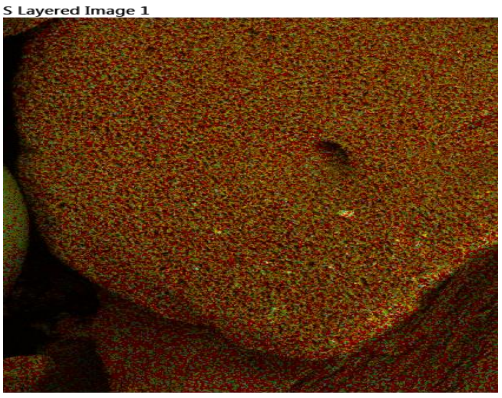

Figure 6.1.9.2: EDS elemental analysis of commercial coal-based AC.

Elemental analysis (EDS) image shows chemical elements in the sample in different colors.

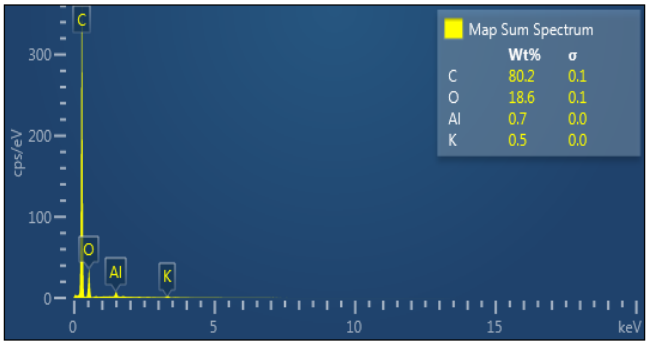

Figure 6.1.9.3: EDS graphs showing weight percentage of elements in commercial AC.

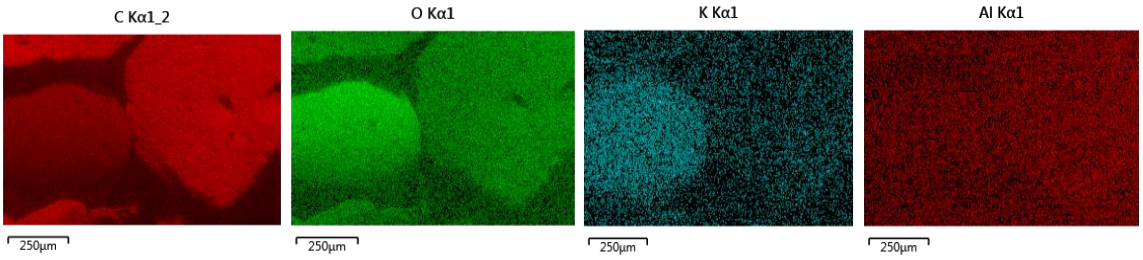

Figure 6.1.9.4: EDS images showing distribution of elements in commercial coal-based AC.

EDS images show the distribution of chemical elements in the sample. Carbon is red, oxygen is green, potassium is blue, and aluminum is red.

6.2 ACTIVATED CARBON ADSORPTION EXPERIMENTS RESULTS

The amount of arsenic adsorbed onto the ACs at equilibrium was quantified using the ICP-OES equipment, and the metalloid analysis was performed using an Inductively Coupled Plasma Optical Emission Spectroscopy ICP-OES Perkin Elmer Optima 7300DV according to standard methods (US EPA 1994 Method 200.7). Dissolved arsenic was determined in filtered samples (filtration removed particles larger than 0.45 μm). The method detection limit (MDL) for the ICP-OES (April 2022) for arsenic was 0.0096 mg/L; MDL was calculated as 3.14 times the standard deviation of seven spikes with recoveries between 50 and 100 % of the spiked concentration.

For the analysis, a small amount (~0. 0025 g) of BBAC from the second repetition (samples 9 to 16) of the DOE and a sample of CCAC were weighed on an aluminum plate. The samples were then dissolved in 0.2 L of water with five different concentrations (~0.25, 0.15, 0.1, 0.05, and 0.025 mg/L) of arsenic compound (Na_2HAsO_4) to obtain the arsenic solution and placed in a magnetic stirrer for 2 hours as discussed in the methodology chapter. With the initial and final concentrations of arsenic dissolved in water, density (qe) and removal percentage achieved by the ACs can be calculated using the formula: $qe = \frac{V}{M}(Co - Ce)$, and isotherms graphs can be developed (Figures 6.2.1 to 6.2.9). The samples were labeled and analyzed according to the arrangement of the DOE matrix. Data obtained from these experiments were used for the statistical analysis (Table 6.2).

Table 6.2: Experimental isotherm data

Sample #	Dosage AC g	Volume L	CoAs mg/L	CeAs mg/L	qe mg/g	Removal %
9E	0.0022	0.2	0.023	0.023	0.004	0.178
9D	0.0022	0.2	0.054	0.054	0.030	0.604
9C	0.0023	0.2	0.105	0.095	0.911	9.830
9B	0.0022	0.2	0.154	0.143	1.068	7.439
9A	0.0021	0.2	0.263	0.237	2.451	9.849
10E	0.0024	0.2	0.023	0.017	0.539	27.507
10D	0.0026	0.2	0.054	0.034	1.594	38.133
10C	0.0022	0.2	0.105	0.105	0.015	0.158
10B	0.0021	0.2	0.154	0.154	0.032	0.222
10A	0.0022	0.2	0.263	0.239	2.088	8.865
11E	0.0021	0.2	0.023	0.023	0.004	0.178
11D	0.0022	0.2	0.054	0.054	0.029	0.604
11C	0.0023	0.2	0.105	0.096	0.829	9.139
11B	0.0023	0.2	0.154	0.141	1.188	8.854
11A	0.0023	0.2	0.263	0.247	1.348	5.902
12E	0.0023	0.2	0.023	0.022	0.048	2.396
12D	0.0023	0.2	0.054	0.035	1.652	34.822
12C	0.0021	0.2	0.105	0.075	2.970	28.948
12B	0.0020	0.2	0.154	0.146	0.830	5.458
12A	0.0020	0.2	0.263	0.245	1.712	6.519
13E	0.0023	0.2	0.023	0.007	1.419	70.531
13D	0.0023	0.2	0.054	0.039	1.319	27.562
13C	0.0022	0.2	0.105	0.090	1.348	14.233
13B	0.0023	0.2	0.154	0.113	3.570	26.487
13A	0.0021	0.2	0.263	0.220	4.090	16.355
14E	0.0021	0.2	0.023	0.022	0.108	4.995
14D	0.0022	0.2	0.054	0.041	1.267	25.298
14C	0.0022	0.2	0.105	0.078	2.532	26.118
14B	0.0021	0.2	0.154	0.146	0.784	5.231
14A	0.0022	0.2	0.263	0.235	2.600	10.644
15E	0.0023	0.2	0.023	0.019	0.374	18.688
15D	0.0022	0.2	0.054	0.051	0.332	6.604
15C	0.0021	0.2	0.105	0.099	0.609	5.935
15B	0.0022	0.2	0.154	0.152	0.216	1.515
15A	0.0020	0.2	0.263	0.239	2.368	8.836
16E	0.0023	0.2	0.023	0.023	0.004	0.178
16D	0.0021	0.2	0.054	0.015	3.807	71.827
16C	0.0022	0.2	0.105	0.079	2.354	24.843
16B	0.0023	0.2	0.154	0.064	7.891	58.542
16A	0.0023	0.2	0.263	0.188	6.559	28.471
COM-E	0.0028	0.2	0.023	0.023	0.003	0.178
COM-D	0.0021	0.2	0.054	0.054	0.031	0.604
COM-C	0.0028	0.2	0.105	0.105	0.012	0.158
COM-B	0.0020	0.2	0.154	0.125	2.912	18.868
COM-A	0.0022	0.2	0.263	0.232	2.805	11.698

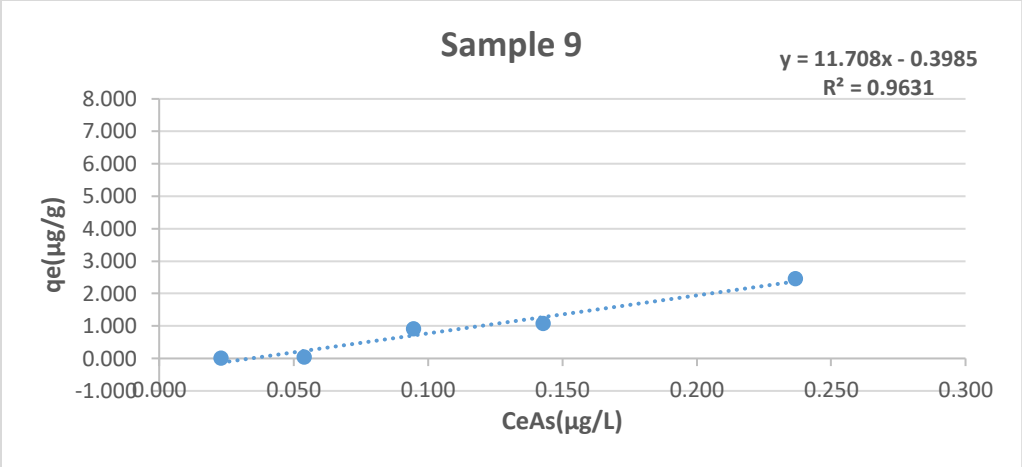

Figure 6.2.1: Adsorption isotherm for binding of Na2HAsO4 onto BBAC-DOE 9 using linear regression.

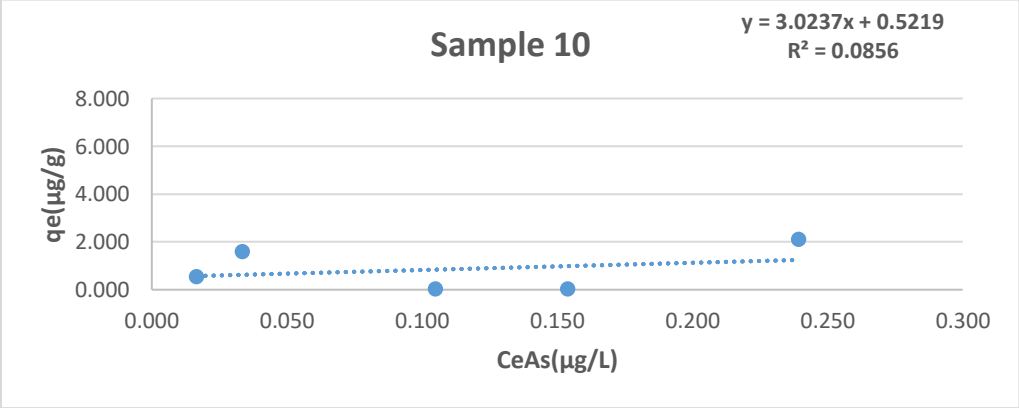

Figure 6.2.2: Adsorption isotherm for binding of Na2HAsO4 onto BBAC-DOE 10 using linear regression.

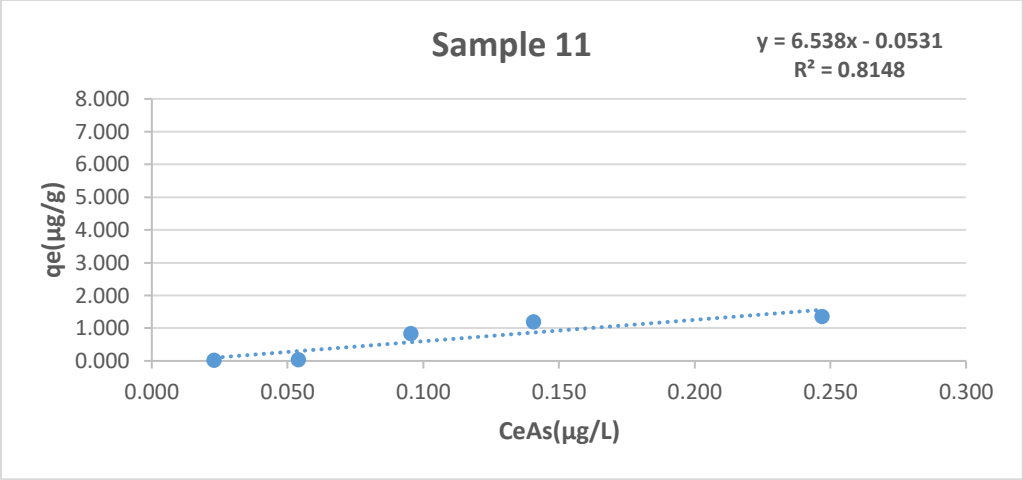

Figure 6.2.3: Adsorption isotherm for binding of Na2HAsO4 onto BBAC-DOE 11 using linear regression.

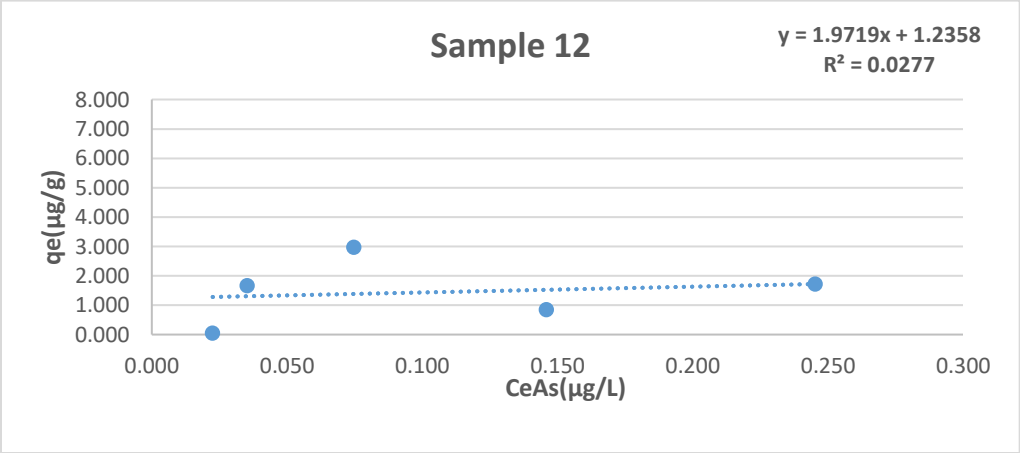

Figure 6.2.4: Adsorption isotherm for binding of Na2HAsO4 onto BBAC-DOE 12 using linear regression.

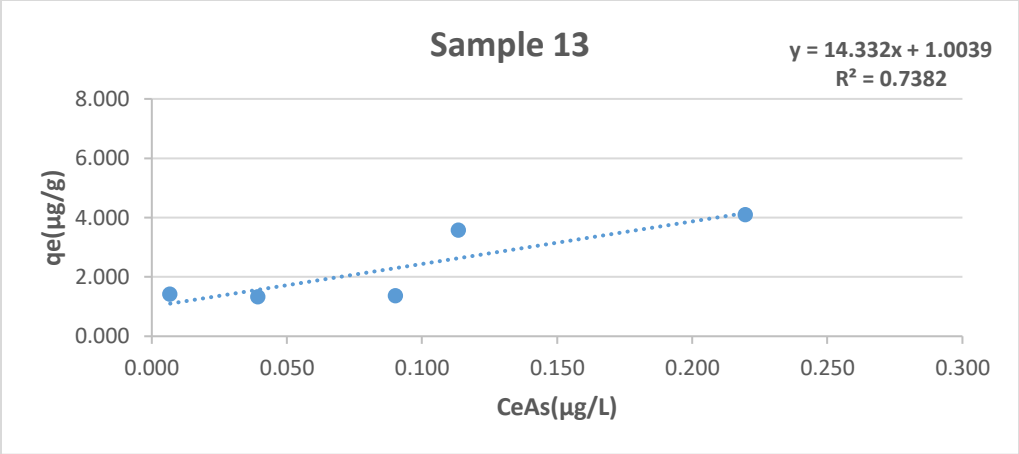

Figure 6.2.5: Adsorption isotherm for binding of Na2HAsO4 onto BBAC-DOE 13 using linear regression.

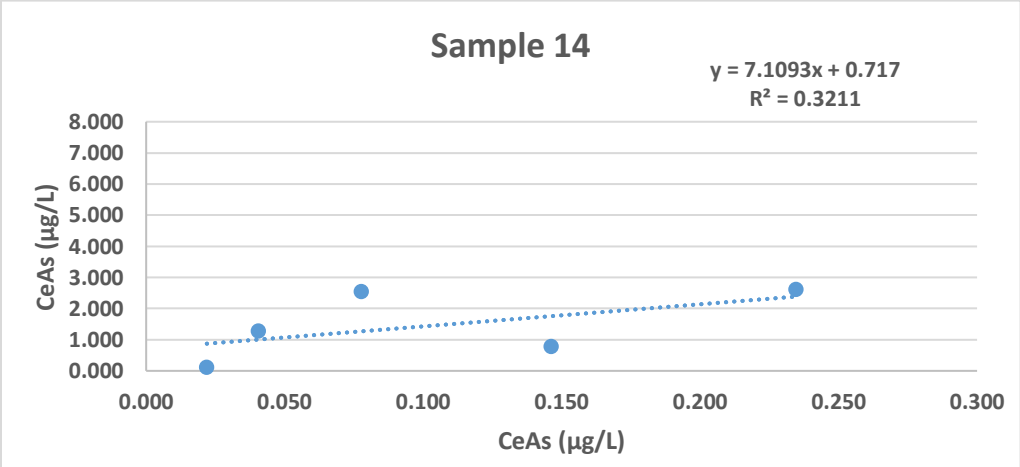

Figure 6.2.6: Adsorption isotherm for binding of Na2HAsO4 onto BBAC-DOE 14 using linear regression.

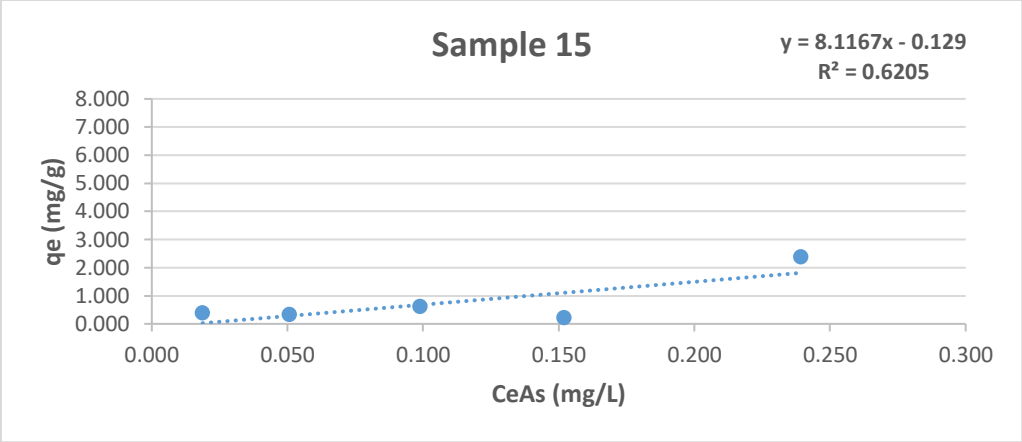

Figure 6.2.7: Adsorption isotherm for binding of Na2HAsO4 onto BBAC-DOE 15 using linear regression.

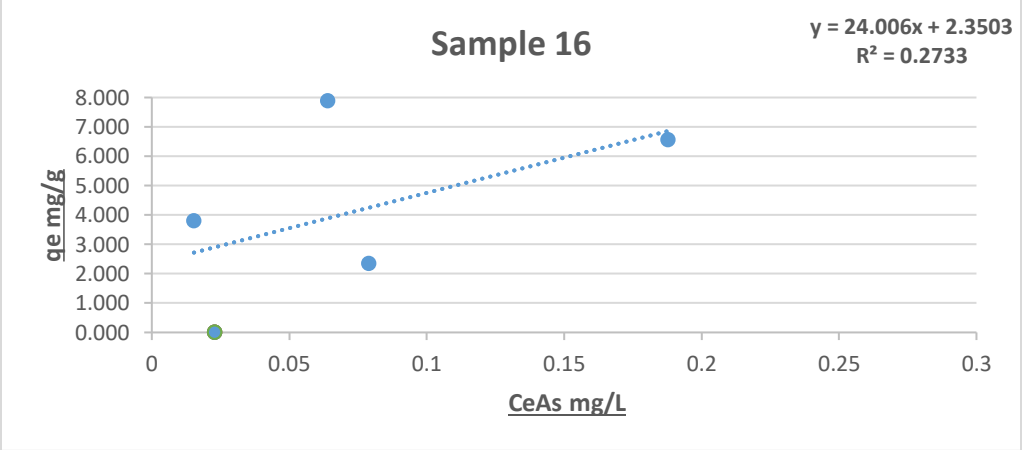

Figure 6.2.8: Adsorption isotherm for binding of Na2HAsO4 onto BBAC-DOE 16 using linear regression.

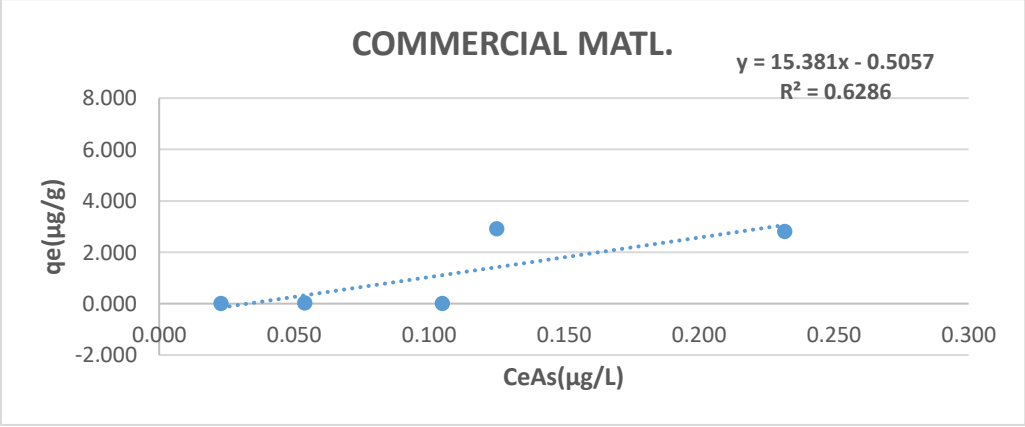

Figure 6.2.9: Adsorption isotherm for binding of Na2HAsO4 onto CCAC using linear regression.

6.3 LIFE CYCLE ASSESSMENT

The LCA methodology was implemented to evaluate and compare the potential environmental impacts of BBAC made from agricultural waste with CCAC made from hard coal. A cradle-to-grave analysis following ISO standards 14040 to 14044 with GaBi modeling software and GaBi Education_database_2020 was used to calculate the TRACI mid-point environmental impact categories (Global warming potential, Acidification potential, Eutrophication potential, Ozone layer depletion potential, Human Health Particulate Air potential, Ecotoxicity potential, Human Toxicity cancer, Human Toxicity non-cancer, Resources depletion fossil fuels and Smog to air). The product system for BBACs made from agricultural waste acquisition until end-of-life and landfill disposal included five main processes with subprocesses depending on the process flow characteristics (Figures 6.3.1, 6.3.3, 6.3.5, 6.3.7, 6.3.9, 6.3.11, 6.3.13, 6.3.15). Inputs and outputs have small differences in the inventory data according to the characteristics of the process set in the DOE matrix.

One of the most critical steps in calculating the environmental impact assessment is the life cycle inventory, including the inputs and outputs values for all the processes needed to produce activated carbon. Data obtained from equipment suppliers' specifications, literature, and databases were used for inputs and outputs inventory. In addition, the study uses publicly available data from the U.S. Department of Energy and EPA. For CCAC production best available technology (BAT) was considered. The study assumed relatively low levels of waste and emissions leaving the system boundaries, recycled and reused water, and distances from production facilities. The following tables show the inventory data for each one of the BBACs and the CCAC (Tables 6.3.1. to 6.3.9).

Table 6.3.1: System Inventory and Data Analysis DOE 1

Raw material acquisition phase for a BBAC

Flow	Material	Amounts/Units	Nation
Input	Peanut shell	7 kg	MX
Output	Peanut shell	7 kg	MX

Transportation of raw material to the processing place (short distance < 10 km)

Flow	Flow type	Amount/Units	Nation
Input	Peanut shell	7 kg	MX
Input	Gasoline/diesel (light cargo vehicle)	5 L (160 oz)	----------
Output	Peanut shell	7 kg	MX
Output	CO_2	1.2 kg	USA
	(Transport input/output source: GaBi Database & CO_2 emissions from EPA website: www.fueleconomy.gov)		

Preparation of Material for Processing Phase

Flow	Flow type	Amount/Units	Nation
Input	Peanut shell	7 kg	MX
Output	Material for production phase	7 kg	MX

Pyrolysis (Processing Phase)

Flow	Flow type	Amount/Units	Nation
Input	Peanut shell	7 kg	MX
Input	LP gas	3 kg	USA
Output	Biochar	1 kg	---------
Output	Ash & residues	6 kg	---------
Output	CO_2	8.97 kg	USA

(Source: U.S. Energy Information Administration: www.eia.gov>environment>emission)

Chemical Activation (Impregnation Phase)

Flow	Flow type	Amount/Units	Nation
Input	Biochar	1 kg	----------
Input	Freshwater	0.3 L (9.6oz)	USA
Input	KOH activating agent	0.1 kg	USA
Output	Activated biochar	1 kg	---------

Washing (Processing Phase)

Flow	Flow type	Amount/Units	Nation
Input	Activated biochar	1 kg	---------
Input	Freshwater	10 L (320oz)	USA
Output	Washed activated biochar	1 kg	---------
Output	Wastewater	10 L (320oz)	USA

Drying (Processing Phase)

Flow	Flow type	Amount/Units	Nation
Input	Washed activated biochar	1 kg	---------
Input	LP gas	1 kg	USA
Output	Dried AC	1 kg	---------
Output	CO_2	2.99 kg	USA

(Source: U.S. Energy Information Administration: www.eia.gov>environment>emission)

Crushing and Sieving (Processing Phase)

Flow	Flow type	Amount/Units	Nation
Input	Dried AC	1 kg	---------
Output	Granular AC (GAC)	1 kg	---------

Packaging and storage (Processing Phase)

Flow	Flow type	Amount/Units	Nation
Input	GAC	1 kg	---------
Output	GAC	1 kg	---------

Transportation of GAC to the place where it is going to be used (short distance < 10 km)

Flow	Flow type	Amount/Units	Nation
Input	GAC	1 kg	MX
Input	Gasoline/diesel (light cargo vehicle)	5 L (160 oz)	---------
Output	GAC	1 kg	MX
Output	CO_2	0.1 kg	USA
	(Transport input/output source: GaBi Database & CO_2 emissions from EPA website: www.fueleconomy.gov)		

GAC Filter (Use Phase)

Flow	Flow type	Amount/Units	Nation
Input	GAC used for filtration	1 kg	---------
Output	GAC used for filtration	1 kg	---------

End of Life Phase (Disassembly Phase of the filter is not considered in the analysis)

Flow	Flow type	Amount/Units	Nation
Input	Used GAC	1 kg	---------
Output	Landfill disposal, municipal solid waste	1 kg	USA

(Landfill disposal source: GaBi Education_database_2020)

Table 6.3.2: System Inventory and Data Analysis DOE 2

Raw material acquisition phase for a BBAC

Flow	Material	Amounts/Units	Nation
Input	Peanut shell	7 kg	MX
Output	Peanut shell	7 kg	MX

Transportation of raw materials to the processing place

Flow	Flow type	Amount/Units	Nation
Input	Peanut shell	7 kg	MX
Input	Gasoline/diesel (light cargo vehicle)	5 L (160 oz)	---------
Output	Peanut shell	7 kg	MX
Output	CO_2	1.2 kg	USA
	(Transport input/output source: GaBi Database & CO_2 emissions from EPA website: www.fueleconomy.gov)		

Preparation of Material for Processing Phase

Flow	Flow type	Amount/Units	Nation
Input	Peanut shell	7 kg	MX
Output	Material for production phase	7 kg	MX

Pyrolysis (Processing Phase)

Flow	Flow type	Amount/Units	Nation
Input	Peanut shell	7 kg	MX
Input	LP gas	2 kg	USA
Output	Biochar	1 kg	---------
Output	Ash & residues	6 kg	---------
Output	CO_2	5.98 kg	USA

(Source: U.S. Energy Information Administration: www.eia.gov>environment>emission)

Chemical Activation (Impregnation Phase)

Flow	Flow type	Amount/Units	Nation
Input	Biochar	1 kg	----------
Input	Freshwater	0.3 L (9.6oz)	USA
Input	KOH activating agent	0.1 kg	USA
Output	Activated biochar	1 kg	---------

Washing (Processing Phase)

Flow	Flow type	Amount/Units	Nation
Input	Activated biochar	1 kg	---------
Input	Freshwater	10 L (320oz)	USA
Output	Washed activated biochar	1 kg	---------
Output	Wastewater	10 L (320oz)	USA

Drying (Processing Phase)

Flow	Flow type	Amount/Units	Nation
Input	Washed activated biochar	1 kg	---------
Input	LP gas	1 kg	USA
Output	Dried AC	1 kg	---------
Output	CO_2	2.99 kg	USA

(Source: U.S. Energy Information Administration: www.eia.gov>environment>emission)

Crushing and Sieving (Processing Phase)

Flow	Flow type	Amount/Units	Nation
Input	Dried AC	1 kg	---------
Output	Granular AC (GAC)	1 kg	---------

Packaging and storage (Processing Phase)

Flow	Flow type	Amount/Units	Nation
Input	GAC	1 kg	---------
Output	GAC	1 kg	---------

Transportation of GAC to the place where it is going to be used (short distance < 10 km)

Flow	Flow type	Amount/Units	Nation
Input	GAC	1 kg	MX
Input	Gasoline/diesel (light cargo vehicle)	5 L (160 oz)	---------
Output	GAC	1 kg	MX
Output	CO_2	0.1 kg	USA
	(Transport input/output source: GaBi Database & CO_2 emissions from EPA website: www.fueleconomy.gov)		

GAC Use Phase

Flow	Flow type	Amount/Units	Nation
Input	GAC used for filtration	1 kg	---------
Output	GAC used for filtration	1 kg	---------

End of Life GAC Phase

Flow	Flow type	Amount/Units	Nation
Input	Used GAC	1 kg	---------
Output	Landfill disposal, municipal solid waste	1 kg	USA
	(Landfill disposal source: GaBi Education_database_2020)		

Table 6.3.3: System Inventory and Data Analysis DOE 3

Raw material acquisition phase for a BBAC

Flow	Material	Amounts/Units	Nation
Input	Peanut shell	7 kg	MX
Output	Peanut shell	7 kg	MX

Transportation of raw materials to the processing place

Flow	Flow type	Amount/Units	Nation
Input	Peanut shell	7 kg	MX
Input	Gasoline/diesel (light cargo vehicle)	5 L (160 oz)	---------
Output	Peanut shell	7 kg	MX
Output	CO_2	1.2 kg	USA
	(Transport input/output source: GaBi Database & CO_2 emissions from EPA website: www.fueleconomy.gov)		

Preparation of Material for Processing Phase

Flow	Flow type	Amount/Units	Nation
Input	Peanut shell	7 kg	MX
Output	Material for production phase	7 kg	MX

Pyrolysis (Processing Phase)

Flow	Flow type	Amount/Units	Nation
Input	Peanut shell	7 kg	MX
Input	LP gas	3 kg	USA
Output	Biochar	1 kg	---------
Output	Ash & residues	6 kg	---------
Output	CO_2	8.97 kg	USA

(Source: U.S. Energy Information Administration: www.eia.gov>environment>emission)

Chemical Activation (Impregnation Phase)

Flow	Flow type	Amount/Units	Nation
Input	Biochar	1 kg	----------
Input	Freshwater	0.3 L (9.6oz)	USA
Input	CaCl activating agent	0.1 kg	USA
Output	Activated biochar	1 kg	---------

Washing (Processing Phase)

Flow	Flow type	Amount/Units	Nation
Input	Activated biochar	1 kg	---------
Input	Freshwater	10 L (320oz)	USA
Output	Washed activated biochar	1 kg	---------
Output	Wastewater	10 L (320oz)	USA

Drying (Processing Phase)

Flow	Flow type	Amount/Units	Nation
Input	Washed activated biochar	1 kg	---------
Input	LP gas	1 kg	USA
Output	Dried AC	1 kg	---------
Output	CO_2	2.99 kg	USA

(Source: U.S. Energy Information Administration: www.eia.gov>environment>emission)

Crushing and Sieving (Processing Phase)

Flow	Flow type	Amount/Units	Nation
Input	Dried AC	1 kg	---------
Output	Granular AC (GAC)	1 kg	---------

Packaging and storage (Processing Phase)

Flow	Flow type	Amount/Units	Nation
Input	GAC	1 kg	---------
Output	GAC	1 kg	---------

Transportation of GAC to the place where it is going to be used (short distance < 10 km)

Flow	Flow type	Amount/Units	Nation
Input	GAC	1 kg	MX
Input	Gasoline/diesel (light cargo vehicle)	5 L (160 oz)	---------
Output	GAC	1 kg	MX
Output	CO_2	1.2 kg	USA
	(Transport input/output source: GaBi Database & CO_2 emissions from EPA website: www.fueleconomy.gov)		

GAC Use Phase

Flow	Flow type	Amount/Units	Nation
Input	GAC used for filtration	1 kg	---------
Output	GAC used for filtration	1 kg	---------

End of Life GAC Phase

Flow	Flow type	Amount/Units	Nation
Input	Used GAC	1 kg	---------
Output	Landfill disposal, municipal solid waste	1 kg	USA

(Landfill disposal source: GaBi Education_database_2020)

Table 6.3.4: System Inventory and Data Analysis DOE 4

Raw material acquisition phase for a BBAC

Flow	Material	Amounts/Units	Nation
Input	Peanut shell	7 kg	MX
Output	Peanut shell	7 kg	MX

Transportation of raw materials to the processing place

Flow	Flow type	Amount/Units	Nation
Input	Peanut shell	7 kg	MX
Input	Gasoline/diesel (light cargo vehicle)	5 L (160 oz)	---------
Output	Peanut shell	7 kg	MX
Output	CO_2	1.2 kg	USA
	(Transport input/output source: GaBi Database & CO_2 emissions from EPA website: www.fueleconomy.gov)		

Preparation of Material for Processing Phase

Flow	Flow type	Amount/Units	Nation
Input	Peanut shell	7 kg	MX
Output	Material for production phase	7 kg	MX

Pyrolysis (Processing Phase)

Flow	Flow type	Amount/Units	Nation
Input	Peanut shell	7 kg	MX
Input	LP gas	2 kg	USA
Output	Biochar	1 kg	---------
Output	Ash & residues	6 kg	---------
Output	CO_2	5.98 kg	USA

(Source: U.S. Energy Information Administration: www.eia.gov>environment>emission)

Chemical Activation (Impregnation Phase)

Flow	Flow type	Amount/Units	Nation
Input	Biochar	1 kg	----------
Input	Freshwater	0.3 L (9.6oz)	USA
Input	CaCl activating agent	0.1 kg	USA
Output	Activated biochar	1 kg	---------

Washing (Processing Phase)

Flow	Flow type	Amount/Units	Nation
Input	Activated biochar	1 kg	---------
Input	Freshwater	10 L (320oz)	USA
Output	Washed activated biochar	1 kg	---------
Output	Wastewater	10 L (320oz)	USA

Drying (Processing Phase)

Flow	Flow type	Amount/Units	Nation
Input	Washed activated biochar	1 kg	---------
Input	LP gas	1 kg	USA
Output	Dried AC	1 kg	---------
Output	CO_2	2.99 kg	USA

(Source: U.S. Energy Information Administration: www.eia.gov>environment>emission)

Crushing and Sieving (Processing Phase)

Flow	Flow type	Amount/Units	Nation
Input	Dried AC	1 kg	---------
Output	Granular AC (GAC)	1 kg	---------

Packaging and storage (Processing Phase)

Flow	Flow type	Amount/Units	Nation
Input	GAC	1 kg	---------
Output	GAC	1 kg	---------

Transportation of GAC to the place where it is going to be used (short distance < 10 km)

Flow	Flow type	Amount/Units	Nation
Input	GAC	1 kg	MX
Input	Gasoline/diesel (light cargo vehicle)	5 L (160 oz)	---------
Output	GAC	1 kg	MX
Output	CO_2	1.2 kg	USA
	(Transport input/output source: GaBi Database & CO_2 emissions from EPA website: www.fueleconomy.gov)		

GAC Use Phase

Flow	Flow type	Amount/Units	Nation
Input	GAC used for filtration	1 kg	---------
Output	GAC used for filtration	1 kg	---------

End of Life GAC Phase

Flow	Flow type	Amount/Units	Nation
Input	Used GAC	1 kg	---------
Output	Landfill disposal, municipal solid waste	1 kg	USA

(Landfill disposal source: GaBi Education_database_2020)

Table 6.3.5: System Inventory and Data Analysis DOE 5

Raw material acquisition phase for a BBAC

Flow	Material	Amounts/Units	Nation
Input	Rice husk	6 kg	MX
Output	Rice husk	6 kg	MX

Transportation of raw materials to the processing place

Flow	Flow type	Amount/Units	Nation
Input	Rice husk	6 kg	MX
Input	Gasoline/diesel (light cargo vehicle)	50 L (160 oz)	---------
Output	Rice husk	6 kg	MX
Output	CO_2	12 kg	USA
	(Transport input/output source: GaBi Database & CO_2 emissions from EPA website: www.fueleconomy.gov)		

Preparation of Material for Processing Phase

Flow	Flow type	Amount/Units	Nation
Input	Rice husk	6 kg	MX
Output	Material for production phase	6 kg	MX

Pyrolysis (Processing Phase)

Flow	Flow type	Amount/Units	Nation
Input	Rice husk	6 kg	MX
Input	LP gas	3 kg	USA
Output	Biochar	1 kg	---------
Output	Ash & residues	6 kg	---------
Output	CO_2	8.97 kg	USA

(Source: U.S. Energy Information Administration: www.eia.gov>environment>emission)

Chemical Activation (Impregnation Phase)

Flow	Flow type	Amount/Units	Nation
Input	Biochar	1 kg	----------
Input	Freshwater	0.3 L (9.6oz)	USA
Input	KOH activating agent	0.1 kg	USA
Output	Activated biochar	1 kg	---------

Washing (Processing Phase)

Flow	Flow type	Amount/Units	Nation
Input	Activated biochar	1 kg	---------
Input	Freshwater	10 L (320oz)	USA
Output	Washed activated biochar	1 kg	---------
Output	Wastewater	10 L (320oz)	USA

Drying (Processing Phase)

Flow	Flow type	Amount/Units	Nation
Input	Washed activated biochar	1 kg	---------
Input	LP gas	1 kg	USA
Output	Dried AC	1 kg	---------
Output	CO_2	2.99 kg	USA

(Source: U.S. Energy Information Administration: www.eia.gov>environment>emission)

Crushing and Sieving (Processing Phase)

Flow	Flow type	Amount/Units	Nation
Input	Dried AC	1 kg	---------
Output	Granular AC (GAC)	1 kg	---------

Packaging and storage (Processing Phase)

Flow	Flow type	Amount/Units	Nation
Input	GAC	1 kg	---------
Output	GAC	1 kg	---------

Transportation of GAC to the place where it is going to be used (short distance < 50 km)

Flow	Flow type	Amount/Units	Nation
Input	GAC	1 kg	MX
Input	Gasoline/diesel (light cargo vehicle)	5 L (160 oz)	---------
Output	GAC	1 kg	MX
Output	CO_2	1.2 kg	USA
	(Transport input/output source: GaBi Database & CO_2 emissions from EPA website: www.fueleconomy.gov)		

GAC Use Phase

Flow	Flow type	Amount/Units	Nation
Input	GAC used for filtration	1 kg	---------
Output	GAC used for filtration	1 kg	---------

End of Life GAC Phase

Flow	Flow type	Amount/Units	Nation
Input	Used GAC	1 kg	---------
Output	Landfill disposal, municipal solid waste	1 kg	USA

(Landfill disposal source: GaBi Education_database_2020)

Table 6.3.6: System Inventory and Data Analysis DOE 6

Raw material acquisition phase for a BBAC

Flow	Material	Amounts/Units	Nation
Input	Rice husk	6 kg	MX
Output	Rice husk	6 kg	MX

Transportation of raw materials to the processing place

Flow	Flow type	Amount/Units	Nation
Input	Rice husk	6 kg	MX
Input	Gasoline/diesel (light cargo vehicle)	50 L (160 oz)	---------
Output	Rice husk	6 kg	MX
Output	CO_2	12 kg	USA
	(Transport input/output source: GaBi Database & CO_2 emissions from EPA website: www.fueleconomy.gov)		

Preparation of Material for Processing Phase

Flow	Flow type	Amount/Units	Nation
Input	Rice husk	6 kg	MX
Output	Material for production phase	6 kg	MX

Pyrolysis (Processing Phase)

Flow	Flow type	Amount/Units	Nation
Input	Rice husk	6 kg	MX
Input	LP gas	2 kg	USA
Output	Biochar	1 kg	---------
Output	Ash & residues	6 kg	---------
Output	CO_2	5.98 kg	USA

(Source: U.S. Energy Information Administration: www.eia.gov>environment>emission)

Chemical Activation (Impregnation Phase)

Flow	Flow type	Amount/Units	Nation
Input	Biochar	1 kg	----------

Input	Freshwater	0.3 L (9.6oz)	USA
Input	KOH activating agent	0.1 kg	USA
Output	Activated biochar	1 kg	---------

Washing (Processing Phase)

Flow	**Flow type**	**Amount/Units**	**Nation**
Input	Activated biochar	1 kg	---------
Input	Freshwater	10 L (320oz)	USA
Output	Washed activated biochar	1 kg	---------
Output	Wastewater	10 L (320oz)	USA

Drying (Processing Phase)

Flow	**Flow type**	**Amount/Units**	**Nation**
Input	Washed activated biochar	1 kg	---------
Input	LP gas	1 kg	USA
Output	Dried AC	1 kg	---------
Output	CO_2	2.99 kg	USA

(Source: U.S. Energy Information Administration: www.eia.gov>environment>emission)

Crushing and Sieving (Processing Phase)

Flow	**Flow type**	**Amount/Units**	**Nation**
Input	Dried AC	1 kg	---------
Output	Granular AC (GAC)	1 kg	---------

Packaging and storage (Processing Phase)

Flow	**Flow type**	**Amount/Units**	**Nation**
Input	GAC	1 kg	---------
Output	GAC	1 kg	---------

Transportation of GAC to the place where it is going to be used (short distance < 50 km)

Flow	Flow type	Amount/Units	Nation
Input	GAC	1 kg	MX
Input	Gasoline/diesel (light cargo vehicle)	5 L (160 oz)	---------
Output	GAC	1 kg	MX
Output	CO_2	1.2 kg	USA
	(Transport input/output source: GaBi Database & CO_2 emissions from EPA website: www.fueleconomy.gov)		

GAC Use Phase

Flow	Flow type	Amount/Units	Nation
Input	GAC used for filtration	1 kg	---------
Output	GAC used for filtration	1 kg	---------

End of Life GAC Phase

Flow	Flow type	Amount/Units	Nation
Input	Used GAC	1 kg	---------
Output	Landfill disposal, municipal solid waste	1 kg	USA

(Landfill disposal source: GaBi Education_database_2020)

Table 6.3.7: System Inventory and Data Analysis DOE 7

Raw material acquisition phase for a BBAC

Flow	Material	Amounts/Units	Nation
Input	Rice husk	6 kg	MX
Output	Rice husk	6 kg	MX

Transportation of raw materials to the processing place

Flow	Flow type	Amount/Units	Nation
Input	Rice husk	7 kg	MX
Input	Gasoline/diesel (light cargo vehicle)	50 L (160 oz)	---------
Output	Rice husk	7 kg	MX
Output	CO_2	12 kg	USA
	(Transport input/output source: GaBi Database & CO_2 emissions from EPA website: www.fueleconomy.gov)		

Preparation of Material for Processing Phase

Flow	Flow type	Amount/Units	Nation
Input	Rice husk	6 kg	MX
Output	Material for production phase	6 kg	MX

Pyrolysis (Processing Phase)

Flow	Flow type	Amount/Units	Nation
Input	Rice husk	6 kg	MX
Input	LP gas	3 kg	USA
Output	Biochar	1 kg	---------
Output	Ash & residues	6 kg	---------
Output	CO_2	8.97 kg	USA

(Source: U.S. Energy Information Administration:
www.eia.gov>environment>emission)

Chemical Activation (Impregnation Phase)

Flow	Flow type	Amount/Units	Nation
Input	Biochar	1 kg	----------
Input	Freshwater	0.3 L (9.6oz)	USA
Input	CaCl activating agent	0.1 kg	USA
Output	Activated biochar	1 kg	---------

Washing (Processing Phase)

Flow	Flow type	Amount/Units	Nation
Input	Activated biochar	1 kg	---------
Input	Freshwater	10 L (320oz)	USA
Output	Washed activated biochar	1 kg	---------
Output	Wastewater	10 L (320oz)	USA

Drying (Processing Phase)

Flow	Flow type	Amount/Units	Nation
Input	Washed activated biochar	1 kg	---------
Input	LP gas	1 kg	USA
Output	Dried AC	1 kg	---------
Output	CO_2	2.99 kg	USA

(Source: U.S. Energy Information Administration:
www.eia.gov>environment>emission)

Crushing and Sieving (Processing Phase)

Flow	Flow type	Amount/Units	Nation
Input	Dried AC	1 kg	---------
Output	Granular AC (GAC)	1 kg	---------

Packaging and storage (Processing Phase)

Flow	Flow type	Amount/Units	Nation
Input	GAC	1 kg	---------
Output	GAC	1 kg	---------

Transportation of GAC to the place where it is going to be used (short distance < 50 km)

Flow	Flow type	Amount/Units	Nation
Input	GAC	1 kg	MX
Input	Gasoline/diesel (light cargo vehicle)	5 L (160 oz)	---------
Output	GAC	1 kg	MX
Output	CO_2	1.2 kg	USA
	(Transport input/output source: GaBi Database & CO_2 emissions from EPA website: www.fueleconomy.gov)		

GAC Use Phase

Flow	Flow type	Amount/Units	Nation
Input	GAC used for filtration	1 kg	---------
Output	GAC used for filtration	1 kg	---------

End of Life GAC Phase

Flow	Flow type	Amount/Units	Nation
Input	Used GAC	1 kg	---------
Output	Landfill disposal, municipal solid waste	1 kg	USA

(Landfill disposal source: GaBi Education_database_2020)

Table 6.3.8: System Inventory and Data Analysis DOE 8

Raw material acquisition phase for a BBAC

Flow	Material	Amounts/Units	Nation
Input	Rice husk	6 kg	MX
Output	Rice husk	6 kg	MX

Transportation of raw materials to the processing place

Flow	Flow type	Amount/Units	Nation
Input	Rice husk	6 kg	MX
Input	Gasoline/diesel (light cargo vehicle)	50 L (160 oz)	---------
Output	Rice husk	7 kg	MX
Output	CO_2	12 kg	USA
	(Transport input/output source: GaBi Database & CO_2 emissions from EPA website: www.fueleconomy.gov)		

Preparation of Material for Processing Phase

Flow	Flow type	Amount/Units	Nation
Input	Rice husk	6 kg	MX
Output	Material for production phase	6 kg	MX

Pyrolysis (Processing Phase)

Flow	Flow type	Amount/Units	Nation
Input	Rice husk	6 kg	MX
Input	LP gas	2 kg	USA
Output	Biochar	1 kg	---------
Output	Ash & residues	6 kg	---------
Output	CO_2	5.98 kg	USA

(Source: U.S. Energy Information Administration: www.eia.gov>environment>emission)

Chemical Activation (Impregnation Phase)

Flow	Flow type	Amount/Units	Nation
Input	Biochar	1 kg	----------
Input	Freshwater	0.3 L (9.6oz)	USA
Input	CaCl activating agent	0.1 kg	USA
Output	Activated biochar	1 kg	---------

Washing (Processing Phase)

Flow	Flow type	Amount/Units	Nation
Input	Activated biochar	1 kg	---------
Input	Freshwater	10 L (320oz)	USA
Output	Washed activated biochar	1 kg	---------
Output	Wastewater	10 L (320oz)	USA

Drying (Processing Phase)

Flow	Flow type	Amount/Units	Nation
Input	Washed activated biochar	1 kg	---------
Input	LP gas	1 kg	USA
Output	Dried AC	1 kg	---------
Output	CO_2	2.99 kg	USA

(Source: U.S. Energy Information Administration: www.eia.gov>environment>emission)

Crushing and Sieving (Processing Phase)

Flow	Flow type	Amount/Units	Nation
Input	Dried AC	1 kg	---------
Output	Granular AC (GAC)	1 kg	---------

Packaging and storage (Processing Phase)

Flow	Flow type	Amount/Units	Nation
Input	GAC	1 kg	---------
Output	GAC	1 kg	---------

Transportation of GAC to the place where it is going to be used (short distance < 50 km)

Flow	Flow type	Amount/Units	Nation
Input	GAC	1 kg	MX
Input	Gasoline/diesel (light cargo vehicle)	5 L (160 oz)	---------
Output	GAC	1 kg	MX
Output	CO_2	1.2 kg	USA
	(Transport input/output source: GaBi Database & CO_2 emissions from EPA website: www.fueleconomy.gov)		

GAC Use Phase

Flow	Flow type	Amount/Units	Nation
Input	GAC used for filtration	1 kg	---------
Output	GAC used for filtration	1 kg	---------

End of Life GAC Phase

Flow	Flow type	Amount/Units	Nation
Input	Used GAC	1 kg	---------
Output	Landfill disposal, municipal solid waste	1 kg	USA

((Landfill disposal source: GaBi Education_database_2020)

Table 6.3.9: System Inventory and Data Analysis of commercial coal-based AC

Raw material acquisition phase for a Commercial AC

Flow	Material	Amounts/Units	Nation
Input	Hard coal mining	1 kg	USA
Output	Hard coal for processing	1 kg	USA

(Functional unit: 1 kg)
(Source: GaBi Education Database)

Transportation of raw material to the processing place (~100 km)

Flow	Flow type	Amount/Units	Nation
Input	Hard coal	1 kg	MX
Input	Gasoline/diesel (light cargo vehicle)	50 L (1600 oz)	---------
Output	Hard coal	7 kg	MX
Output	CO_2	12 kg	USA
	(Transport input/output source: GaBi Database & CO_2 emissions from EPA website: www.fueleconomy.gov)		

Preparation of Material for the Processing Phase (Crushing)

Flow	Flow type	Amount/Units	Nation
Input	Hard coal	1 kg	MX
Input	Electricity (coal & natural gas burning plants)	25 kWh	USA
Output	Material for production phase	1 kg	MX
Output	Carbon dioxide	~33.75 kg	USA

Activation (steam & other gases)

Flow	Flow type	Amount/Units	Nation
Input	Hard coal crushed	1 kg	USA
Input	Freshwater	0.3 L (9.6oz)	USA
Input	Electricity	1 kWh	USA
Input	LP gas	13.73 kg (~7.5 m^3)	USA
Output	Carbon dioxide	41 kg	USA

Washing (Processing Phase)

Flow	Flow type	Amount/Units	Nation
Input	COM-AC	1 kg	USA
Input	Freshwater	10 L (320oz)	USA
Input	Electricity	1 kWh	USA
Output	Washed activated carbon	1 kg	USA
Output	Wastewater	10 L (320oz)	USA

Drying (Processing Phase)

Flow	Flow type	Amount/Units	Nation
Input	Washed activated carbon	1 kg	---------
Input	LP gas	12 kg	USA
Input	Electricity	1 kWh	USA
Output	Dried AC	1 kg	---------
Output	CO_2	35.88 kg	USA

(Source: U.S. Energy Information Administration: www.eia.gov>environment>emission)

Sieving (Processing Phase)

Flow	Flow type	Amount/Units	Nation
Input	Dried AC	1 kg	---------
Output	Granular AC (GAC)	1 kg	---------

Packaging and storage (Processing Phase)

Flow	Flow type	Amount/Units	Nation
Input	GAC	1 kg	---------
Output	GAC	1 kg	---------

Transportation of GAC to the place where it is going to be used (> 100 km)

Flow	Flow type	Amount/Units	Nation
Input	GAC	1 kg	MX
Input	Gasoline/diesel (light cargo vehicle)	50 L (1600 oz)	USA
Output	GAC	1 kg	MX
Output	CO_2	12 kg	USA
	(Transport input/output source: GaBi Database & CO_2 emissions from EPA website: www.fueleconomy.gov)		

GAC Use Phase

Flow	Flow type	Amount/Units	Nation
Input	GAC used for filtration	1 kg	---------
Output	GAC used for filtration	1 kg	---------

End of Life GAC Phase

Flow	Flow type	Amount/Units	Nation
Input	Used GAC	1 kg	---------
Output	Landfill disposal, municipal solid waste	1 kg	USA

(Landfill disposal source: GaBi Education_database_2020)

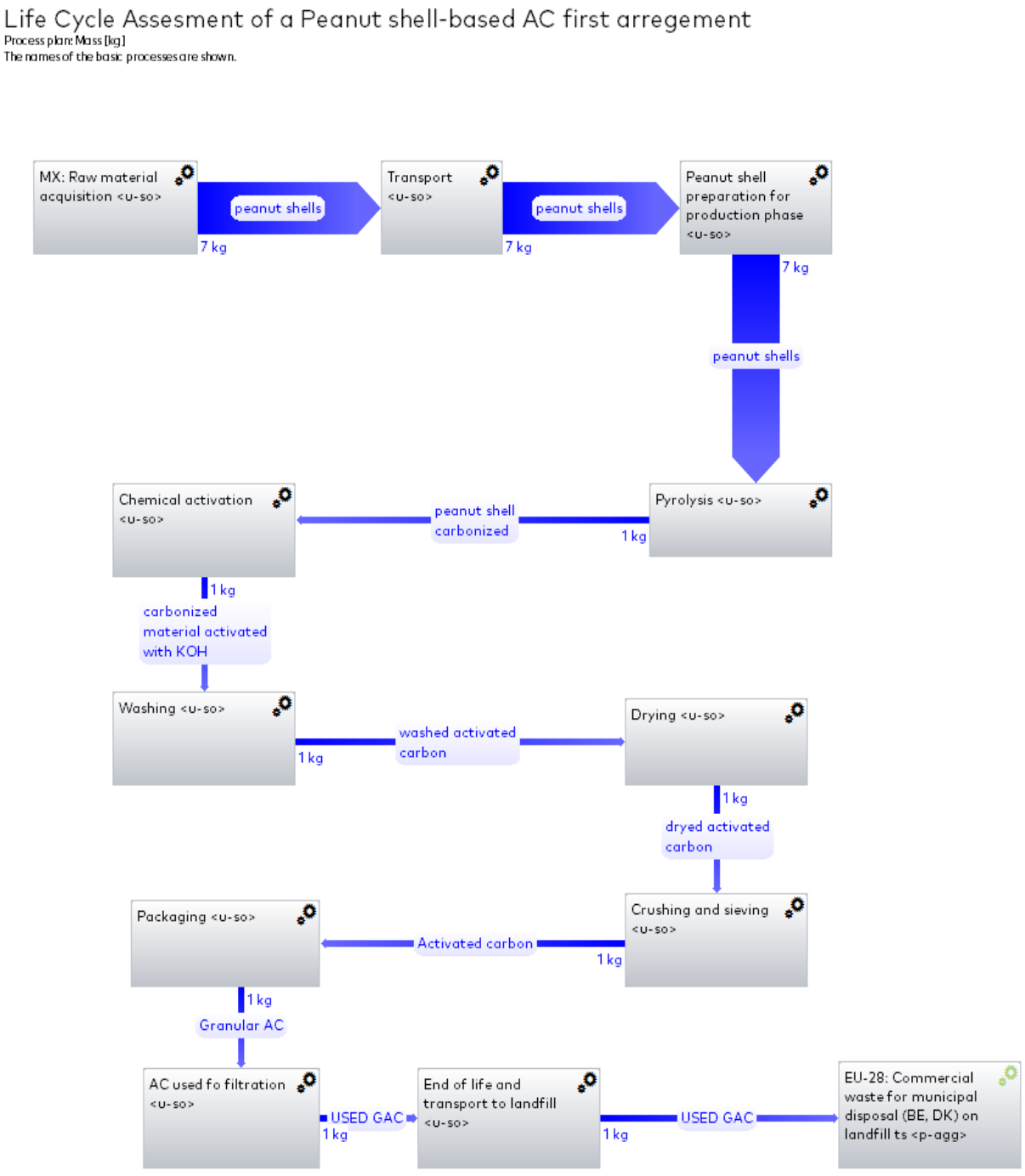

Figure 6.3.1: Process flow diagram of BBAC-DOE 1 production using GaBi software and Education_database_2020.

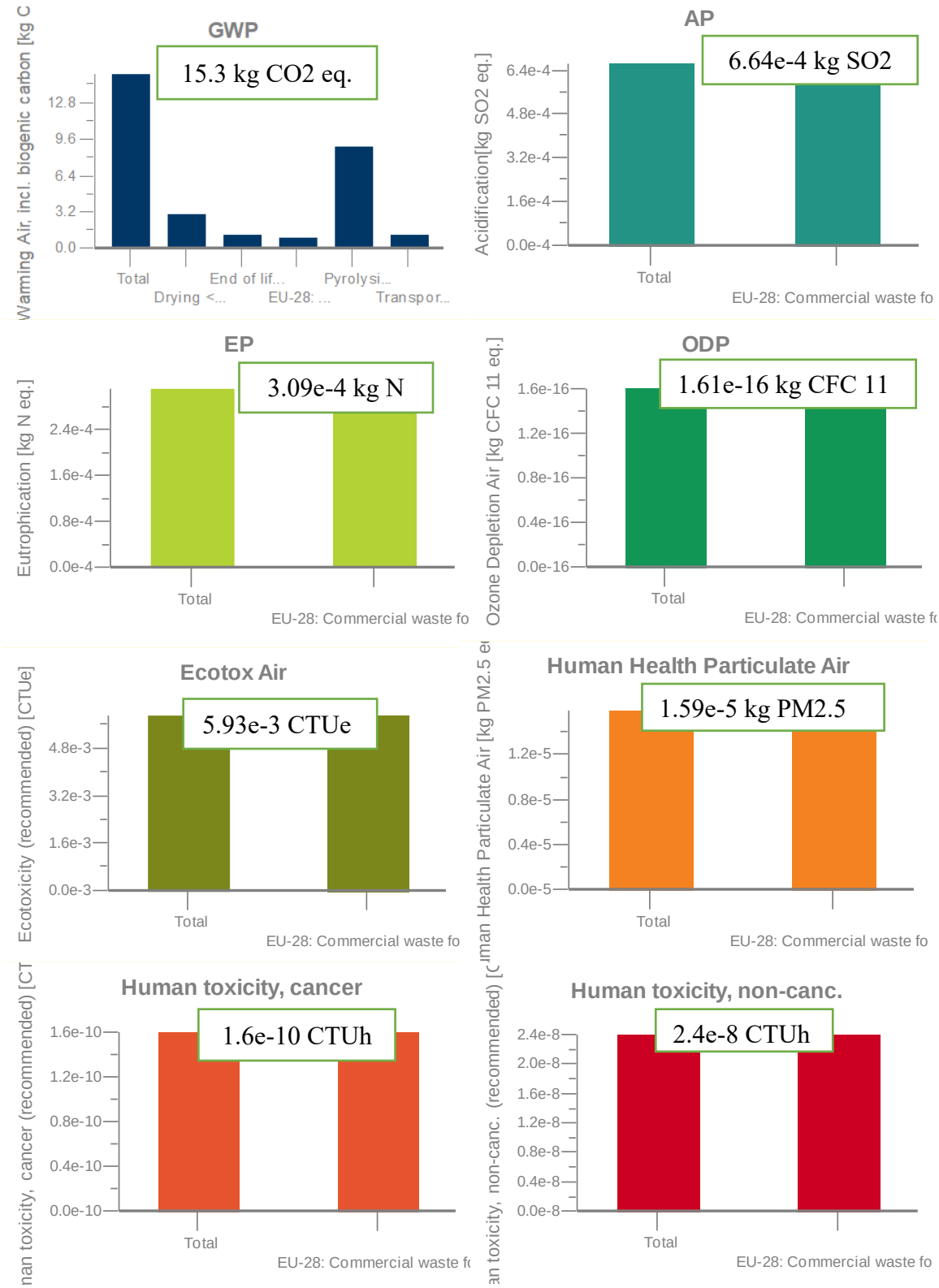
GWP
15.3 kg CO2 eq.
Warming Air, incl. biogenic carbon [kg C
12.8
9.6
6.4
3.2
0.0
Total
End of lif...
Pyrolysi...
Drying <...
EU-28: ...
Transpor...
AP
6.64e-4 kg SO2
Acidification[kg SO2 eq.]
6.4e-4
4.8e-4
3.2e-4
1.6e-4
0.0e-4
Total
EU-28: Commercial waste fo
EP
3.09e-4 kg N
Eutrophication [kg N eq.]
2.4e-4
1.6e-4
0.8e-4
0.0e-4
Total
EU-28: Commercial waste fo
ODP
1.61e-16 kg CFC 11
Ozone Depletion Air [kg CFC 11 eq.]
1.6e-16
1.2e-16
0.8e-16
0.4e-16
0.0e-16
Total
EU-28: Commercial waste fo
Ecotox Air
5.93e-3 CTUe
Ecotoxicity (recommended) [CTUe]
4.8e-3
3.2e-3
1.6e-3
0.0e-3
Total
EU-28: Commercial waste fo
Human Health Particulate Air
1.59e-5 kg PM2.5
uman Health Particulate Air [kg PM2.5 e
1.2e-5
0.8e-5
0.4e-5
0.0e-5
Total
EU-28: Commercial waste fo
Human toxicity, cancer
1.6e-10 CTUh
nan toxicity, cancer (recommended) [CT
1.6e-10
1.2e-10
0.8e-10
0.4e-10
0.0e-10
Total
EU-28: Commercial waste fo
Human toxicity, non-canc.
2.4e-8 CTUh
an toxicity, non-canc. (recommended) [C
2.4e-8
2.0e-8
1.6e-8
1.2e-8
0.8e-8
0.4e-8
0.0e-8
Total
EU-28: Commercial waste fo

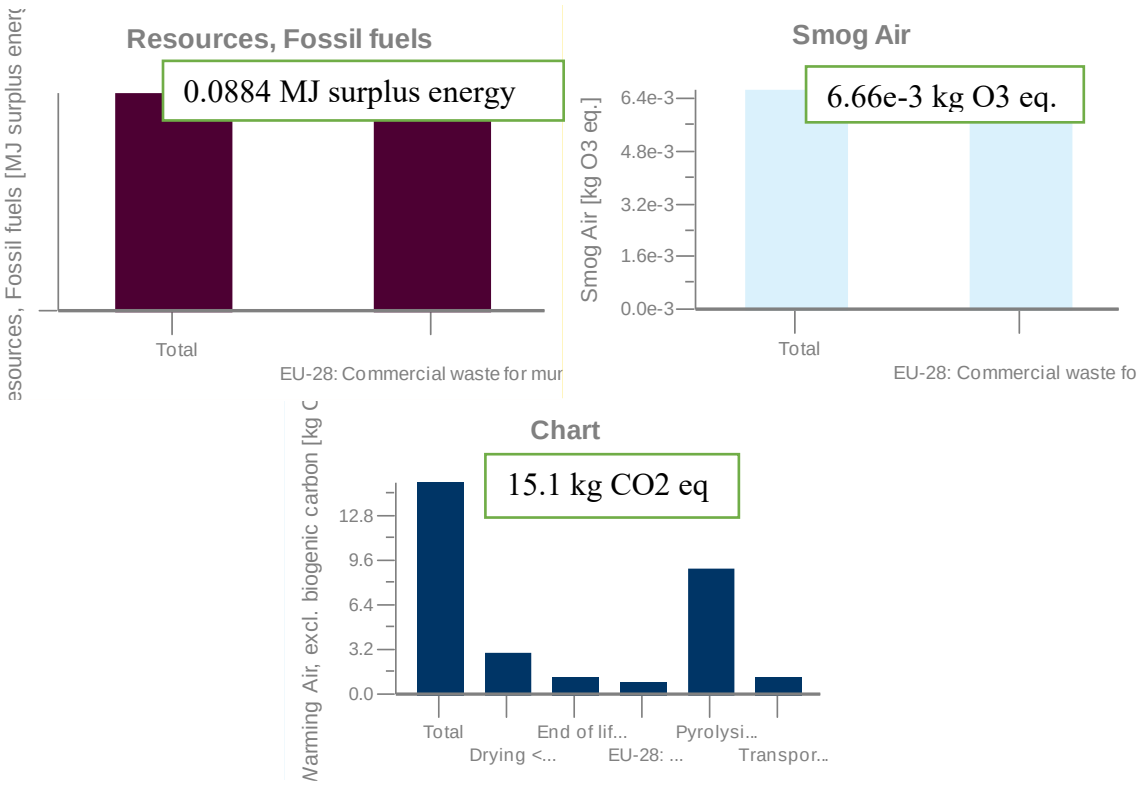

Figure 6.3.2: Life cycle impact assessment according to TRACI mid-point impact categories for BBAC-DOE 1.

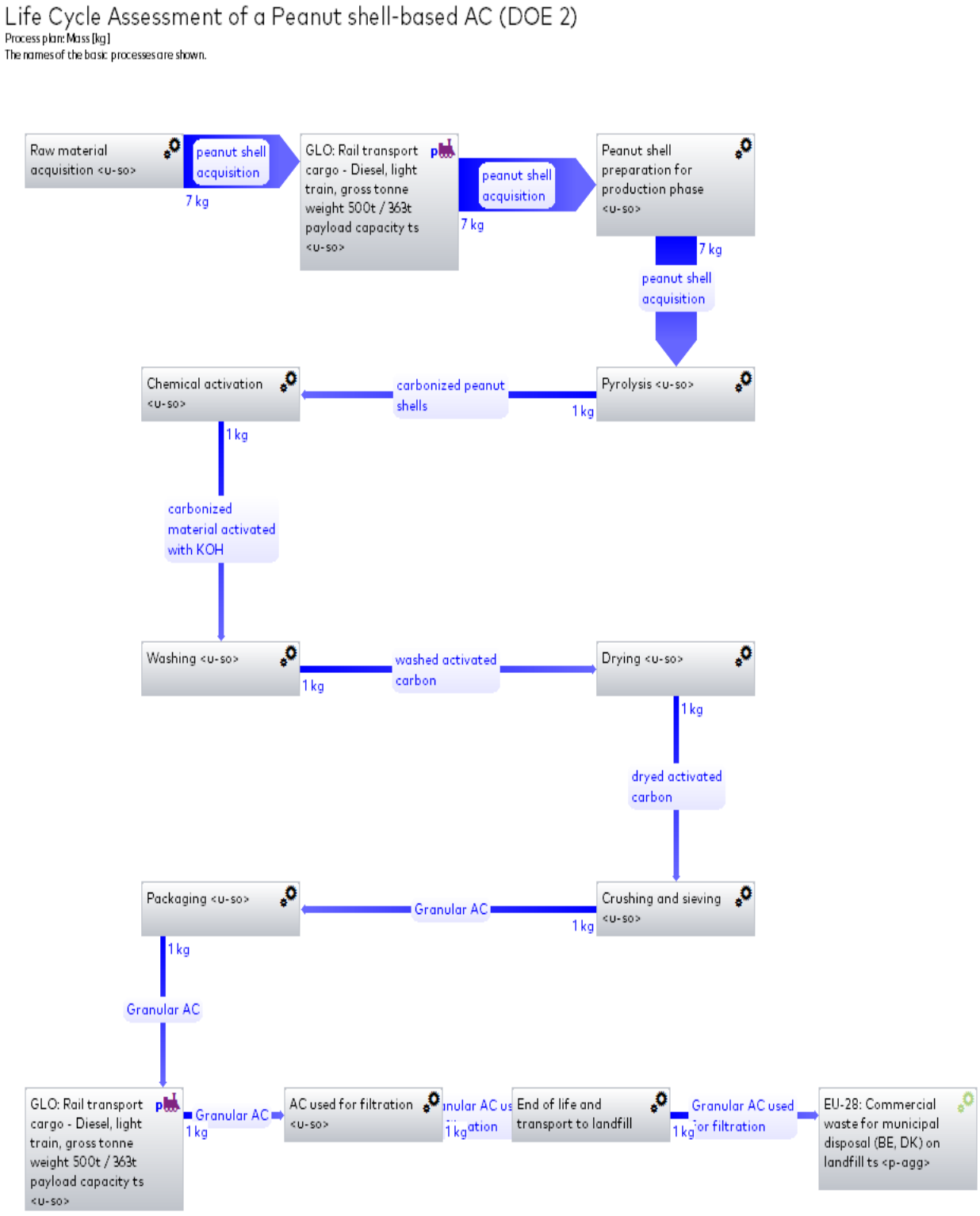

Figure 6.3.3: Process flow diagram of BBAC-DOE 1 production using GaBi software and Education_database_2020.

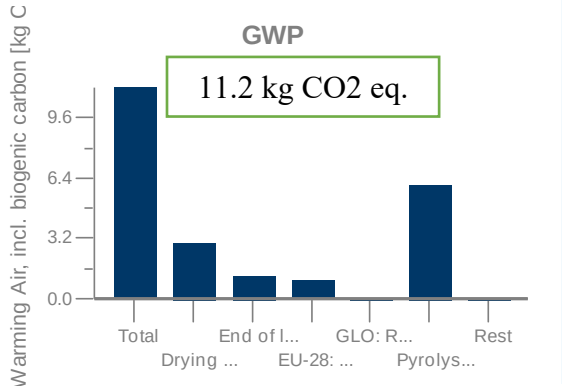
GWP
11.2 kg CO2 eq.
Warming Air, incl. biogenic carbon [kg C
9.6
6.4
3.2
0.0
Total
Drying ...
End of l...
EU-28: ...
GLO: R...
Pyrolys...
Rest

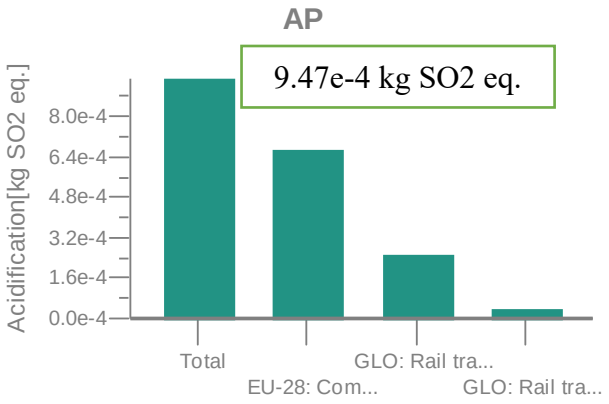
AP
9.47e-4 kg SO2 eq.
Acidification[kg SO2 eq.]
8.0e-4
6.4e-4
4.8e-4
3.2e-4
1.6e-4
0.0e-4
Total
EU-28: Com...
GLO: Rail tra...
GLO: Rail tra...

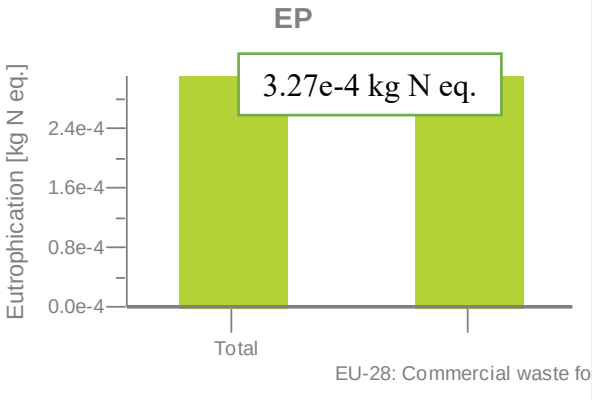
EP
3.27e-4 kg N eq.
Eutrophication [kg N eq.]
2.4e-4
1.6e-4
0.8e-4
0.0e-4
Total
EU-28: Commercial waste fo

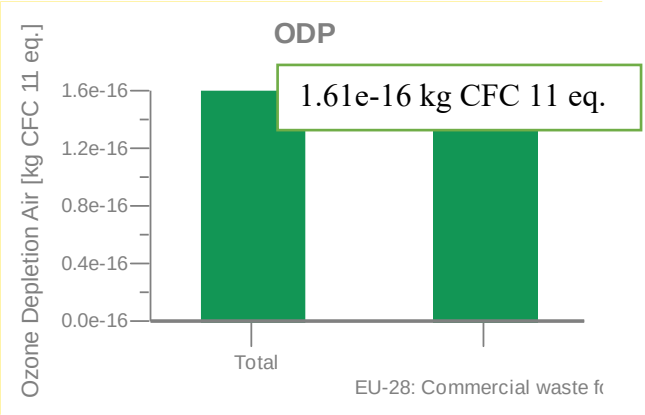
ODP
1.61e-16 kg CFC 11 eq.
Ozone Depletion Air [kg CFC 11 eq.]
1.6e-16
1.2e-16
0.8e-16
0.4e-16
0.0e-16
Total
EU-28: Commercial waste fo

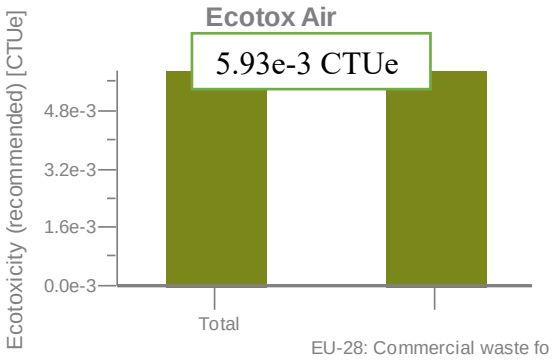
Ecotox Air
5.93e-3 CTUe
Ecotoxicity (recommended) [CTUe]
4.8e-3
3.2e-3
1.6e-3
0.0e-3
Total
EU-28: Commercial waste fo

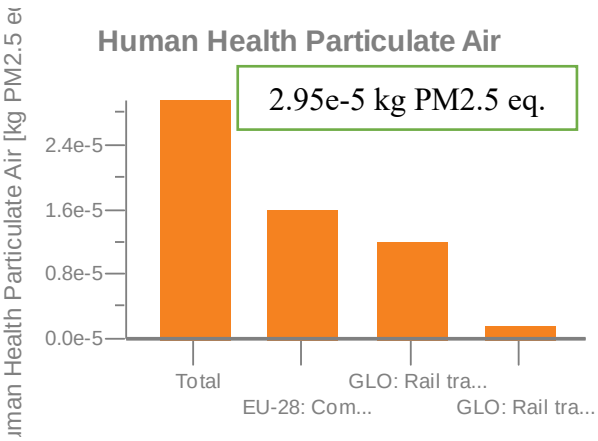
Human Health Particulate Air
2.95e-5 kg PM2.5 eq.
Human Health Particulate Air [kg PM2.5 eq
2.4e-5
1.6e-5
0.8e-5
0.0e-5
Total
EU-28: Com...
GLO: Rail tra...
GLO: Rail tra...

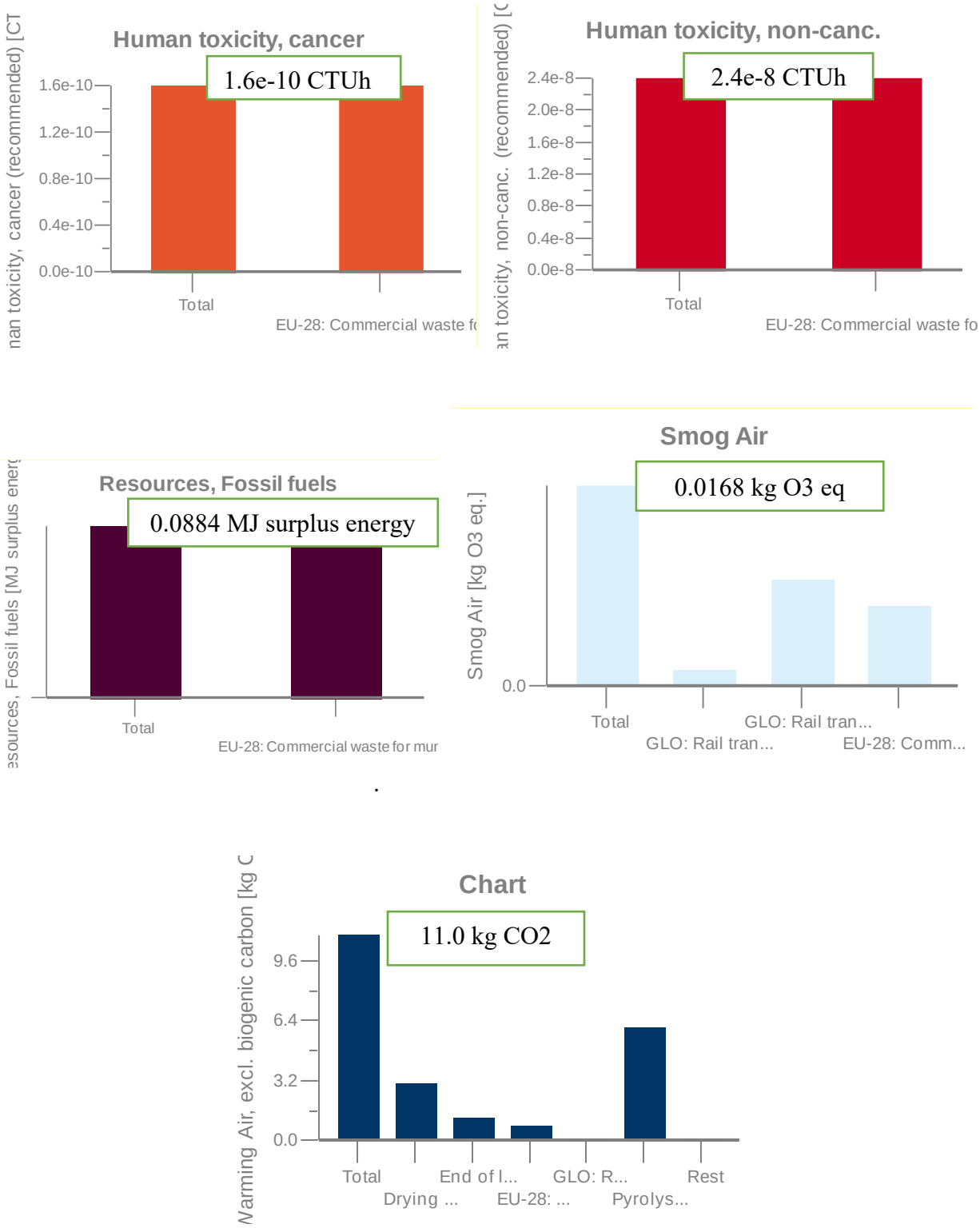

Figure 6.3.4: Life cycle impact assessment according to TRACI mid-point impact categories for BBAC-DOE 2.

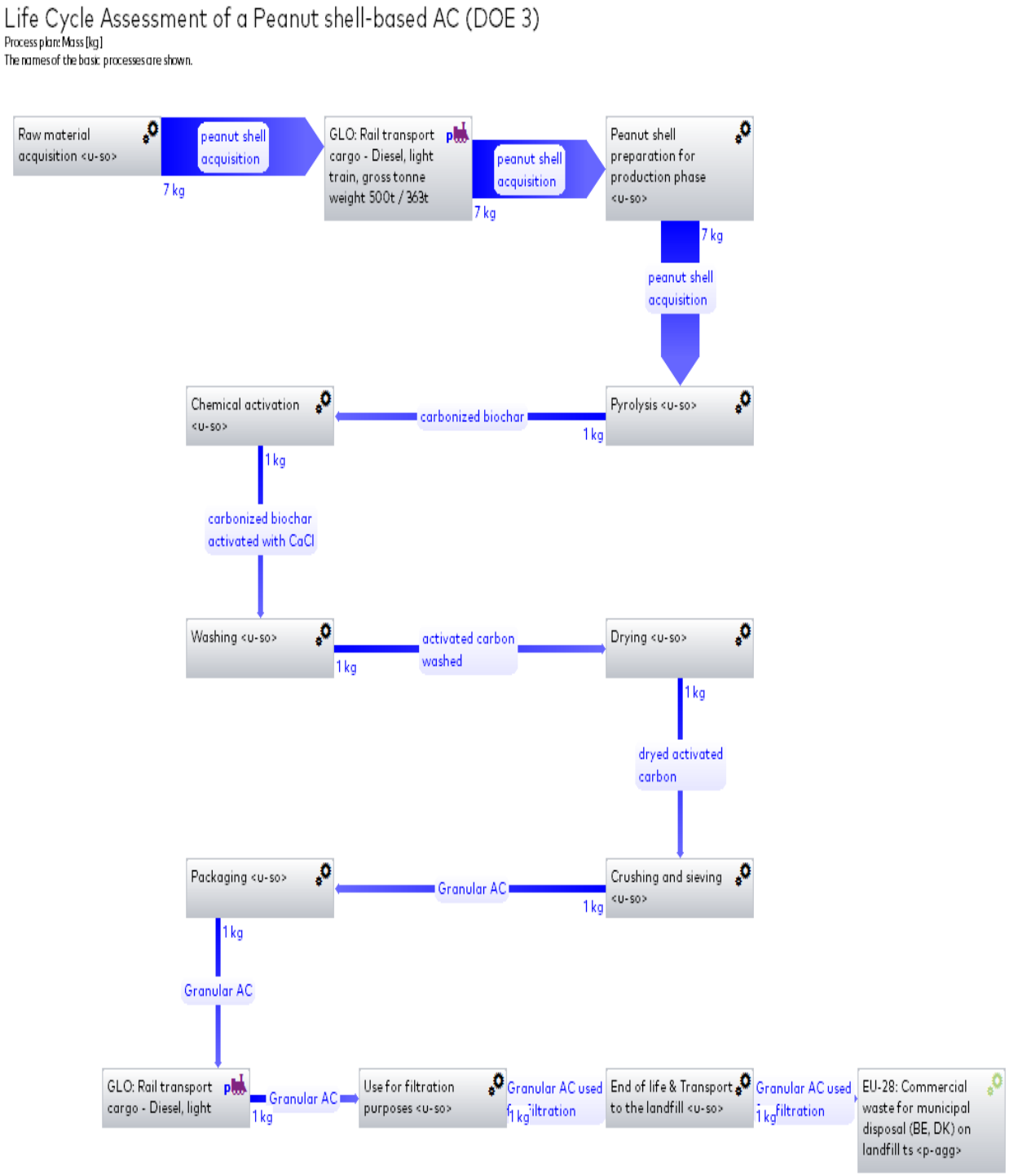

Figure 6.3.5: Process flow diagram of BBAC-DOE 3 production using GaBi software and Education_database_2020.

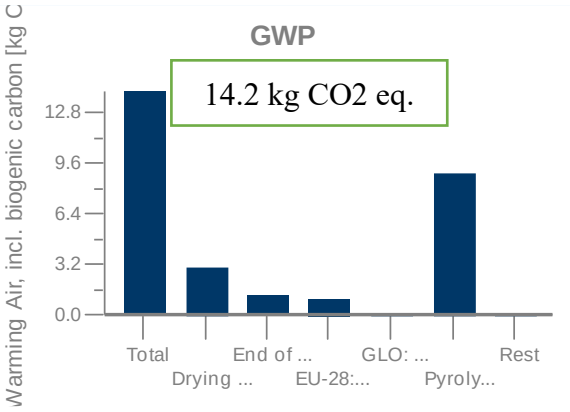
GWP
14.2 kg CO2 eq.
Warming Air, incl. biogenic carbon [kg C
12.8
9.6
6.4
3.2
0.0
Total
Drying ...
End of ...
EU-28:...
GLO: ...
Pyroly...
Rest

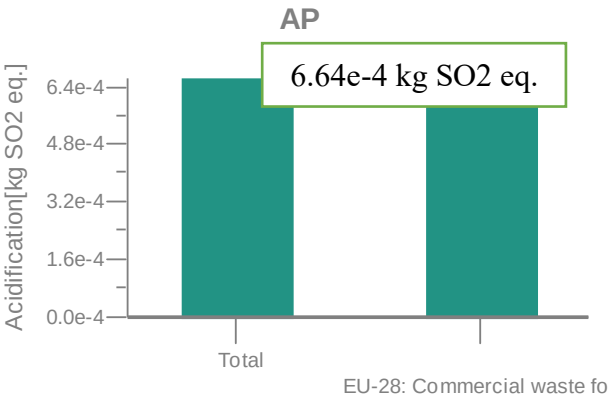
AP
6.64e-4 kg SO2 eq.
Acidification[kg SO2 eq.]
6.4e-4
4.8e-4
3.2e-4
1.6e-4
0.0e-4
Total
EU-28: Commercial waste fo

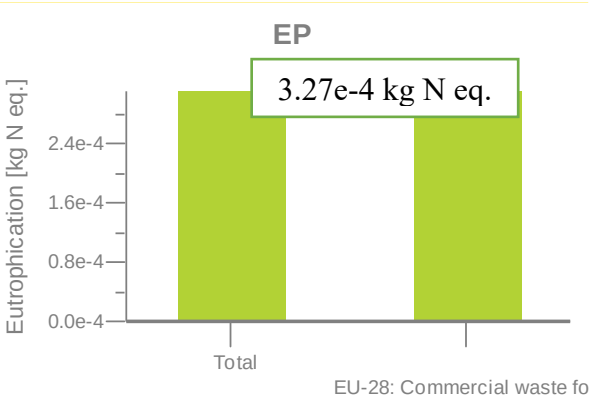
EP
3.27e-4 kg N eq.
Eutrophication [kg N eq.]
2.4e-4
1.6e-4
0.8e-4
0.0e-4
Total
EU-28: Commercial waste fo

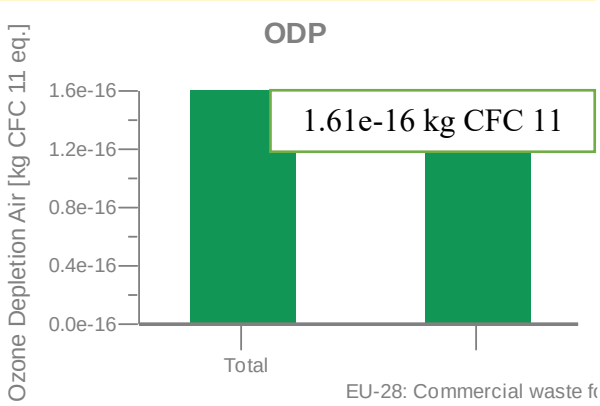
ODP
1.61e-16 kg CFC 11
Ozone Depletion Air [kg CFC 11 eq.]
1.6e-16
1.2e-16
0.8e-16
0.4e-16
0.0e-16
Total
EU-28: Commercial waste fo

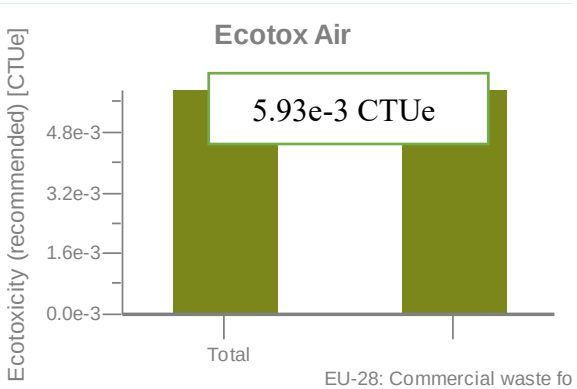
Ecotox Air
5.93e-3 CTUe
Ecotoxicity (recommended) [CTUe]
4.8e-3
3.2e-3
1.6e-3
0.0e-3
Total
EU-28: Commercial waste fo

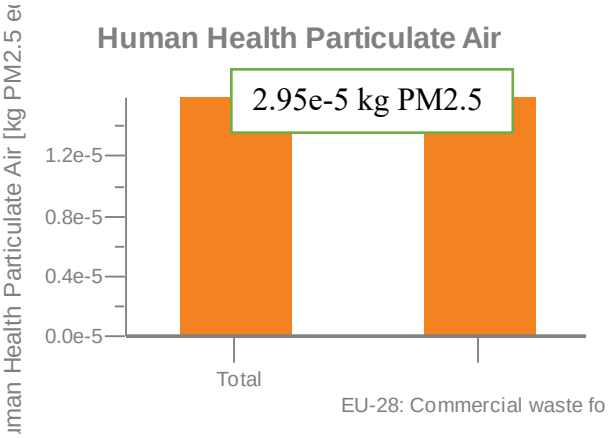
Human Health Particulate Air
2.95e-5 kg PM2.5
uman Health Particulate Air [kg PM2.5 e
1.2e-5
0.8e-5
0.4e-5
0.0e-5
Total
EU-28: Commercial waste fo

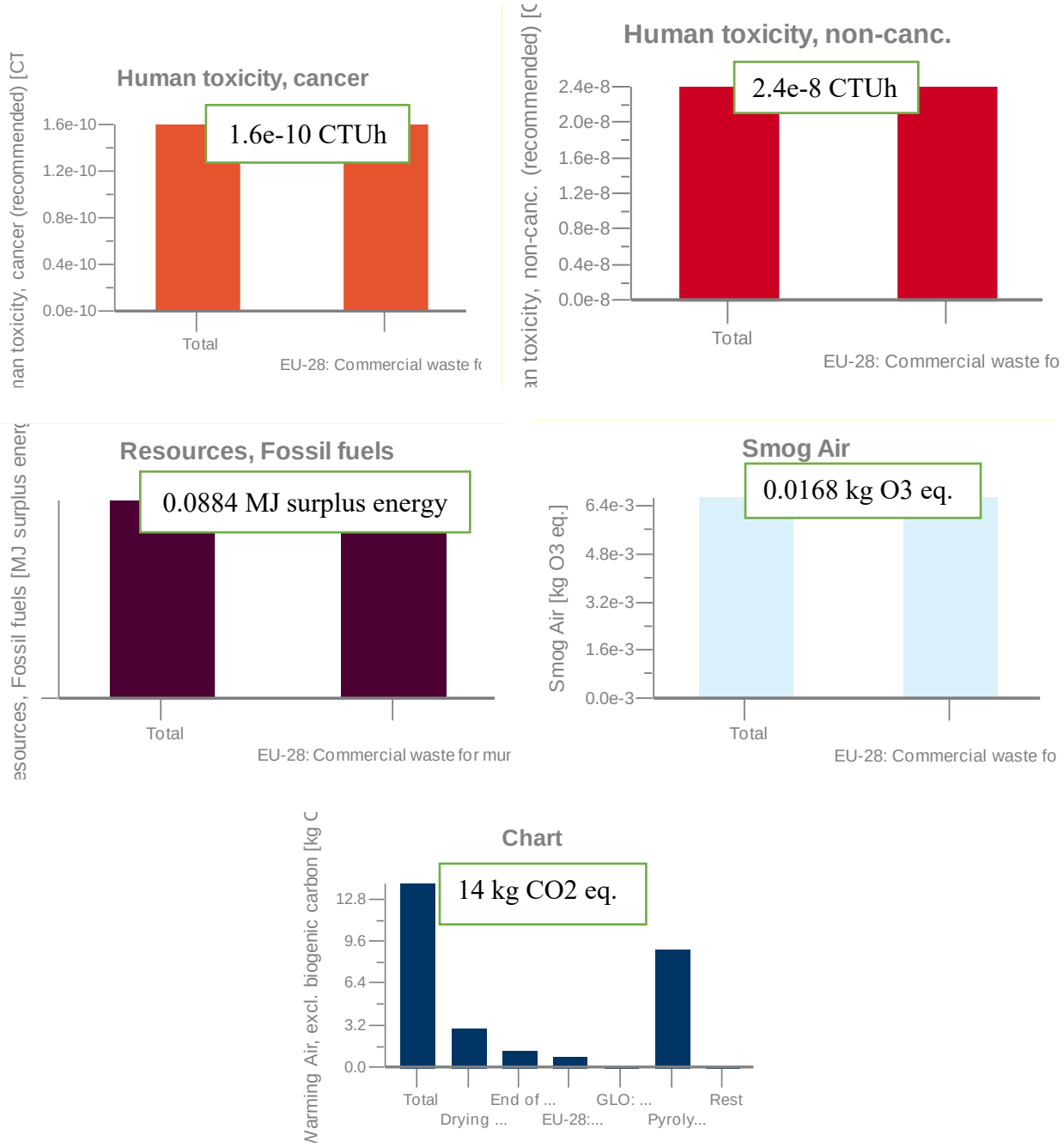

Figure 6.3.6: Life cycle impact assessment according to TRACI mid-point impact categories for BBAC-DOE 3.

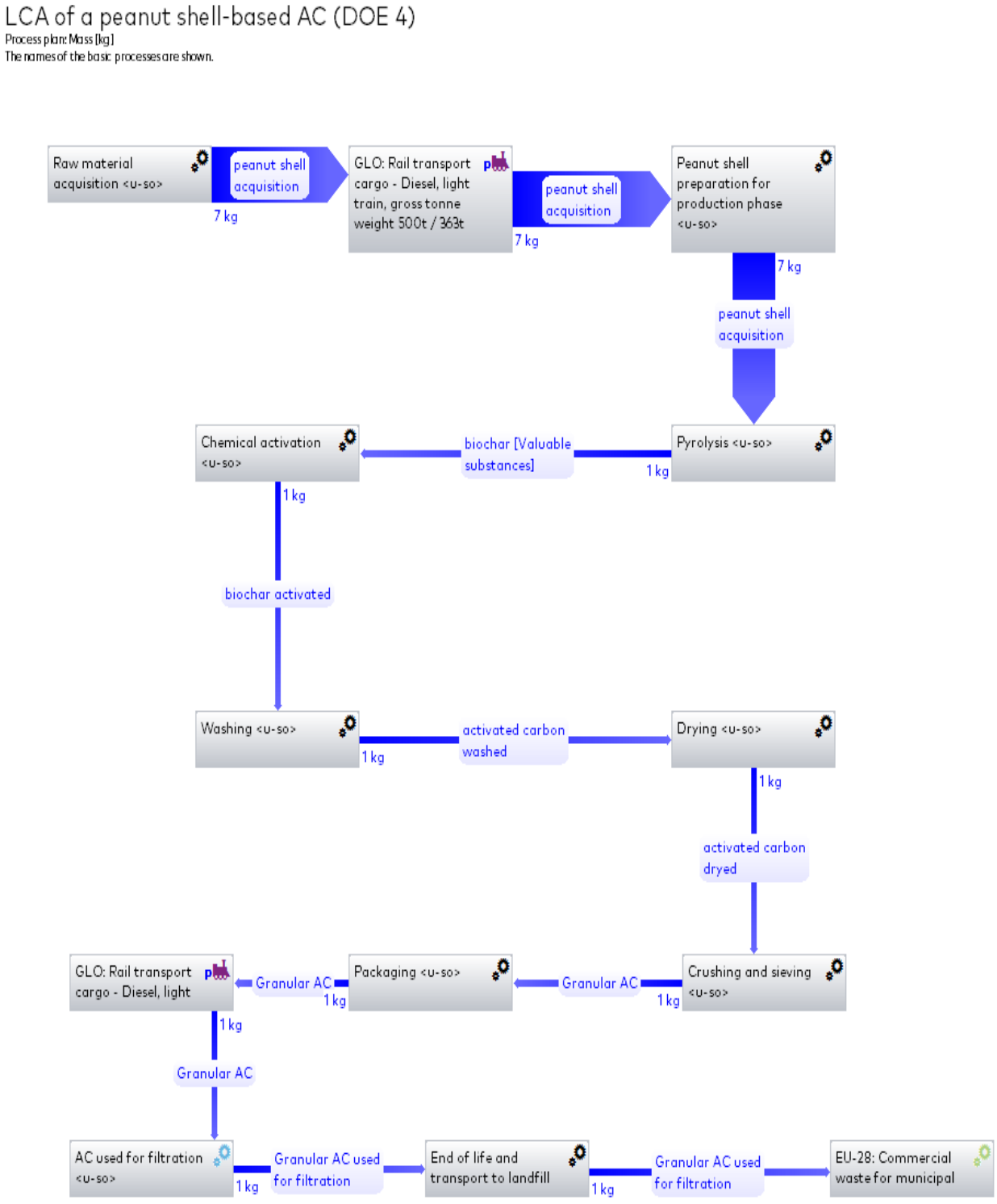

Figure 6.3.7: Process flow diagram of BBAC-DOE 4 production using GaBi software and Education_database_2020.

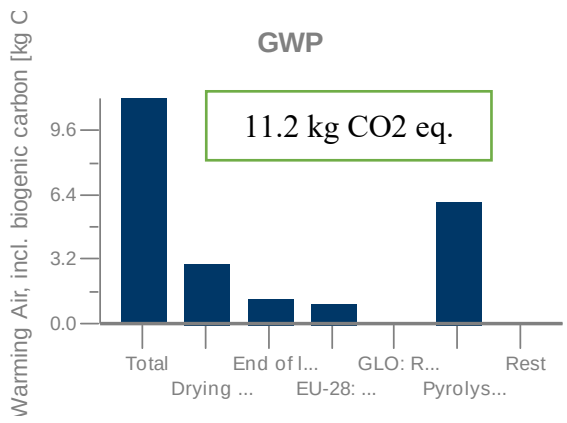
GWP
Warming Air, incl. biogenic carbon [kg C
11.2 kg CO2 eq.
9.6
6.4
3.2
0.0
Total
End of l...
GLO: R...
Rest
Drying ...
EU-28: ...
Pyrolys...

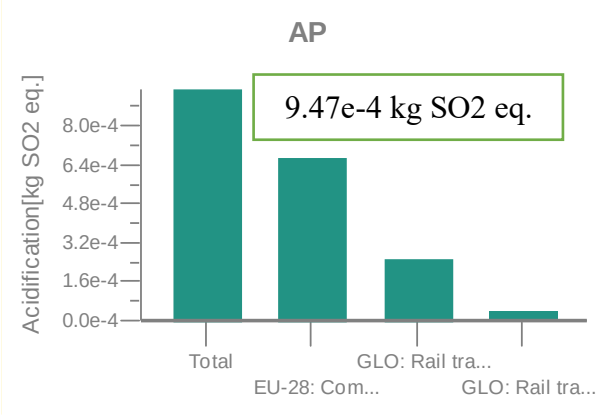
AP
Acidification[kg SO2 eq.]
9.47e-4 kg SO2 eq.
8.0e-4
6.4e-4
4.8e-4
3.2e-4
1.6e-4
0.0e-4
Total
GLO: Rail tra...
EU-28: Com...
GLO: Rail tra...

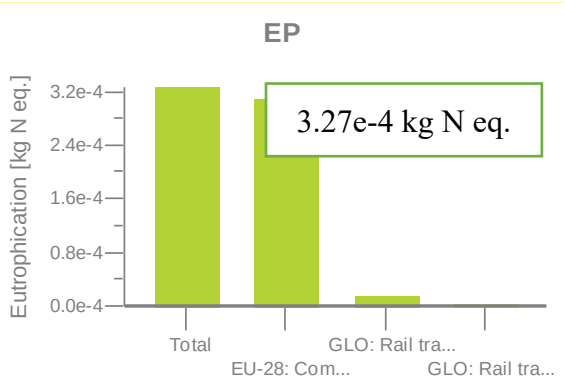
EP
Eutrophication [kg N eq.]
3.27e-4 kg N eq.
3.2e-4
2.4e-4
1.6e-4
0.8e-4
0.0e-4
Total
GLO: Rail tra...
EU-28: Com...
GLO: Rail tra...

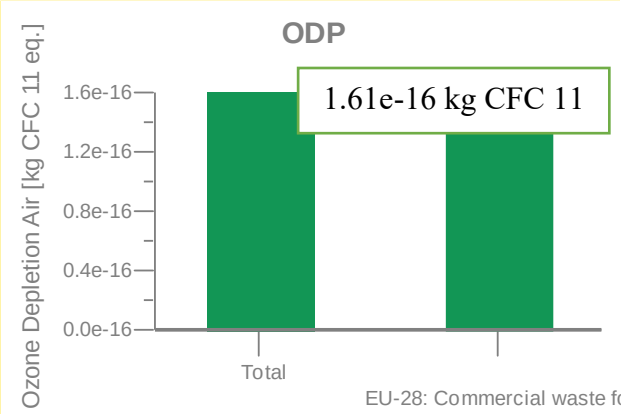
ODP
Ozone Depletion Air [kg CFC 11 eq.]
1.61e-16 kg CFC 11
1.6e-16
1.2e-16
0.8e-16
0.4e-16
0.0e-16
Total
EU-28: Commercial waste fo

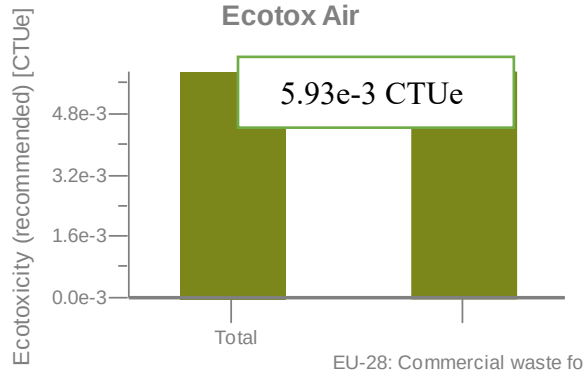
Ecotox Air
Ecotoxicity (recommended) [CTUe]
5.93e-3 CTUe
4.8e-3
3.2e-3
1.6e-3
0.0e-3
Total
EU-28: Commercial waste fo

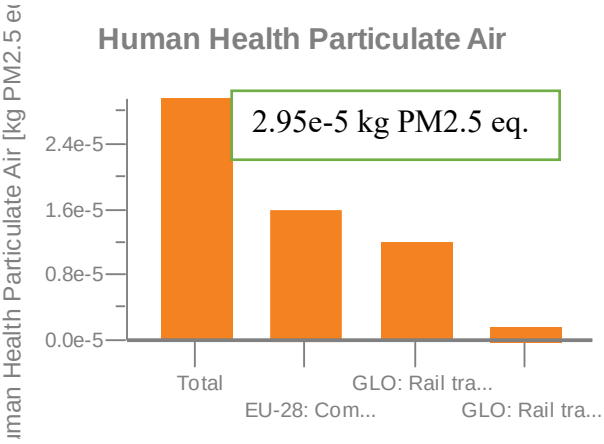
Human Health Particulate Air
man Health Particulate Air [kg PM2.5 eq
2.95e-5 kg PM2.5 eq.
2.4e-5
1.6e-5
0.8e-5
0.0e-5
Total
GLO: Rail tra...
EU-28: Com...
GLO: Rail tra...

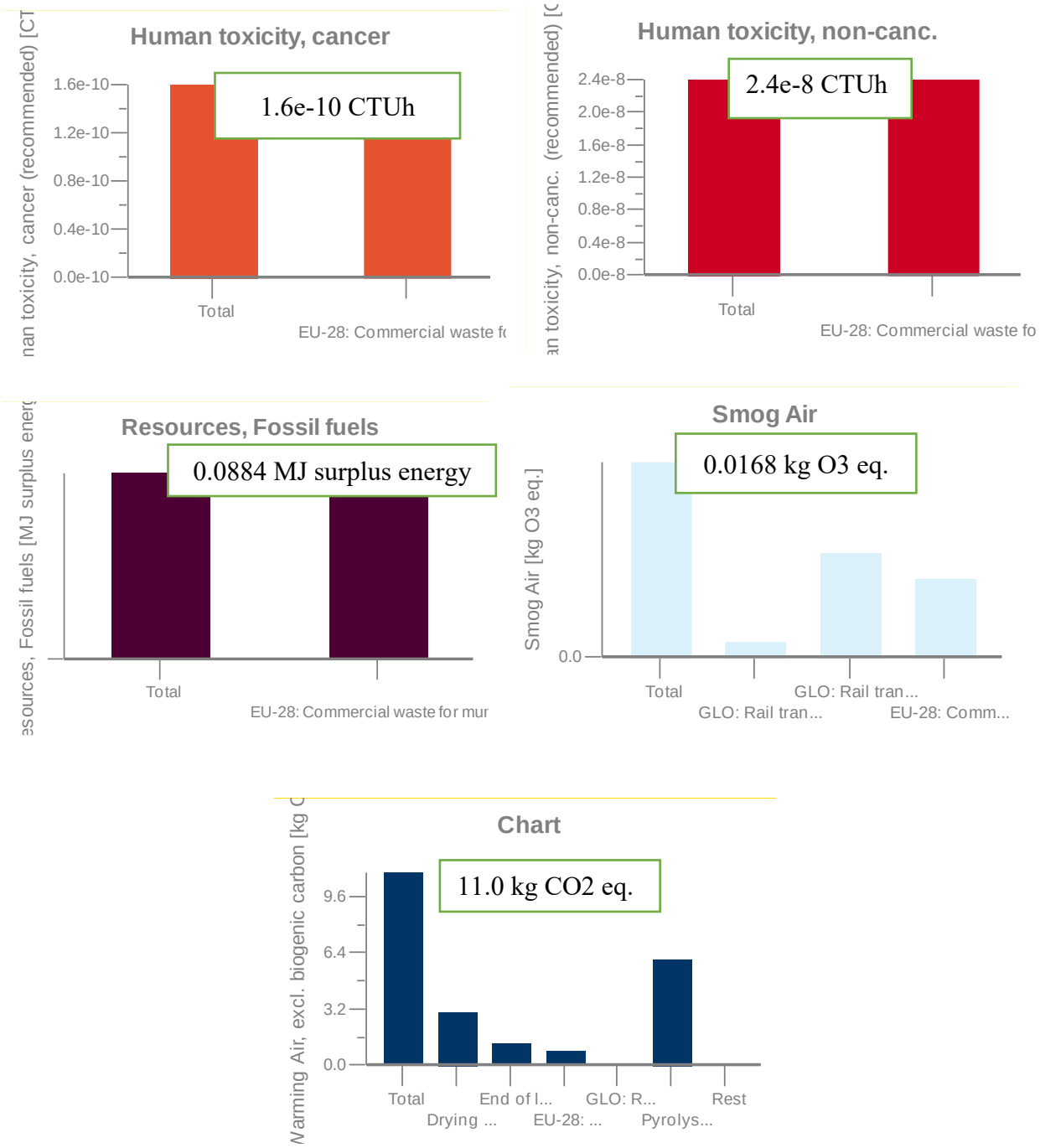

Figure 6.3.8: Life cycle impact assessment according to TRACI mid-point impact categories for BBAC-DOE 4.

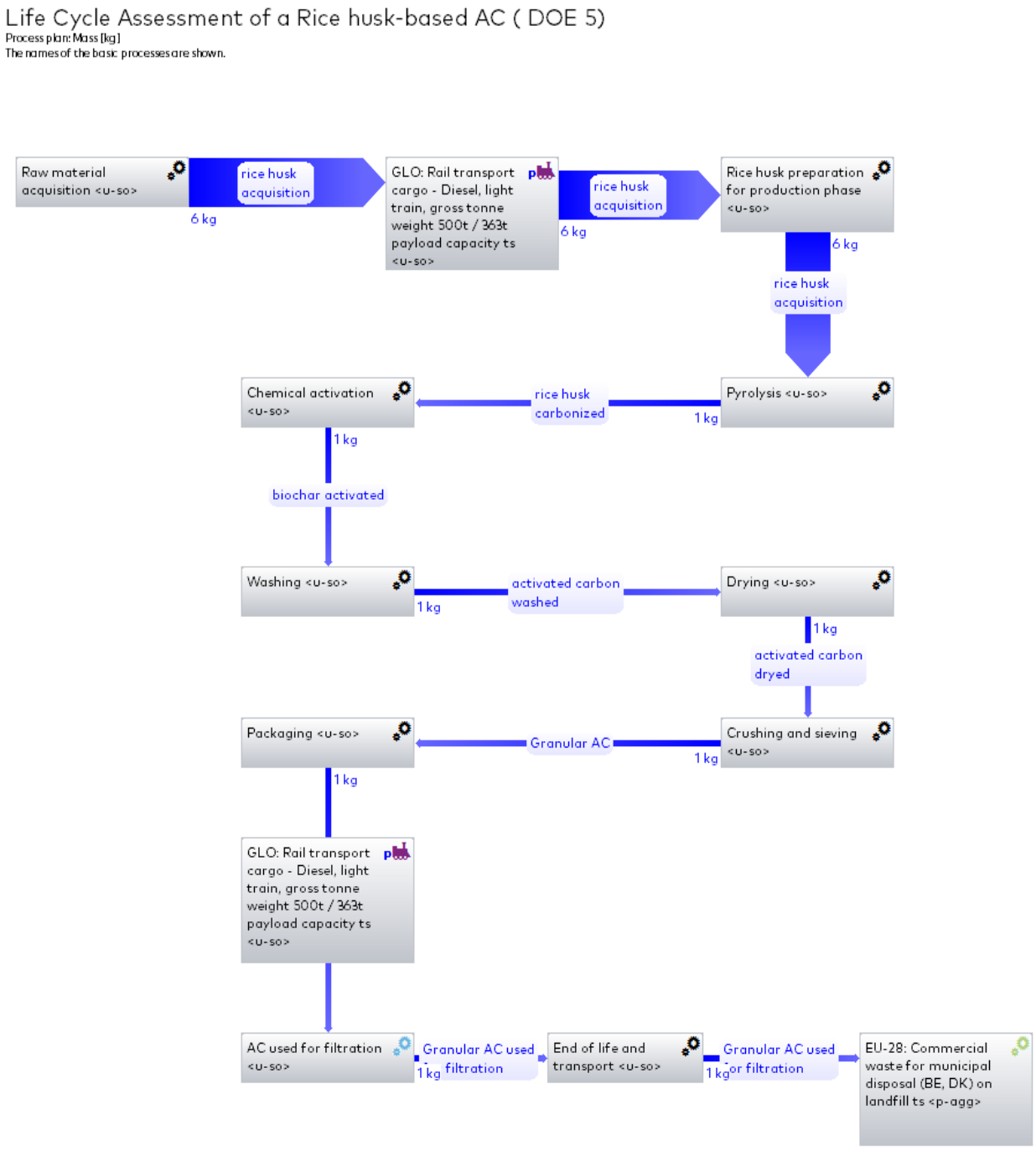

Figure 6.3.9: Process flow diagram of BBAC-DOE 5 production using GaBi software and Education_database_2020.

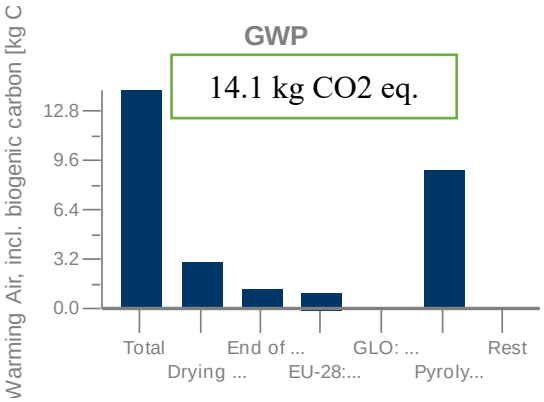
GWP
14.1 kg CO2 eq.
Warming Air, incl. biogenic carbon [kg C
12.8
9.6
6.4
3.2
0.0
Total
Drying ...
End of ...
EU-28:...
GLO: ...
Pyroly...
Rest

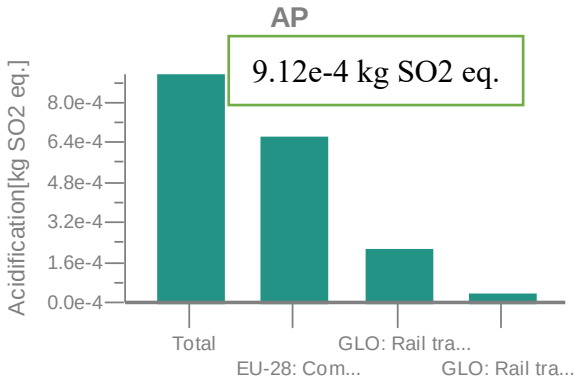
AP
9.12e-4 kg SO2 eq.
Acidification[kg SO2 eq.]
8.0e-4
6.4e-4
4.8e-4
3.2e-4
1.6e-4
0.0e-4
Total
EU-28: Com...
GLO: Rail tra...
GLO: Rail tra...

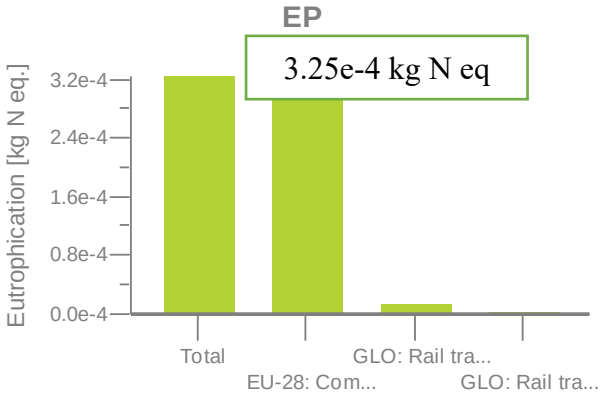
EP
3.25e-4 kg N eq
Eutrophication [kg N eq.]
3.2e-4
2.4e-4
1.6e-4
0.8e-4
0.0e-4
Total
EU-28: Com...
GLO: Rail tra...
GLO: Rail tra...

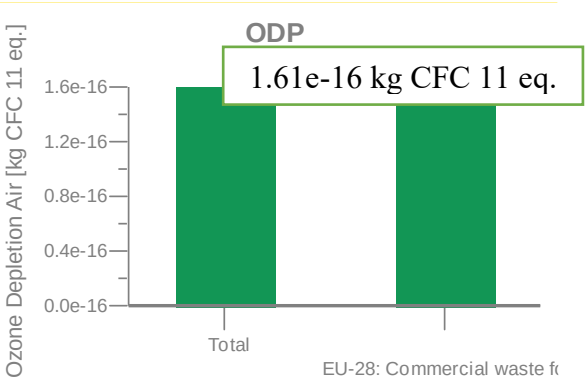
ODP
1.61e-16 kg CFC 11 eq.
Ozone Depletion Air [kg CFC 11 eq.]
1.6e-16
1.2e-16
0.8e-16
0.4e-16
0.0e-16
Total
EU-28: Commercial waste fo

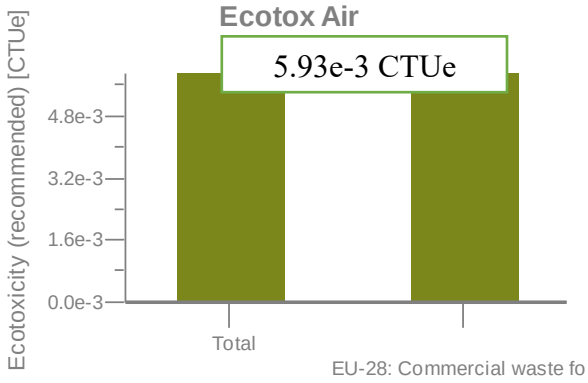
Ecotox Air
5.93e-3 CTUe
Ecotoxicity (recommended) [CTUe]
4.8e-3
3.2e-3
1.6e-3
0.0e-3
Total
EU-28: Commercial waste fo

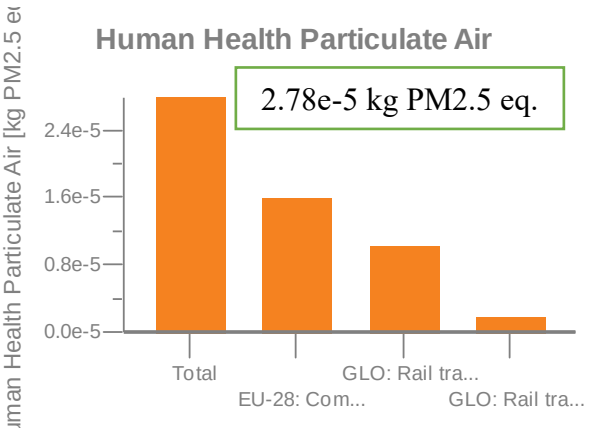
Human Health Particulate Air
2.78e-5 kg PM2.5 eq.
uman Health Particulate Air [kg PM2.5 e
2.4e-5
1.6e-5
0.8e-5
0.0e-5
Total
EU-28: Com...
GLO: Rail tra...
GLO: Rail tra...

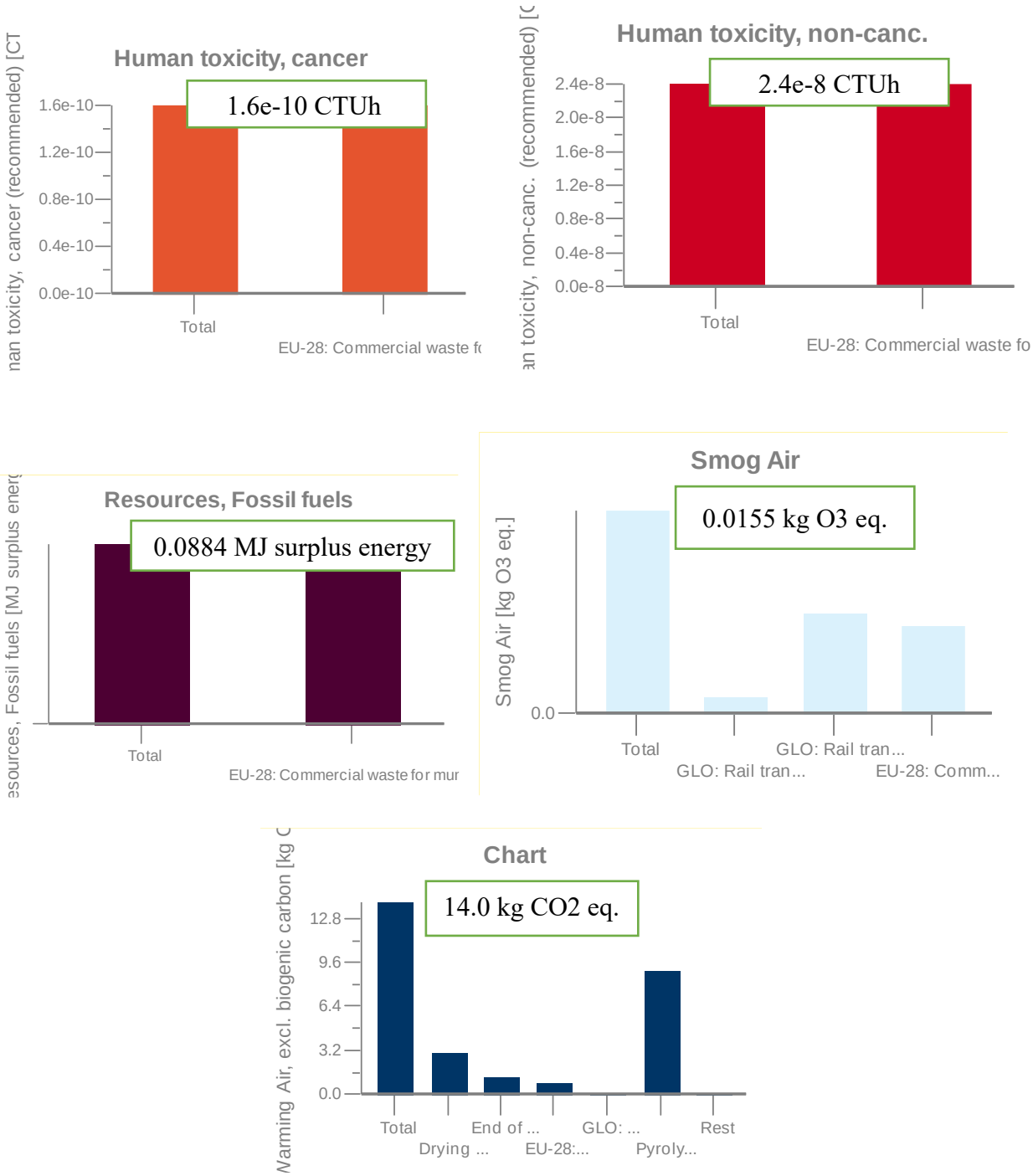

Figure 6.3.10: Life cycle impact assessment according to TRACI mid-point impact categories for BBAC-DOE 5.

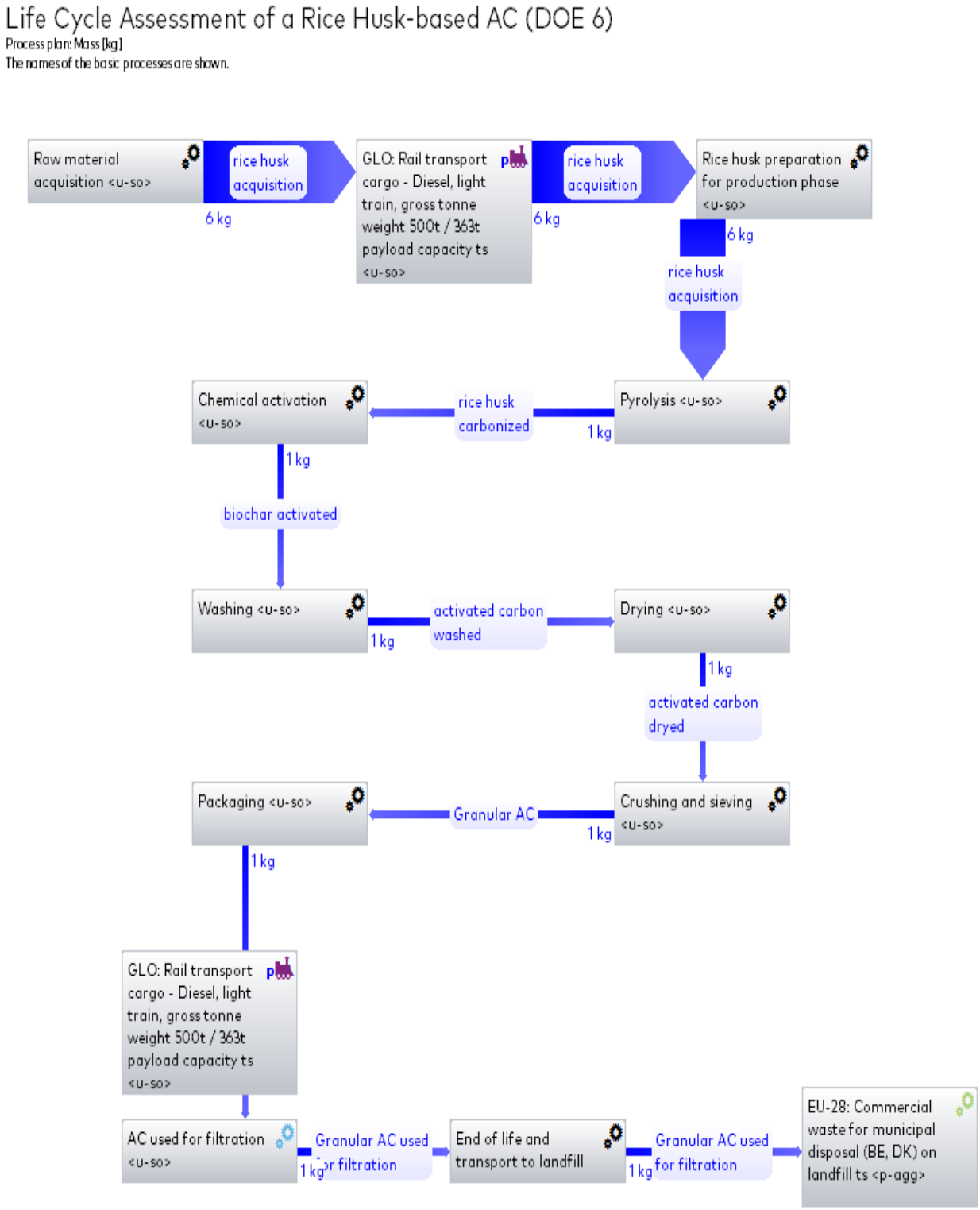

Figure 6.3.11: Process flow diagram of BBAC-DOE 6 production using GaBi software and Education_database_2020.

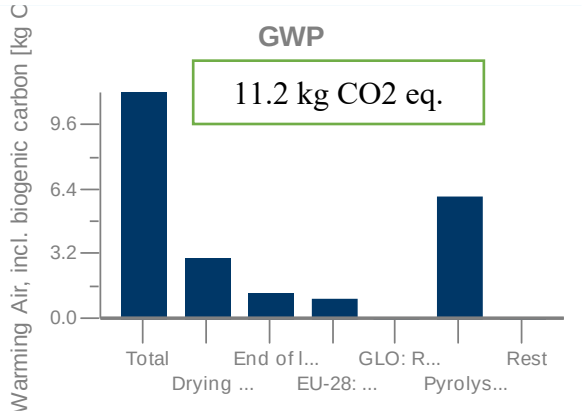
GWP
11.2 kg CO2 eq.
Warming Air, incl. biogenic carbon [kg C
9.6
6.4
3.2
0.0
Total
Drying ...
End of l...
EU-28: ...
GLO: R...
Pyrolys...
Rest

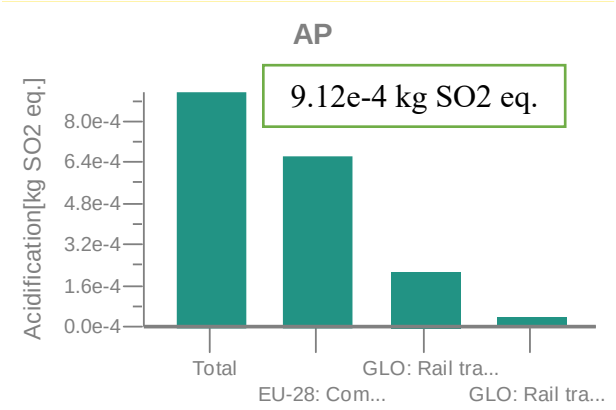
AP
9.12e-4 kg SO2 eq.
Acidification[kg SO2 eq.]
8.0e-4
6.4e-4
4.8e-4
3.2e-4
1.6e-4
0.0e-4
Total
EU-28: Com...
GLO: Rail tra...
GLO: Rail tra...

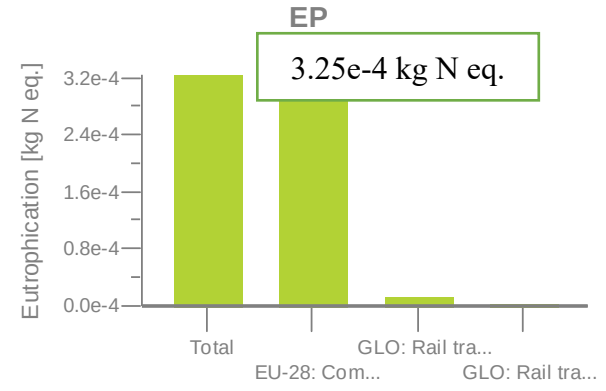
EP
3.25e-4 kg N eq.
Eutrophication [kg N eq.]
3.2e-4
2.4e-4
1.6e-4
0.8e-4
0.0e-4
Total
EU-28: Com...
GLO: Rail tra...
GLO: Rail tra...

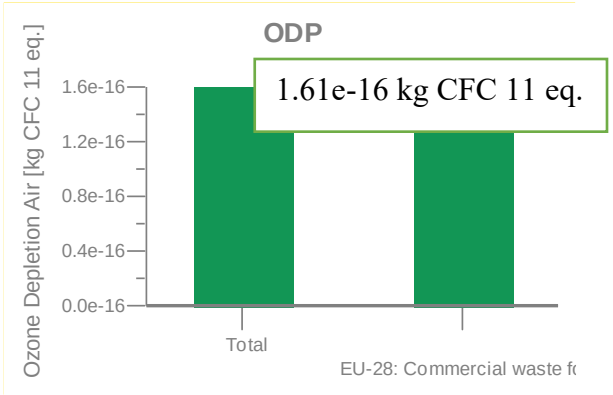
ODP
1.61e-16 kg CFC 11 eq.
Ozone Depletion Air [kg CFC 11 eq.]
1.6e-16
1.2e-16
0.8e-16
0.4e-16
0.0e-16
Total
EU-28: Commercial waste fc

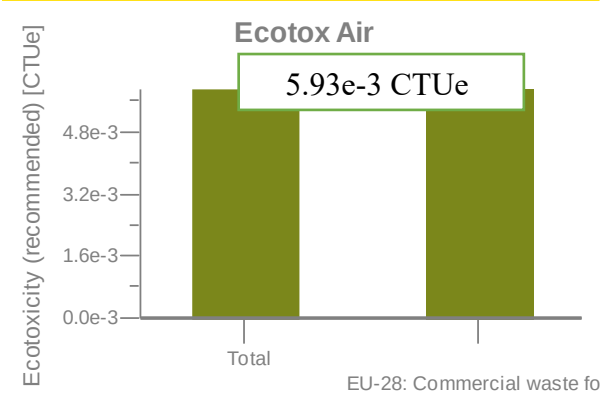
Ecotox Air
5.93e-3 CTUe
Ecotoxicity (recommended) [CTUe]
4.8e-3
3.2e-3
1.6e-3
0.0e-3
Total
EU-28: Commercial waste fo

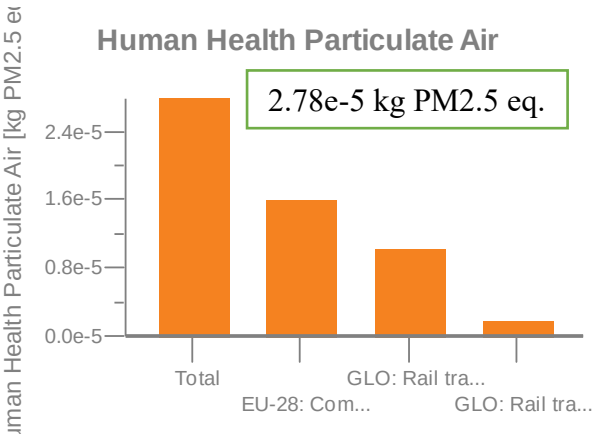
Human Health Particulate Air
2.78e-5 kg PM2.5 eq.
Iman Health Particulate Air [kg PM2.5 e
2.4e-5
1.6e-5
0.8e-5
0.0e-5
Total
EU-28: Com...
GLO: Rail tra...
GLO: Rail tra...

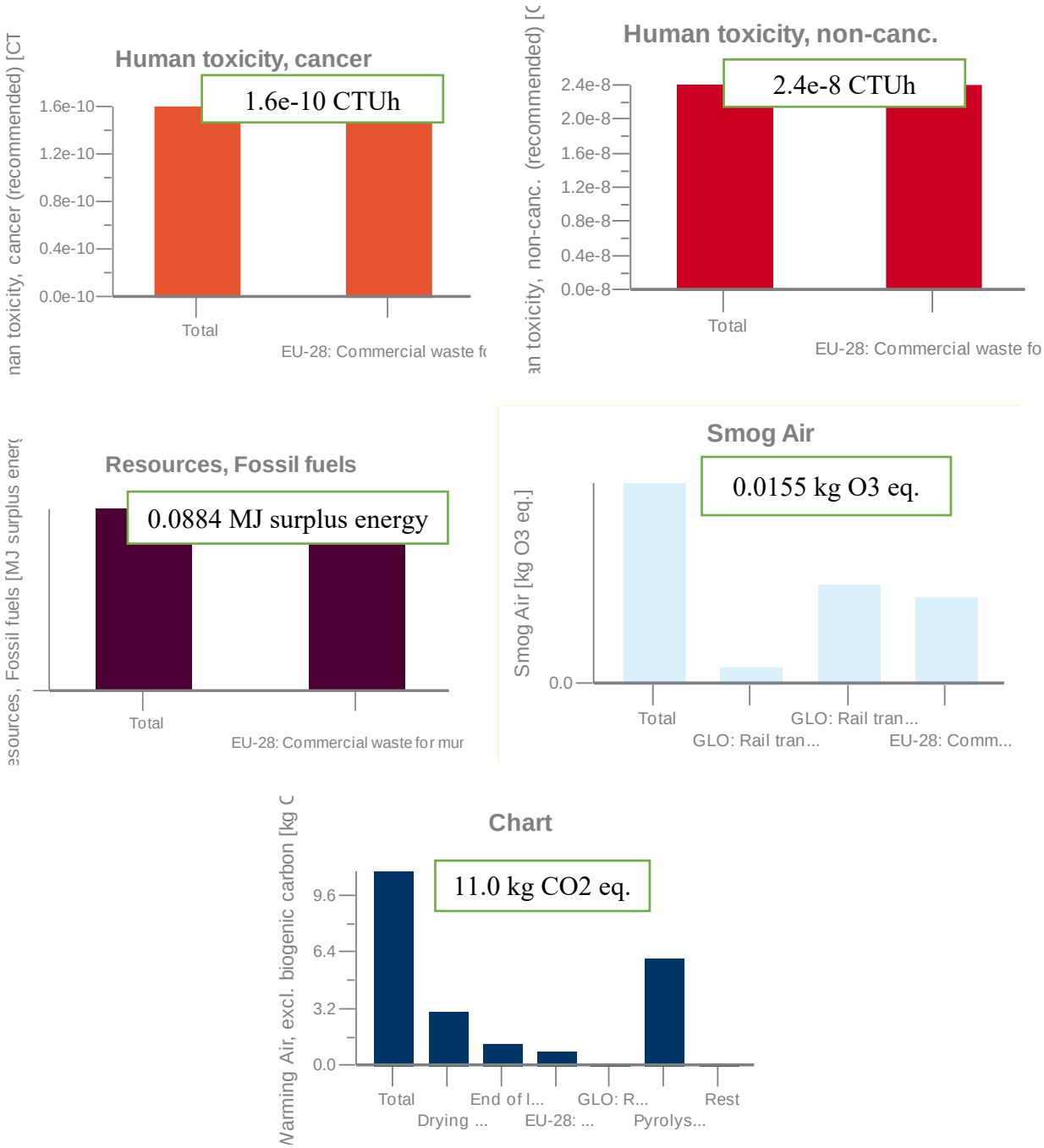

Figure 6.3.12: Life cycle impact assessment according to TRACI mid-point impact categories for BBAC-DOE 6.

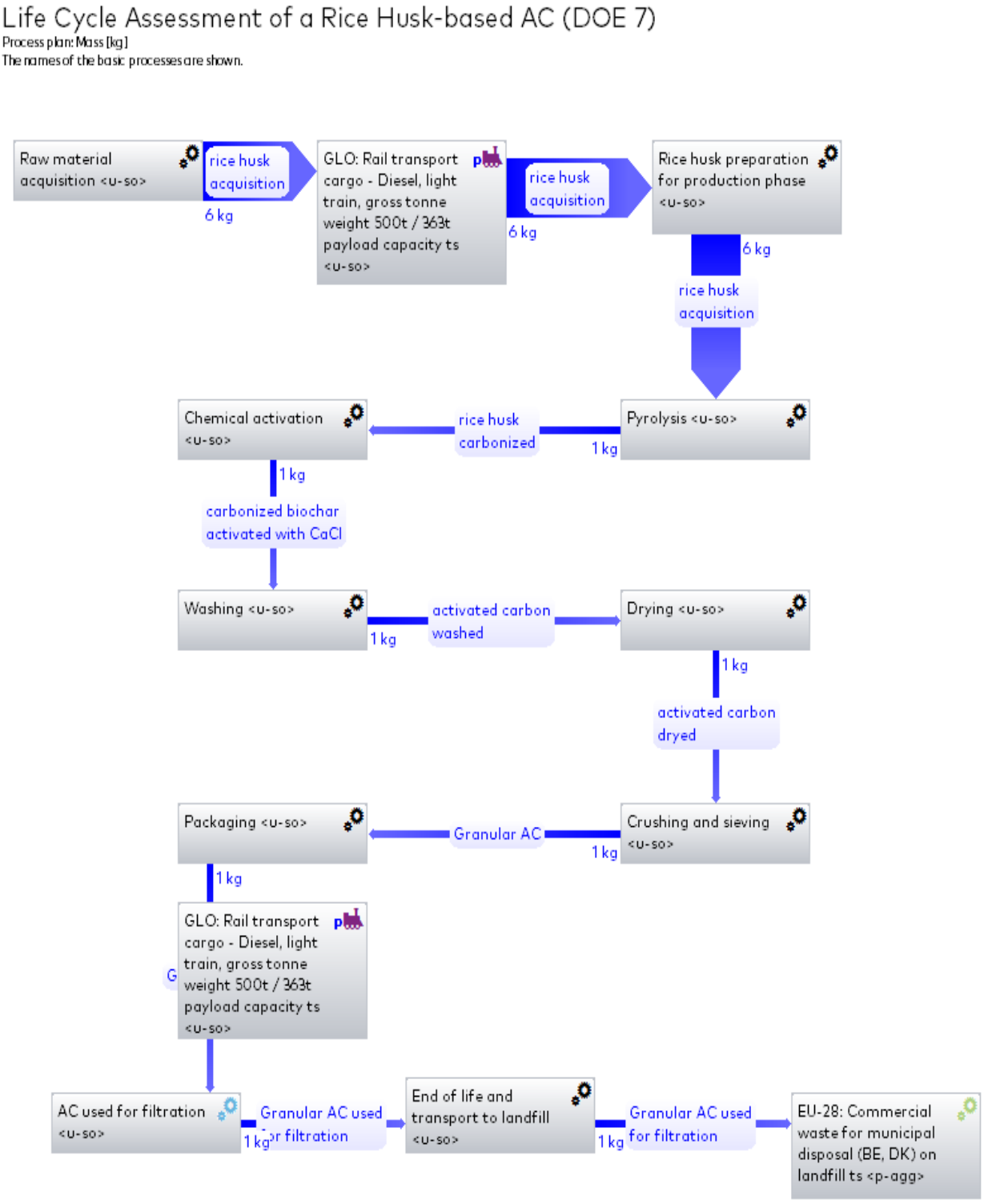

Figure 6.3.13: Process flow diagram of BBAC-DOE 7 production using GaBi software and Education_database_2020.

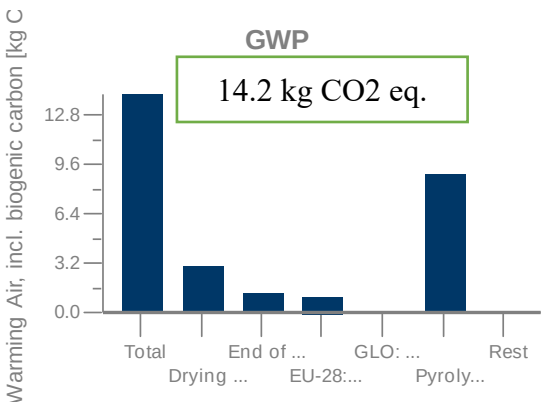
GWP
14.2 kg CO2 eq.
Warming Air, incl. biogenic carbon [kg C
12.8
9.6
6.4
3.2
0.0
Total
Drying ...
End of ...
EU-28:...
GLO: ...
Pyroly...
Rest

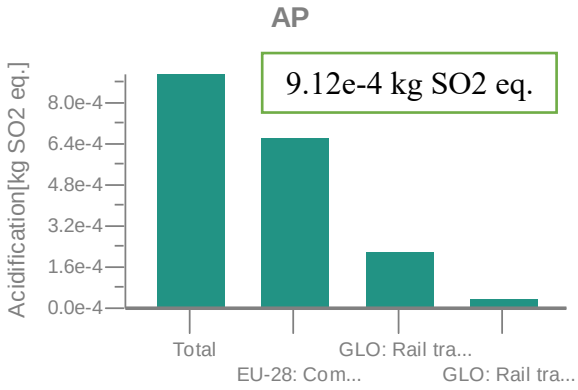
AP
9.12e-4 kg SO2 eq.
Acidification[kg SO2 eq.]
8.0e-4
6.4e-4
4.8e-4
3.2e-4
1.6e-4
0.0e-4
Total
EU-28: Com...
GLO: Rail tra...
GLO: Rail tra...

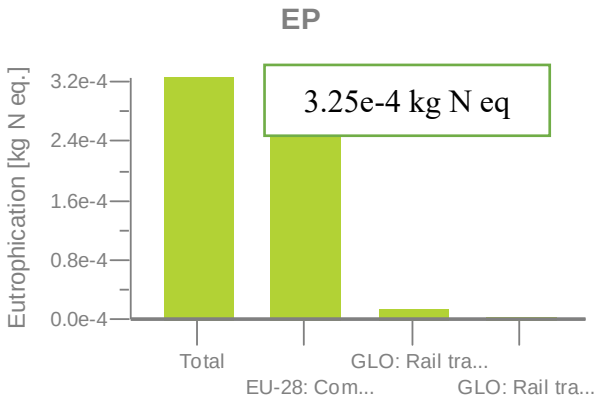
EP
3.25e-4 kg N eq
Eutrophication [kg N eq.]
3.2e-4
2.4e-4
1.6e-4
0.8e-4
0.0e-4
Total
EU-28: Com...
GLO: Rail tra...
GLO: Rail tra...

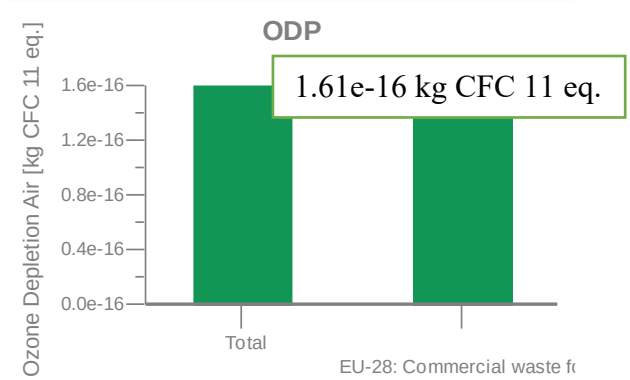
ODP
1.61e-16 kg CFC 11 eq.
Ozone Depletion Air [kg CFC 11 eq.]
1.6e-16
1.2e-16
0.8e-16
0.4e-16
0.0e-16
Total
EU-28: Commercial waste fo

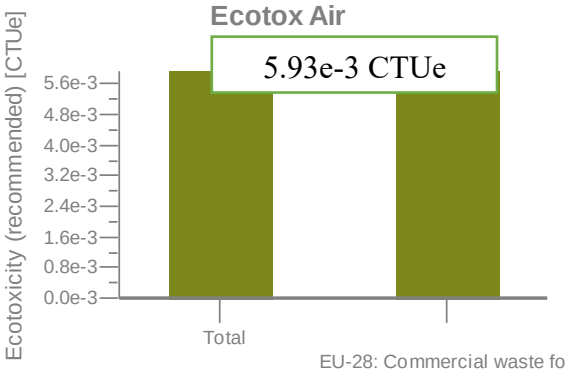
Ecotox Air
5.93e-3 CTUe
Ecotoxicity (recommended) [CTUe]
5.6e-3
4.8e-3
4.0e-3
3.2e-3
2.4e-3
1.6e-3
0.8e-3
0.0e-3
Total
EU-28: Commercial waste fo

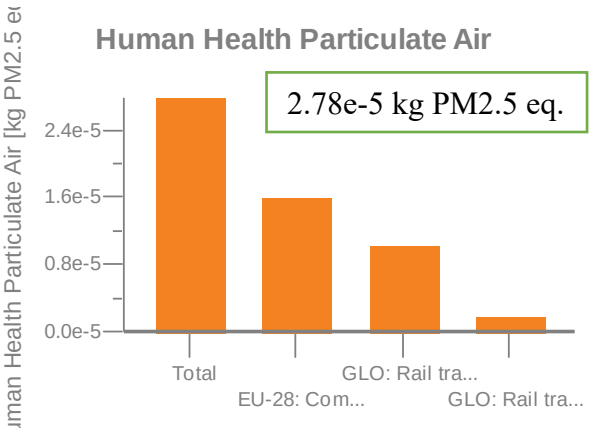
Human Health Particulate Air
2.78e-5 kg PM2.5 eq.
uman Health Particulate Air [kg PM2.5 e
2.4e-5
1.6e-5
0.8e-5
0.0e-5
Total
EU-28: Com...
GLO: Rail tra...
GLO: Rail tra...

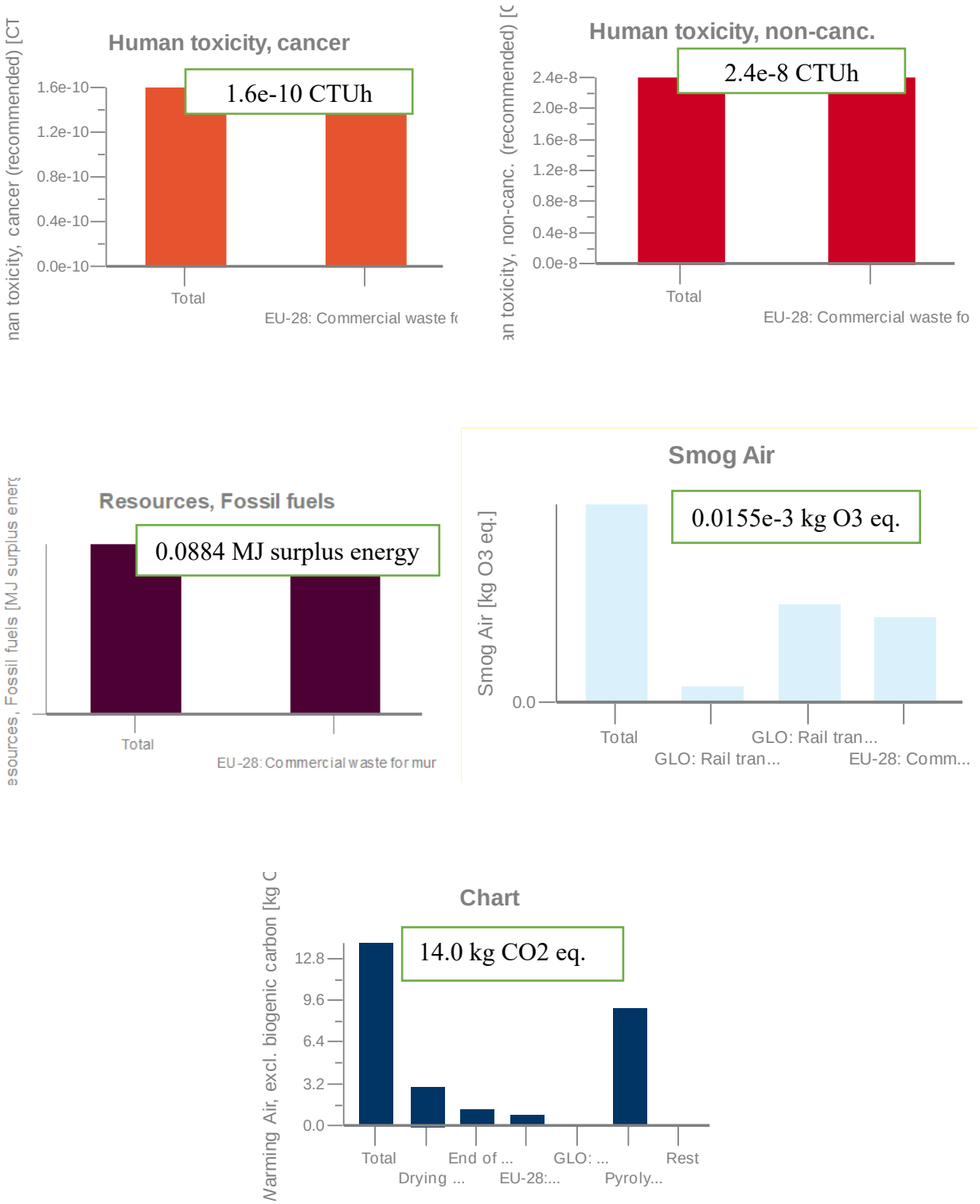

Figure 6.3.14: Life cycle impact assessment according to TRACI mid-point impact categories for BBAC-DOE 7.

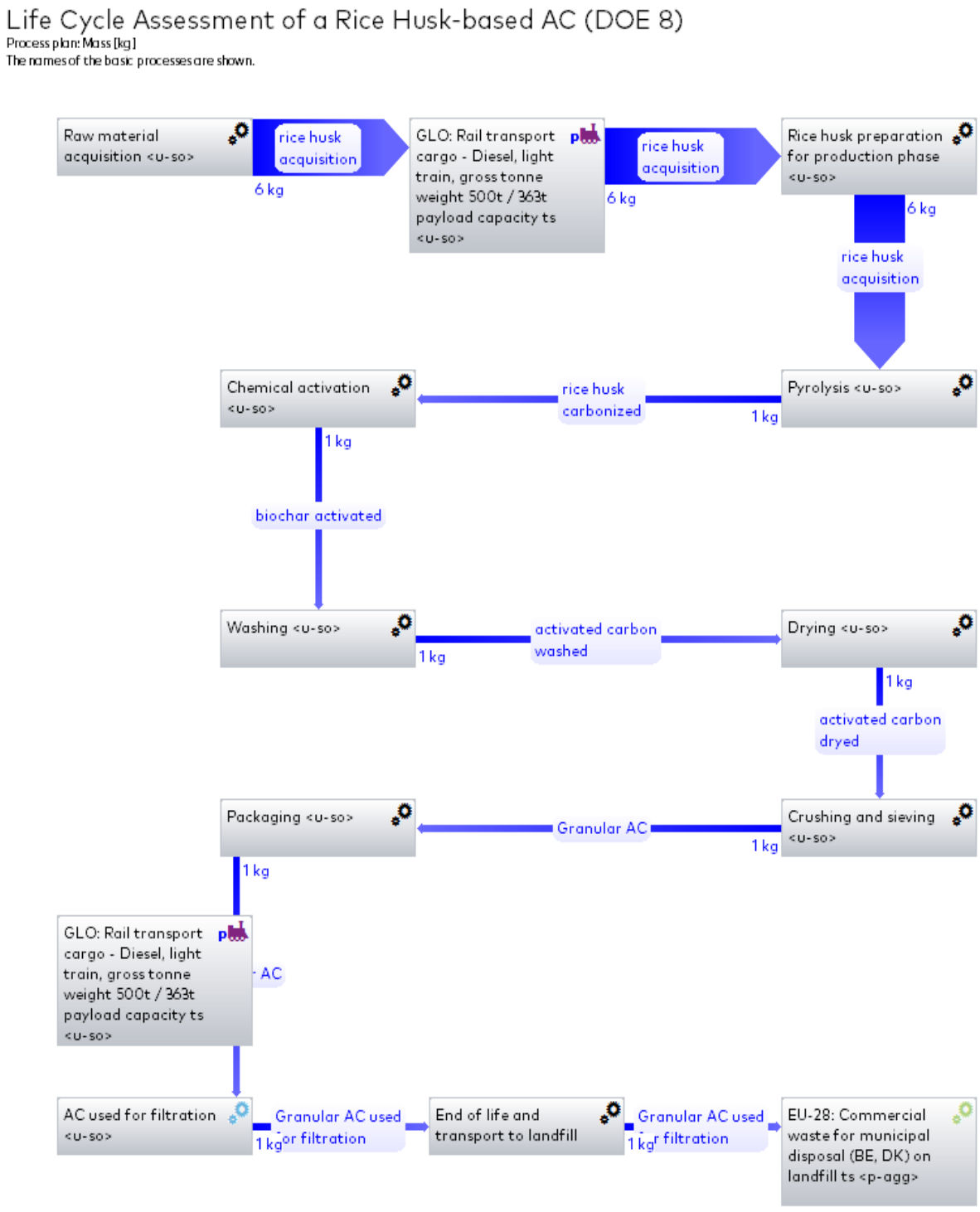

Figure 6.3.15: Process flow diagram of BBAC-DOE 8 production using GaBi software and Education_database_2020.

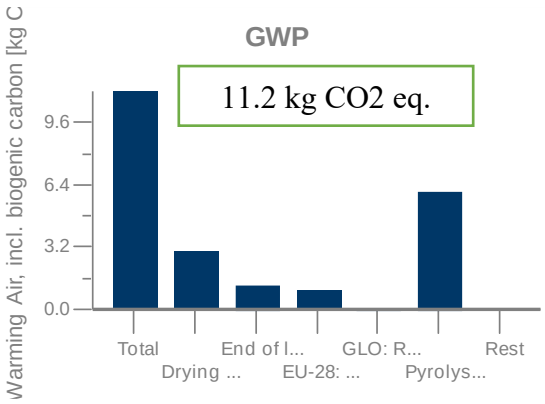
GWP
11.2 kg CO2 eq.
Warming Air, incl. biogenic carbon [kg C
9.6
6.4
3.2
0.0
Total
End of l...
GLO: R...
Rest
Drying ...
EU-28: ...
Pyrolys...

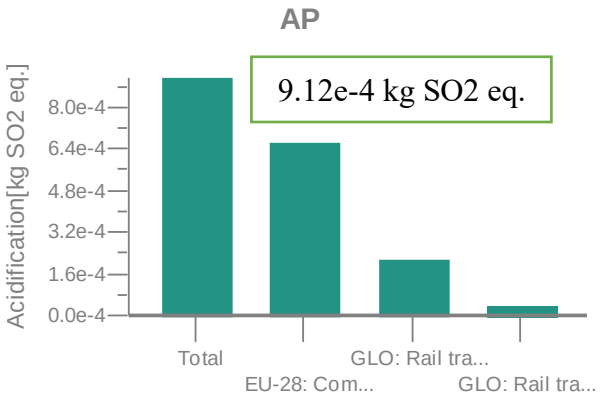
AP
9.12e-4 kg SO2 eq.
Acidification[kg SO2 eq.]
8.0e-4
6.4e-4
4.8e-4
3.2e-4
1.6e-4
0.0e-4
Total
GLO: Rail tra...
EU-28: Com...
GLO: Rail tra...

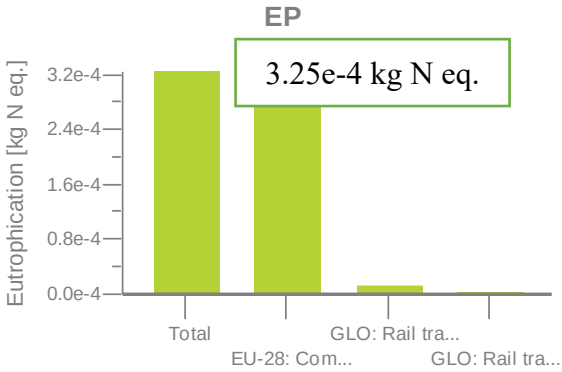
EP
3.25e-4 kg N eq.
Eutrophication [kg N eq.]
3.2e-4
2.4e-4
1.6e-4
0.8e-4
0.0e-4
Total
GLO: Rail tra...
EU-28: Com...
GLO: Rail tra...

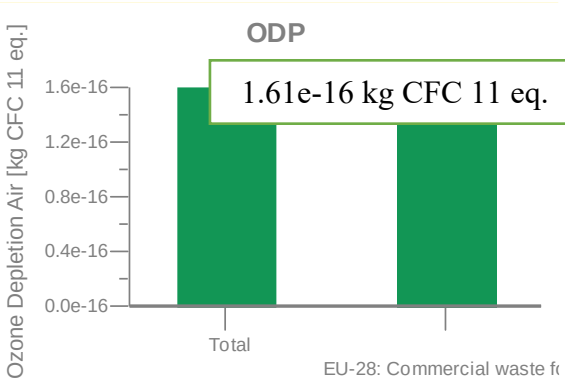
ODP
1.61e-16 kg CFC 11 eq.
Ozone Depletion Air [kg CFC 11 eq.]
1.6e-16
1.2e-16
0.8e-16
0.4e-16
0.0e-16
Total
EU-28: Commercial waste fo

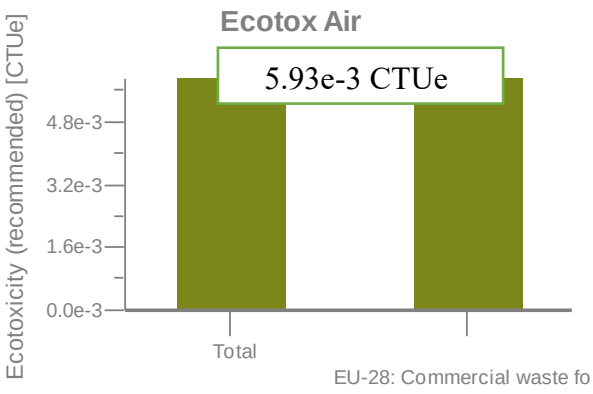
Ecotox Air
5.93e-3 CTUe
Ecotoxicity (recommended) [CTUe]
4.8e-3
3.2e-3
1.6e-3
0.0e-3
Total
EU-28: Commercial waste fo

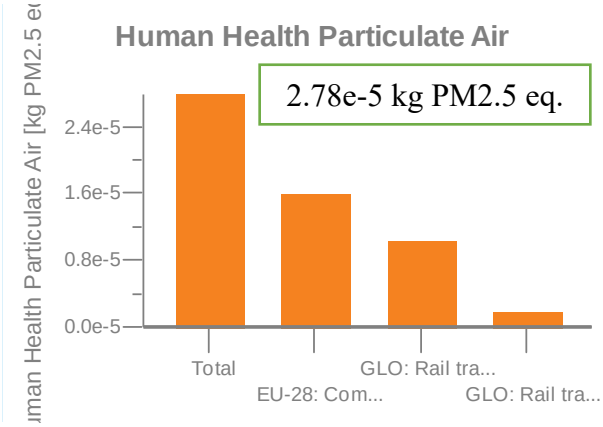
Human Health Particulate Air
2.78e-5 kg PM2.5 eq.
uman Health Particulate Air [kg PM2.5 e
2.4e-5
1.6e-5
0.8e-5
0.0e-5
Total
GLO: Rail tra...
EU-28: Com...
GLO: Rail tra...

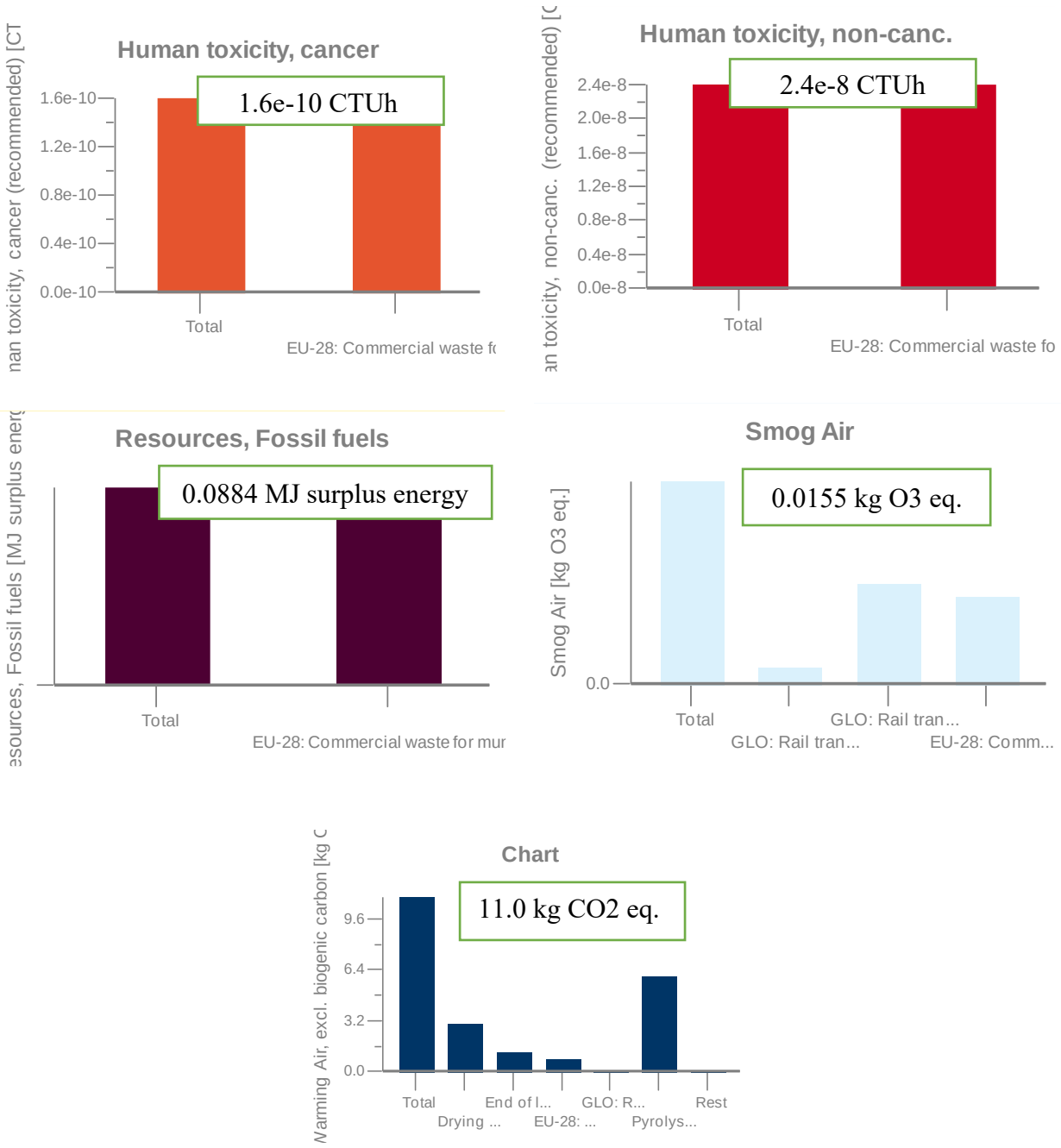

Figure 6.3.16: Life cycle impact assessment according to TRACI mid-point impact categories for BBAC-DOE 8.

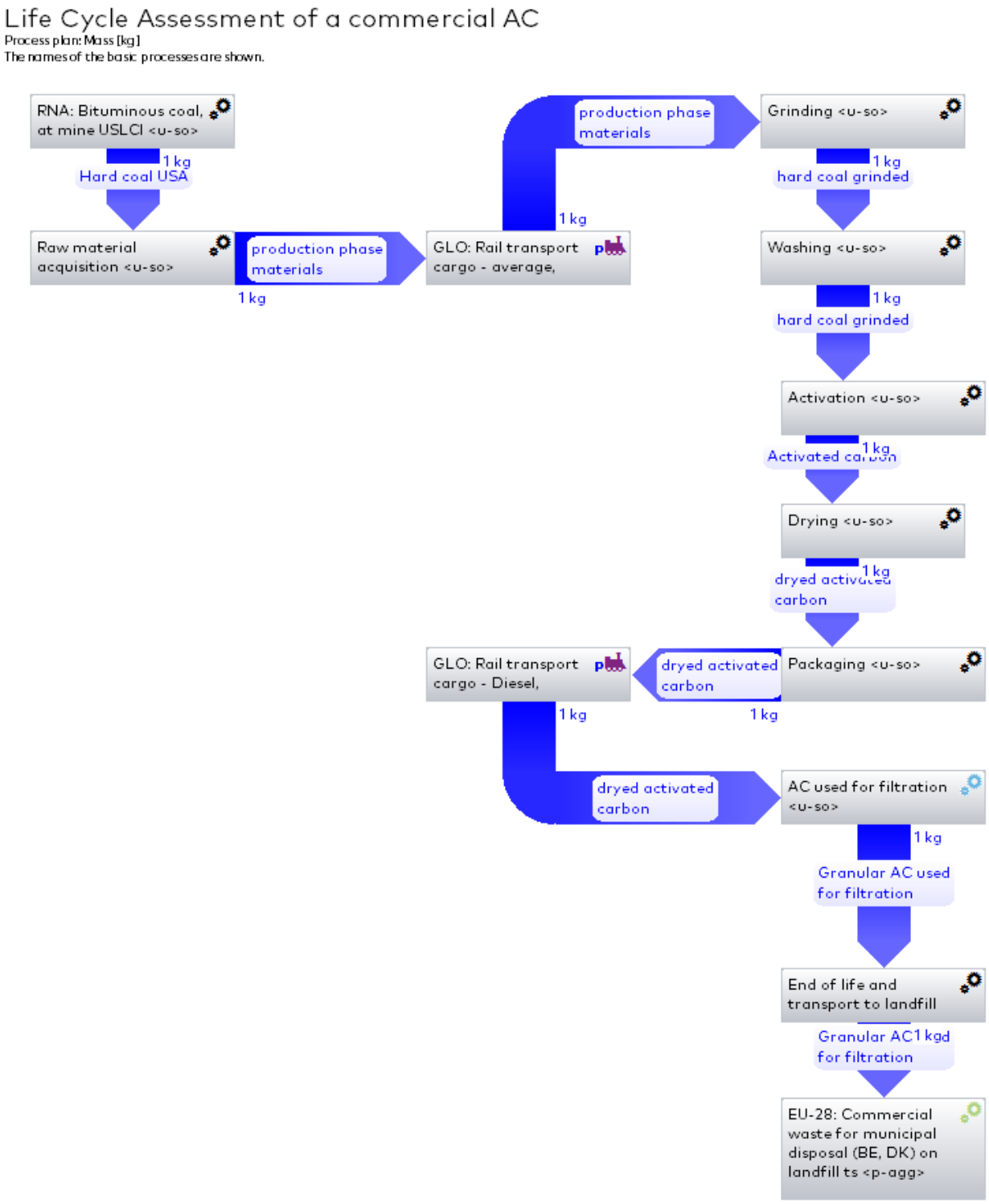

Figure 6.3.17: Process flow diagram of CCAC production using GaBi software and Education_database_2020.

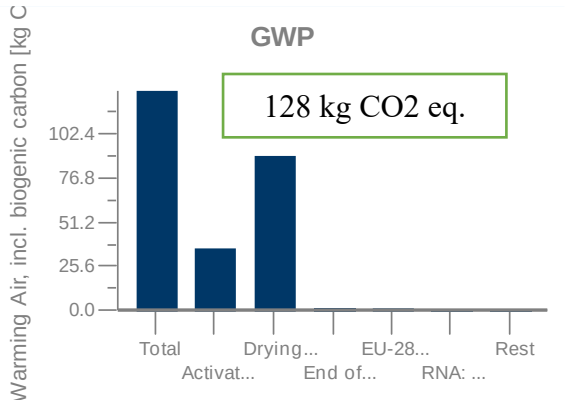
GWP
128 kg CO2 eq.
Warming Air, incl. biogenic carbon [kg C
102.4
76.8
51.2
25.6
0.0
Total
Activat...
Drying...
End of...
EU-28...
RNA: ...
Rest

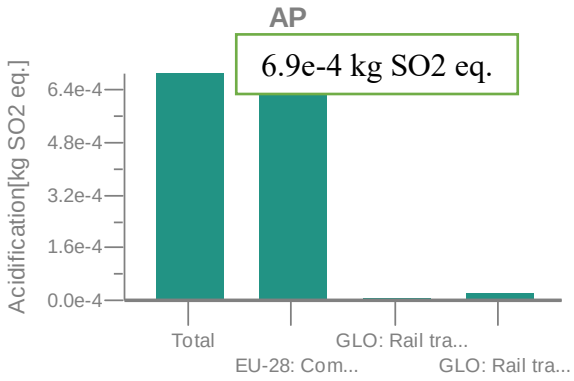
AP
6.9e-4 kg SO2 eq.
Acidification[kg SO2 eq.]
6.4e-4
4.8e-4
3.2e-4
1.6e-4
0.0e-4
Total
EU-28: Com...
GLO: Rail tra...
GLO: Rail tra...

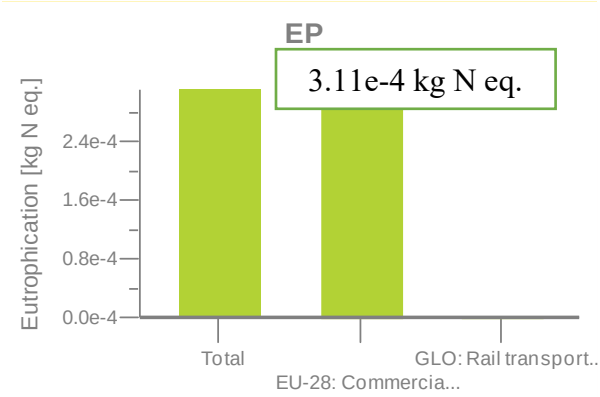
EP
3.11e-4 kg N eq.
Eutrophication [kg N eq.]
2.4e-4
1.6e-4
0.8e-4
0.0e-4
Total
EU-28: Commercia...
GLO: Rail transport..

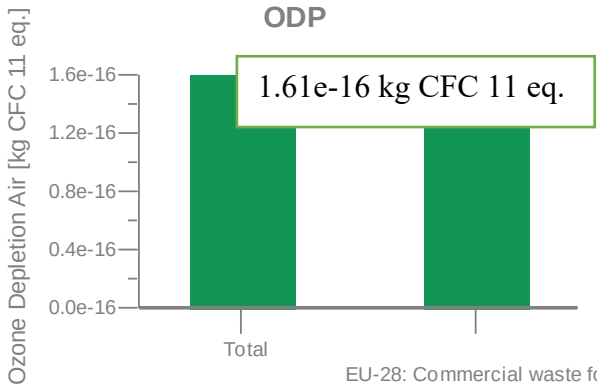
ODP
1.61e-16 kg CFC 11 eq.
Ozone Depletion Air [kg CFC 11 eq.]
1.6e-16
1.2e-16
0.8e-16
0.4e-16
0.0e-16
Total
EU-28: Commercial waste fo

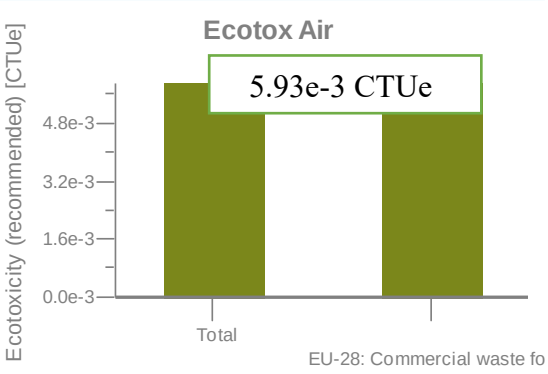
Ecotox Air
5.93e-3 CTUe
Ecotoxicity (recommended) [CTUe]
4.8e-3
3.2e-3
1.6e-3
0.0e-3
Total
EU-28: Commercial waste fo

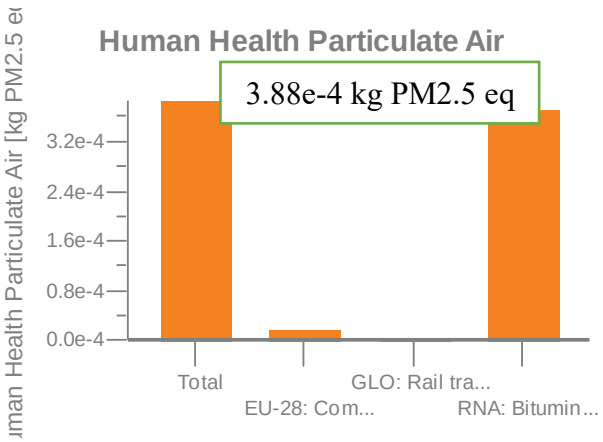
Human Health Particulate Air
3.88e-4 kg PM2.5 eq
uman Health Particulate Air [kg PM2.5 e
3.2e-4
2.4e-4
1.6e-4
0.8e-4
0.0e-4
Total
EU-28: Com...
GLO: Rail tra...
RNA: Bitumin...

.

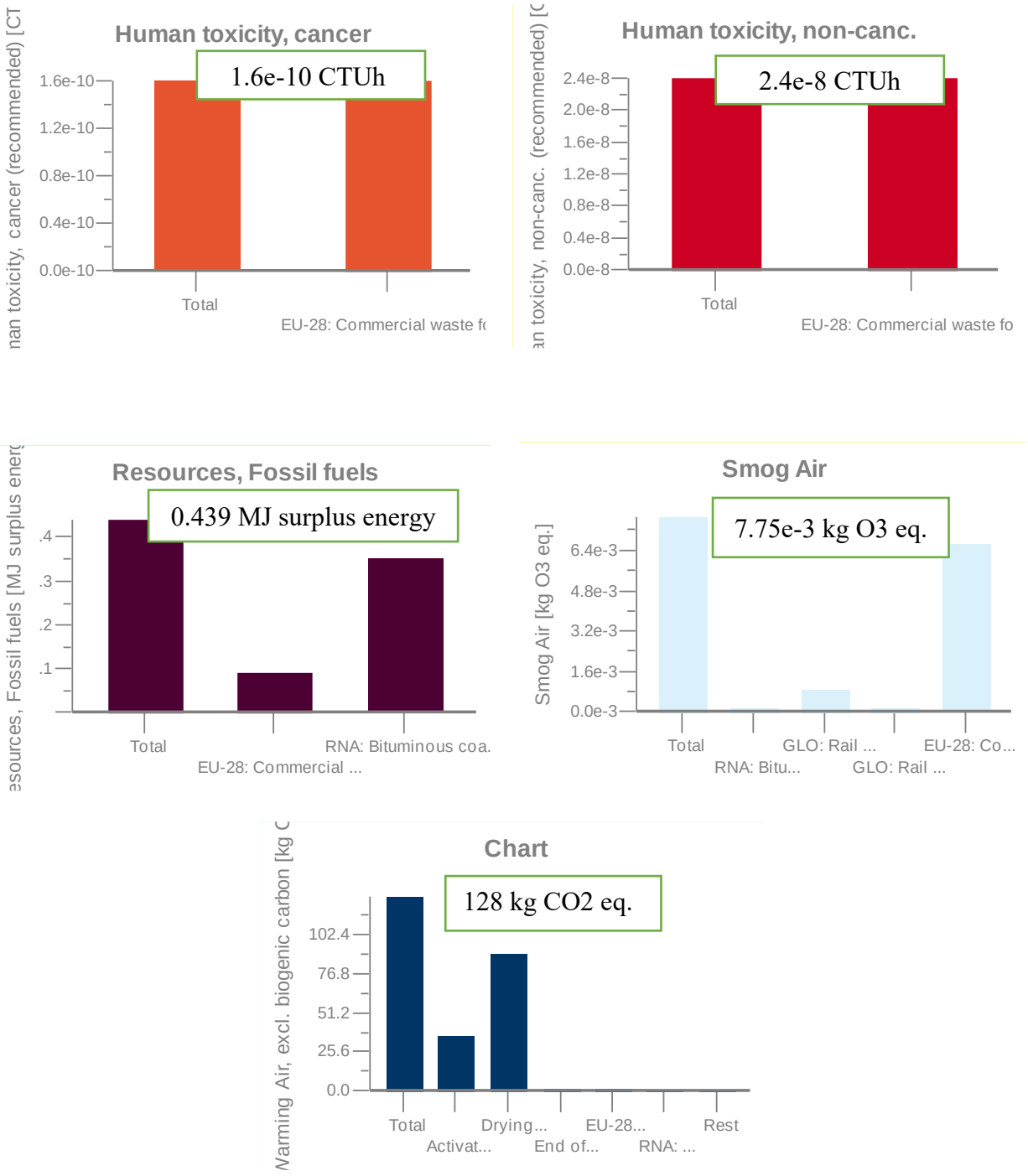

Figure 6.3.18: Life cycle impact assessment according to TRACI mid-point impact categories for CCAC.

6.4 STATISTICAL ANALYSIS

The hypothesis can be accepted or rejected once pyrolysis and activation processes are statistically evaluated through a DOE. DOE is designed to determine the main effects of the factors (precursor material, carbonization temperature, and chemical activating agent) and their interactions over the response variables (adsorption equilibrium capacity and carbon content) in the manufacture of BBAC. After the analysis, the best levels for each factor are obtained with the cube plot and/or optimizer plot to improve the production process in BBAC preparation.

$H_{0:}$ The ACs made of agricultural waste do not have better or equal adsorption equilibrium capacity for arsenic adsorption and lower production cost with less environmental impact than the commercial coal-based AC.

$$\mu 1 \geq \mu 2,$$

$\mu 1$= The response variable: physical properties of the CCAC: adsorption capacity of arsenic from water, carbon content, production cost, and environmental impact scores.

$\mu 2$= The response variable of the BBAC: adsorption capacity of arsenic from water, production cost, and environmental impact scores.

H_1: The BBAC has better or comparable adsorption properties and a lower cost of production for arsenic removal from water with less environmental impact than CCAC.

$$\mu 1 < \mu 2$$

The environmental assessment results and production cost for producing 1 kg BBAC and 1 kg CCAC will be compared, and conclusions will be documented.

6.4.1 Analysis of variance of Adsorption Equilibrium Capacity

Analysis of variance (ANOVA Unilateral) will allow for comparison of the equilibrium adsorbent-phase concentration of adsorbate (adsorption equilibrium capacity) and variation for each bio-based activated carbon prepared and commercial coal-based AC. Statistical analyses used a significance level of 0.05 ($\propto$=0.05) to determine if the means of adsorption equilibrium capacity of the samples evaluated were significantly different. All means were compared using Tukey Pairwise comparisons under the null hypothesis that all means are equal (H_0: μ_1=…= μ_8). Statistical analyses are completed using Minitab 18® (Minitab Inc.).

The mean varies from BBAC "C" (sample 11) to BBAC "H" (sample 16), ranging from 0.673 to 4.12. The adsorption capacities are statistically different among some BBACs. According to Tukey Pairwise comparisons, this difference was accounted for by five AC samples, sample 16 (H) and samples 9, 10,11, and 15 (A, B, C, and G), and are not significantly different between commercial coal-based AC and the BBAC samples according to the Tukey Method, where the means of the CCAC and BBAC share a letter.

Grouping Information Using the Tukey Method and 95% Confidence (Minitab Inc.).

Table 6.4.1: Tukey Pairwise comparisons

ARRANGEMENT	N	Mean	Grouping	
H (sample 16)	5	4.12	A	
E (sample 13)	5	2.350	A	B
F (sample 14)	5	1.458	A	B
D (sample 12)	5	1.442	A	B
I (commercial AC)	5	1.143	A	B
A (sample 9)	5	0.886		B
B (sample 10)	5	0.844		B
G (sample 15)	5	0.780		B
C (sample 11)	5	0.673		B

Means that do not share a letter are significantly different.

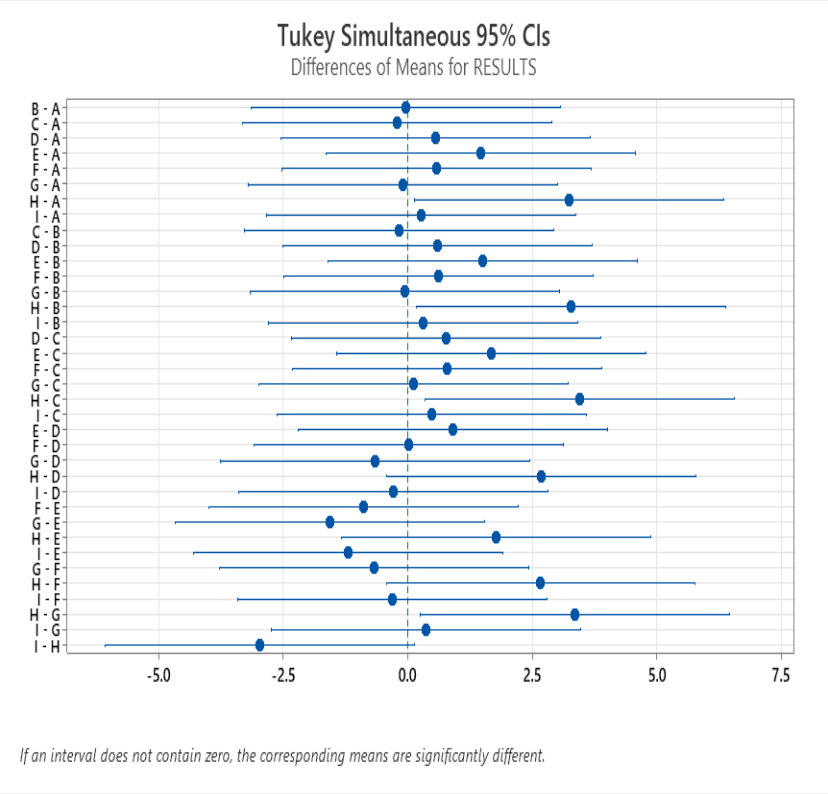

Figure 6.4.1: Adsorption equilibrium capacity (qe) mean intervals.

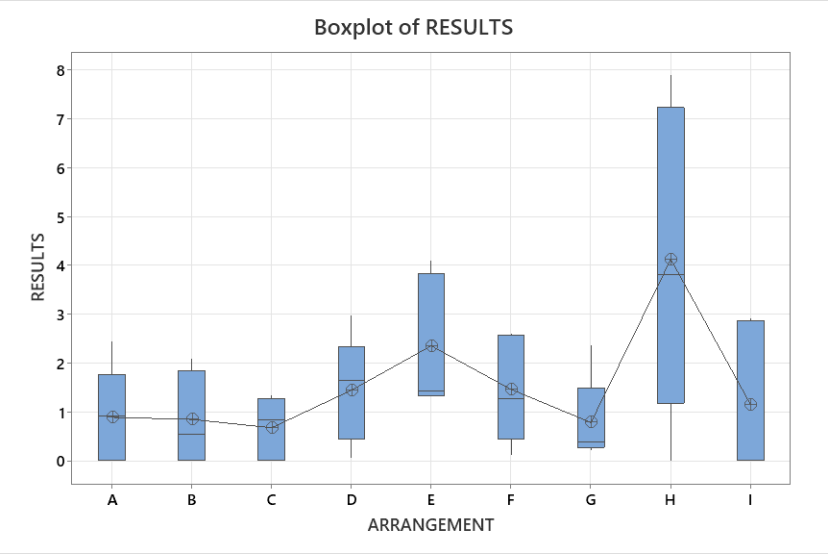

Figure 6.4.2: Adsorption equilibrium capacity (qe) boxplot showing data intervals and means.

6.4.1.1 Test for Equal Variances

The test for equal variances shows that the standard deviations of the ACs (BBACs and CCAC) are not significantly different, with a P value of 0.123 and 0.149 (P>0.05). The graph for equal variances shows overlaps between all ACs, indicating that standard deviations are not significantly different.

Table 6.4.2: Test for Equal Variances: RESULTS versus ARRANGEMENT

Method

Null hypothesis	All variances are equal
Alternative hypothesis	At least one variance is different
Significance level	$\alpha = 0.05$

95% Bonferroni Confidence Intervals for Standard Deviations

ARRANGEMENT	N	StDev	CI
Sample 9 A	5	1.00678	(0.186746, 12.1857)
Sample 10 B	5	0.95222	(0.296519, 6.8652)
Sample 11 C	5	0.64244	(0.226681, 4.0877)
Sample 12 D	5	1.09200	(0.220248, 12.1553)
Sample 13 E	5	1.36473	(0.472184, 8.8555)
Sample 14 F	5	1.09220	(0.334337, 8.0105)
Sample 15 G	5	0.89909	(0.103375, 17.5560)
Sample 16 H	5	3.17651	(0.838922, 27.0031)
Commercial AC I	5	1.56623	(0.598612, 9.2002)

Individual confidence level = 99.4444%

Tests

Method	Test Statistic	P-Value
Multiple comparisons	—	0.123
Levene	1.64	0.149

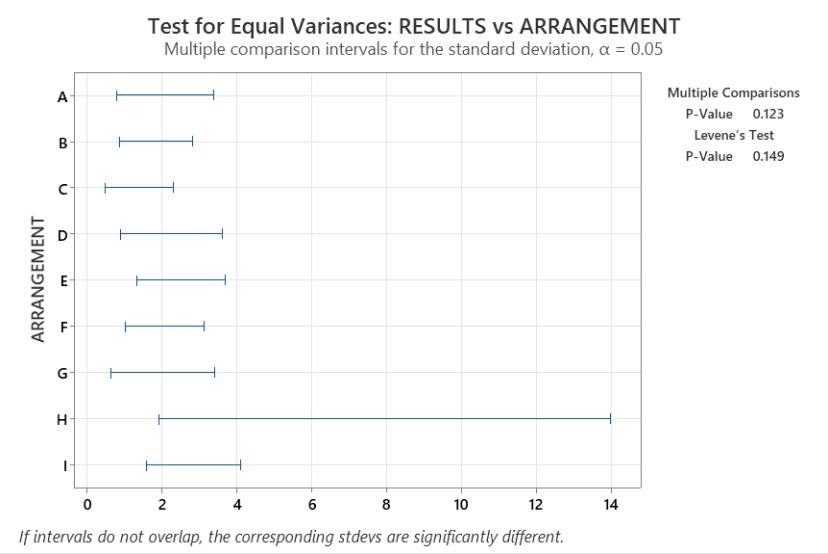

Figure 6.4.3: Graph for Equal Variances of adsorption equilibrium capacity (qe).

The test for normal/abnormal results indicates in the graph that sample 16 (H) has an adsorption equilibrium capacity very different from the other BBAC samples and the CCAC (Figure 6.4.4).

One-Way Normal ANOM for RESULTS

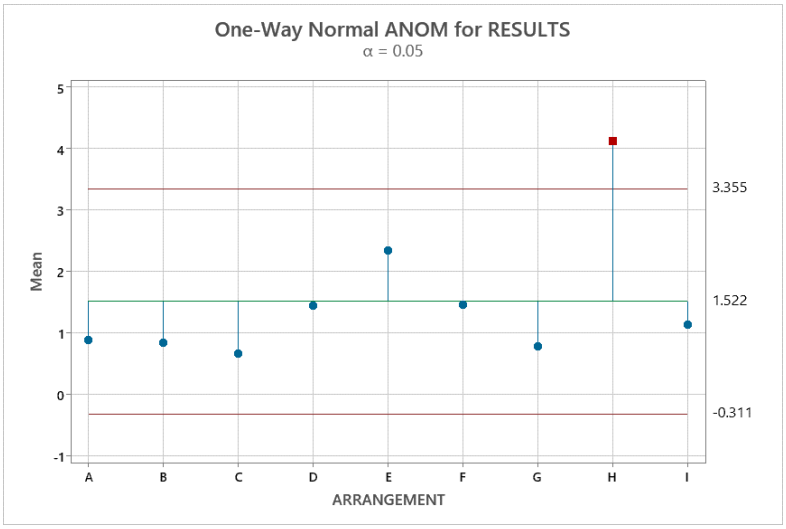

Figure 6.4.4: Graph showing ACs adsorption equilibrium capacity means for normal results.

6.4.1.2 Factorial Plots for adsorbate concentration of ~0.25mg/L

DOE graphical analysis shows in the plot of main effects that the most significant factor is raw material, followed by the carbonization temperature and the activation agent. The interaction plot shows that the combination of factors raw material/activating agent and the combination of activating agent/carbonization temperature is the most significative interaction.

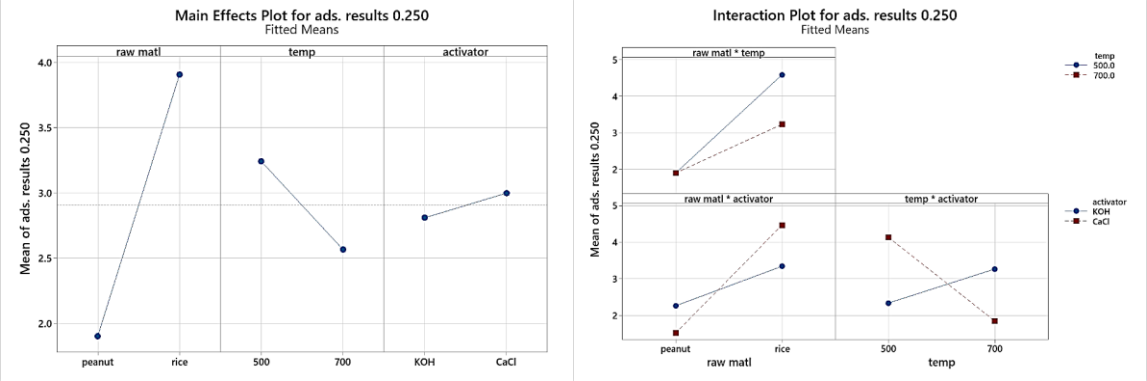

Figure 6.4.5: Factorial Plots for adsorption equilibrium capacity, arsenic solution ~0.25mg/L.

6.4.1.3 Cube Plot (fitted means)

The cube plot shows the best combination of factors to obtain the best equilibrium adsorbent-phase concentration of adsorbate (qe) in DOE for an adsorbate concentration of ~0.25mg/L. The best combination of factors, in this case, is: rice husk carbonized at 500-600°C using as activating agent calcium chloride (the largest number in the cube indicates the best combination of factors:6.55851)

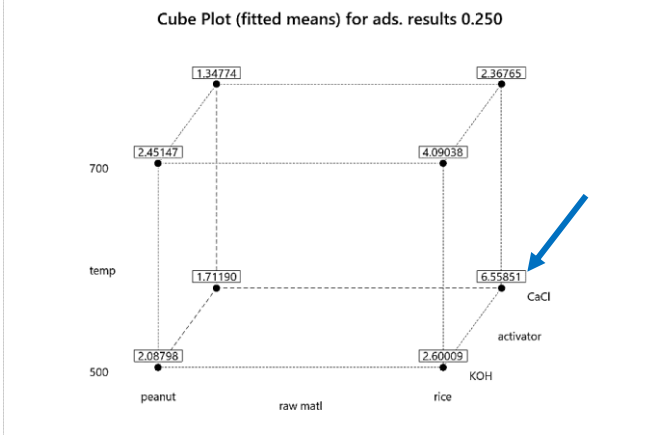

Figure 6.4.6: Cube Plot (fitted means) for adsorption equilibrium capacity (qe), adsorbate concentration ~0.25mg/L.

6.4.1.4 Factorial Plots for adsorbate concentration of ~0.15mg/L

DOE graphical analysis shows in the plot of main effects that the most significant factor is raw material, followed by the activating agent and carbonization temperature. The interaction plot shows that the combination of factors raw material/carbonization temperature and the combination of activating agent/carbonization temperature are the most significative interactions for adsorption equilibrium capacity (qe) results at adsorbate concentration of ~0.15mg/L.

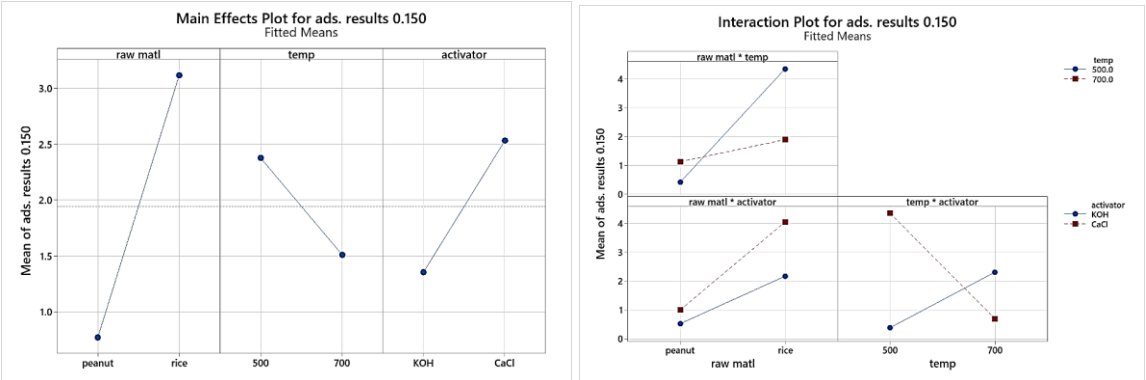

Figure 6.4.7: Factorial Plots for adsorption equilibrium capacity (qe), arsenic solution concentration ~0.15mg/L.

6.4.1.5 Cube Plot (fitted means)

The cube plot shows the best combination of factors to obtain the best equilibrium adsorbent-phase concentration of adsorbate (qe) in DOE for an adsorbate concentration of ~0.15mg/L. In this case, the best combination of factors is rice husk carbonized at 500-600°C using as activating agent calcium chloride (the largest number in the cube indicates the best combination of factors:7.89127).

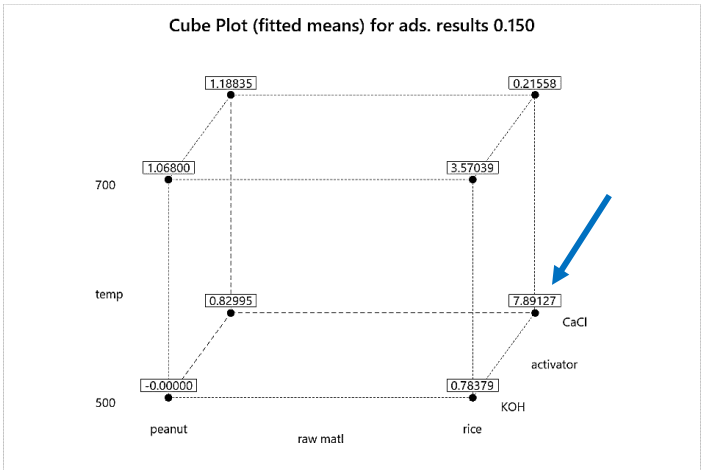

Figure 6.4.8: Cube Plot (fitted means) for adsorption equilibrium capacity (qe), adsorbate concentration ~0.15mg/L.

6.4.1.6 Factorial Plots for adsorbate concentration of ~0.100mg/L

DOE graphical analysis shows in the plot of main effects that the most significant factor is carbonization temperature. Furthermore, the interaction plot shows that the combination of factors raw material/activating agent and the combination of activating agent/carbonization temperature is the most significative interaction for adsorption equilibrium capacity (qe) results at adsorbate concentration of ~0.100mg/L.

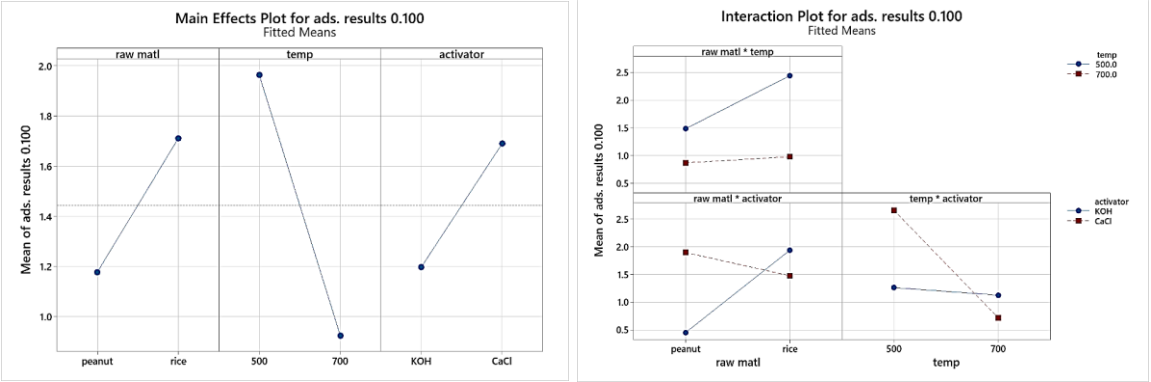

Figure 6.4.9: Factorial Plots for adsorption equilibrium capacity (qe), adsorbate concentration ~0.100mg/L.

6.4.1.7 Cube Plot (fitted means)

The cube plot shows the best combination of factors to obtain the best equilibrium adsorbent-phase concentration of adsorbate (qe) in DOE for an adsorbate concentration of ~0.100mg/L. In this case, the best combination of factors is peanut shell carbonized at 500-600°C using as activating agent calcium chloride (the largest number in the cube indicates the best combination of factors:2.97005).

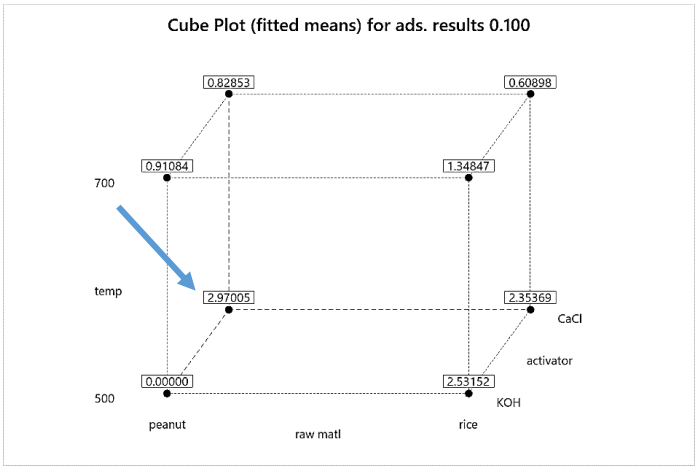

Figure 6.4.10: Cube Plot (fitted means) for adsorption equilibrium capacity (qe), adsorbate concentration ~0.100mg/L.

6.4.1.8 Factorial Plots for adsorbate concentration of ~0.050mg/L

DOE graphical analysis shows in the plot of main effects that the most significant factor is carbonization temperature. Furthermore, the interaction plot shows that the combination of factors activating agent/carbonization temperature is the most significative interaction for adsorption equilibrium capacity (qe) results at an adsorbate concentration of ~0.050mg/L. The other interactions seem to have no effect.

The interaction plot shows that the combination of factors raw material/activating agent and the combination of activating agent/carbonization temperature is the most significative interaction for adsorption equilibrium capacity (qe) results at adsorbate

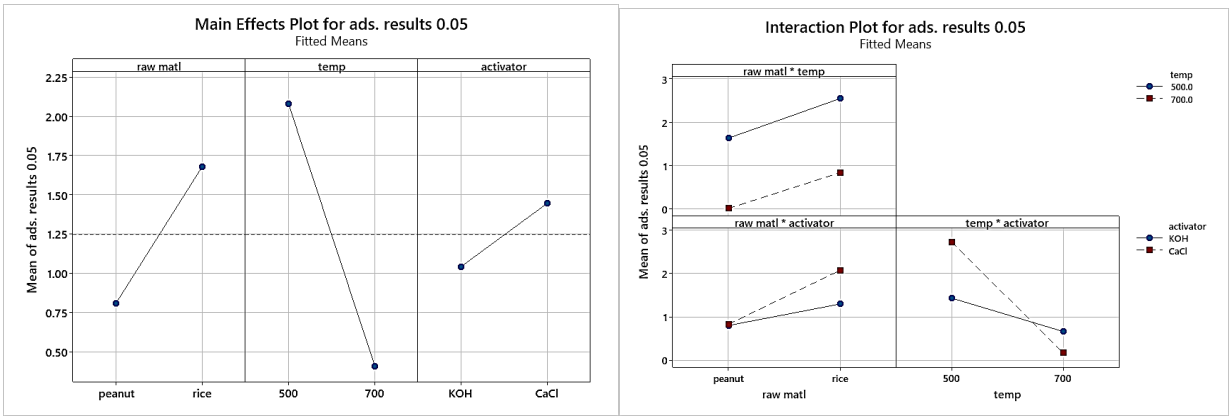

Figure 6.4.11: Factorial Plots for adsorption equilibrium capacity (qe), adsorbate concentration ~0.050mg/L.

6.4.1.9 Cube Plot (fitted means)

The cube plot shows the best combination of factors to obtain the best equilibrium adsorbent-phase concentration of adsorbate (qe) in DOE for an adsorbate concentration of ~0.050mg/L. In this case, the best combination of factors is rice husk carbonized at 500-600°C using as activating agent calcium chloride (the largest number in the cube indicates the best combination of factors:3.80702).

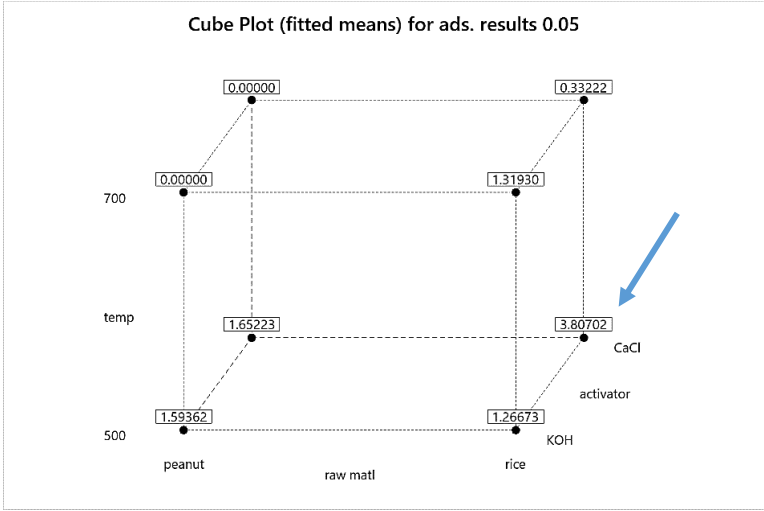

Figure 6.4.12: Cube Plot (fitted means) for adsorption equilibrium capacity (qe), adsorbate concentration ~0.050mg/L.

6.4.1.10 Factorial Plots for adsorbate concentration of ~0.025mg/L

DOE graphical analysis shows in the plot of main effects that the most significant factor is activating agent, followed by the other two factors with almost similar effects. The interaction plot shows that the combination of factors raw material/carbonization temperature is the most significative interaction. The other interactions seem to have no effect.

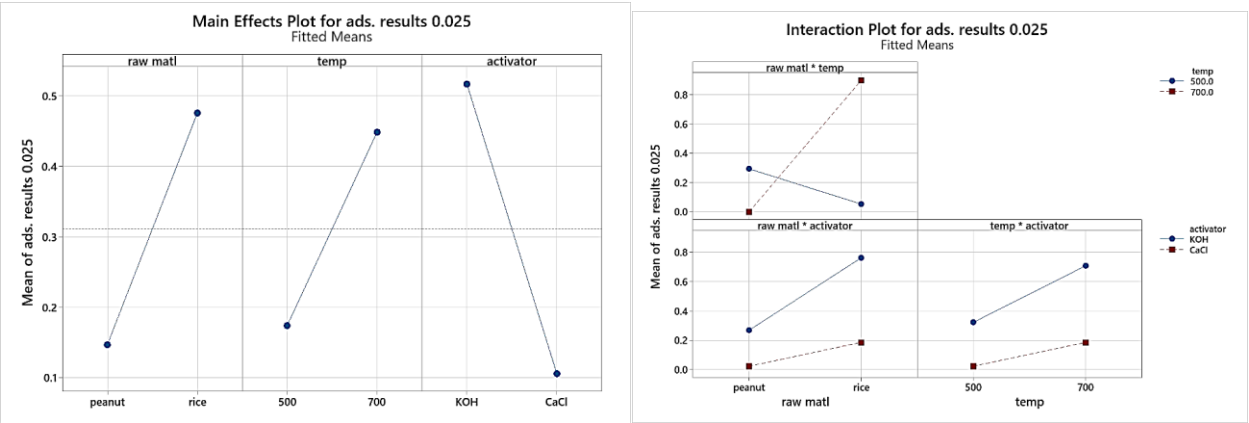

Figure 6.4.13: Factorial Plots for adsorption equilibrium capacity (qe), adsorbate concentration ~0.025mg/L.

6.4.1.11 Cube Plot (fitted means)

The cube plot shows the best combination of factors to obtain the best equilibrium adsorbent-phase concentration of adsorbate (qe) in DOE for an adsorbate concentration of ~0.025mg/L. In this case, the best combination of factors is rice husk carbonized at 600-800°C using as activating agent potassium hydroxide (the largest number in the cube indicates the best combination of factors:1.41930).

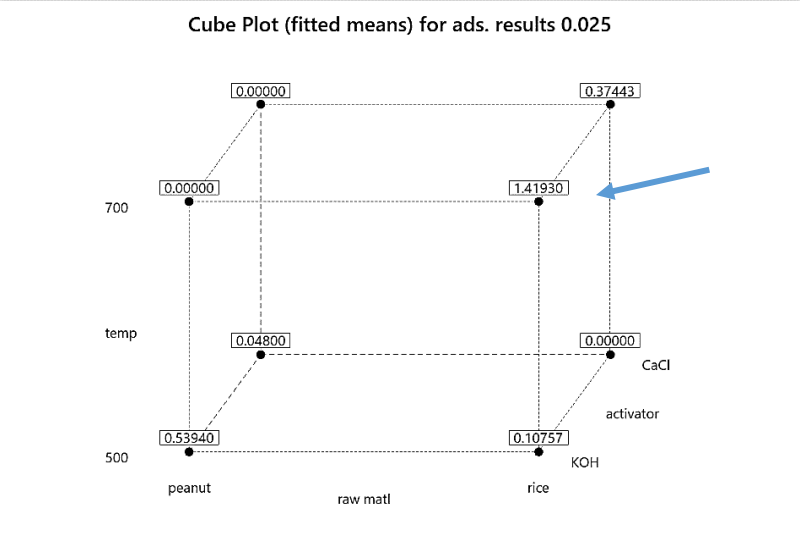

Figure 6.4.14: Cube Plot (fitted means) for adsorption equilibrium capacity (qe), adsorbate concentration ~0.025mg/L.

6.4.2 Factorial design analysis of the DOE 2^3

Full factorial design allows us to determine the main effects of the controllable factors on the response variable and thus estimate the levels of the factors and their interactions to obtain the best results. The factors and levels selected for this DOE are based on previous studies using similar agricultural waste. This DOE aims to find factors, levels, and interactions for the preparation of BBACs capable of adsorbing arsenic from water, prepared with agricultural waste from the region, better or at least equal to the CCAC. The factors considered are precursor material (peanut shell and rice husk), pyrolysis temperature (500-600 and 600-800°C), and chemical

activation material (KOH and CaCl) (Table 6.1 DOE matrix). One of the significant response variables considered for this DOE is carbon content percentage. Also, oxygen and activating elements (potassium, chlorine, and calcium) content are considered for comparative analysis.

The DOE contains a total of 24 runs, with three factors at two levels. The base runs contain eight distinct combinations of factors and levels, followed by two repetitions of each combination, thus creating a total of three replicates.

Table 6.4.3: Design of experiments summary indicating the total number of experiments, factor information, and analysis of variance results.

Design Summary

Factors:	3	Replicates:	3
Base runs:	8	Total runs:	24
Base blocks:	1	Total blocks:	1

Factor Information

Factor	Levels	Values
RAW MATL	2	1, 2
PYROLYSIS TEMP	2	1, 2
ACT. AGENT	2	1, 2

Analysis of Variance

Source	DF	Adj SS	Adj MS	F-Value	P-Value
Model	7	3097.98	442.57	2.26	0.084
Linear	3	1890.21	630.07	3.22	0.051
RAW MATL	1	1081.38	1081.38	5.52	0.032
PYROLYSIS TEMP	1	597.00	597.00	3.05	0.100
ACT. AGENT	1	211.82	211.82	1.08	0.314
2-Way Interactions	3	674.78	224.93	1.15	0.360
RAW MATL*PYROLYSIS TEMP	1	123.76	123.76	0.63	0.438
RAW MATL*ACT. AGENT	1	465.52	465.52	2.38	0.143
PYROLYSIS TEMP*ACT. AGENT	1	85.50	85.50	0.44	0.518
3-Way Interactions	1	532.98	532.98	2.72	0.119
RAW MATL*PYROLYSIS TEMP*ACT. AGENT	1	532.98	532.98	2.72	0.119
Error	16	3135.21	195.95		
Total	*23*	*6233.19*			

Analysis of the variance above indicates that the raw material is a significative factor for the response variable carbon content, with a value of P=0.032 (P<0.05). Pareto Chart below also indicates that the most significative factor crossing the red dotted line, in this case, is the raw material used to prepare the BBAC (peanut shell/ rice husk). The carbonization temperature, activating material and their interactions are not statistically significative for the response variable.

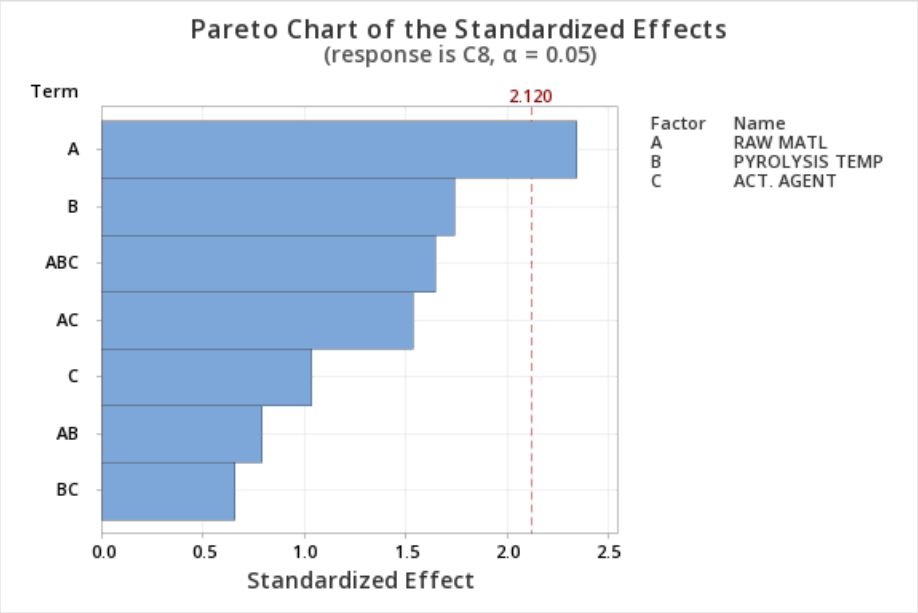

Figure 6.4.15: Pareto chart for carbon content indicating factors and interactions.

6.4.2.1 DOE Factorial Plots for carbon content

DOE graphical analysis shows in the plot of main effects that the most significant factor for carbon content percentage is the raw material (peanut shell/rice husk). Furthermore, the interaction plot shows that the combination of factors of raw material/activating agent is the most significative interaction for carbon content results. The other interactions seem to have no effect.

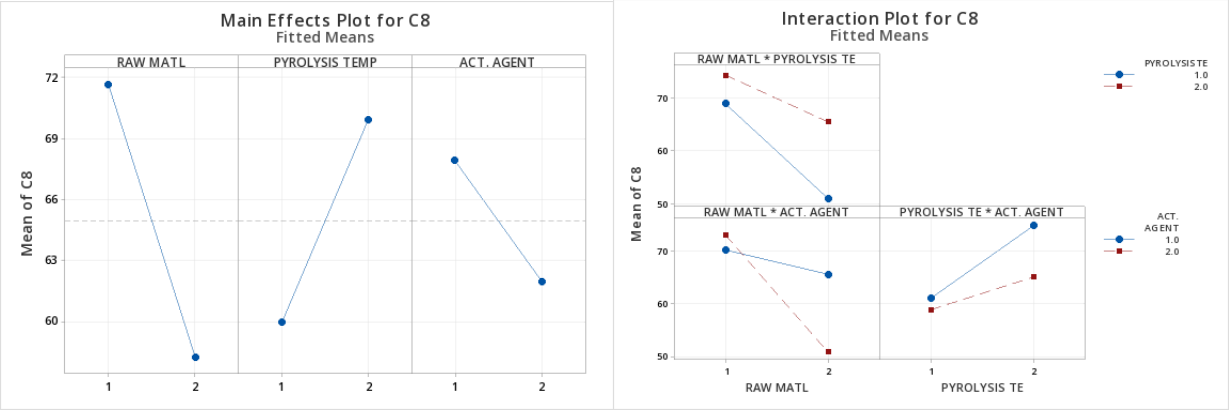

Figure 6.4.16: Factorial plots for main effects and interaction for the response variable carbon content (C8).

6.4.2.2 Optimizer

The optimizer shows the best combination of factors to obtain the best carbon content in DOE. The best combination of factors, in this case, are: peanut shell carbonized at 600-800°C using as activating agent potassium hydroxide

Table 6.4.4: Optimizer calculations in Minitab18®

Parameters

Response	Goal	Lower	Target	Upper	Weight	Importance
C8	Maximum	22.3	86.2		1	1

Solution

Solution	RAW MATL	PYROLYSIS TEMP	ACT. AGENT	C8 Fit	Composite Desirability
1	1	2	1	79.5667	0.896192

Multiple Response Prediction

Variable	Setting
RAW MATL	1
PYROLYSIS TEMP	2
ACT. AGENT	1

Response	Fit	SE Fit	95% CI	95% PI
C8	79.57	8.08	(62.43, 96.70)	(45.30, 113.83)

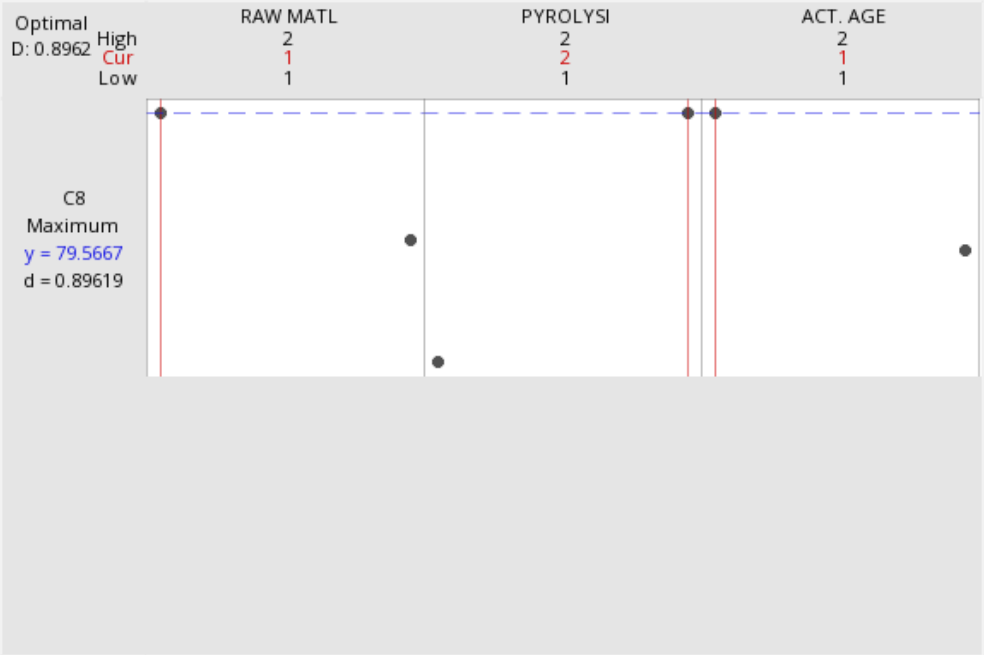

Figure 6.4.17: Optimizer plot for the best combination of factors for the response variable carbon content.

6.4.3 Analysis of variance (ANOVA Unilateral) of carbon content percentage

Each bio-based activated carbon prepared was analyzed using the analysis of variance (ANOVA) to compare carbon content percentage and variation. Statistical analyses used a significance level of 0.05 ($\propto$=0.05) to determine if the means of carbon content percentage of samples evaluated differed significantly. All means were compared using Tukey Pairwise comparisons under the null hypothesis that all means are equal (H_0: μ_1=…= μ_8). Statistical analyses were done using Minitab 18® (Minitab Inc.).

The mean varies from 40.80% to 80.1%. The carbon content percentage is statistically different among BBAC samples 3 and 6, and the CCAC is only statistically different with sample 6 according to the variance analysis (ANOVA, F=2.66, P=0.04) and Tukey Pairwise comparisons. Grouping Information using the Tukey Method and 95% Confidence confirm that means that do not share a letter are significantly different; in the intervals graph, samples 6 and 3 and 6 and 9 do

not contain zero, confirming that the means of these samples are statistically different. Null hypothesis can be rejected.

Table 6.4.5: ANOVA Minitab 18® results for carbon content percentage

Analysis of Variance

Source	DF	Adj SS	Adj MS	F-Value	P-Value
sample	8	3708	463.5	2.66	0.040
Error	18	3135	174.2		
Total	26	6844			

Grouping Information Using the Tukey Method and 95% Confidence

sample	N	Mean	Grouping	
9	3	80.1000	A	
3	3	79.57	A	
2	3	77.00	A	B
7	3	70.07	A	B
4	3	69.23	A	B
5	3	61.20	A	B
8	3	61.0	A	B
1	3	60.9	A	B
6	3	40.80		B

Means that do not share a letter are significantly different.

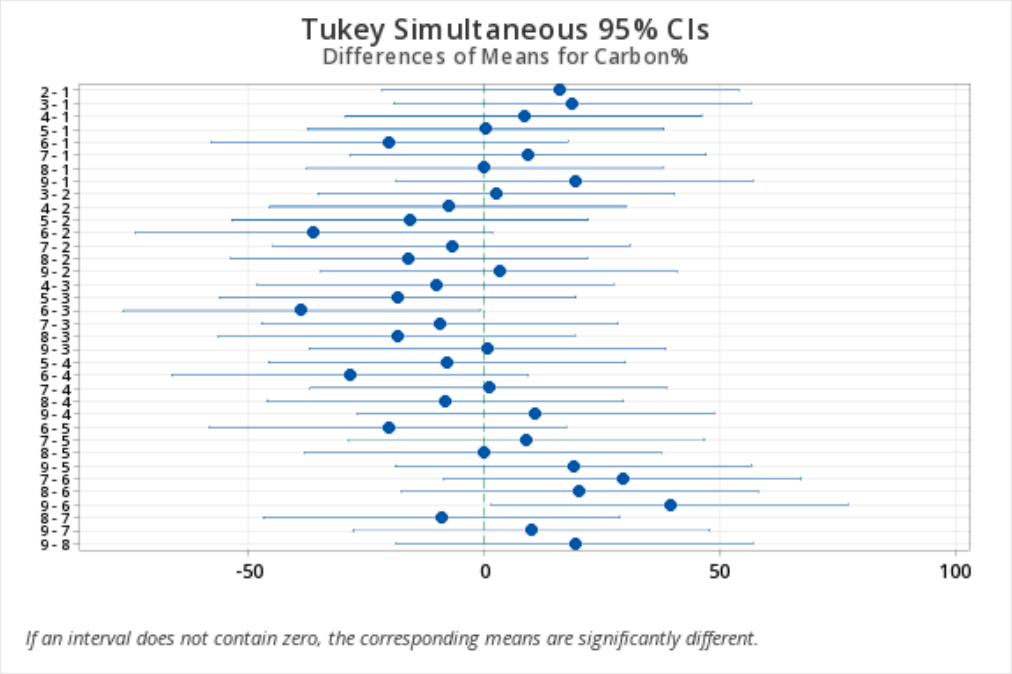

Figure 6.4.18: Interval plot for Tukey comparison method for the response variable carbon content.

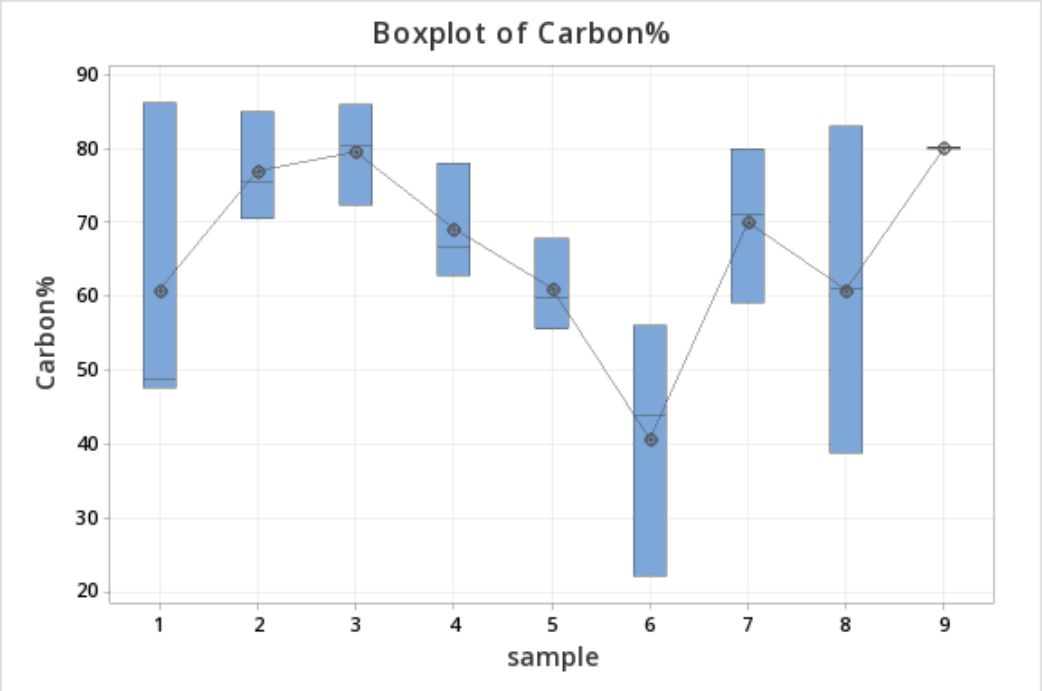

Figure 6.4.19: Boxplot showing data intervals and means for the response variable carbon content.

6.4.4 Analysis of variance (ANOVA Unilateral) of oxygen content percentage

The mean varies from 10.97% to 35.23%. The oxygen content percentage is statistically different among BBACs samples 3 and 6, but BBACs are not statistically different from CCAC according to the variance analysis (ANOVA, F=2.32, P=0.066) and Tukey Pairwise comparisons. Grouping Information Using the Tukey Method and 95% Confidence confirm that means that do not share a letter are significantly different; in the intervals graph samples, 6 and 3 do not contain zero, confirming that the means of these samples are statistically different.

Table 6.4.6: ANOVA Minitab 18® results for oxygen content percentage

Analysis of Variance

Source	DF	Adj SS	Adj MS	F-Value	P-Value
Sample	8	1211	151.33	2.32	0.066
Error	18	1173	65.19		
Total	26	2384			

Grouping Information Using the Tukey Method and 95% Confidence

Sample	N	Mean	Grouping	
6	3	35.23	A	
5	3	27.17	A	B
8	3	22.17	A	B
1	3	21.33	A	B
7	3	19.20	A	B
9	3	18.300	A	B
2	3	17.53	A	B
4	3	14.77	A	B
3	3	10.97		B

Means that do not share a letter are significantly different.

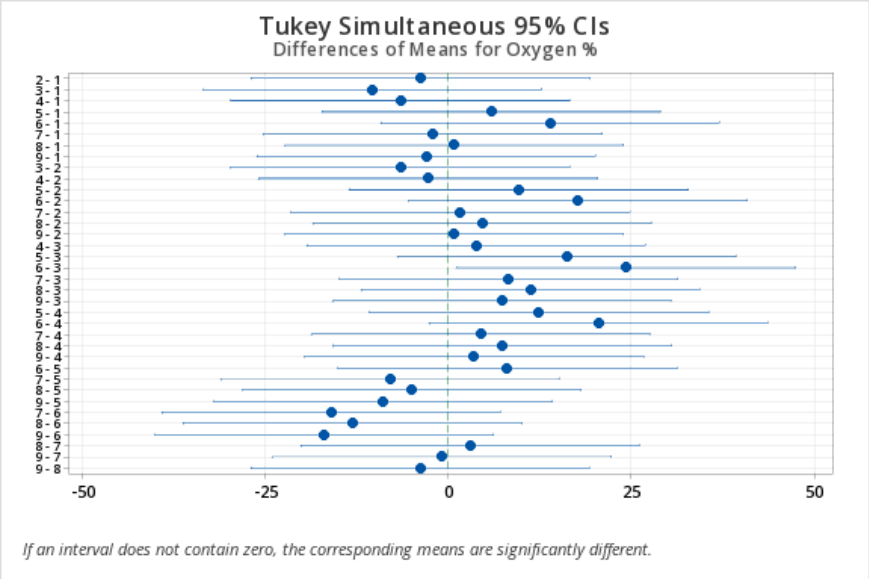

Figure 6.4.20: Interval plot for Tukey comparison method for the response variable oxygen content.

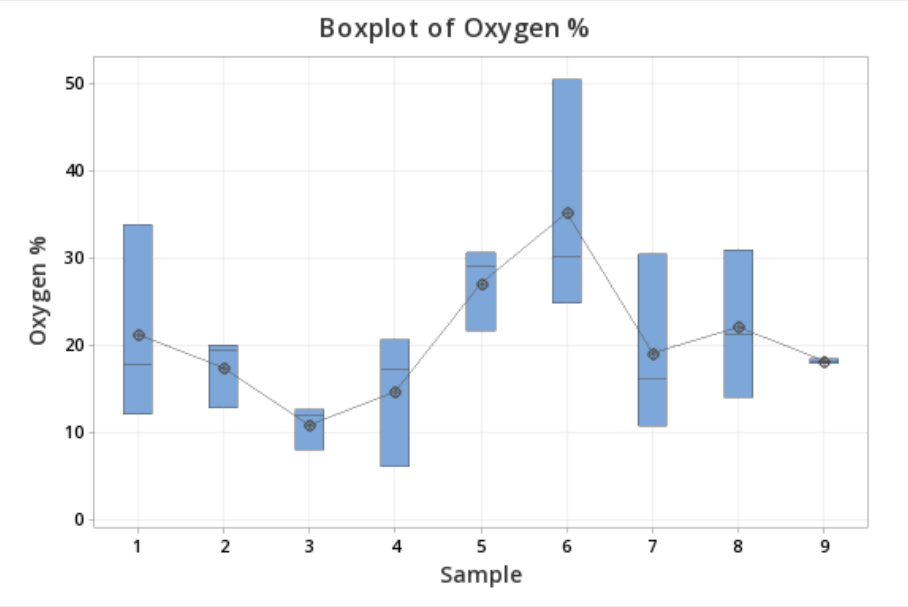

Figure 6.4.21: Boxplot showing data intervals and means for the response variable oxygen content.

6.4.5 Analysis of variance (ANOVA Unilateral) of potassium content percentage

The mean varies from 5.20% to 21.27%. The potassium content percentage is not statistically different among BBAC samples according to the variance analysis (ANOVA, F=3.304, P=0.093) and Tukey Pairwise comparisons. CCAC was not included in this analysis as information about the activating agent is not publicly available.

Table 6.4.7: ANOVA Minitab 18® results for potassium content percentage

Analysis of Variance

Source	DF	Adj SS	Adj MS	F-Value	P-Value
sample	3	560.9	186.97	3.04	0.093
Error	8	492.4	61.55		
Total	11	1053.3			

Tukey Pairwise Comparisons

Grouping Information Using the Tukey Method and 95% Confidence

sample	N	Mean	Grouping
6	3	21.27	A
1	3	15.20	A
5	3	5.30	A
2	3	5.20	A

Means that do not share a letter are significantly different.

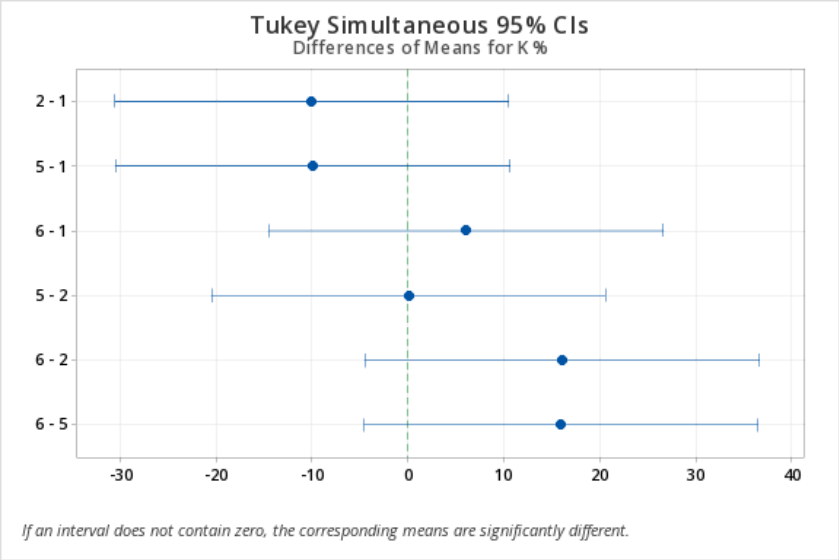

Figure 6.4.22: Interval plot for Tukey comparison method for the response variable potassium content.

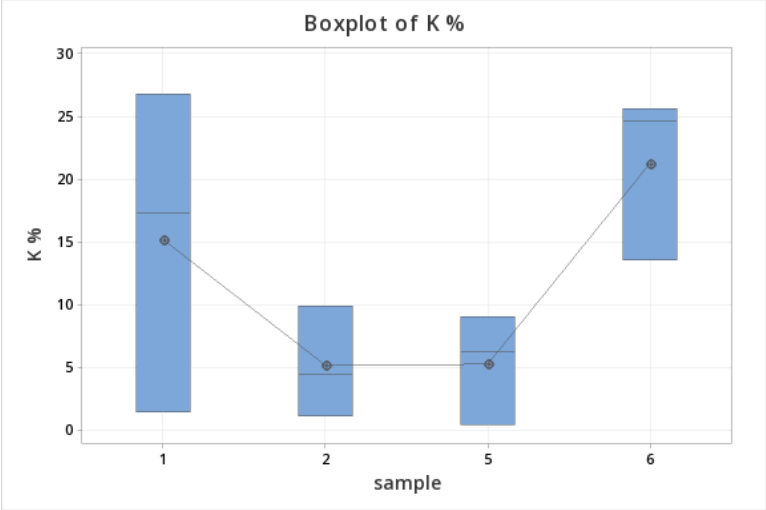

Figure 6.4.23: Boxplot showing data intervals and means for the response variable potassium content.

6.4.6 Analysis of variance (ANOVA Unilateral) of chlorine content percentage

The mean varies from 3.80% to 9.70%. The chlorine content percentage is not statistically different among BBACs according to the variance analysis (ANOVA, F=0.49, P=0.696) and Tukey Pairwise comparisons. Grouping Information Using the Tukey Method and 95% Confidence confirm that means that do not share a letter are significantly different. Furthermore, in this case, all share the letter and contain zero in the interval plot, confirming that the means of these samples are not statistically different for the content of this activating material.

Table 6.4.8: ANOVA Minitab 18® results for chlorine content percentage.

Analysis of Variance

Source	DF	Adj SS	Adj MS	F-Value	P-Value
sample	3	53.46	17.82	0.49	0.696
Error	8	288.51	36.06		
Total	11	341.97			

Grouping Information Using the Tukey Method and 95% Confidence

sample	N	Mean	Grouping
4	3	9.70	A
8	3	6.20	A
3	3	6.03	A
7	3	3.80	A

Means that do not share a letter are significantly different.

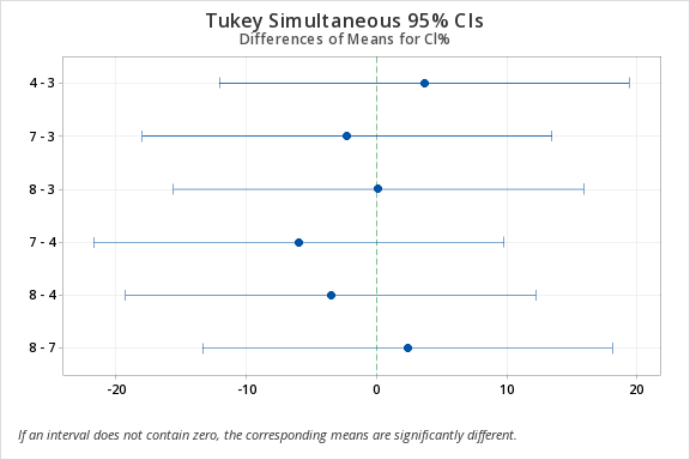

Figure 6.4.24: Interval plot for Tukey comparison method for the response variable chlorine content.

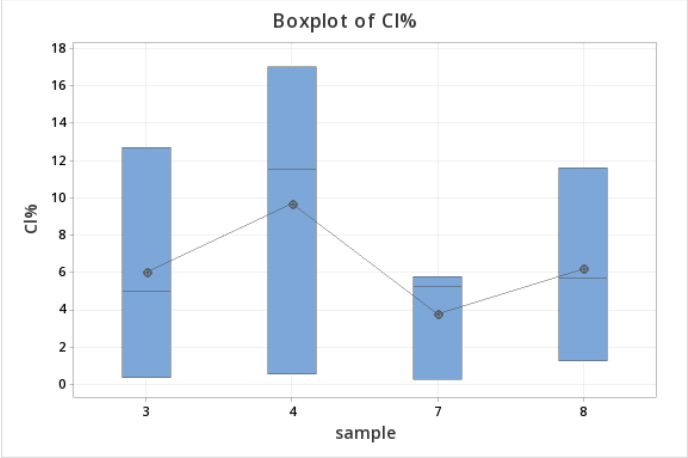

Figure 6.4.25: Boxplot showing data intervals and means for the response variable chlorine content.

6.4.7 Analysis of variance (ANOVA Unilateral) of calcium content percentage

The mean varies from 2.033% to 4.97%. The calcium content percentage is not statistically different among BBACs according to the variance analysis (ANOVA, F=0.46, P=0.716) and Tukey Pairwise comparisons. Grouping Information Using the Tukey Method and 95% Confidence confirm that means that do not share a letter are significantly different. Furthermore, in this case, all share the letter and contain zero in the interval plot, confirming that the means of these samples are not statistically different for the content of this activating material.

Table 6.4.9: ANOVA Minitab 18® results for calcium content percentage.

Analysis of Variance

Source	DF	Adj SS	Adj MS	F-Value	P-Value
sample	3	12.97	4.322	0.46	0.716
Error	8	74.77	9.347		
Total	11	87.74			

Means

sample	N	Mean	StDev	95% CI
3	3	3.40	3.08	(-0.67, 7.47)
4	3	4.97	4.21	(0.90, 9.04)
7	3	2.033	1.701	(-2.037, 6.104)
8	3	3.60	2.70	(-0.47, 7.67)

Pooled StDev = 3.05723

Grouping Information Using the Tukey Method and 95% Confidence

sample	N	Mean	Grouping
4	3	4.97	A
8	3	3.60	A
3	3	3.40	A
7	3	2.033	A

Means that do not share a letter are significantly different.

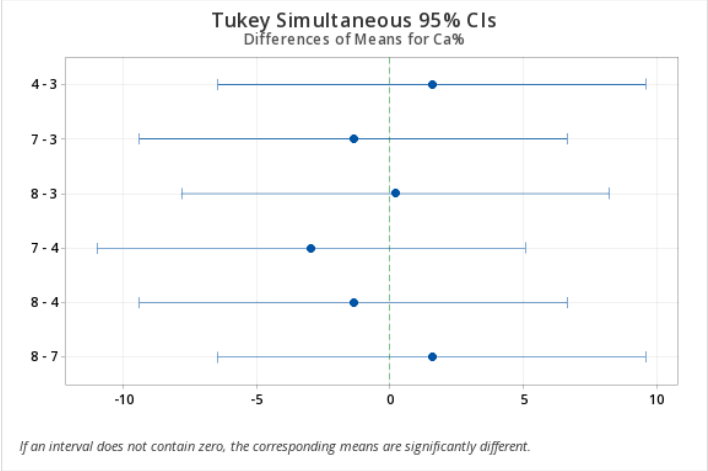

Figure 6.4.26: Interval plot for Tukey comparison method for the response variable calcium content.

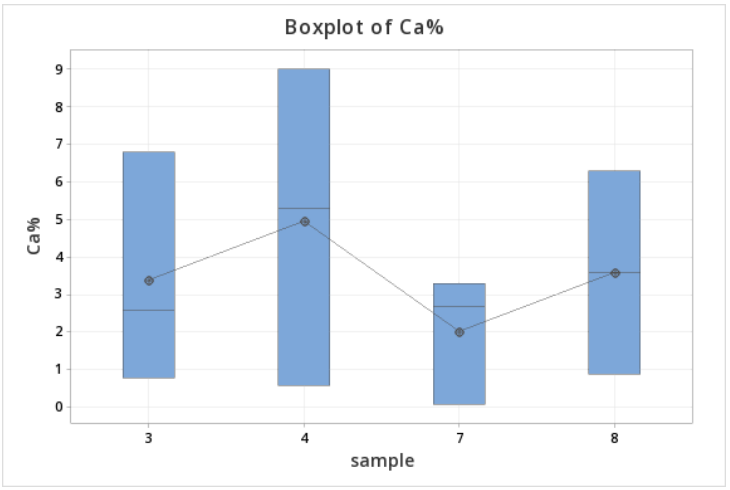

Figure 6.4.27: Boxplot showing data intervals and means for the response variable calcium content.

6.5 COMPARATIVE ANALYSIS

The comparative analysis in the following section shows all the results obtained from SEM/EDS, ICP-OES and LCA in graph form. These graphs allow for a better result-comprehension and assist with final analysis.

6.5.1 Adsorption equilibrium capacity

The results obtained of equilibrium adsorbent-phase concentration of adsorbate (qe) in mg adsorbate/g adsorbent units were used to perform the isotherms. The isotherms obtained provide the nature of the distribution of qe versus Ce. Based on the plots, the isotherms fit better to a linear form (using linear regression) and showed a better correlation in BBAC samples 9, 11,13, and 15 than the CCAC. The adsorption equilibrium capacity (qe) at arsenic concentration initial solution of 0.250 mg/L is higher in BBAC samples 13 and 16 than in the CCAC. The adsorption equilibrium capacity (qe) at an arsenic initial concentration of 0.15 mg/L is higher in BBAC samples 13 and 16 than in the CCAC. The adsorption equilibrium capacity (qe) at an arsenic initial concentration of 0.10 mg/L is higher in BBAC samples 9, 11, 12, 13, 14, 15, and 16 than in the CCAC. The adsorption equilibrium capacity (qe) at an arsenic initial concentration of 0.05 mg/L is higher in BBAC samples 10, 12, 13, 14, 15, and 16 than in the CCAC. The adsorption equilibrium capacity (qe) at an arsenic initial concentration of 0.025 mg/L is higher in BBAC samples10, 13, 14, and 15 than in the CCAC. In summary, BBAC samples 13 and 16, made from rice husk at different pyrolysis temperatures and different activating agents, show better adsorption equilibrium capacity than CCAC at the different initial concentrations of arsenic.

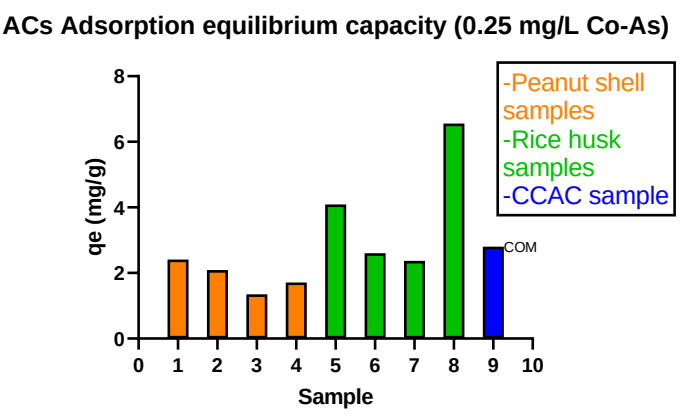

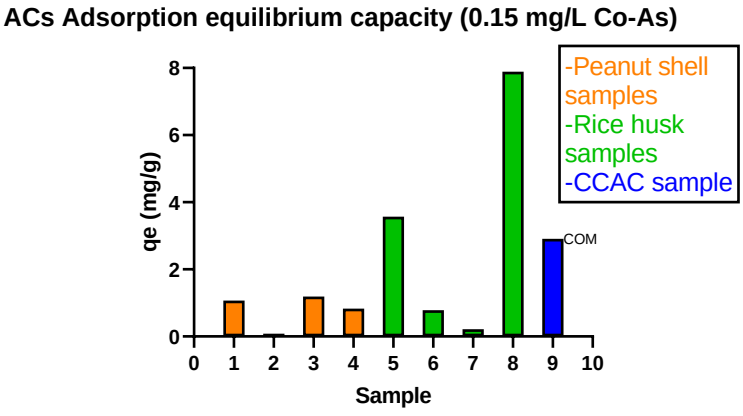

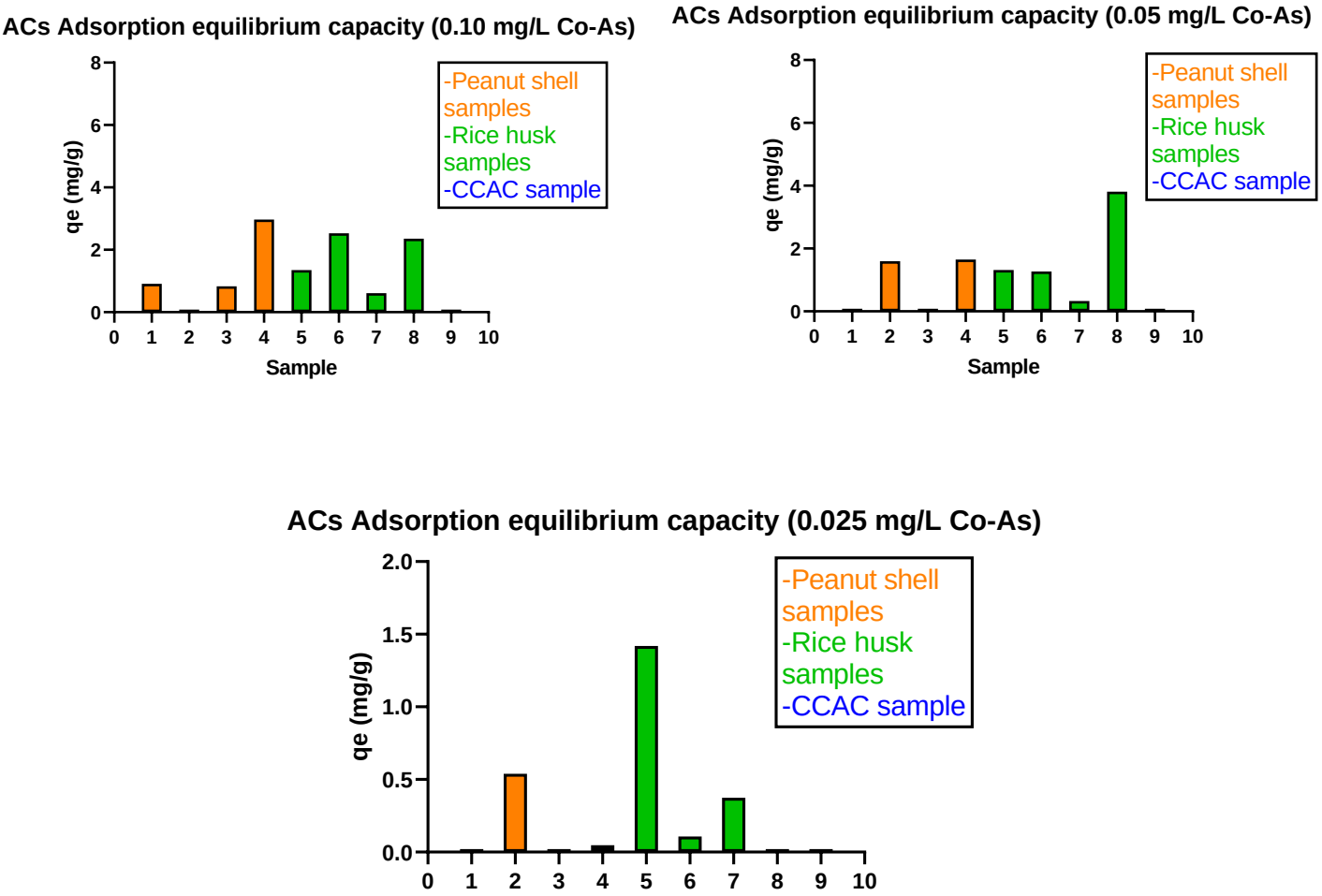

Figure 6.5.1: Comparative graphs of qe at different arsenic concentration solutions.

Adsorption equilibrium capacity (qe) comparative graphs of BBACs and CCAC samples, from sample 9 to sample 16 of BBACs (bars 1 to 8 respectively) and CCAC at the end of the bars (number 9), are seen above.

6.5.2 Life Cycle Assessment

In the LCA studies made from cradle-to-grave to different ACs products for comparative purposes, the results show that the CCAC has a larger Global Warming impact potential (128 kg-CO_2 eq.) than the BBACs (ranging from 11.2 to 15.3 kg-CO_2 eq.) in all samples analyzed according to the DOE matrix. The main contributor to the reduced score was the drying process in the CCAC

and the pyrolysis process in the BBACs (Figure 6.5.2). The acidification potential impact of each BBAC samples (ranging from 0.000664 to 0.000947 kg-SO_2 eq.) and CCAC sample (0.00069 kg-SO_2 eq.) show a small difference in the results and that the landfill disposal is the main contributor to the score in all ACs (Figure 6.5.2). The Eutrophication potential impact also shows a small difference between BBACs (ranging from 0.000309 to .000325 kg-N eq.) and CCAC (.000311 kg-N eq.), and the main contributor to the score is the landfill disposal process in all ACs (Figure 6.5.2). The ozone layer depletion potential impact and Ecotoxicity air impact show the same result for all BBACs and CCAC (1.61 x 10^{-16} kg-CFC 11 eq. for ODP and .00593 CTUe for Ecotoxicity air), and the main contributor to the scores is the landfill disposal process (Figure 6.5.2). CCAC has a more harmful Human Health Particulate impact (0.000388 kg-PM 2.5 eq.) than the BBACs (ranging from 1.59 x 10^{-5} to 2.59 x 10^{-5} kg-PM 2.5 eq.) being the main contributors to the scores the raw material mining process for CCAC and the transportation and landfill disposal for BBACs (Figure 6.5.2). The Human toxicity cancer and non-cancer potential impacts are the same for all BBACs and CCAC (1.6 x 10^{-10} CTUh for HT cancer and 2.4 x 10^{-8} CTUh for HT non-cancer); the main contributor to the scores is the landfill disposal process. The Smog in air potential impact results shows a small difference between BBACs (ranging from 0.00666 to 0.0168 kg-O_3 eq.) and CCAC (0.00775 kg-O_3 eq.), the main contributor to the scores are transportation and landfill disposal processes for BBACs and landfill disposal for CCAC (Figure 6.5.2). Finally, CCAC has larger Resources fossil fuels depletion impact (0.439 MJ surplus energy) than BBACs (0.0884 MJ surplus energy), being the main contributor to the score the raw material mining for CCAC and the landfill disposal for BBACs (Figure 6.5.2)

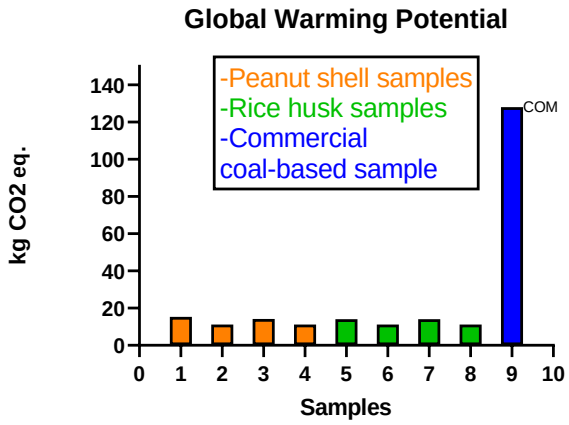
Global Warming Potential
-Peanut shell samples
-Rice husk samples
-Commercial coal-based sample
kg CO2 eq.
140
120
100
80
60
40
20
0
0 1 2 3 4 5 6 7 8 9 10
Samples
COM

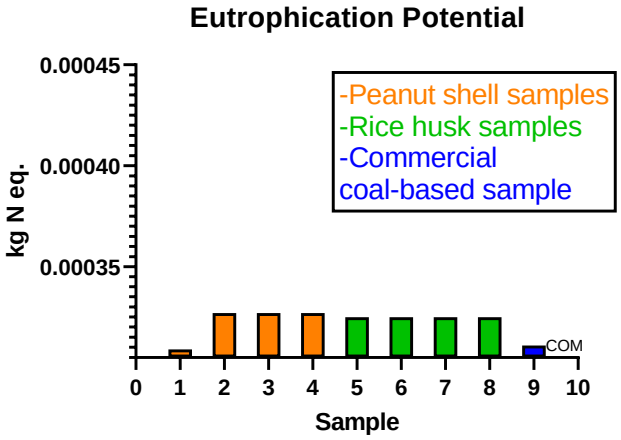
Eutrophication Potential
-Peanut shell samples
-Rice husk samples
-Commercial coal-based sample
kg N eq.
0.00045
0.00040
0.00035
0 1 2 3 4 5 6 7 8 9 10
Sample
COM

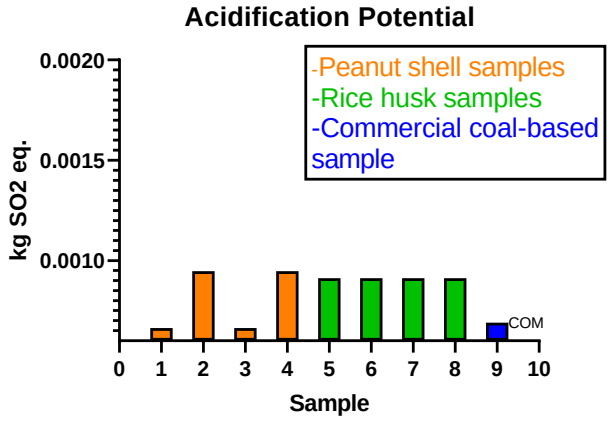
Acidification Potential
-Peanut shell samples
-Rice husk samples
-Commercial coal-based sample
kg SO2 eq.
0.0020
0.0015
0.0010
0 1 2 3 4 5 6 7 8 9 10
Sample
COM

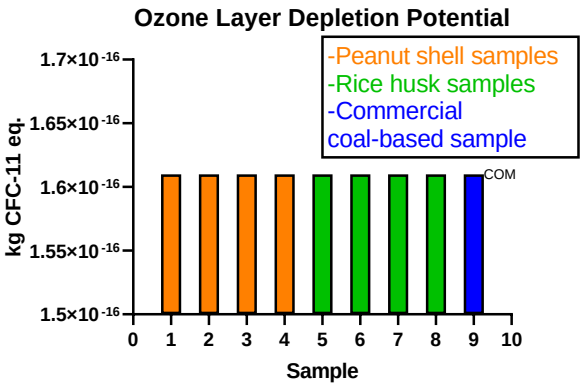
Ozone Layer Depletion Potential
-Peanut shell samples
-Rice husk samples
-Commercial coal-based sample
kg CFC-11 eq.
1.7×10-16
1.65×10-16
1.6×10-16
1.55×10-16
1.5×10-16
0 1 2 3 4 5 6 7 8 9 10
Sample
COM

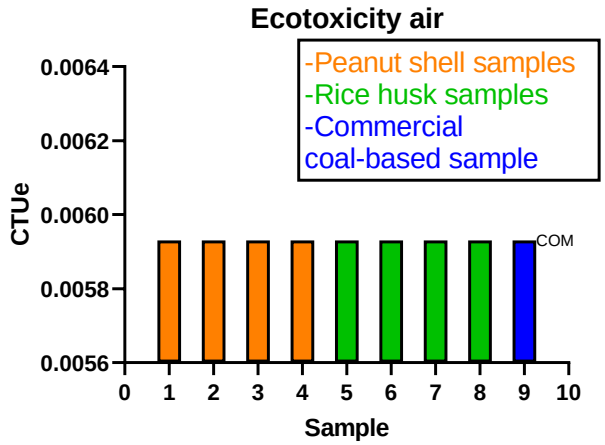
Ecotoxicity air
-Peanut shell samples
-Rice husk samples
-Commercial coal-based sample
CTUe
0.0064
0.0062
0.0060
0.0058
0.0056
0 1 2 3 4 5 6 7 8 9 10
Sample
COM

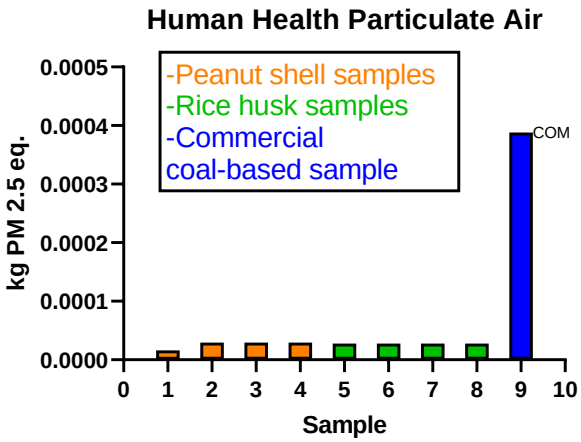
Human Health Particulate Air
-Peanut shell samples
-Rice husk samples
-Commercial coal-based sample
kg PM 2.5 eq.
0.0005
0.0004
0.0003
0.0002
0.0001
0.0000
0 1 2 3 4 5 6 7 8 9 10
Sample
COM

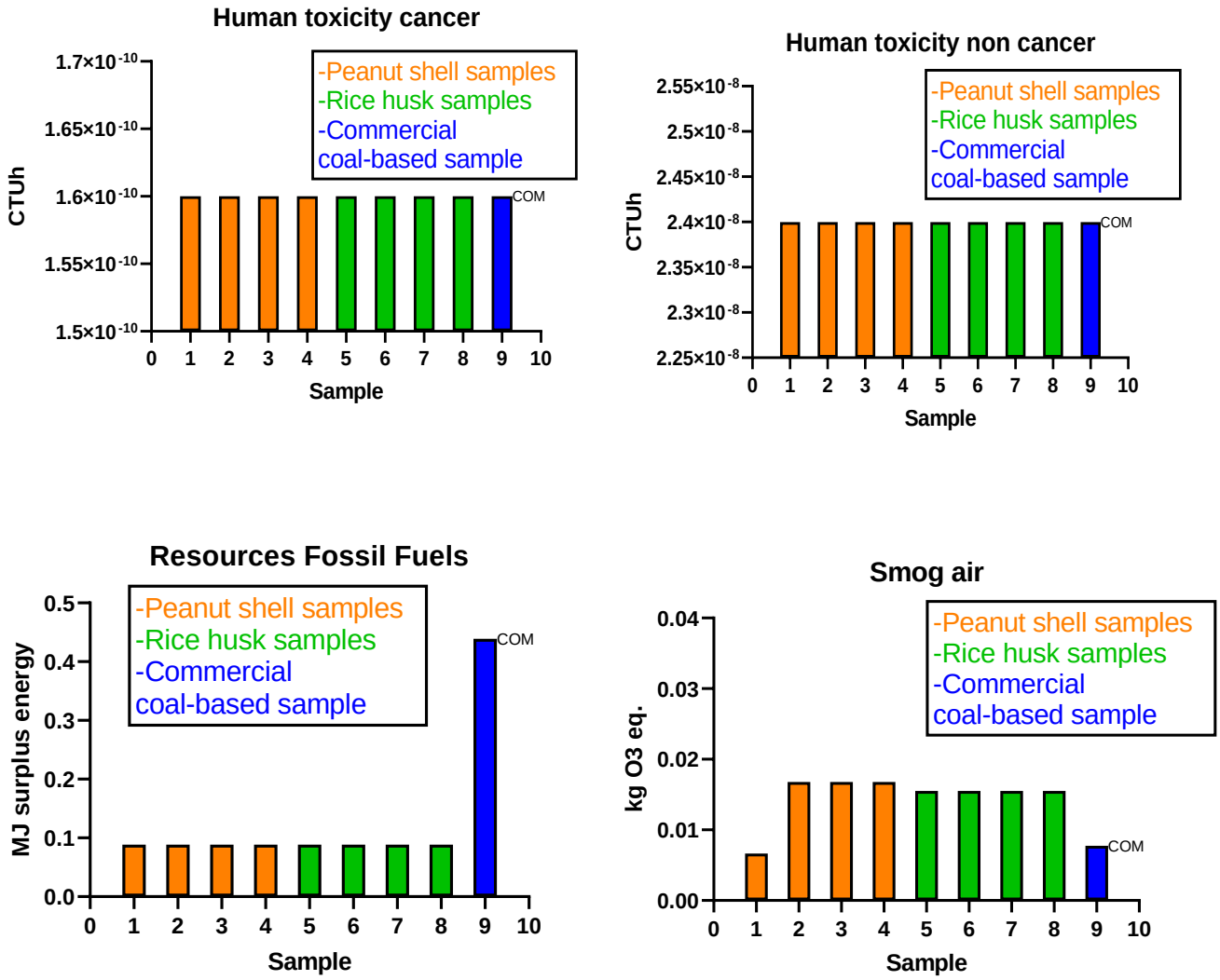

Figure 6.5.2: Comparative graphs of LCIA TRACI categories results.

LCIA-TRACI impact categories of BBACs compared to CCAC.

6.5.3 Characterization and elemental analysis

Once the physical, chemical and structural characteristics of ACs are known, a comparative analysis between BBACs and the CCAC can occur. All the combinations of DOE factors show as main effects of a large surface area with a high volume of macro and mesopores and a homogeneous distribution of the activating agents on the surface of the BBACs. CCAC

also shows a large surface area with a high volume of macro and mesopores and a homogeneous distribution of the activating agent. EDS analysis show the relative abundance of elements present in the sample being the carbon content higher in BBAC samples 2 (85%), 7 (80%), 9 (86.2%), 11 (80.3%), 16 (83%), and 19 (86%) than CCAC (80.2%). BBAC samples show no significant variation between experiment repetitions for the activating elements potassium, calcium, and chlorine and no significant variation between experiments for carbon and oxygen content. The higher content of activating elements in BBACs than in CCAC is attributed to the washing process, which can remove less activating substance than the activating agent found in CCAC (the CCAC show less percentage content of activating agent potassium). (Apparently, CCAC has a better process for activating agent removal).

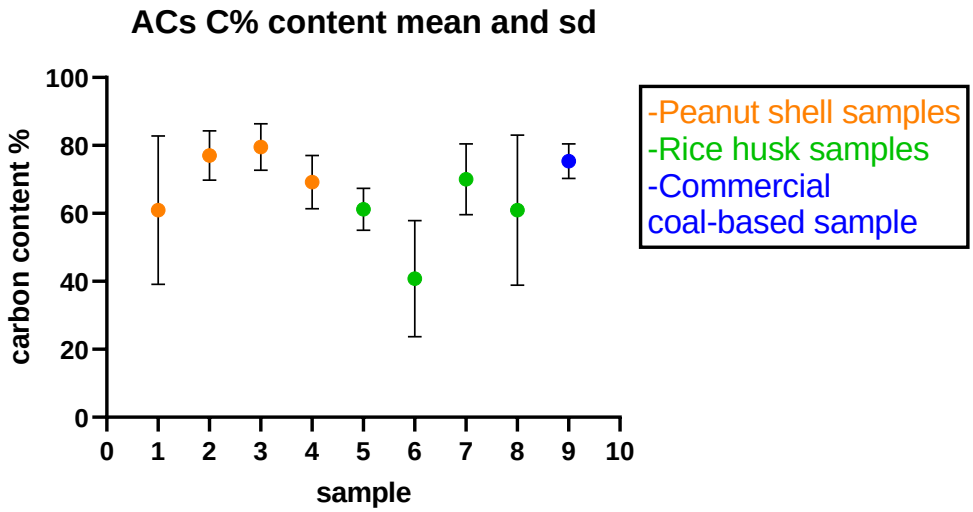

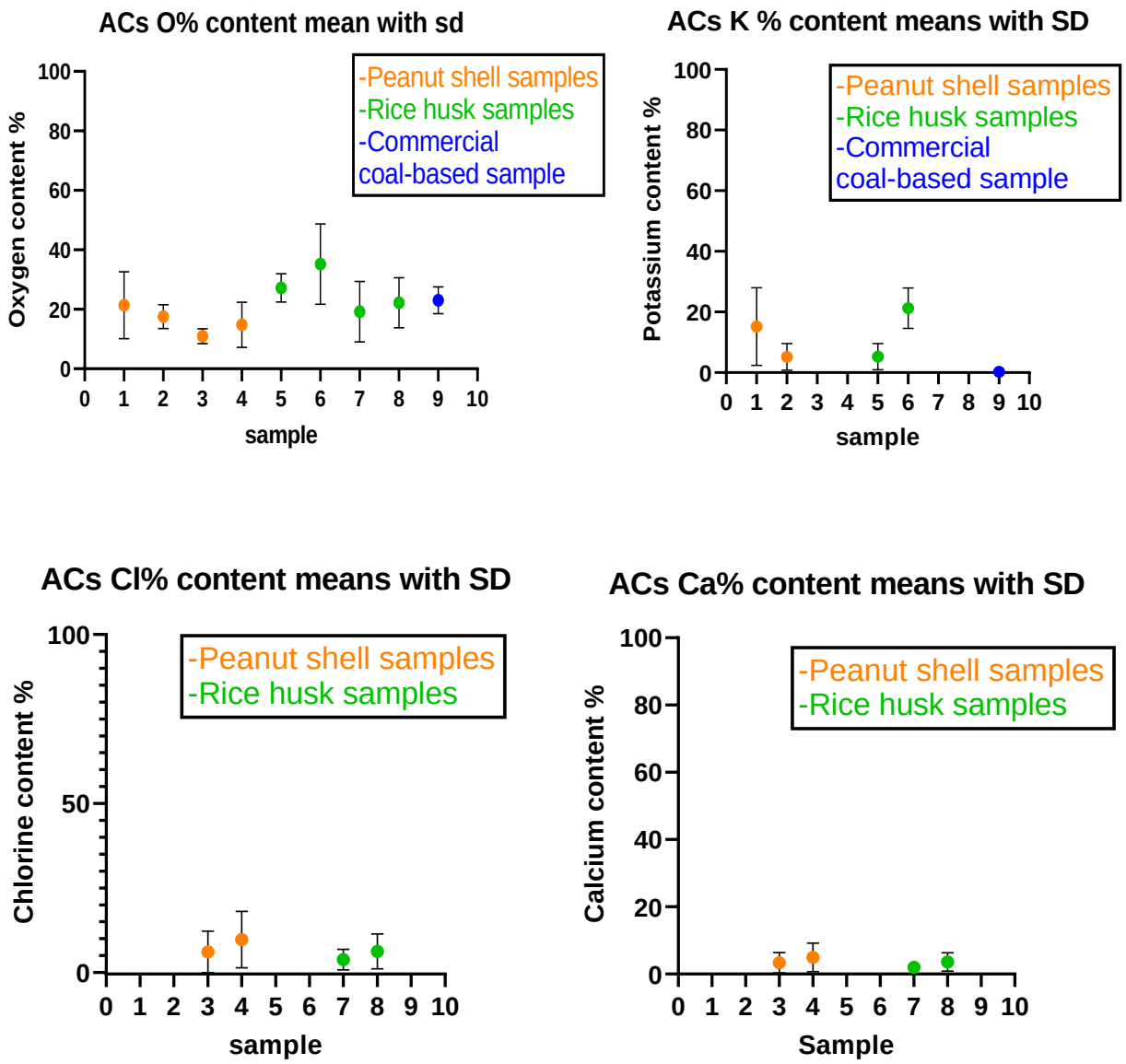

Figure 6.5.3: Comparative graphs of relative abundance of elements present in ACs.

Relative abundance of elements C, O, K, Cl, and Ca present in ACs samples of the DOE matrix and the CCAC.

Chapter 7: Conclusions

7.1 INTRODUCTION

Water quality analysis conducted in the Bustillos lagoon showed that arsenic levels were above standard environmental regulations. Arsenic in water can be potentially harmful at very low concentrations because of its high toxicity and bioaccumulation ability. Thus, treating water used for agricultural and livestock production is highly recommended.

This dissertation focused on a query to find a simple, low cost and environmentally sustainable method to reduce the levels of the arsenic element and obtain water suitable for irrigation and livestock consumption. As discussed in Chapter 4, using an activated carbon filter potentially meets the required physical, environmental and economic characteristics needed to treat water with arsenic. This study manipulated some manufacturing parameters in the activated carbon preparation through a DOE to achieve the adsorption of arsenic with less environmental impact and lower cost of production than the commercial coal-based activated carbon. As mentioned earlier, in multiple studies found in the literature review section of this work, activated carbon made from agricultural residues has shown improved adsorption properties of arsenic with less environmental impact. In this context, the proposed BBAC made with locally available biomass (peanut shell and rice husk) achieved the three main objectives of the research study: equal or improved adsorption of arsenic from water samples, lower cost of BBAC production and equivalent or improved environmental performance results in comparison to CCAC.

7.2 PHYSICAL AND ELEMENTAL ANALYSIS

The characterization analysis of the different ACs performed using the SEM show in the twenty-four samples of BBAC prepared according to the DOE factors and levels that the particle size corresponds to a granular activated carbon with a particle size >180 μm. This is mainly due to the crushing and sieving processes with large and very irregular surface areas and with a high volume of macropores and mesopores (pores >2 nm), as expected in biomass with a greater content of lignin.

In the energy-dispersive X-ray spectroscopy analysis (EDS), the relative abundance of carbon, oxygen, and the activating elements potassium, calcium, and chlorine (KOH and CaCl as activating substances) are different varying from 86.2% of carbon to 22.3%, 6.2% to 50.5% oxygen, 26.8% to 0.3% potassium, 17% to 0.3% chlorine, and 9% to 0.1% calcium.

An EDS analysis determines which BBAC is equal or greater in carbon content than the CCAC. This EDS showed that samples 2 (85%), 9 (86.2%), 11 (80.3%), 16 (83%), and 19 (86%) of BBACs have more carbon content than the CCAC (80.2%) and the rest of the samples with a carbon content ranging from 22 to 80%. The first run and the two replicates of the DOE means are not statistically different among BBACs (ANOVA unilateral). In the DOE variance analysis, a value of $P=0.032$ and $F=5.52$ ($P<0.05$) for raw material was obtained, indicating that precursor material (peanut shell/rice husk) is a significative factor in the response variable (carbon content). The other factors and interactions are not significant. The optimal parameters for maximum carbon content according to DOE optimizer are the following: peanut shell as precursor material, pyrolyzed at high temperature (600-800°C), using the activating agent potassium hydroxide.

7.3 ADSORPTION EXPERIMENTS

The adsorption equilibrium capacity (qe) of BBACs and CCAC obtained in the study show that samples 13 (1.419, 1.319, 1.348, 3.57, and 4.09 mg/g) and 16 (0.004, 3.807, 2.354, 7.891, and 6.559 mg/g) have higher scores than the CCAC (0.003, 0.031, 0.012, 2.912, and 2.805 mg/g) at all the different initial concentrations of arsenic in the DOE and the CCAC only has better adsorption performance in samples 9, 10, 11, 12, 14, and 15 at 0.25 mg/L and 0.15 mg/L arsenic concentrations. Adsorption equilibrium isotherms plotted using linear regression describe a linear relationship between adsorption equilibrium capacity (qe) versus ACs aqueous-phase concentration (Ce) in most of the experiments. Sample 16 of the BBACs shows an abnormal result for adsorption equilibrium capacity above the other BBACs and CCAC scores. In conclusion, samples 13 and 16 show better adsorption equilibrium capacity than CCAC. This improvement identifies that one of the main objectives of the research, to physically improve the AC, is achieved.

7.4 STATISTICAL ANALYSIS

The objectives of the DOE are to find factors, levels, and interactions for the preparation of BBACs capable of adsorbed arsenic from water, prepared with agricultural waste from the region with improved or equal physical, chemical, and structural properties than CCAC. One of the response variables considered for this DOE is adsorption equilibrium capacity (qe). In the statistical analysis, the mean of qe varies from sample to sample, ranging from 0.673 to 4.12. The adsorption capacities are statistically different among some BBACs, but they are not statistically different from CCAC according to the Tukey method, with a level of confidence of 95%. The test for equal variances shows that the standard deviations of the ACs (BBACs and CCAC) are not significantly different. Still, the test for normality/abnormality results shows that sample 16 is not

normal compared to the other BBACs and CCAC. Sample 16 shows a lot greater adsorption capacity performance than the other BBACs of the DOE and the CCAC.

DOE graphical analysis shows in the plot of main effects that raw material and carbonization temperature are the most significant factors. Only the interaction of activating agent and carbonization temperature is significative in most of the experiments for the different arsenic solutions. However, the cube plot shows that the best combination of factors to obtain the best equilibrium adsorbent-phase concentration of adsorbate (qe) in DOE is: rice husk carbonized at 500-600°C using calcium chloride as activating agent. The largest number in the cube indicates the best combination of factors, highest score 7.89127.

The statistical analysis of variance indicates that the raw material is a significative factor in the response variable carbon content and that the other factors and interactions between them are not significative. The factorial plot of main effects indicates that raw material and its interaction with an activating agent are not statistically significative. The analysis determines that the best combination of factors for carbon content are: peanut shell, pyrolyzed at 600-800°C using potassium hydroxide as activating agent.

In summary, samples 13 and 16 of BBAC (both made with rice husk) have better adsorption capacity than the CCAC, and samples 2, 9, 11, 16, and 19 (2, 9, 11, and 19 made with peanut shell and 16 with rice husk) have higher carbon content. The DOE and statistical analysis results show that the carbon content is not the major contributor to the adsorption equilibrium capacity. Peanut shell samples show higher carbon content but not better adsorption equilibrium capacity than samples of BBAC made with rice husk. Furthermore, an improved porosity and surface area are also needed to increment the adsorption equilibrium capacity; the activation process is the major contributor for pores and surface area development. Lastly, rice husk can be

used to produce activated carbon with equal and better adsorption properties than CCAC. The production process setups significantly affect significatively the adsorption equilibrium capacity at the parameters used for this DOE and the carbon content, which is an essential characteristic of activated carbons and is affected significatively by the raw material used and its interaction with the activating agent.

7.5 LIFE CYCLE ASSESSMENT

The results of the LCIA show that BBACs made with agricultural waste have a potentially less environmental impact than a CCAC. The impact categories: global warming potential, human health particulate air potential, and resource fossil fuels depletion potential all have higher scores in CCAC. Ozone depletion potential, ecotoxicity potential, human toxicity cancer, and human toxicity non-cancer impact categories have the same scores in all ACs. While air potential impact categories: eutrophication potential, acidification potential, and smog, have a higher score in BBACs, this is only a small difference in all ACs. However, there is an extremely large difference between the CCAC and BBACs GWP scores: 128 kg-CO_2 eq. for CCAC compared to 11.2 to 15.3 kg-CO_2 eq. for BBACs. The major contributors to the CCAC's GWP score are drying, activation process, and landfill disposal. Pyrolysis and landfill disposal are the major contributors to the BBACs' GWP and smog score. The raw material mining process is the major contributor to the human health particulate air potential and resources fossil fuel depletion impact categories for the CCAC. In conclusion, BBACs have a better environmental performance potential than the CCAC, achieving the environmental performance objective of this research.

7.6 COST ANALYSIS

The cost analysis developed in Table 5.3 indicates that the production cost of BBACs made with agricultural waste is lower than the price of the CCAC in retail stores. The difference is approximately 4.0976 USD for BBAC made with rice husk, about 3.8356USD for BBAC made with peanut shell, and roughly 16.29USD for CCAC. The comparative analysis used CCAC consumer costs as the production cost information is unavailable. The use of agricultural waste eliminates the cost of the raw material needed in the first step of the life cycle for the ACs production compared with the higher cost of mining the hard coal used in the CCAC. The transportation cost is reduced as the materials are sourced within the region which will use them. Crushing the raw material and removing rocks and other contaminants can be completed manually without electricity or other energy sources. Manual crushing costs of raw materials are considerably lower than the mechanical crushing of hard coal, using electricity for the CCAC preparation. Pyrolysis is the most energy-intensive process in BBAC production; energy is provided by fossil fuel combustion in this study, LP gas. Pyrolysis is also considered the most energy-consumption process and the major BBAC cost contributor. The chemical activation process in BBAC production is also made manually and requires a heating process using LP gas and its associated cost (see cost analysis Table 5.3). The activation of hard coal to produce CCAC by chemical or physical activation requires electricity, gas, and water to prepare the activating agent or the steam, as well as the heating of the material and activating agent depending on the process used to activate the material (Table 5.3). These processes are energy consumers due to the high temperatures they need to produce steam and/or the activation temperature they need to apply to hard coal. Removal of the chemical is required in the BBAC preparation and chemically activated CCAC, so water consumption is needed in this part of the life cycle (the same amount of

water is considered in the cost analysis for all ACs). For the drying process, CCAC production needs fossil fuel or electricity; gas costs are considered for CCAC, and drying at room temperature at no cost is considered for BBAC. Finally, the ACs are sieved and packed according to specifications. Cost analysis did not consider the life cycle's end-of-life and land-fill disposal steps. Nonetheless, the BBACs' cost of production is one-fourth of the CCAC price, thus fulfilling the cost reduction objective of this research.

Chapter 8: Future work

Further work in LCA and LCIA arena would be helpful to provide a more in depth understanding of the potential environmental impacts of Bio-based Activated Carbons (BBAC). Data on energy consumption, emissions to the environment and measuring methods should be collected for a large-scale production process. The adsorption experiment should be repeated to determine the BBACs adsorption equilibrium capacity in a natural aquatic ecosystem (lagoon surface water in natural conditions) to compare to the lab-controlled results obtained in this investigation.

An ecological handprint analysis, is a new method to facilitate the measurement, evaluation and communication of the ecological, economic, and social sustainability impacts of products, could be done to include the positive feedbacks from BBAC. This new concept provides a positive and realistic framework for evaluating sustainability including issues of social justice and human rights alongside the rights of the environment, animals, and species inhabiting the planet (Husgafvel, 2021).

References

Agency for Toxic Substances and Disease Registry. U.S Department of Health and Human Services (2013). Toxicological profile for uranium. Available online: https://www.atsdr.cdc.gov/toxprofiles/tp150.pdf (accessed on 25 February 2018).

Acero, A. P., Rodriguez, C., Ciroth A. (2015). LCIA methods: Impact assessment methods in Life Cycle Assessment and their impact categories. Green Delta, Germany. https://www.openlca.org/wp-content/uploads/2015/11/LCIA-METHODS-v.1.5.4.pdf (accessed 29 January 2020).

Ahmaruzzaman, M. (2011). Industrial Wastes as Low-Cost Potential Adsorbents for Treatment of Wastewater Laden with Heavy Metals. *Advances in Colloid and Interface Science*, 166, 36-59.

Amado-Álvarez, J.P. (2011). Uso y Manejo Eficiente del Agua. Reporte. Cuauhtémoc, Chihuahua: Instituto Nacional de Investigaciones Forestales, Agrícolas y Pecuarias (inifap).

Anirudhan, T.S., & Sreekumari, S.S. (2011). Adsorptive Removal of Heavy Metal Ions from Industrial Effluents Using Activated Carbon Derived from Waste Coconut Buttons. *Journal of Environmental Sciences,* 23, 1989-1998.

Angin, D. (2014). Production and Characterization of Activated Carbon from Sour Cherry Stones by Zinc Chloride. Department of Food Engineering, Sokarya University, 3-8.

Anoop Krishnan, K., & Anirudhan, T.S. (2002). Removal of Mercury (II) from Aqueous Solutions and Chlor-Alkali Industry Effluent by Steam Activated and Sulphurised Activated Carbons Prepared from Bagasse Pith: Kinetics and Equilibrium Studies. *Journal of Hazardous Materials*, 161-183.

Arena, N., Lee, J., & Clift, R. (2016). Life Cycle Assessment of Activated Carbon Production from Coconut Shells. *Journal of Cleaner Production*, (125), 68-77.

Avesmx. Available online: http://avesmx.conabio.gob.mx/ficharegion.html # AICA-62 (accessed on June 23, 2018).

Aygun, A., Yenisoy-Karakas, S., & Duman, I. (2003). Production of Granular Activated Carbon from Fruit Stones and Nutshells and Evaluation of Their Physical, Chemical and Adsorption Properties. Department of Metallurgical Engineering, Institute of Science and Technology, 189-195.

Bansode, R.R., Losso, J.N., Marshall, W.E., Rao, R.M., & Portier, R.J. (2003). Adsorption of Metal Ions by Pecan Shell-Based Granular Activated Carbons. Department of Food Science, Louisiana State University Agricultural Center, 115-119.

Bare, J.C., Hofstetter, P., Pennington, D.W. and H.A. Udo de Haes (2000). Life Cycle Impact Assessment Workshop Summary. Midpoints versus Endpoints: The Sacrifices and Benefits. *The International Journal of Life Cycle Assessment*, 5(6):319-326.

Barroso-Bogeat, A., Alexandre-Franco, M., Fernandez-Gonzalez, C., & Gomez-Serrano, V. (2016). Activated Carbon Surface Chemistry: Changes Upon Impregnation with Al (III), Fe (III) and Zn (II)- metal Oxide Catalyst Precursors from Non-Aqueous Solutions. *Arabian Journal of Chemistry*, 1-11

Benjamin M.M., (2015). Water Chemistry, second edition. Waveland Press, Inc., Long Grove, IL.

Bernardo, M., Lapa, N., Matos, I., & Fonseca, I. (2016). Critical Discussion on Activated Carbons from Bio- Wastes – Environmental Risk Assessment. Chemistry Department, University of Lisboa.

Bhakar, V., Kumar, H., Sai, N., Sangwan, K., & Raghuvanshi, S. (2016). Life Cycle Assessment of Filtration Systems of Reverse Osmosis Units: A Case Study of a University Campus. Research School Department of Mechanical Engineering, 40, 268-273.

Biswas, B., Pandey, N., Bisht, Y., Singh, R., Kumar, J., & Bhaskar, T. (2017). Pyrolysis of Agricultural Biomass Residues: Comparative Study of Corn Cob, Wheat Straw, Rice Straw and Rice Husk. *Bioresource Technology Journal*, (102), 501-511

Bonton, A., Bouchard, C., Barbeau, B., & Jedsejak, S. (2011). Comparative Life Cycle Assessment of Water Treatment Plants. *Desalination Journal*, (102), 501-511

Ching, Wah., Srinvasakannan, C., & Shoaibi, A. (2015). Cleaner Production of Porous Carbon from Palm Shells Through Recovery and Reuse of Phosphoric Acid. *Journal of Cleaner Production,* (102), 501-511.

Comisión para la cooperación ambiental. Tareas importantes para la conservación de las aves de América del Norte: Directorio de 150 sitios relevantes. Available online: http://www3.cec.org/islandora/es/item/1664-north-american-important-bird-areas-directory-150-key-conservation-sites-es.pdf (accessed on 20 June 2018).

Crittenden J.C., Rhodes Trusell R., Hand D.W., Howe K.J., Tchobanoglous G. (2012). Water treatment principles and design, third edition. Published by John Wiley & Sons, Inc., Hoboken, New Jersey.

Corsi, I., Fiorati, A., Grassi, G., Bartolozzi, I., Daddi, T., Melone, L., & Punta, C. (2018). Environmentally Sustainable and Ecosafe Polyssaccharide-Based Materials for Water Nano-Treatment: An Eco-Design Study. Materials.

Daifullah, A.A.M., Girgis, B.S., & Gad, H. (2002). Utilization of Agro-Residues (rice husk) in Small Waste Water Treatment Plans. Laboratory and Waste Management Center, 1723-1731.

Danish, M., & Ahmad, T. (2018). A Review on Utilization of Wood Biomass as a Sustainable Precursor for Activated Carbon Production and Application. *Renewable and Sustainable Energy Reviews*, 87, 1-21.

Demiral, H., Demiral, I., Karabacakoglu, B., & Tumsek, F. (2011). Production of Activated Carbon from Olive Bagasse by Physical Activation. Department of Chemical Engineering, Faculty of Engineering and Architecture, 206-213.

Demiral, H., & Gunduzoglu, G. (2010). Removal of Nitrate from Aqueous Solutions by Activated Carbon Prepared from Sugar Beet Bagasse. *Bioresource Technology Journal*, 101, 1675-1680.

Dias, J.M., Alvim-Ferraz, C.M., Almeida, M., Rivera-Utrilla, J., & Sanchez-Polo, M. (2007). Waste Materials for Activated Carbon Preparation and Its Use in Aqueous-Phase Treatment. *Journal of Environmental Management*, 833-846.

Fierro, V., Muniz, G., Basta, A.H., & Celzard, A. (2010). Rice Straw as Precursor of Activated Carbons: Activation with Ortho-Phosphoric Acid. *Journal of Hazardous Materials*, 181, 27-34.

Fu, R., Liu, Y., Lou, Z., Wang, Z., Baig, S.A., & Xu, X. (2016). Adsorptive Removal of Pb (II) by Magnetic Activated Carbon Incorporated with Amino Groups from Aqueous Solutions. *Journal of the Taiwan Institute of Chemical Engineers,* 247-258.

Fujiwara, M., Hayashi, N., Kanai, K., Kiyozuka, M., Matsui, Y., Mori, K., & Sakakibara, Y. (2006). Application of Life Cycle Assessment (LCA) to Water Purification Facilities: Inventory Analysis for Comparison Between "Coagulation Sedimentation + Sand Filtration" and "Membrane Filtration."

GaBi Software and Education database, 2020 UTEP, MyApps.

Gavankar, S., Suh, S., & Keller, A.F. (2012). Life Cycle Assessment at Nanoscale: Review and Recommendations. International *Journal Life Cycle Assessment*, 17:295-303.

Georgin, J., Luiz, G., Mazutti, M.A., & Foletto, E. (2015). Preparation of Activated Carbon from Peanut Shell by Conventional Pyrolysis and Microwave Irradiation-Pyrolysis to Remove Organic Dyes from Aqueous Solutions. *Journal of Environmental Chemical Engineering*, 266-275.

Grande, C.A., Blom, R., Spjelkavik, A., Moreau, V., & Payet, J. (2017). Life Cycle Assessment as a Tool for Eco-design of Metal-Organic Frameworks. *Sustainable Materials and Technologies*, 14, 11-18.

Gu, H., Bergman, R., Anderson, N., & Alanya-Rosenbaum, S. (2018). Life Cycle Assessment of Activated Carbon from Woody Biomass. *Wood and Fiber Science*, 50(3), 1-15.

Hadi, P., To, M.H., Hui, C.W., Ki Lin, C., & McKay, G. (2015). Aqueous Mercury Adsorption by Activated Carbons. Chemical and Biomolecular Engineering Department, Hong Knog University of Science and Technology, 73, 37-55.

Hauschild, M.Z., Huijbregts, M., Jolliet, O., Macleod, M., Margni, M., Van DeMeent, D., Rosenbaum, R.K., McKone, T.E. (2008). *Environmental Science and Technology*, 42, 7032-7037.

Heijungs, R., Guinee J.B. (1993). Environmental life cycle assessment of products: guide and backgrounds. Institute of Environmental Sciences. Leiden Netherlands.

Hieu, N.M., Korobochkin, V.V. & Tu, N.V. (2015). A Study of Silica Separation in the Production of Activated Carbon from Rice Husk in Vietnam. *Department of Chemical Engineering*, 15, 308-312.

Hjaila, K., Baccar, R., Sarra, M., Gasol, C.M., Blanquez, P. (2013). Environmental impact associated with activated carbon preparation from olive-waste cake via life cycle assessment. *Journal of Environmental Management*, 130, 242-247.

Husgafvel, R. Exploring Social Sustainability Handprint—Part 1: Handprint and Life Cycle Thinking and Approaches. Sustainability 2021, 13, 11286. https://doi.org/10.3390/su132011286

Hwan Oh, G., & Rae Park, C. (2002). Preparation and Characteristics of Rice- Straw Based Porous Carbons with High Adsorption Capacity. *Enviro-Polymers Design Laboratory*, 327-336.

INEGI (2003) & (2010). Instituto Nacional de Estadistica y Geografia. Síntesis de Información Geográfica del Estado de Chihuahua 2010.

Ioannidou, O., & Zabaniotou, A. (2007). Agricultural Residues as Precursors for Activated Carbon Production. *Renewable and Sustainable Energy Reviews*, 11, 1966-2005.

Jeswani, H.K., Gujba, H., Brown, N.W., Roberts, E., & Azapagic, A. (2015). Removal of Organic Compounds from Water: Life Cycle Environmental Impacts and Economic Costs of the Arvia Process Compared to Granulated Activated Carbon. *Journal of Cleaner Production*, 89, 203-213.

Jijakli, K., Arafat, H., Kennedy, S., Mande, P., & Theeyattuparampil, V.V. (2012). How Green Solar Desalination Really is? Environmental Assessment Using Life-Cycle Analysis (LCA) Approach. *Desalination Journal*, 287, 123-131.

Jung, S.H., & Kim, J. (2014). Production of Biochars by Intermediate Pyrolysis and Activated Carbons from Oak by Three Activation Methods Using CO2. *Journal Analytical and Applied Pyrolysis*, (107), 116-122.

Kadirvelu, K., Kavipriya, M., Karthika, C., Radhika, M., Vennilamani, N., & Pattabhi, S. (2003). Utilization of Various Agricultural Wastes for Activated Carbon Preparation and Application for the Removal of Dyes and Metal Ions from Aqueous Solutions. Department of Environmental Science, *PSG College of Arts and Science*, 87, 129-132.

Karnib, M., Kabbani, A., Holail, H., & Olama, Z. (2014). Heavy Metals Removal Using Activated Carbon, Silica and Silica Activated Carbon Composite. The International Conference on Technologies and Materials for Renewable Energy, *Environment and Sustainability*, 50, 113-120.

Kim, M.H., Jeong, I.T., Park, S.B., Kim, J.W. (2019). Analysis of environmental impact of activated carbon production from wood waste. *Environ. Eng. Res*. 24(1), 117-126.

Kumar, A., & Jena, H. (2016). Preparation and Characterization of High Surface Area Activated Carbon from Fox Nut (Euryale ferox) Shell by Chemical Activation with H3PO4, 651-658.

Lanzetta, M., & Di Blasi, C. (1998). Pyrolysis Kinetics of Wheat and Corn Straw. *Journal of Analytical and Applied Pyrolysis*, (44), 181-192.

Le Van, K., & Thuy Luong Thi, T. (2014). Activated Carbon Derived from Rice Husk by NaOH Activation and Its Application in Supercapacitor. Physical Chemistry Department, Hanoi University of Education, 191-198.

Li, S., Han, K., Li, J., Li, M., & Lu, C. (2017). Preparation and Characterization of Super Activated Carbon Produced from Gulf weed by KOH Activation. *Microporous and Mesoporous Materials*, 243, 291-300.

Lillo-Rodenas, M.A., Cazorla-Amoros, D., & Linares-Solano, A. (2002). Understanding Chemical Reactions Between Carbons and NaOH and KOH. An Insight into the Chemical Activation Mechanism. Department of Inorganic Chemistry, University of Alicante, 1-9.

Lori, J.A., Lawal, A.O., & Ekanem, E.J. (2008). Active Carbons from Chemically Mediated Pyrolysis of Agricultural Wastes: Application of Simultaneous Removal of Binary Mixture of Benzene and Toluene from Water. Department of Chemistry, Ahmadu Bello University.

Lo, S.F., Wang, S.Y., Tsai, M.J., & Lin, L.D. (2012). Adsorption Capacity and Removal Efficiency of Heavy Metal Ions by Moso and Ma Bamboo Activated Carbons. *Chemical Engineering Research and Design*, 90, 1397-1406.

Manjare, S.D., Khan, A.Y. (2006). A cradle to grave approach: an effective solution for reduction in environmental pollution. *Chemical Weekly Journal*, October 24, 2006.

Mohammad-Khah, A., & Ansari, R. (2009). Activated Charcoal: Preparation, Characterization and Application: A Review Article. *International Journal of ChemTech Research*, (4), 859-864.

Mohamed-Lamine, S., Ridha, C., Mohammed-Mahfoud, H., Mouad, C., Lotfi, B., & Al-Dujaili, A.H. (2014). Chemical Activation of an Activated Carbon Prepared from Coffee Residue. The International Conference on Technologies and Materials for Renewable Energy, *Environment and Sustainability*, 393-400.

Ng, C., Marshall, W., Rao, R.M., Bansode, R.R., Losso, J.N., & Portier, R.J. (2003). Granular Activated Carbons from Agricultural By-products: Process Description and Estimated Cost of Production.

Nienborg, B., Helling, T., Frohlich, D., Horn, R., Munz, G., & Schossig, P. (2018). Closed Adsorption Heat Storage-A Life Cycle Assessment on Material and Component Levels. *Energies*, 11, 3421.

Noijuntira, I. & Kittisupakorn, P. (2010). Life cycle assessment for the activated carbon production by coconut shells and palm-oil shells. Green Technology and Productivity. *The 2nd RMUTP International Conference 2010*. 228-231.

Ochoa-Rivero, J., Reyes, A., Peralta, R., Zavala, F., Ballinas, L., Salmerón, I., Rubio, H., Rocha-Gutiérrez, B. (2017). Levels and Distribution of Pollutants in the Waters of an Aquatic Ecosystem

in Northern Mexico. *International Journal of Environmental Research and Public Health.* 2017,14,456

Pallares, J., Gonzalez-Cencerrado, A., & Arauzo, I. (2018). Production and Characterization of Activated Carbon from Barley Straw by Physical Activation with Carbon Dioxide and Steam. *Biomass and Bioenergy Journal*, (115), 64-73.

Pode, R. (2016). Potential Application of Rice Husk Waste from Rice Husk Biomass Power Plant. *Renewable and Sustainable Energy Reviews*, 53, 1468-1485.

Quintana, R., Espinoza, J. Frescas, J., Pinedo A. (2015). The importance of assessing water quality in Laguna Bustillos, Chihuahua, Mexico. *Revista Latinoamericana el Ambiente y las Ciencias*, 6(13), 187-203.

Raghuvanshi, S., Bhakar, V., Sowmya, C., & Sangwan, K.S. (2017). Waste Water Treatment Plant Life Cycle Assessment: Treatment Process to Reuse of Water. Department of Mechanical Engineering.

Ras, C., & Blottniz, H. A Comparative Life Cycle Assessment of Process Water Treatment Technologies at the Secunda Industrial Complez South Africa. Environmental Process Systems Engineering Research Group, Department of Chemical Engineering, 549-554.

Ribas, M.C., Adebayo, M.A., Prola, L., Lima, E., Cataluna, R., Feris, L., Puchana-Rosero, M.J., Machado, F., Pavan, F., & Calvete, T. (2014). Comparison of a Homemade Cocoa Shell Activated Carbon with Commercial Activated Carbon for the Removal of Reactive Violet 5 Dye from Aqueous Solutions. *Chemical Engineering Journal*, 315-326.

Ricordel, S., Taha, S., Cisse, I., & Dorange, G. (2001). Heavy Metal Removal by Adsorption onto Peanut Husks Carbon: Characterization, Kinetic Study and Modeling. *Separation and Purification Technology*, 24, 389-401.

Seager, T.P., & Linkov, I. (2008). Coupling Multicriteria Decision Analysis and Life Cycle Assessment for Nanomaterials. *LCA in North America*, 282-285.

Shamsuddin, M.S., Yusoff, N.R.N., & Sulaiman, M.A. (2016). Synthesis and Characterization of Activated Carbon Produced from Kenaf Core Fiber Using H3PO4 Activation. Faculty of Earth Science, University Malaysia Kelantan, 19, 558-565.

Sharaai, A.H., Mahmood, N.Z. & Sulaiman, A.H. (2010). Life cycle impact assessment (LCIA) using TRACI methodology: an analysis of potential impact on potable water production. *Australian Journal of Basic and Applied Sciences*. 4(9), 4313-4322.

Sharma, A., Pareek, V., & Zhang, D. (2015). Biomass Pyrolysis- A review of Modelling, Process Parameters and Catalytic Studies. *Renewable and Sustainable Energy Reviews*, 1081-1096.

Stavropoulos, G.G., & Zabaniotou, A.A. (2005). Production and Characterization of Activated Carbons from Olive-Seed Waste Residue. Department of Chemical Engineering, Aristotle University of Thessaloniki, 79-85.

SEMARNAT. Secretaria de Medio Ambiente y Recursos Naturales. 2003. Norma Oficial Mexicana NOM-001/002-SEMARNAT-1996. Publicada el 30 de octubre de 1996 en el Diario Oficial de la Federación. Texto vigente.

Sudaryanto, Y., Hartono, S.B., Irawaty, W., Hindarso, H., & Ismadji, S. (2005). High Surface Area Activated Carbon Prepared from Cassava Peel by Chemical Activation. *Bioresource Technology*.

Sun, K., & Chun Jiang, J. (2009). Preparation and Characterization of Activated Carbon from Rubber-Seed Shell by Physical Activation with Steam. *Institute of Chemical Industry of Forest Products*, 539-544.

Sun, Y., Li, H., Li, G., Gao, B., Yue, Q., & Li, X. (2016). Characterization and Ciprofloxacin Adsorption Properties of Activated Carbons Prepared from Biomass Wastes by H3PO4 Activation. *Bioresource Technology Journal*, 217, 239-244.

Sun, Y., & Weblay, P. (2010). Preparation of Activated Carbons from Corncob with Large Specific Area by a Variety of Chemical Activators and Their Application in Gas Storage. *Chemical Engineering Journal*, (162), 883-892.

Taha, S., Ricodel, S., & Cisse, I. (2011). Kinetic Study and Modeling of Heavy Metals Removal by Adsorption onto Peanut Husks Incinerated Residues. *Energy Procedia*, 6, 143-152.

Tsai, W.T., Chang, C.Y., & Lee, S.L. (1997). A Low-Cost Adsorbent from Agricultural Waste Corn by Zinc Chloride Activation. Department of Environmental Engineering and Health.

Tsai. W.T., Chang, C.Y., Wang, S.Y., Chang, C.F., Chien, S.F., & Sun, H.F. (2001). Cleaner Production of Carbon Adsorbents by Utilizing Agricultural Waste Corncob, 43-53.

Tsai, W.T., Chang, C.Y., Wang, S.Y., Chang, C.F., Chien, S.F., & Sun, H.F. (2000). Preparation of Activated Carbons from Corn Cob Catalyzed by Potassium Salts and Subsequent Gasification with CO2. Department of Environmental Engineering and Health, *Chia Nan College of Pharmacy and Science*. 203-208

Uner, O., Gecgel, U., & Bayrak, Y. (2015). Preparation and Characterization of Mesoporous Activated Carbons from Waste Watermelon Rind by Using the Chemical Activation Method with Zinc Chloride. *Arabian Journal of Chemistry*.

United States Environmental Protection Agency (US EPA). (2009). National Primary and Secondary Drinking Water Regulation. Available online: http://www.epa.gov/safewater/ (accessed on 15 March 2018).

United States Environmental Protection Agency (US EPA). (2016). Health Effect Notebook. Available online: https://www.epa.gov/sites/production/files/2013-11/documents/nla_newlowres_fullrpt.pdf (accessed on 15 March 2018).

Vanderheyden, G., & Aerts, J. (2014). Comparative LCA Assessment of Fontinet Filtered Tap Water vs. Natural Sourced Water in a PET Bottle.

Vittrup, E. Lopez-Moreno, A. Iracheta, L.C. Herrera, R. Orvananos, M. Sliwa, B. Gordyn. (2016). Indice Basico de las Ciudades Prosperas. *ONU-Habitat Mexico* 2016, INFONAVIT and SEDATU.

Wu, M., Guo, Q., & Fu, G. (2013). Preparation and Characteristics of Medicinal Activated Carbon Powders by CO2 Activation of Peanut Shells. *College of Chemical Engineering*, 188-196.

Xu, X., Schierz, A., Xu, N., & Cao, X. (2016). Comparison of the Characteristics and Mechanisms of HG(II) Sorption by Biochars and Activated Carbon. *Journal of Colloid and Interface Science*, 55-60.

Yahya, M.A., Al-Qodah, Z., & Zanariah Ngah, C.W. (2015). Agricultural Bio-Waste Materials as Potential Sustainable Precursors Used for Activated Carbon Production. *Renewable and Sustainable Energy Reviews*, (46), 218-235.

Yakout, S.M., & Sharaf El-Deen, G. (2011). Characterization of Activated Carbon Prepared by Phosphoric Acid Activation of Olive Stones. *Arabian Journal of Chemistry*.

Yang, D., Jiang, L., Yang, S., & Wei, S. (2017). Experimental Study on Preparation of Straw Activated Carbon by Microwave Heating. School of Thermal Engineering.

Yang, Q., Wu, S., Lou, R., & Lv, G. (2010). Analysis of Wheat Straw Lignin by Thermogravimetry and Pyrolysis-Gas Chromatography/Mass Spectrometry.

Yorgun, S., & Yildiz, D. (2015). Preparation and Characterization of Activated Carbons from Paulownia Wood by Chemical Activation with H3PO4. *Journal of the Taiwan Institute of Chemical Engineers,* (53), 122-131.

Zhang, F.S., Nriagu, J.O, & Itoh, H. (2005). Mercury Removal from Water Using Activated Carbons Derived from Organic Sewage Sludge. *Department of Environmental Health Sciences*, 39, 389-395.

Zhang, S., Tao, L., Jiang, M., Gou, G., & Zhou, Z. (2015). Single Step Synthesis of Magnetic Activated Carbon from Peanut Shell. *Materials Letters Journal*, 157, 281-284.

Zhang, T., Walawender, W., Fan. L.T., Fan, M., Daugaard, D., & Brown, R.C. (2004). Preparation of Activated Carbon from Forest and Agricultural Residues Through CO2 Activation. *Chemical Engineering Journal*, 53-59.

Vita

Leticia E. Rodriguez Prieto
Environmental Science and Engineering Department
University of Texas at El Paso
500 W. University Ave.
El Paso, TX 79968-0517
Email: lerodriguez12@miners.utep.edu

Short Biosketch

Leticia E. Rodriguez is a teacher assistant in the Department of Environmental Science and Engineering at the University of Texas at El Paso. She holds a BS in Electronic and Industrial Engineering from Instituto Tecnologico de Chihuahua, an MS in Manufacturing Engineering from the Instituto Tecnologico de Cd. Juarez, and Ph.D. degree in Environmental Science and Engineering from University of Texas at El Paso. Her research strenghts involve the development of ecofriendly materials, sustainable process design, and Life Cycle Assessment methodology for environmental impacts assessment. Leticia E. Rodriguez has published the manuscript "Comparative LCA of glass containers made from recycled and virgin raw material" in Proceedings of the Industrial and Systems Engineering Research Conference. Orlando, FL. May 2019.

Current Position
Teacher assistant. From Fall 2017 - to date
Department of Environmental Science and Engineering
The University of Texas at El Paso

Education
Ph.D. in Environmental Science and Engineering Program at the University of Texas at El Paso. From Fall 2017- to Fall 2022.
Manufacturing Engineering Master's degree. Universidad Autónoma de Ciudad Juárez. Instituto de Ingeniería y Tecnología. Professional specialization: Process Design and Lean Manufacturing. Master's Thesis: Manufacture of a tin-copper solder compound with alumina (Al_2O_3) nanoparticles as a reinforcing material. Graduated in June 2016.
Industrial Electronic Engineer Bachelor. Instituto Tecnológico de Chihuahua. Graduated in June 1998.

Work experience
Delphi Automotive Systems. Manufacturing Engineer for Sensors and Solenoids division. Responsible for the Design and implementation of production lines for the manufacture of

sensors and solenoids for the control of emissions of BMW, Opel GM, and Toyota models. From 1998-2006.
Zenith Cableproductos de Chihuahua. Production Supervisor of main boards of tv cable equipment, responsible for automatic insertion and test equipment. From 1996-1997.

Research Interests:
Sustainable Engineering
Life Cycle Assessment
Engineering Materials
Water treatment methods
Production systems statistical analysis

Other Relevant Coursework
MINITAB (statistical analysis).
ABACUS (finite element analysis).
MASTERCAM (computer aided manufacturing CAD/CAM software application).
SOLID WORKS (3D CAD design).
FluidSIM (simulation program for pneumatics, hydraulics, and electrical engineering by FESTO).
PFMEA & PCP (process failure mode and effect analysis and process control plan)
Failure analysis by statistical methods (SHAINING, DOE, TAGUSHI, 6 SIGMA).
JIT (just in time), KAN BAN, POKA YOKE.
Geometric dimensioning and tolerances (GD & T).
Transmission and Engine Teardown.
Robust Engineering.
Lean Equipment Design.

Contact Information: lerodriguez12@miners.utep.edu